Consumer Behaviour Integrated Dynamic-Life Cycle Assessment of Car-based Sharing Economy

Chalaka Fernando

February 2023

A thesis submitted for the degree of Doctor of Philosophy of
The Australian National University

DECLARATION

This thesis contains no material which has been accepted for the award of any other degree or diploma in any university. To the best of the author's knowledge, it contains no material previously published or written by another person, except where due reference is made in the text.

Chalaka Fernando

February 2023

DEDICATION

to

those who *Share* and *Pool* by compromising their comfort…

On the whole, you find wealth more in use than in ownership Aristotle, 350BC

ACKNOWLEDGEMENTS

Praises and Thanks to God!

The completion of this study could not have been possible without my chair supervisor, Associate Professor Matthew Doolan, and panel advisers Dr Vi Kie Soo, Prof Paul Compston and Dr Hyung Chul Kim from Ford USA.

A great appreciation to Dr Gary Buttriss from the Research School of Management, Dr Hwan-Jin Yoon from the CSIRO (former ANU Statistic Consulting Unit), Robert De Klaine from the Ford USA and Dr Chris Brown from the College of Science for diversified research collaborations and guidance.

Dear Andi, Victoria, Saeed, John, Chris and Mengyuan and all office mates, thanks for the chit-chats and sharing, and also Dustin Weigl from US NREL Denver for the system dynamics modelling discussions.

I greatly appreciate the support from Ed and Marie Otoole, Marie Elspeth, Roger Fitzgerald, Roger Paul, Megan Thompson, Sean Perera, Barbara Burns and Nancy Clerk for proofreading support.

I also appreciate Conjoint.ly for providing a free academic license.

Last but not least, a great thanks to my loving family: Achala, Vinuk and Jemith, for joining me in coming to Australia and going through all the changes with patience and all support, and to my loving parents and in-laws.

This study is supported by the ARC Training Centre in Lightweight Automotive Structure (project number IC160100032), the Australian National University, and is funded by the Australian Government.

ABSTRACT

Personal mobility modes, such as private vehicles, contribute significantly to the increase in greenhouse gas (GHG) emissions. Car-based sharing economy modes are considered a solution for reducing personal mobility-related GHG impacts. These car-based Mobility as a Service (MaaS) modes have lowered the barrier of affording vehicle usage compared to the product-based linear economy, thus changing consumer decision-making attributes. Their fleets have also transformed technologically to face increased pressure to incorporate environmental responsibilities. MaaS consumer preferences can influence fleet changes. This thesis quantifies the environmental impacts of the transition to MaaS from private vehicles, considering consumer preferences and their feedback on timely varying fleet technological changes.

The Consumer Behaviour Integrated Dynamic Life Cycle Assessment (C-DLCA) methodology framework is introduced as a structured approach to integrating MaaS consumer behaviour into a dynamic Life Cycle Assessment (LCA). It employs the System Dynamics (SD) technique as the modelling interface. The full life cycle of personal mobility fleets was chosen as the LCA scope and the 2014 to 2050 time period as the temporal scope for dynamic modelling. The United States (US) GREET model-based lightweighting and life cycle inventory and the US electric grid factor GHG changes are incorporated in the modelling. A policy scenario is chosen for adopting a high-Battery Electric Vehicle (BEV) based on market and policy dynamics.

The US round-trip to work, the most frequent and increasing routine journey type, is chosen as the case study to analyse the consumer preferences and decision-making attributes for private vehicles, carpooling, solo-ridesourcing and pooled-ridesourcing. An extensive market survey was administered to 2,968 qualified samples representing US geography and public transit ridership. Cost, journey time, number of passengers, body style, and powertrain type were chosen as choice-based conjoint analysis attributes to integrate the Discrete Choice Experiment (DCE) features and the MaaS modes. The results show that cost, journey time, and occupancy are significant attributes, and the powertrain type is the least. Also, utility outcomes are directed towards more environmentally unsustainable gasoline and Sports Utility Vehicles (SUVs). In summary, the results show a value-action gap associated with transitioning to MaaS. The Bass model (Bass, 1969) is adopted to simulate the transition to MaaS by incorporating DCE outcomes, and the vehicle body type provided an endogenous explanation in the SD model.

The dynamic LCA outcomes show a significant GHG emission reduction in aggregated personal mobility and a further reduction in the high BEV adoption scenario. The results suggest a decline in carpooling, the least GHG-emitting car-based MaaS mode. The aggregated MaaS GHG emissions considerably increased owing to solo-occupancy, deadheading contribution, and SUV dominance from the extensively increasing BEV-supported solo-ridesourcing fleet. However, the GHG emission trends show a decline in all modes when interpreted using p.km, the chosen functional unit that correlates with the number of users. The high BEV adoption scenario attracts more MaaS consumers, while emitting more GHG emissions from SUV prominent solo-ridesourcing. Dynamic fleet technology changes increase production emissions while reducing use-phase emissions with the support of vehicle lightweighting, increasing survivability, and the US electric grid GHG factor.

This research concludes that consumer preferences and fleet changes incorporated dynamic LCA on the transition to MaaS in trips to work in the US have shown that the car-based sharing economy is a pathway to reduce GHG emissions in personal mobility with specific fleets and consumer preference combinations. The shift to BEV-driven pooling modes reduces life-cycle GHG emissions in personal mobility. It also highlights the significance of combining consumer preferences and dynamic fleet technology changes to determine GHG emissions in the transition to sharing economy-based car modes.

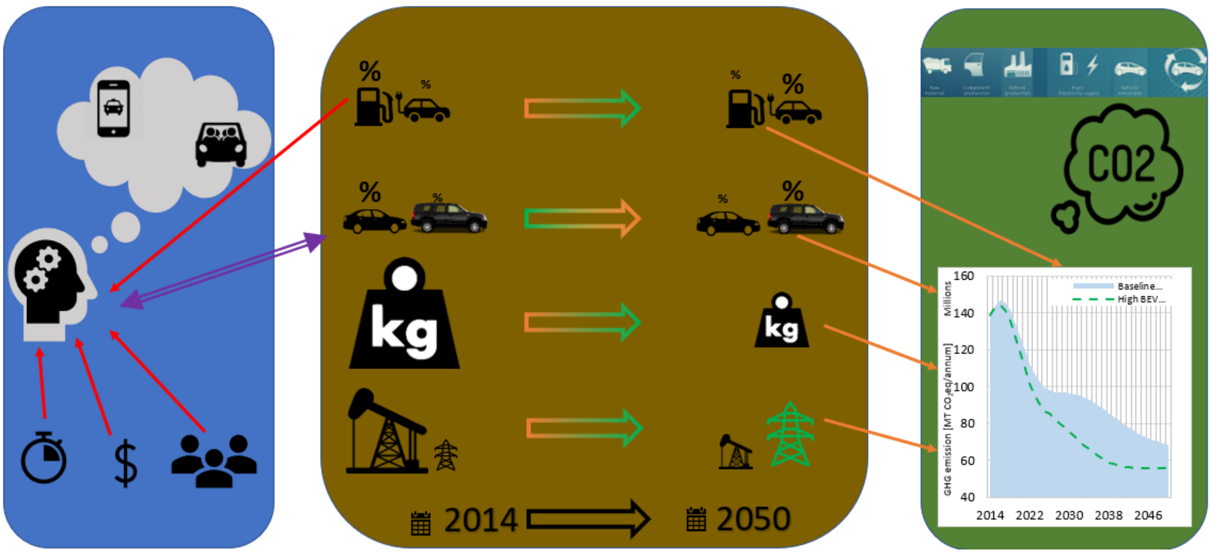

Figure 0-1: Graphical abstract

Publications

The following publications were developed during my PhD candidature:

Fernando, C., Soo, V. K., & Doolan, M. (2020). Life Cycle Assessment for Servitization: A Case Study on Current Mobility Services. *Procedia Manufacturing*, *43*, 72–79. https://doi.org/10.1016/j.promfg.2020.02.112

Fernando, C., Soo, V. K., Compston, P., Kim, H. C., De Kleine, R., Weigl, D., Keith, D. R., & Doolan, M. (2020). Life cycle environmental assessment of a transition to mobility servitization. *Procedia CIRP*, *90*, 238–243. https://doi.org/10.1016/j.procir.2020.01.098

Fernando, C., Soo, V. K., Compston, P., & Doolan, M. (2022). Life Cycle Environmental Impact of Mobility Servitization: The Effect of Fleet Technology Changes. *Procedia CIRP*, *105*, 829–834. https://doi.org/10.1016/j.procir.2022.02.137

Fernando, C., Buttriss, G., Yoon, H.-J., Soo, V. K., Compston, P., & Doolan, M. (Accepted). Integration of consumer behaviour into dynamic life cycle assessment for the sharing economy: Methodology and case study for shared mobility. *International Journal of Life Cycle Assessment*.
Status: Accepted

Fernando, C., Buttriss, G., Yoon, H.-J., Soo, V. K., Compston, P., Kim, H. C., De Kleine, R., & Doolan, M. (Under review). Characterising the consumer preferences of car-based mobility for a round-trip to work. *Journal of Consumer Behaviour*.
Status: Reviewer comments address in-progress

Fernando, C., Soo, V. K., Compston, P., & Doolan, M. (Under review). The impact of car-based shared mobility on greenhouse gas emissions: A review. *Transportation Safety and Environment*.
Status: Reviewer comments address in-progress

TABLE OF CONTENTS

LIST OF TABLES

LIST OF FIGURES

ACRONYMS AND NOMENCLATURE

ARQ – Associated Research Question

BEV – Battery Electric Vehicle

DCE – Discrete Choice Experiment

DPI – Dynamic Process Inventory

EoL – End-of-Life

GHG – Greenhouse Gas

HEV – Hybrid Electric Vehicle

ICEV – Internal Combustion Engine Vehicle

LCA – Life Cycle Assessment

LCI – Life Cycle Inventory

LCIA – Life Cycle Impact Assessment

MaaS – Mobility as a Service

MNL – Multinomial Logistic

p.km – passenger kilometre

SD – System Dynamics

SQLR – Systematic Quantitative Literature Review

SUV – Sports Utility Vehicle

v.km – vehicle kilometre

WoM – Word-of-Mouth

1 INTRODUCTION

1.1 Context of the study

Personal mobility modes, such as private vehicles, contribute significantly to increasing greenhouse gas (GHG) emissions. From 2000 to 2019, passenger cars recorded the highest global increase in GHG emission (1 Gt CO_2 per year) compared to other road-sector transport mediums, such as commercial trucks and buses (International Energy Agency (IEA), 2021a). Light-duty vehicles, mostly used for personal mobility, accounted for the most significant transport GHG emission contribution (57 to 59%) in the USA (US EPA, 2020a, 2022). Car-based sharing economy modes are considered a solution for reducing personal mobility-related GHG emission impacts. Alternatives available for personal mobility have increased in recent times. Carpooling has been in use for decades, and pooled-ridesourcing is the newest addition to the car-based Mobility as a Service (MaaS) market. In MaaS [1], vehicles are not owned but are utilised for journey purposes from a fleet. Thus, the adoption of MaaS for different types of journeys has become widespread. Some metro areas and cities promote the use of MaaS as a substitute for private vehicles, for its environmental benefits (Metropolitan Transportation Commission, 2019b, 2019a; Wenzel *et al.*, 2019). Nevertheless, the contribution of car-based MaaS modes to GHG emissions remains unclear (Union of Concerned Scientists, 2020b).

Several factors that influence GHG emissions when using shared mobility modes are highlighted in recent research findings. Transition to fleet electrification is an example of GHG emissions changes in MaaS that are driven by policies and adopted faster than the private vehicle fleet by shared mobility operators targeting sustainability commitments (Lyft, 2020; Uber, 2020; US EPA, 2021). The higher adoption of Sports Utility Vehicles (SUVs) in these modes is another factor that influences GHG emissions. The automobile industry has reduced its GHG footprint by introducing newer technologies that are lightweight, energy efficient (these factors are further discussed in Section 2.4), having higher survivability (Lu, 2006; Davis and Boundy, 2021). In summary, the changes in MaaS fleets are temporal, and their consequences on the GHG emissions of MaaS are dynamic.

Car-based MaaS adoption depends on decisions made by the consumer. Hence, understanding consumer preferences and preferred choices from available options is critical for evaluating the transition to MaaS usership. Consumers decide on the transition to MaaS based on attributes such as journey fare, time (door-to-door) and convenience (Lippke and Noyce, 2020). The type of

[1] The term MaaS (Mobility as a Service) is used to represent the car-based sharing economy modes in this thesis

journey is also an important factor determining the use of MaaS mode (McGuckin and Fucci, 2018), as well as fleet technology, such as body style (Uber, 2021c). A detailed literature-based analysis of consumer preference attributes in MaaS is listed in Appendix B. According to the collection of literature, changing fleet technology can influence the choice of the MaaS mode based on consumer preference. On the other hand, consumers can affect the MaaS industry based on their fleet technology preferences when ordering a ride. As shown in Figure 1-1, consumers can show their interest in body type while selecting fleet options provided in a journey (ride) request in transport network company apps. There is a causality relationship between consumer preferences, fleet technology and MaaS use, subsequently influencing GHG emissions based on usership and dynamic fleet technology types.

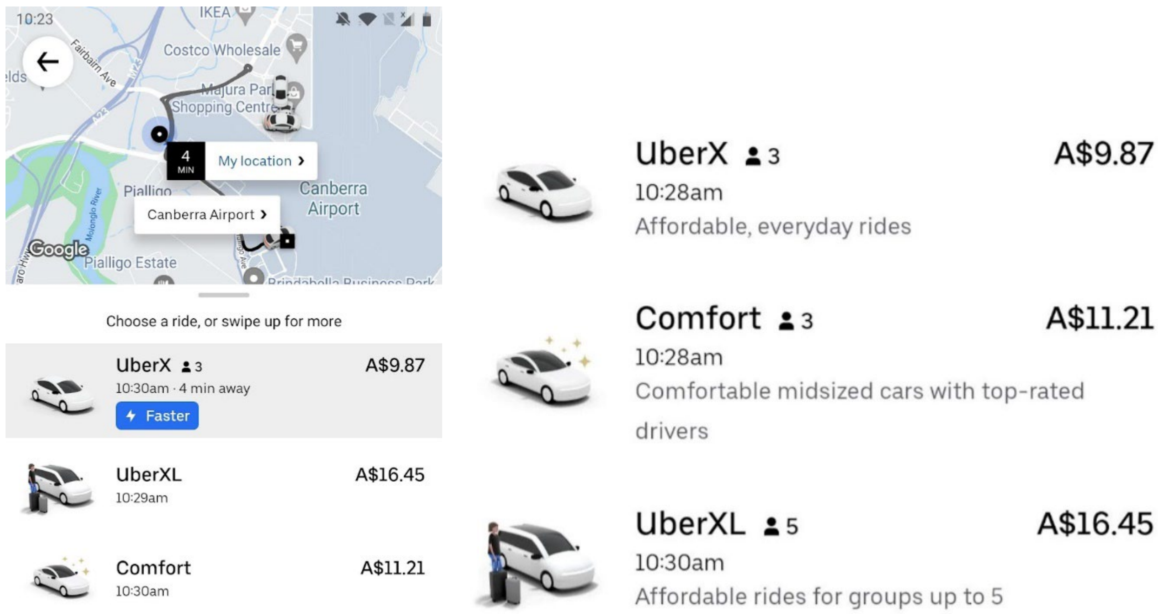

Figure 1-1 Fleet options provided for a journey by a transport network company mobile app

Note: Using the Uber mobile App

The Life Cycle Assessment (LCA) method (ISO, 2006) is commonly used to determine the environmental impacts of the entire life cycle of a product like a car or service, such as shared mobility modes. In LCA, the use phase is often the focus of the studies on shared mobility, due to its considerable contribution of GHG emissions and since the fleet is not owned by the user (H. Zhang *et al.*, 2020; Pinto and Rossetti, 2020; Dang, von Arx and Frölicher, 2021). Hence, the influence of MaaS fleet technology changes on production[2] and End-of-Life (EoL) does not fully

[2] In this thesis term production is used to represent the scope of raw material, manufacturing energy, battery manufacturing and other production related processes.

capture the scope of the study from *cradle-to-grave*. With rapid fleet technology changes, these emission profiles are dynamic and depend on consumer preferences in the shared mobility modes. As the above facts suggest, it is critical to assess consumer preferences, integrated with temporal fleet technology changes, considering all phases of the product in the fleet to determine the impact on GHG emissions of the transition to car-based sharing economy modes.

1.2 Problem statement

In the standard LCA method, it is assumed that input parameters are constant or static. Therefore, it is impossible to integrate timely changes in MaaS fleet technology by employing a standard LCA method other than scenario analysis. The scenario approach utilised to model exogenic influence does not support integrating causality from consumer preferences of MaaS. Therefore, the problem statement addressed in this study is:

> To understand the GHG emissions impact of the transition from private vehicles to MaaS options on personal mobility in the context of consumer preferences and fleet technology changes.

1.3 Purpose and aim

The purpose of this investigation is to determine the life-cycle GHG emissions of the transition to car-based shared mobility from private vehicles by combining consumer preferences and changes in MaaS fleet technology. The specific aims of this study are as follows:

- **Aim 1:** Establish a methodological framework to combine consumer preferences and fleet technology changes, considering their causality and temporal effects to assess the life cycle GHG impacts of the transition to car-based sharing economy modes.

- **Aim 2:** Assess the attributes of consumer preference and the characteristics of car-based sharing economy modes.

- **Aim 3:** Determine the significance of consumer preferences and fleet technology changes on the dynamic GHG emission changes of the transition to car-based sharing economy modes over time by selecting a case study.

The scope of this thesis includes a comprehensive LCA analysis of the transition to MaaS in the United States (US) for the ride to work based on primary market survey data. By understanding the existing work, consumer decisions and temporal fleet technology influences on GHG emissions can be determined based on consumer preferences, System Dynamics (SD), and an LCA combined methodology framework. The temporal scope of this work covers the period from 2014 to 2050.

1.4 Research approach

To achieve the aims of this research, a combined methodology framework of consumer preference, SD and LCA was developed. The SD method was introduced as a modelling and simulation tool to analyse complex and dynamic problems. Dynamic problems involve quantities that change over time and involve the notion of feedback (Richardson and Pugh III, 1981, chap. 1.1). Therefore, the SD method is utilised as the interface to combine the causality of consumer preferences and time-dependent MaaS fleet technology changes into the LCA. Standard LCA methodology is commonly employed to measure the environmental impact of a product or service (ISO, 2006). SD and LCA models are integrated to assess the temporal environmental impact of sharing economy systems (Stasinopoulos, Shiwakoti and Beining, 2021). Consumer preference studies and the combined SD model approach have also been used in fleet technology studies (Jiang, 2019). The consumer behaviour integrated dynamic-life cycle assessment methodology framework is introduced to combine the consumer preference, SD and LCA methods and is employed to analyse the impact of transition to MaaS on GHG emissions by integrating the causal and temporal elements.

The integrated modelling approach is started by setting up LCA goals, objectives and scope. The SD modelling objectives are identified based on the defined LCA objectives. Preliminary SD feedback structures were then constructed. The innovation and diffusion model was adopted to demonstrate the transition to MaaS behaviour (Bass, 1969; Sterman, 2000, chap. 9.3.3). Consumer preference attributes with endogenous and exogenous foci are identified, and their data requirements are listed.

The Discrete Choice Experiment (DCE) model provides consumer choice-based market survey outcomes, which are the inputs for the combined modelling approach. The market survey sample is selected based on the selected case study, and the survey instrument is designed in four parts. The two key parts are consumer preference choice-based analyses based on a conjoint choice set (DCE) and descriptive questions to characterise the sample influence. The results highlight the importance of attributes and utility values, which are the key inputs to the SD model.

The SD model then encapsulates the interaction and feedback of consumer preferences and MaaS fleet technology changes. It depicts system changes over time and causality elements. Next, fleet behaviour is modelled based on consumer responses and system feedback. Finally, the LCA calculation model is built as an extension of fleet behaviour in the SD model. The GREET model-based Life Cycle Inventory (LCI) outcomes are employed to calculate the dynamic life-cycle impacts (Wang *et al.*, 2021). Vehicle lightweighting scenario based on the GREET model is also considered. The LCI results are combined with the SD model outcomes of fleet behaviour, consumer behaviour and other exogenous variables to derive the GHG emissions of the transition over time.

Life Cycle Impact Assessment (LCIA) scenarios are generated by selecting the high adoption of electric vehicles as an SD policy scenario. Policy scenario generation is based on the increased drive for fleet electrification by MaaS modes (Lyft, 2020; Uber, 2020) and policy instruments (The White House, 2021). Overall, the derived scenario represents GHG changes based on the possible dynamic fleet technology behaviour in MaaS and market responses.

Finally, the results are presented in two forms. The specific GHG results are presented based on the functional unit p.km (Union of Concerned Scientists, 2020b) and absolute GHG emissions expressed in tCO_2eq[3] over a year or throughout the modelling period considered (Yu *et al.*, 2017a; Jenn, 2020).

[3] t represents metric tonnes equals to 1,000kg or 1 Mega gram

1.5 Contribution of the study

This research provides new insights into which car-based sharing economy mode can be used to reduce life-cycle GHG emissions in personal mobility by combining consumer preferences and dynamic fleet technology changes. Hence, the influence of temporal powertrain types and vehicle body style on shared mobility GHG emissions is investigated. In addition, forecasted automobile improvements, such as lightweighting and increasing survivability are integrated into dynamic LCA assessments. These developments are discussed further in Section 2.4, and the utilised quantitative scenarios are listed in Table 6-3. This allows for a better understanding of how different fleet technologies and vehicle improvement elements impact the personal mobility life cycle GHG emissions of the chosen round-trip to work journey in the US.

This study introduces a novel approach by combining consumer preference, SD and LCA into a methodology framework that supports the assessment of sharing economy systems. Therefore, the feedback loop integrating consumer preferences and fleet technology elements incorporates both market causality and temporal technology influences on life-cycle emission calculations. This work generates fresh insights by considering the vehicle body style and powertrain system as attributes in the market survey and allows for the integration of consumer preferences with respect to fleet technology elements. Investigations on choosing vehicle body style as an endogenous variable demonstrated the influence of consumer preference and fleet changes on the life-cycle GHG emissions of shared mobility systems. The high-battery electric vehicle (BEV) adoption scenario results provide changes in full life cycle GHG emissions, considering the influence of policy instruments and transport network companies' commitments. As a whole, this study contributes significantly to understanding the complex interconnection between market and fleet technology through a life cycle GHG emissions assessment of shared mobility modes.

These issues are important for both current and future personal mobility alternatives. The findings of this study can be used by various parties, including shared mobility operators (e.g., transport network companies), policymakers and auto manufacturers. The outcomes of this research will facilitate interested parties in making informed decisions by providing a better understanding of the influences of consumer preferences and fleet technology changes on car-based sharing economy industry GHG emissions.

1.6 Structure of the thesis

This section provides an overview of the thesis structure.

Chapter 2 reviews developments in sharing economy modes, particularly in the shared mobility industry, consumer preferences and environmental consequences. The challenges of assessing environmental impacts by combining consumer preferences and temporal fleet changes are highlighted. This is followed by an overview of the approaches commonly used to investigate temporal systems, quantitative environmental assessments, and their combinations. The research questions identified to address the aims of this study are derived from observations in the literature.

Chapter 3 describes the methods used in this study. LCA, SD and DCE methods are identified as the analytical research tools, and the importance of the combined approach of the above techniques is explained. The chosen case study is introduced to obtain results aligned with the research questions addressed in Chapter 2.

Chapter 4 introduces the novel, systematic and structured methodology framework to combine consumer preference, SD and LCA to evaluate sharing economy systems such as MaaS. The proposed framework provides a solution to the defined research Aim 1 in Section 1.3. The LCA goals and objectives are identified to address the research aims, and the SD process steps are established to align with the LCA objectives. High BEV adoption is recognised as the SD policy scenario that also influences GHG of the transition to MaaS.

Chapter 5 presents the primary data collection process to quantify the consumer preference attributes as defined in the research Aim 2 in Section 1.3. A market survey is performed to obtain the case study-specific consumer preference data for SD modelling. The DCE-based choice-based conjoint analysis model collects consumer preferences based on the available choice combinations. Random utility method and multinomial logistics model were employed as data analysis techniques to derive the importance of attributes and utility values.

Chapters 6 and 7 present the simulation of the dynamic behaviours of the transition to MaaS, fleet changes and the derived dynamic LCA results over the modelling period established in Section 1.3 to determine the significance of consumer preferences and fleet technology changes on the dynamic GHG emission changes of the transition to car-based sharing economy modes (research Aim 3).

The main observations from the case study results and the user, fleet and GHG behaviour outcomes are discussed and concluded in Chapters 8 and 9. Recommendations for potential future research work are briefly described in Chapter 8. A discussion of the direction for future research work is presented in Chapter 9.

2 BACKGROUND AND LITERATURE REVIEW

Publication relevant to this chapter

Fernando, C., Soo, V. K., Compston, P., & Doolan, M. (Under review). The impact of car-based shared mobility on greenhouse gas emissions: A review. *Transportation Safety and Environment.*

Introduction

This chapter reviews the literature on car-based sharing economy modes, consumer characteristics, preferences, fleet behaviour and how they lead to non-conventional dynamic environmental assessments. Sections 2.1 to 2.4 provide the historical trend of car-based MaaS, consumer preferences and changes in personal mobility fleets. Thereafter, the approaches widely used to assess dynamics and environmental assessment are explored and discussed. Finally, combining those approaches and their limitations is examined to provide some background on the chosen approaches and methodologies for this study.

2.1 Evolution of sharing economy systems

Sharing economy models are becoming more widespread in the current business context as a potential solution to economic and environmental considerations (Amasawa *et al.*, 2020). The sharing economy is defined as an economic model that shares the underutilised pool of existing assets among users for monetary or non-monetary benefits without changing ownership (Botsman, 2015; Gobble, 2017). The commonly known product service system is a subset of the sharing economy modes. Some sharing economy modes, such as carsharing, have existed since the 1950s (Shaheen, Sperling and Wagner, 1998). Airbnb, Uber, Lime (e-scooter sharing), private parking space rental in city areas, and Lease A Jeans are a few known sharing economy brands and platforms in the current business. The sharing economy model is a sustainable business model connected and accepted by society (Curtis and Lehner, 2019; Curtis and Mont, 2020) and a transition platform to business model innovation (Ritter and Schanz, 2019). Today, the majority of sharing economy business models are facilitated by internet-based platforms (Gobble, 2017). The internet-based solutions, primarily the Apps, have significantly enhanced the connection of sharing economy models with their customers in both peer-to-peer and business-to-consumer markets.

Consumer behaviour in SE models differs from the traditional linear economy system. A sharing economy system provides access to products without owning them based on their functionality.

This form of access is characterised differently from the linear economy model by changing from ownership to usership (Botsman, 2015; Amasawa *et al.*, 2020), which is also significantly dependent on the context of user characteristics, social norms and influencing institutes (Retamal, 2019). Features commonly considered in conventional purchase decision-making processes, such as upfront capital investment, longevity of the product, and variable cost (maintenance and repair cost), are not the key factors in sharing economy mode decision-making. Overall, the sharing economy models remove the burden of the upfront capital investment and convert it to a variable expense through hiring/lending. This change in expenditure in SE models allows greater access to expensive high-tech products (Ajanovic, 2015; Chuah *et al.*, 2021; Carissimi and Creazza, 2022).

Technology upgrades are faster in sharing economy modes compared to the conventional ownership model (Kumar *et al.*, 2020; Si *et al.*, 2020). This trend results from diverse user expectations, like newer vehicle technologies in shared mobility (Qian and Soopramanien, 2011; Dewalska-Opitek, 2017; Hoerler *et al.*, 2020). The technology upgrades are also supported by sharing economy mode operators' service pitching and sustainability commitments (Lyft, 2020; Uber, 2020, 2021a). Therefore, consumers have more opportunities to access newer products in sharing economy modes with better technology than in traditional ownership modes. For example, the Hybrid Electric Vehicles (HEVs) composition of the Uber fleet in the US is six times higher than the country's average (Uber, 2020). The vehicle age limits enforced on ridesourcing fleets are lower than the average vehicle usage (Lu, 2006; Davis and Boundy, 2021, pp. 3–20; Uber, 2021a).

Applications in the personal mobility space are considered the fastest growing and most globally accepted among sharing economy systems (Novikova, 2017). The utilisation of shared mobility as an alternative to personal mobility has increased significantly in the last decade (US Census Bureau, 2020a). However, the use of popular carpooling as a service has been reduced (US Census Bureau, 2020a). On the other hand, the industry has also grown by introducing a few MaaS modes that provide more customised services to personal mobility requirements compared to conventional modes such as taxis. The use of ridesourcing is higher than traditional taxis in some major cities in the US (Schneider, 2021b, 2021a). In the US and Canada alone, the ridesourcing company Uber had an average of 4 billion monthly riders in 2017-2019 (Uber, 2020).

2.1.1 Car-based Mobility as a Service modes

Based on the operational characteristics, there are four car-based MaaS modes (Shaheen and Chan, 2016; Jin *et al.*, 2018). Figure 2-1 presents a customised classification of car-based MaaS modes. These modes are defined in Table 2-1 with subcategories, and the SAE International taxonomy is used in this thesis to minimise the confusion in shared mobility terms (SAE International, 2018).

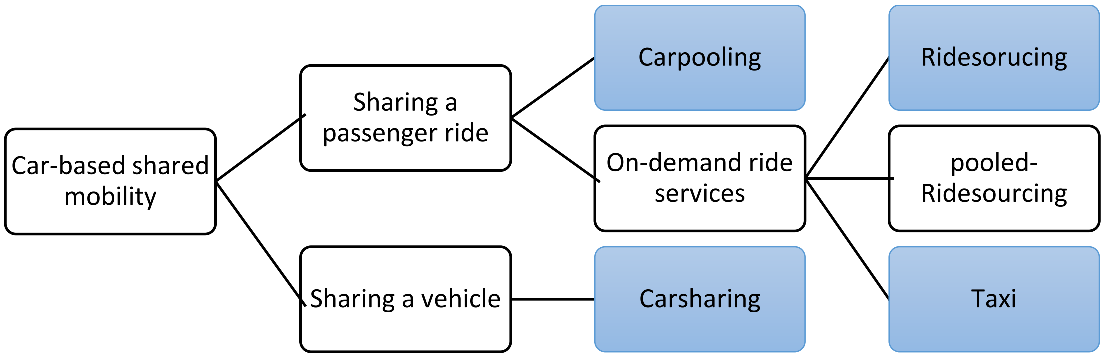

Figure 2-1 Categories of car-based MaaS modes based on ridership

Note: Adopted based on (Shaheen and Chan, 2016; Jin *et al.*, 2018), Blue boxes represent the key modes

Table 2-1 Definitions of the popular car-based MaaS modes and different terms used

MaaS Mode* (abbreviation)	Definition	Existing subcategories and *examples*
Carsharing (CS)	Carsharing offers members access to vehicles by joining an organisation that provides and maintains a fleet of cars and/or light trucks. These vehicles may be located within neighbourhoods, public transit stations, employment centres, universities, etc. (SAE International, 2018).	Regular car hire *Avis, Hertz* Two-way, station-based, two nodes (t-n) One-way, free-floating *DriveNow, Car2go* Round-trip *GoGet, Flexicar* Peer-to-peer (P2P) *Turo, SnappCar, Car Next Door*
Carpooling (CP), rideshare, ride-splitting	Ridesharing facilitates formal or informal shared rides between drivers and passengers with similar origin-destination pairings (SAE International, 2018; Shaheen and Cohen, 2019)	*GoCarma, Waze Carpool, Scoop, Carzac, Ride, LifeSocial, CoSeats; ShareURide*
Ridesourcing (RS), ride-hailing, on-demand rides	Prearranged and on-demand transportation services for compensation in which drivers and passengers connect via digital applications typically used for booking, electronic payment, and ratings. Ridesourcing services are not allowed to street hail (SAE International, 2018).	*Uber; Lift, DiDi, Shebah, GoCatch* Pooled-ridesourcing (pRS) *UberPool, LyftShare*

MaaS Mode* (abbreviation)	Definition	Existing subcategories and *examples*
Taxi, hailing	Prearranged and on-demand transportation services for compensation through a negotiated price, zone pricing, or taximeter (either traditional or GPS-based) (SAE International, 2018).	*Yellow taxis, Black cabs*

Note: *term used in this paper is underlined

The consumer characteristics of car-based MaaS also differ from those of conventional product-based private vehicle ownership. These are further discussed in Section 2.2.

2.2 Consumer characteristics of MaaS

Unlike private vehicle ownership, consumer decision-making in shared mobility modes does not focus on product acquisition but on its service functionality for the journey. Hence, consumer preferences for shared mobility modes differ from those for conventional vehicle ownership. Namazu and Dowlatabadi (2015) found that the average age of the sharing mobility fleet is a key factor for consumers. Conventional consumer preference attributes such as the capital investment of a vehicle in the linear economy are not part of the decision-making process in the transition to shared mobility; instead, it is the journey fare (Tirachini and del Río, 2019; Vij *et al.*, 2020). Hence, this change in expenditure in shared mobility modes enables greater access to expensive, high-tech products (Ajanovic, 2015). In summary, consumer preferences for MaaS differ from those for private vehicle ownership.

The recent COVID-19 global pandemic has impacted the car-based MaaS business differently within different modes. The pandemic has reduced overall personal mobility, and ‘driving alone’ has picked up much faster than public transit (Shokouhyar *et al.*, 2021). COVID-19 has created a ‘relatively risky’ perception in car-based shared mobility modes compared with private vehicle use (Rahimi *et al.*, 2021, sec. 3). Studies have also found that consumers expect extra measures, such as avoiding crowding and increased cleanliness to continue with or join MaaS modes (Awad-Núñez *et al.*, 2021). Their findings align with those of Garaus and Garaus (2021) on the least negative perception of carsharing compared to modes such as ridesourcing and carpooling. Ridesourcing modes, such as Uber, have shown a slower recovery compared to the other modes (Wang *et al.*, 2022). The above facts suggest a comparison of consumer characteristics is not sensible in the

COVID-19 recovery era until mobility and user perception stability are reached. This fact must be considered in consumer preference studies on shared mobility modes.

Consumers' socioeconomic and demographic profiles also impact the transition decision to MaaS as part of their choice of transport mode (Prieto, Baltas and Stan, 2017; Davlembayeva, Papagiannidis and Alamanos, 2019; Flores and Jansson, 2021). Pooled-ridesourcing is more widely accepted by the young (<30 yrs) and lower-income (<$[4]50,000/household per annum) consumer population (Sarriera *et al.*, 2017), while higher household income consumers use more transport network company trips (Schaller, 2018). Clewlow and Mishra (2017) and Schaller (2018) found that ridesourcing was more dominant among college-educated individuals than among the general population. The above outcomes imply a strong relationship between socioeconomic, demographic and educational attainment levels and consumer preferences for car-based MaaS modes. In summary, the above factors must be considered in the consumer preference studies of car-based MaaS assessments.

Most studies on car-based mobility have been conducted in cities and metro areas. Many were from North America and larger European cities (Dumas and Dobson, 1979; Carroll, Caulfield and Ahern, 2017; Lavieri and Bhat, 2019; Alonso-González *et al.*, 2020). Studies have also shown that the population density of the user location impacts the MaaS mode usage (Firnkorn and Müller, 2011; Vasconcelos *et al.*, 2017), supported by the household vehicle availability, which also varies based on the living location (McGuckin and Fucci, 2018, p. 65). Case studies from the locations such as Malaysia and Australia have also shown similar findings (Zulhelmi *et al.*, 2018; Vij *et al.*, 2020). Previous studies have found that MaaS mode selection correlates with the public transport level of the location and varies considerably across cities (Shaheen and Chan, 2016; US Census Bureau, 2019b; Yan, Levine and Zhao, 2019). In summary, resident location and public transit status are significant factors for understanding consumer behaviour in car-based MaaS modes in different journey types.

The journey type substantially influences user characteristics. The average daily trip rates in US households are 0.59 and 1.3 person trips per day for the round-trip to work and shopping cum errands, respectively (McGuckin and Fucci, 2018, p. 41). However, *sharing* modes are more prevalent in the journey type 'usual commute to work' in the largest household community survey in the USA (McGuckin and Fucci, 2018, p. 78). While the carpooling mode is extensively used on

[4] $ represents the USD values.

to/from work journeys (Ben-Akiva and Atherton, 1977; Nurul Habib, Tian and Zaman, 2011; Malodia and Singla, 2016; US Census Bureau, 2020a), ridesourcing is generally used for social and recreational journeys (Rayle *et al.*, 2014; Henao, 2017; Alemi *et al.*, 2018). Overall, the journey type significantly influences the utilised car-based MaaS mode and is an important factor to consider in consumer preference studies.

MaaS consumers have salient user characteristics compared to private vehicle ownership and are highly dependent on socioeconomic, demographic and living location based on public transit facilities and journey type. Overall, identifying consumer preference attributes is critical for understanding the transition to MaaS. These attributes are explored in Section 2.3.

2.3 Consumer preference attributes of MaaS mode selection

A literature review was performed to understand the consumer preference attributes of car-based MaaS. Three MaaS modes—carpooling, solo-ridesourcing, and pooled-ridesourcing—were chosen to represent the high- and low-occupancy modes. The review was limited to data collected before early 2020 to exclude COVID-19 implications on MaaS modes, as discussed in Section 2.2. The findings are presented in Figure 2-2 and further discussed below.

The literature highlights the significance of cost and journey time as the most important attributes in selecting mobility modes. Figure 2-2 shows the influence of cost and time recognised by the users of all three MaaS modes (Palma and Rochat, 2000; Henao, 2017; Sarriera *et al.*, 2017; Amirkiaee and Evangelopoulos, 2018; Alonso-González *et al.*, 2020; Lippke and Noyce, 2020). Novikova (2017) also found that the importance of time (total duration to accomplish the trip), cost of the journey, and perceived convenience are crucial in selecting a mobility solution based on their interviews. The above findings indicate that cost, time (door-to-door), and convenience are the key consumer preference attributes in car-based MaaS modes.

However, the results in Figure 2-2 highlight that convenience is a mode-dependent attribute rather than a generic one. Individual attributes such as interaction comfort (Carrese *et al.*, 2017; Cui *et al.*, 2020), privacy concerns (Lavieri and Bhat, 2019; Lippke and Noyce, 2020), extra distance and trip distance (Hunt and McMillan, 1997) affect the number of passengers (measured in occupancy rate) in a MaaS-mode ride. The transition to higher occupancy modes, such as carpooling and pooled-ridesourcing, presents more challenges than lower occupancy modes (for example, ridesourcing) based on the above findings. Hence, considering the number of passengers and relevant convenience fleet characteristics, such as vehicle body style (representing the size of the vehicle), is significant in the transition to MaaS consumer decision-making. This selection also distinguishes preference studies using high- or low-occupancy-based MaaS modes. However, in past studies, the vehicle body style was not identified as a specific attribute.

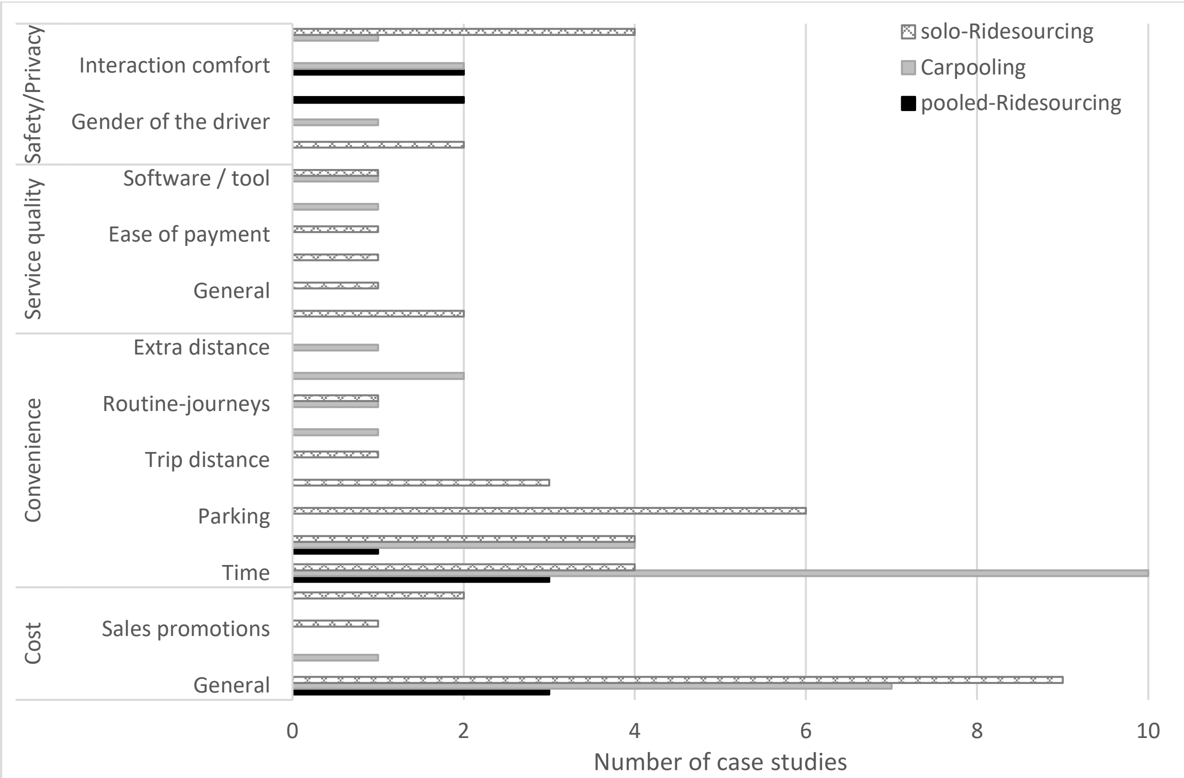

Figure 2-2 Graphical summary of the literature review on the influence of consumer preference attributes in the selection of MaaS modes

Note: search criteria: before 1st quarter 2020, to avoid COVID-19 implications

Past studies have highlighted the use of the stated preference-based conjoint analysis technique to analyse consumer preferences in MaaS modes (Hildebrandt *et al.*, 2015; König, Bonus and Grippenkoven, 2018; An *et al.*, 2021). This method has also been utilised to analyse consumer preferences for fleet electrification (Jenn, Laberteaux and Clewlow, 2018; Jiang, 2019; Qian, Grisolía and Soopramanien, 2019). Cohen (1997) states, "the best features of discrete choice models and conjoint analysis are married in choice-based conjoint analysis". The choice-based conjoint analysis mode facilitates the comparison of brands (alternatives) and aligns with the DCE model. It is commonly utilised in mobility-related consumer preference studies (Cohen, 1997; Bierlaire, 1998; El Zarwi, Vij and Walker, 2017). Previous studies have collectively chosen the

Multinomial Logit Model (MNL) with the choice-based conjoint analysis technique to quantify stated preference analysis (Qian, Grisolía and Soopramanien, 2019; Berneiser *et al.*, 2021).

The literature highlights the significance of trip purpose in selecting car-based MaaS modes. Most carpooling studies have targeted work journeys. At the same time, the two ridesourcing options are often used in social and recreational trips and are underrepresented in other types of journeys. The journey type (trip purpose) and detailed analysis with the list of sources utilised are presented in Table B-1 to Table B-3 in Appendix B.

2.3.1 MaaS user preference in fleet technology elements

Car-based MaaS consumers have shown interest in fleet technological features (Spurlock *et al.*, 2019). Studies have found a higher consumer preference for BEVs in ridesourcing (Jenn, Laberteaux and Clewlow, 2018) and e-car pooling (Galatoulas *et al.*, 2017). Hence, car-based MaaS users are influenced by fleet technology elements, particularly the powertrain types, similar to private vehicle users (Qian and Soopramanien, 2011). Therefore, the powertrain type can be considered a MaaS consumer attribute based on rapid fleet electrification (Lyft, 2020; Uber, 2020).

The vehicle body type can also be considered a factor affecting the occupancy rate, which influences journey comfort. No study has been undertaken to understand vehicle body style as an attribute, although the light-duty vehicle fleet has been shifting from sedans to SUVs aggressively (Cozzi and Apostolos, 2021). It is also a choice provided by MaaS-mode apps for consumers to decide on fleet options (see Figure 1-1). In summary, considering vehicle body style as an attribute in a consumer preference study can generate more realistic results similar to previously identified conventional user attributes (see Section 2.3).

MaaS consumer preference outcomes have shown the importance of fleet technology attributes, such as powertrain type and body style, apart from the typical cost of the journey, total time taken to accomplish a trip, and passenger convenience factors, such as the number of passengers. Section 2.4 explores changes in fleet technology.

2.4 Technology changes in personal mobility fleets

The light-duty vehicle segment, primarily used in personal mobility fleets, has undergone many technological changes (U.S. Energy Information Administration - EIA, 2016, 2021; Davis and Boundy, 2021). Fleet electrification, shift to SUVs from most sedans, and overall lightweighting trends are the most significant related to the life-cycle GHG emissions of light-duty vehicles. Consumers react differently to these changes, such as fleet electrification (Kudoh and Motose, 2010; Liao, Molin and van Wee, 2017). The willingness to pay for these fleet technology changes is also heterogenic (Qian and Soopramanien, 2015). As a whole, these changes influence the consumers' value-action gap, the 'discrepancy' between stated attitudes, preferences, and behaviour (Kollmuss and Agyeman, 2002; Young *et al.*, 2010). Subsequently, they impact the relevant GHG emissions (Guyon, 2017; California Air Resource Board, 2019; Maciel Fuentes and González, 2021; Akimoto, Sano and Oda, 2022). These technological changes are discussed in Sections 2.4.1 to 2.4.3.

2.4.1 Fleet powertrain systems changes

The transition from Internal Combustion Engine Vehicles (ICEVs) to BEVs has significantly increased in recent years. The global electric vehicle market share for passenger light-duty reached almost 10 million by 2020, starting from nearly zero in 2010 (International Energy Agency (IEA), 2021b). This same study also highlighted that passenger light-duty vehicles mainly utilised in personal mobility represent the highest uptake, from 1.2 million in 2015 to 10.2 million in 2020. Fleet electrification significantly depends on the government's policy support (Qian, Grisolía and Soopramanien, 2019; The White House, 2021). More than 34 countries have set up policies to ban new registrations of ICEVs in the future (Cozzi and Apostolos, 2021). Automakers like Ford have committed to phasing out ICEV production lines in the future (Neate, 2021). Studies have shown that consumer preferences for BEV usage are different for many reasons, including the policy and awareness of BEVs (Kudoh and Motose, 2010; Wang, Tang and Pan, 2018). Technology aspects, such as range anxiety and financial attributes, such as purchase and operating costs, also influence consumer acceptance of BEVs (Liao, Molin and van Wee, 2017; Jiang, 2019). Also, MaaS consumer acceptance of fleet electrification differs from that of private vehicle fleets (Hoerler *et al.*, 2020).

Shared mobility operators have adopted powertrain types, such as HEVs and BEVs in their fleets. Uber has more than a five-fold higher HEV fleet composition than in private fleet (Uber, 2020).

Transport network companies also lead their fleet electrification goals to comply with state policies and demonstrate environmental sustainability commitments. Two large ridesourcing companies, Uber and Lyft, have pledged to achieve a 100% EV fleet by 2040 and 2030, respectively, compared to the US president's executive order on 50% sales share of BEVs by 2030 (Lyft, 2020; Uber, 2020; The White House, 2021). These company-based decisions are also supported by local initiatives such as zero-emission zones and fiscal support schemes like tax benefits on BEVs (Wolf *et al.*, 2015). As a whole, the above findings suggest that powertrain types and their temporal changes are significant in car-based MaaS GHG emission assessments.

2.4.2 Fleet changes in the vehicle body styles

The transition from a sedan body style to SUVs is widespread among personal mobility users. SUVs' global share has increased from 16.5% in 2010 to 45.9% in 2021 (Cozzi and Apostolos, 2021). In the last few decades, the transition to the SUV body type in the US auto market has aligned with global trends (US EPA, 2021), increased from 6.9% in 1995 to 23.7% in 2017 in the US household-based vehicle distribution, representing 34% of SUV fleets less than two-year-old SUV fleet (McGuckin and Fucci, 2018, p. 66, 2018, fig. 12). The shift to SUVs has also been represented in commercial and state fleets (Davis and Boundy, 2021, sec. 8). SUVs are often used as multipurpose vehicles, although they are branded as *sports utility*. The average occupancy of SUVs (1.70 to 1.90) is higher than that of sedans (1.54 to 1.59) (McGuckin and Fucci, 2018; Davis and Boundy, 2021, fig. 9.1). Overall, SUV fleets support a higher occupancy of both private vehicles and MaaS modes.

SUV adoption is higher in MaaS modes, such as ridesourcing, and is influenced by the higher SUV dominance private vehicle fleet in the US (US EPA, 2021, p. 15). The use of SUVs in pooled-ridesourcing is demanded by the nature of the mode to cater to many passengers compared to solo-ridesourcing. Transport network companies demand larger vehicles for pooled-ridesourcing than for solo-ridesourcing (Uber, 2021a). For example, driving partners with only six passenger-seated vehicles can join UberXL and Uber Black SUV service categories (Uber, 2021a). They can earn more if their vehicles are larger (Uber, 2021b). These factors passively influence to use of more SUVs and larger vehicles in transport network company fleets to earn more.

Studies have shown that larger body style vehicles emit more life-cycle GHG than medium-sized vehicles. The model year 2019 Car SUVs[5] have a 15% higher production-weighted annual carbon footprint (well-to-wheel[6]) than a sedan car that emits 5.4 tCO_2/year (Davis and Boundy, 2021, pp. 12–16). Although SUVs have shown a 1.9% well-to-wheel carbon footprint reduction from 2009 to 2019 (Davis and Boundy, 2021, pp. 12–16), the shift to SUVs increased annual CO_2 emissions by 120 million tonnes (Cozzi and Apostolos, 2021). These findings confirm that BEV GHG benefits are offset by the growth in sales of SUVs (Heubl, 2020).

Hence, the vehicle body style composition changes significantly influence GHG changes in personal fleets, and its consideration is critical based on the set research aim. In addition, the SUV models that started with bulky LandCruisers, Patrols and Pajeros have shifted to mid-size and lighter SUVs, such as Hyundai Tucson and Mazda CX series (Corby, 2018). The vehicle lightweighting changes are explored in Section 2.4.3.

2.4.3 Car technology changes – lightweighting

Vehicle lightweighting is a conventional approach used by auto manufacturers to increase the energy economy and reduce GHG emissions (Elgowainy *et al.*, 2016; Kim and Wallington, 2016; Wang *et al.*, 2021). The latest GREET model has shown an estimated 16% and 20% weight reduction in petrol-driven and BEV sedans, respectively and 15% and 19% for SUVs in future vehicle models (Wang *et al.*, 2021). This observation does not align with the US EPA (2021, pp. 19–20) records based on the increasing trend of vehicle weight during the last two decades. However, automakers significantly increase research and development and rely on lightweighting as a critical element to achieve the Corporate Automobile Fuel Economy (CAFE) Standards (U.S. Department of Transportation, 2014; WardsAuto, 2014). Lightweighting improves the energy efficiency of vehicles through various pathways. In addition to the overall weight reduction, the resized powertrain further enhances energy efficiency improvements (Kim and Wallington, 2016). However, no studies have explored the impact of automobile lightweighting on car-based MaaS

[5] Often SUVs are categorised under light truck vehicle class (Davis and Boundy, 2021). However, under Corporate Average Fuel Economy (CAFE) methodology, "two-wheel and all-wheel drive sport utility vehicles that are under 2,721kg gross vehicle weight and have off road capabilities will be held to the same standards as cars" (Davis and Boundy, 2021, pp. 4–13).

[6] Tailpipe emissions plus emissions associated with upstream fuel/energy production i(ncluding refinery) and distribution

fleets. Therefore, analysing the influence of vehicle lightweighting on personal mobility GHG emissions calculation is considered in this study.

While achieving an overall GHG reduction, vehicle lightweighting influences GHG emissions differently in the life-cycle phases (Wang *et al.*, 2021). Wang et al. (2021) determined that production impacts are higher in lightweight vehicle body scenarios. This change is mainly due to changes in material composition during the vehicle lightweighting process. Soo et al. (2015) suggest that lightweighting used multi material vehicle design is a short-term solution with the long-term effect of increasing waste. The complexity of EoL impacts increases with the higher utilisation of composite materials (Yang *et al.*, 2012) and the recycling of batteries used in BEVs (Boyden, Soo and Doolan, 2016). In summary, a complete life-cycle GHG assessment scope is crucial when considering vehicle lightweighting.

Further, newer SUVs (manufacturing years 2022-2026) are expected to have increased survival rates compared to previous manufacturing eras (Lu, 2006, p. 8; Davis and Boundy, 2021, pp. 3–20). The increased survival rates have been demonstrated by the increased average age of vehicles (European Environment Agency (EEA), 2018; U.S. Department of Transportation, 2018; Federal Highway Administration (FHWA), 2019). Davis and Boundy (2021, pp. 3–19) have shown an increase of 3.5 years of the average vehicle age for US light vehicles from 8.4 years in 1994 to 2019. While relatively cheaper cars can be manufactured with relatively lower survival rates, the dominant car players have increased the survival rates, which can also be observed with their increased lifetime distances (iSeeCars, 2022).

Fleet technologies in personal mobility fleets have shown significant changes, and their influence on GHG emissions has changed equally. The adoption of electrification and more SUVs is higher in MaaS modes, and their effects on GHG emission changes have not been collectively assessed. In summary, integrating temporal fleet technology changes into GHG assessments of the transition to MaaS is critical.

2.5 Utilising system dynamics technique in car-based MaaS

The system dynamics method has been used to investigate temporal variables and their causal interaction in car-based sharing economy modes (Geum, Lee and Park, 2014; Wang *et al.*, 2018; Wasserbaur *et al.*, 2020). This method has also been employed as the temporal analysis technique for assessing the environmental impacts of car-based shared mobility (Luna *et al.*, 2020; Stasinopoulos, Shiwakoti and Beining, 2021) and shared-micro mobility (Astegiano, Fermi and Martino, 2019). The most pivotal element of the SD model is its ability to connect causality to the system (Meadows, 2008). It provides the ability to integrate market dynamics without holding to exogenous characteristics (Geum et al., 2014) and combines consumer preferences into the modelling system (Wang, Lai and Chang, 2016; Jiang, 2019). Overall, the SD technique can be used to analyse the sharing economy case studies, integrating consumer preferences and fleet technologies to determine GHG emission outcomes by incorporating the temporal and relevant causality elements.

A few common modes of behaviour in SD, such as exponential growth, S-shaped growth, goal-seeking and growth and overshoot, are used to explain the system (Sterman, 2000, sec. 4.1). The selection of the mode of behaviour depends on the investigating system and its behavioural characteristics. The Bass diffusion model (Bass, 1969) is explored based on its applicability, considering the behaviour of car-based MaaS modes and their maturing market stages.

2.5.1 The Bass diffusion model

The Bass diffusion model is commonly used in product and product innovation-based SD analyses (see Figure 2-3). The model depicts the behaviour of the early stages of innovation. Many car-based MaaS modes remain in the innovation phase. The Bass model is adopted to explain the one-way carsharing case study (C. Zhang *et al.*, 2020) and explore Product Service System approaches, a subset of sharing economy systems (Franco, 2019). The Bass model can be employed to analyse car-based sharing economy modes' behaviour by integrating relevant temporal and causal variables.

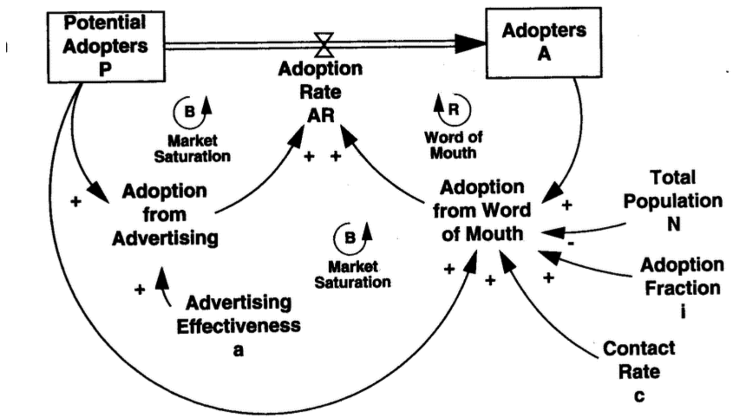

Figure 2-3 The Bass diffusion model: the adoption relationship of innovators and imitators

Source: Business Dynamics Systems Thinking and Modeling for a Complex World, John D. Sterman (2000), Commercial Electronic and Print Use, copyright © McGraw Hill, reprinted by permission of McGraw Hill (CHA887761455-1), https://www.mheducation.com/permissions.html

The Bass model divides adopters into two sets: innovators and imitators (Sterman, 2000, sec. 9.3.3). These two sets of adopters are represented by two key feedback loops. In Figure 2-3, positive feedback (R) represents adoption from Word-of-Mouth (WoM). The WoM loop represents the adopter-group, imitators. Higgins et al. (2012) have defined the imitators as "influenced in the timing of adoption by the pressures of the social system". The other set of adopters, innovators, choose to accept innovation, irrespective of the decisions of other individuals in the system. They are represented by negative feedback (B) in Figure 2-3 due to market saturation based on external sources of awareness and adoption. The latter is usually interpreted as the effect of advertising (Sterman, 2000, sec. 9.3.3). With reference to the model, the introduced innovation or new product adopters initially depend on external information, such as advertising. The advertising contribution to the system drops with the decline of potential adopters and the growth of the adopted population. This behaviour results in reinforcement of the WoM loop. The mathematical expression of the Bass model can be found in Equation (6-1) in Section 6.1.1.

The Bass model behaviour is suitable for explaining car-based MaaS modes behaviour during their start-up time and ongoing market maturity. In summary, the Bass model can be employed to provide a better interpretation of the transition to/adopting car-based MaaS models (C. Zhang *et al.*, 2020), integrating technology-based attributes (Higgins *et al.*, 2012) and causality into the system.

2.5.2 Consideration of causality

Consumer preference attributes can add causality to MaaS user behaviour models by combining consumer preferences and Bass model-based systems. Geum et al. (2014) integrated causal relationships into their SD model based on fuel consumption, traffic congestion and total profit variables. Luna et al. (2020) chose the 'working-age population' as the causality-connecting variable in assessing the transition from ICEVs to BEVs. Stasinopoulos et al. (2021) and H. Wang et al. (2018) adopted a similar approach by integrating causality in their MaaS-based research. A feedback system that incorporates causality is unique to each study. However, no research has incorporated primary data into car-based MaaS SD modelling based on consumer preference results. Taken together, incorporating consumer preference data to integrate casual feedback is identified as a research gap in car-based sharing economy models.

The product attractiveness concept introduced by Schmidt and Gary (2002) provides an approach for incorporating consumer preference attributes into SD models. They define product attractiveness as "the additive utility of each product attribute". According to this definition, consumer preference attributes can be combined into feedback loops by employing the utility values of attribute and attribute distributions. The utility functions were operationalised to the SD model combining product attractiveness (Schmidt and Gary, 2002, fig. 6). These steps are part of the dynamic problem formulation and hypothesising steps (Sterman, 2000, sec. 3.5.2) to understand the endogenous and exogenous explanations of the variables resulting from the SD model structure. The product attractiveness approach can be customised and utilised to incorporate attributes significant to GHG emission changes, fleet electrification and higher SUV body style (Section 2.4) into car-based MaaS SD models.

The SD technique is utilised, and the Bass model is adopted to incorporate temporal and causal changes into the GHG impacts of car-based MaaS modes. The product attractiveness approach connects consumer preference attributes to the SD model by linking causality. The studies carried out to determine the life cycle GHG emissions of MaaS are explored in Section 2.6.

2.6 Environmental life-cycle assessments of car-based MaaS

Studies on car-based MaaS mode GHG emission assessments have yielded a range of outcomes. GHG emission results have differed due to the selection of the scope of the emission assessment

(Ding *et al.*, 2019), the research intent (Briceno *et al.*, 2005; Caulfield, 2009; Carranza *et al.*, 2016; Wu *et al.*, 2018), and considering different powertrain systems, such as electrification (Kim, Ko and Park, 2015; Jung and Koo, 2018; Jenn, 2020). Furthermore, the assessment methodology ranges from simple carbon factor-based analysis (Ryden and Morin, 2005; Te and Lianghua, 2020) to complete LCAs beyond mid-point analysis (Vedrenne *et al.*, 2014; Shi *et al.*, 2016a; Cai *et al.*, 2019; Shinde, Dikshit and Singh, 2019; Sun and Ertz, 2021). Overall, multiple variables influence the GHG emission assessment results of MaaS modes, and comparing the study outcomes is not straightforward.

The use of multiple functional units in the car-based MaaS assessments also significantly influences the interpretation of the results. The traditional product-based functional units are unsuitable for assessing sharing economy systems such as MaaS as they differ from the ownership-driven system. The functional units of the SE models have to represent the exact functionality of the use of the service. Studies that chose occupancy-based functional units, such as passenger kilometres (p.kms) have shown adverse GHG impacts by employing certain MaaS modes (Union of Concerned Scientists, 2020b, 2020b). In contrast, studies using distance-based units have shown lower GHG emissions in MaaS than in private vehicle fleets (Myers and Cairns, 2009; Loose, 2010; Vasconcelos *et al.*, 2017; Jenn, 2020). However, Goedkoop et al. (1999) have highlighted the importance of using a wider definition, such as the actual monthly transport activities of two persons. The recent studies on shared mobility have widely used occupancy-integrated functional units such as p.km to interpret the LCA outcomes of car-based MaaS modes, which can also be utilised to compare private and sharing mobility modes (Ertz, Durif and Arcand, 2016; California Air Resource Board, 2019; Aamas and Andrew, 2020; Amatuni *et al.*, 2020; Union of Concerned Scientists, 2020b; Dang, von Arx and Frölicher, 2021).

A comprehensive literature review was conducted to explore the quantitative GHG emissions of car-based MaaS modes and the factors affecting them. The outcomes of a quantitative literature review provide the factors and elements that must be considered in the GHG emission assessment phase. It also prioritises them to avoid complexities in the assessment process.

The Systematic Quantitative Literature Review (SQLR) method (Pickering and Byrne, 2014) was employed to perform this review. The SQLR method has been adopted for specific engineering applications and quantitative sustainability assessments (Lim, Antony and Albliwi, 2014; McAnulty, Jeswiet and Doolan, 2017; Tarne, Traverso and Finkbeiner, 2017). The SQLR method comprises 15 steps (Pickering and Byrne, 2014). Step 2, the research question, is defined as:

'What GHG impact outcomes are implied by the research into car-based shared mobility modes?'

A list of the keywords employed in the literature search is presented in Table 2-2. This is the third step in the SQLR method. The search was extended to similar terms used in different geographical locations and a combination of both terms for MaaS modes and assessment types. Scopus, Science Direct, Google Scholar and ProQuest were used as search databases based on previous literature review experience, aligned with the fourth step in the SQLR method.

Table 2-2 Keywords used in the SQLR search

Assessment types	Terms used for car-based MaaS modes
Greenhouse gas, GHG, Carbon footprint Life cycle assessment, LCA Global warming potential, GWP, global warming impacts	Taxi, hail, hailing Carpooling, carpool, ridesharing, slugging, ridesharing Carshare, carsharing, car-share, car-sharing Ridesourcing, ride-hail, ride-hailing, pooled-ride-hailing, pooled-ridesourcing, on-demand mobility

Note: GWP – global warming potential

A set of 121 publications with 214 case studies was shortlisted based on SQLR. The selection covers 20 years of work from 2001 to 2021 inclusive. The detailed results are listed for 15 fields (see Table A-1 in Appendix A). The results were categorised based on the four prominent car-based MaaS types: carsharing, ridesourcing, carpooling and taxi. Appendix A shows an analysis of the shortlisted sources based on research location, type of source and publication year.

The GHG emissions results are interpreted compared to private vehicle use to avoid any influencing variables and to compare the results. The shortlisted results for carpooling and ridesourcing are presented in Section 2.6.1. These modes were chosen based on the range of occupancy rates. The assessment scope with different powertrain systems and employed functional units is also explored in Section 2.6.1. Section 2.6.2 investigates the external indirect factors that influence the GHG emission results of car-based MaaS.

2.6.1 Influence of life cycle scope and powertrain type

<u>Carpooling case studies</u>

Unsurprisingly, all shortlisted carpooling-based studies have shown lower GHG emissions than private vehicle use (see Figure 2-4).

ICEVs represent the largest powertrain fraction (80%) in the carpool SQLR collection, and the results determine the overall skewed mean as -26% to -50% GHG change. Nurhadi et al. (2017) found a 50% to 70% GHG reduction in their study with an extended scope of production and EoL treatment of BEV batteries. The rest of the BEV studies have shown a GHG decrease of 27% to 75%, 85% and 21% (Ding *et al.*, 2019; Aamas and Andrew, 2020). These findings highlight the importance of scope and powertrain types in comparing the GHG emission outcomes of personal mobility modes.

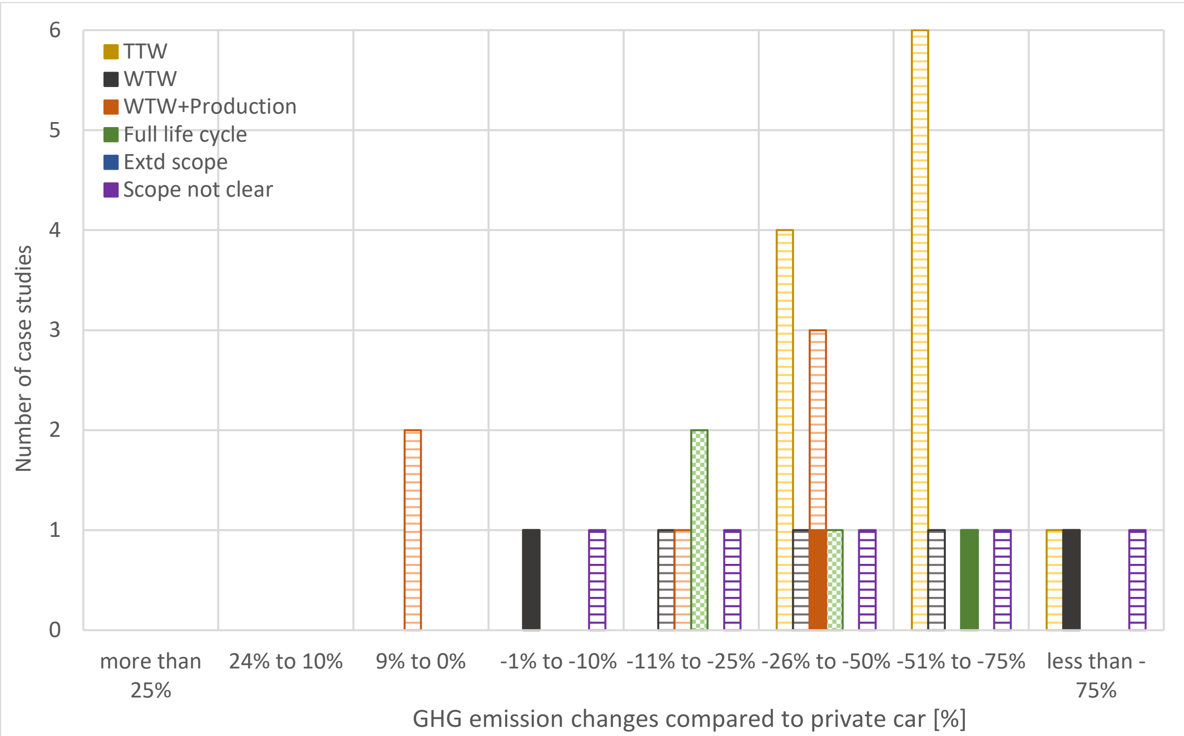

Figure 2-4 Case studies collection of Carpooling: GHG emission changes compared to private car use based on powertrain system

Note: solid fill – BEVs, pattern fill- ICEVs, dotted fill-mix fleet of ICEVs and BEVs. WTW – well-to-wheel, TTW-tank-to-wheel, The complete SQLR outcome can be found in Table A-5 and Table A-6 of Appendix A.

Ridesourcing case studies

The ridesourcing mode is the smallest in the SQLR collection because it is the most recently introduced car-based MaaS mode (see Figure 2-5). The collection has three case studies investigating BEVs, with six on ICEVs and two on mixed fleets.

Nine of the twelve shortlisted sources have shown a GHG reduction compared to private vehicles supported by two peer review sources (H. Zhang *et al.*, 2020; Jenn, 2020) (see Figure 2-5). On the other hand, the Union of Concerned Scientists (2020b) showed a 47% GHG increase compared to the private vehicle fleet but a 53% and 68% reduction when using BEVs solo-resourcing and BEV pooled-ridesourcing, respectively. These findings highlight the importance of electrification and ride-splitting to achieve a lower GHG emission profile in ridesourcing mode, which also aligns with the commitments of transport network companies (Lyft, 2020; Uber, 2020). The SQLR results for carsharing and taxis can be found in Figure A-1 and Figure A-2 in Appendix A.

A diverse set of functional units are employed in the LCA/GHG assessment of car-based MaaS. The distance-based units dominate in the SQLR collections, while passenger and distance-integrated units such as p.km record the second highest (see Figure A-3 in Appendix A.). Distance-based functional units are often used to compare different powertrain types and alternative fuel vehicles (Qian and Li, 2014; Teixeira and Sodré, 2016; Nilrit, Sampanpanish and Bualert, 2018). However, only the occupancy (passenger) and distance combined functional unit can incorporate the net occupancy and avoid non-productive distances, such as deadheading, pick-up, and relocation. Komanduri et al. (2018) have highlighted the 37% of vehicle kilometres (v.kms) spent deadheading in Ride Austin, a local non-profit-based ridesourcing service, while Uber and Lyft drivers spent an additional 69% v.km in deadheading (Henao, 2017). Henao and Marshall, 2018 have found that the average of 1.4 passengers per ride (occupancy rate) decreases to 1.3 when the distance is weighted and 0.8 when accounting for deadheading. In summary, the integration of net-occupancy in the functional unit calculation of p.km increases the accuracy of the interpretation of GHG emission results in MaaS modes (Henao, 2017; Union of Concerned Scientists, 2020b).

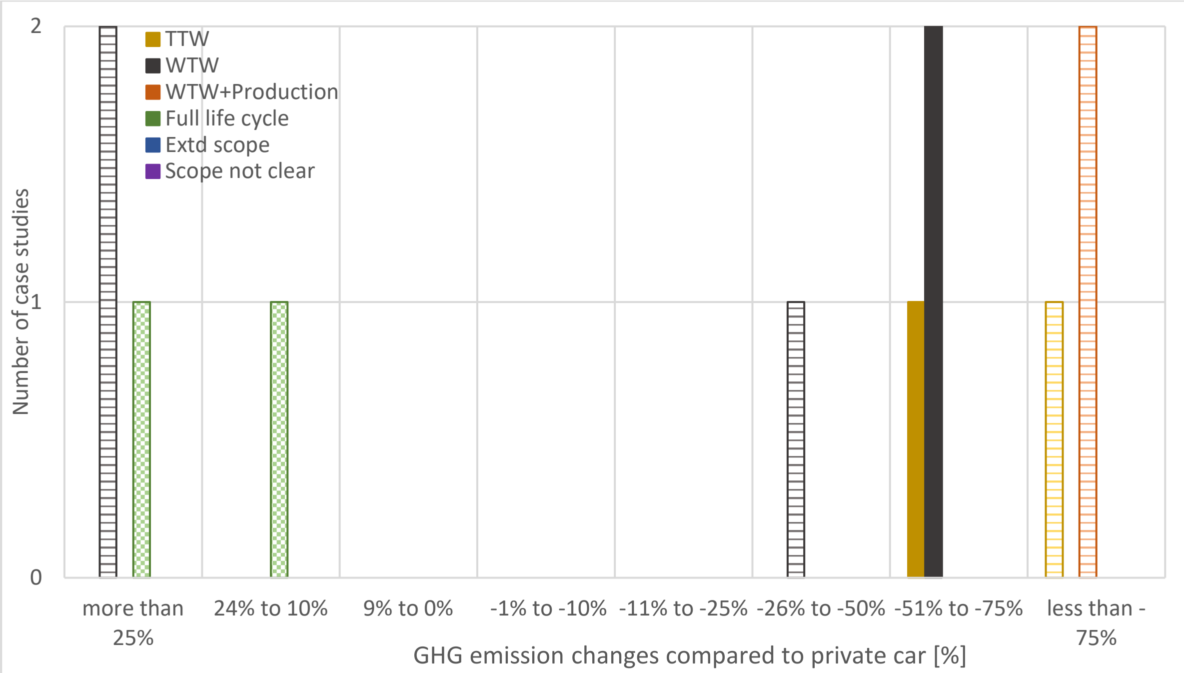

Figure 2-5 Case studies collection of ridesourcing: GHG emission changes compared to private car use based on powertrain system

Note: solid fill – BEVs, pattern fill- ICEVs, dotted fill-mix fleet of ICEVs and BEVs. WTW – well-to-wheel, TTW-tank-to-wheel, The complete SQLR outcome is presented in Table A-4 in Appendix A.

Goedkoop et al. (1999, p. 42) have highlighted the importance of using a wider definition beyond p.km, such as the actual monthly transport activities of two people. Their study further elaborated on the importance of equal levels of user satisfaction in these modes to use a wider definition. Hence, the level of satisfaction differs between car-based MaaS modes, and this approach does not suit for evaluating car-based MaaS modes. Also, to compare the transition between car-based personal mobility modes, a functional unit that can distinguish the effect of occupancy rate is essential, and p.km serves that purpose. It also provides a practical approach to communicating and interpreting results with fewer assumptions compared to wider definitions, such as transport during a month. Therefore, the above findings highlight the importance of employing net occupancy-based functional units, such as p.km, instead of conventional product-based units (e.g., per car, v.km) to interpret the LCA/GHG emissions results of the car-based sharing economy modes. This p.km-based GHG interpretation is aligned with several other studies (Mccarthy, 2017; Union of Concerned Scientists, 2020b; Arbeláez Vélez and Plepys, 2021; Berjisian, 2021; Dang, von Arx and Frölicher, 2021; Sun and Ertz, 2021). Furthermore, the selection above supports an effective comparison with other personal mobility modes.

The overall outcomes of the SQLR findings suggest that car-based MaaS modes reduce GHG emissions and are further supported by fleet electrification. The interpretation of GHG results has also varied vastly due to the differences in selected assessment methods, life cycle scope, functional units, and research intentions. Hence, defining the scope by considering the total life cycle (cradle-to-grave) is a more meaningful and unbiased approach for assessing GHG emission changes in sharing mobility modes. These conclusions are further aligned with Nordelöf et al. (2014), which conclude the importance of a comprehensive and clear goal, and scope while environmentally evaluating different powertrain options of MaaS fleets. The most prominent finding from the systematic review is that there is no solid quantitative signal of the change in GHG results compared to private vehicles in car-based MaaS modes. The above findings indicate that fleet changes, such as electrification, are influential in assessing the GHG emission changes of the transition to car-based MaaS from private vehicle use.

2.6.2 Influence of electricity grid factor on car-based MaaS GHG

The electricity grid GHG factor has become a significant external influencer in personal mobility fleets in the context of increasing the BEV composition in light-duty passenger vehicles (Girard *et al.*, 2019; International Energy Agency (IEA), 2021b) (see Section 2.4.1). In 2014, the US electricity grid GHG factor was 519 gCO_2eq/kWH. It is expected to decrease to 246 gCO_2eq/kWh by 2050, representing the baseline modelling scenario (U.S. Energy Information Administration - EIA, 2016, 2019, 2021). Studies have highlighted a range of BEV GHG impacts when the charging energy source is changed, such as the grid mix and solar-generated electricity (Hawkins *et al.*, 2013; Girard *et al.*, 2019). In summary, the electricity grid GHG factor is temporal, and combining it with personal mobility fleet GHG emission assessments is crucial, considering the increasing passenger light-duty vehicle BEV composition.

The SQLR collection of car-based LCA/GHG assessments has provided a range of outcomes, including the influence of the assessment scope and powertrain types on the assessment results. Hence, integrating external factors, such as changes in the electricity grid, is critical for setting the scope of fleet-electrification-based assessments. Overcoming the limitations of temporal flexibility in the conventional LCA method is identified as a critical requirement, considering the influence of time-varying variables in the GHG emission calculations of MaaS. Alternative approaches to overcome this limitation are explored in Section 2.7.

2.7 Combining the temporal effect in LCA in the sharing economy

The LCA method was established and standardised based on the ISO 14040 and 14044 principles and frameworks (ISO, 2006, 2006). It consists of four major phases: a) goal and objectives, b) life cycle inventory, c) life cycle impact assessment, and d) interpretation, and capable of applying in the environmental assessments of products and services (ISO, 2006). Therefore, this method supports the analysis of the environmental assessments of service systems in the sharing economy and compares them against their products in the traditional linear economy. This method has been extensively used to analyse sharing economy services (Farrant, Olsen and Wangel, 2010; Amasawa *et al.*, 2020; Klint and Peters, 2021). However, previous studies found temporal flexibility to be a well-known limitation of the LCA method (Udo de Haes *et al.*, 2004; Levasseur *et al.*, 2010; Pinsonnault *et al.*, 2014; Hu, 2018). LCA is a static environmental assessment methodology that does not support time-varying input. Studies have found that the precision of LCA outcomes is challenged when the entire range of temporal (dynamic) issues is not integrated (Lueddeckens, Saling and Guenther, 2020). Lueddeckens et al. (2020) have further highlighted, stressing the findings of Pinto and Rossetti (2020:3,5), the dependency of exogenous sources on future trends or behaviour as a threat to the LCA method and emphasise maximising endogenous dynamics. Techniques such as dynamic LCA have been proposed to overcome this issue (Kim, 2003; Levasseur *et al.*, 2010; Pinsonnault *et al.*, 2014; Hu, 2018).

Consideration of temporal effects is essential for assessing the environmental implications of long-lived products (Herrchen, 1998). Two common examples of long-lived products include automobiles and buildings. They are commonly offered as services in a sharing economy system (e.g., a car in the Uber fleet and a rented or leased building). Dynamic LCA is a widely used method to account for the temporal effects of long-term products (Levasseur *et al.*, 2010; Pinsonnault *et al.*, 2014; Hu, 2018; Sohn *et al.*, 2020). This section explores the suitability of the extensively used dynamic LCA method as a methodological alternative to overcome the challenge of integrating temporal flexibility and assessing its compatibility for sharing economy modes such as car-based MaaS. In addition, the limitations of incorporating consumer preferences are explored.

2.7.1 Dynamic-life cycle assessment method

The dynamic LCA method has emerged as the most frequently used technique to combine temporal effects with LCA, existing since 1991 with 165 applications by 2016 (Sohn *et al.*, 2020).

The dynamic LCA is defined as "an LCA that incorporates elements of temporally induced changes that affect results and interpretation of the modelled system" (Sohn *et al.*, 2020). The dynamic LCA method provides methodological solutions to the identified limitations of conventional LCA applications in temporal space (Stasinopoulos, 2013; Sohn *et al.*, 2020). Most of the method applications are aligned with the ISO 14040-based four LCA phases with some extensions to integrate the temporal modelling flexibility, as shown in Figure 2-6. Overall, it is a structured and systematic approach.

The dynamic LCA method has extensively utilised SD and LCA methods (Stasinopoulos, 2013; Ilhamsah, Prasetyo and Mustajib, 2017; McAvoy *et al.*, 2021). Hence, in addition to temporal flexibility, the dynamic LCA can be utilised to incorporate the modelling capability of causal (feedback) effects beyond the functions of conventional LCA applications (Stasinopoulos, 2013; Sigüenza, Cucurachi and Tukker, 2021; Stasinopoulos, Shiwakoti and Beining, 2021). The dynamic LCA method has also been employed to determine the GHG emissions associated with changes in powertrain types, such as the transition to BEV (Garcia, Gregory and Freire, 2015). It has also been identified as an approach to integrating other tools (Udo de Haes *et al.*, 2004). Therefore, the dynamic LCA method can incorporate the causal consumer preferences discussed in Section 2.3 and the related technology changes discussed in Section 2.4.

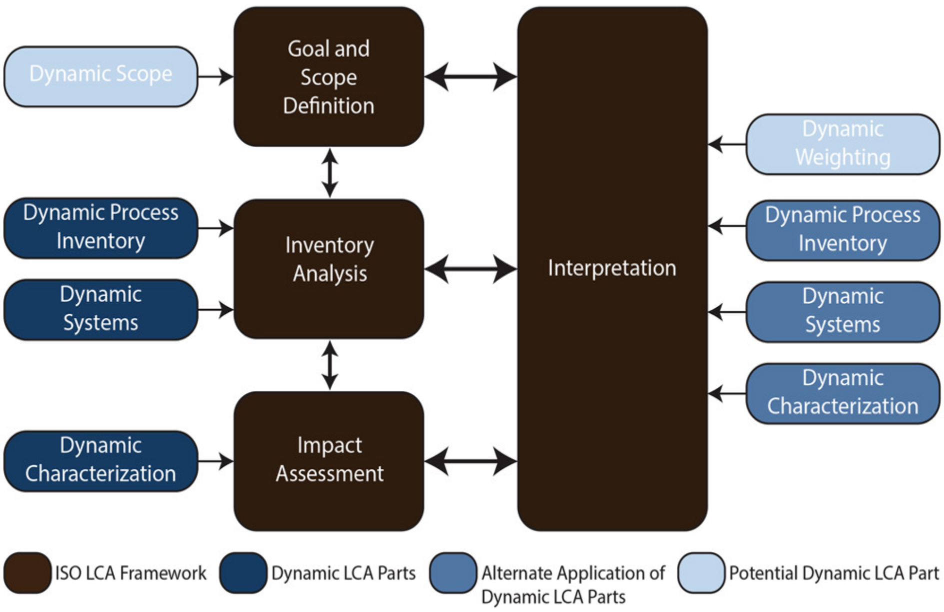

Figure 2-6 Additional dynamic LCA sections associated with the conventional 4 phases of the LCA method (ISO, 2006)

Source: Defining Temporally Dynamic-Life Cycle Assessment: A Review, Sohn et al. (2020), copyright © reprinted by permission of John Willy and Sons

2.7.2 Integration of SD and LCA methods

The SD method has been utilised to integrate causal and temporal effects into LCAs and other quantitative environmental sustainability assessments (McAvoy *et al.*, 2021). As shown in Figure 2-7, two approaches have commonly been used to combine SD and LCA (or GHG or sustainability assessments). Halog and Manik (2011) have developed Approach 1, which is frequently used. In their approach, LCA results are calculated conventionally, and those results are used as the input of the SD model (Onat, Kucukvar, and Tatari 2016; Pinto, Sverdrup, and Diemer 2019; Stasinopoulos 2013). Approach 2 combines the two methods differently. It utilises the casual and temporal effects considered SD outcomes as inputs to the LCI (Changsirivathanatahathamrong, Moore and Linard, 2001; Kumar, Hoadley and Shastri, 2019). Though some studies have not indicated the term 'dynamic LCA' for the methodology, the combined approach of temporal and casual SD outcomes and LCA results implies a similar application. However, the primary data-generated consumer preferences have not been integrated into any SD and LCA combined (dynamic LCA) studies.

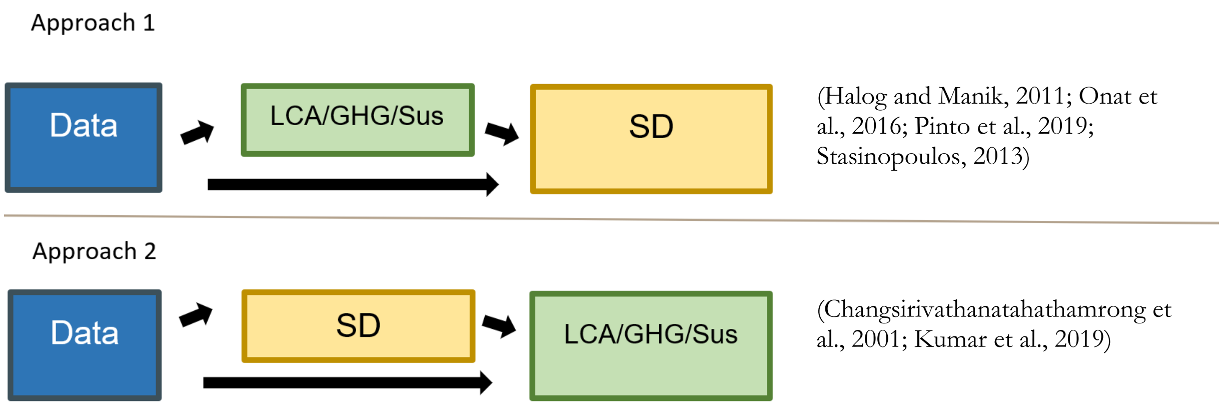

Figure 2-7 Two main approaches to combining SD and LCA/GHG/Sustainability indicators

Note: Modified based on (McAvoy *et al.*, 2021, fig. 7), *Sus=Sustainability indicators,

2.7.3 Dynamic LCA use in sharing economy systems

There is limited research combining time-dependent temporal variables into LCA studies of sharing economy systems. Only two scenario-based case studies have been identified using the dynamic LCA method in the sharing economy of shared-own autonomous vehicle fleets (Stasinopoulos, Shiwakoti and Beining, 2021) and pay-per-wash washing machine services (Sigüenza, Cucurachi and Tukker, 2021). Both studies utilised secondary literature for consumer adoption scenarios. Although Amasawa et al. (2020) identified the importance of considering the sharing economy asset changes in a consumer-to-consumer carsharing case study, they did not integrate temporal or causality effects into their LCA calculations. Therefore, existing work confirms the importance of integrating temporal variables in environmental assessments of the sharing economy systems considering the associated dynamic nature. They also confirm the suitability of adopting the emerging dynamic LCA method as a technique for such assessments. The existing literature also highlights the importance of integrating primary data into the assessments by employing the dynamic LCA method (Stasinopoulos, Shiwakoti and Beining, 2021). The method integrates the causality elements to deliver a more realistic assessment.

2.7.4 Limitations of dynamic LCA alone for use in the transition to MaaS

The dynamic LCA method alone is not capable of incorporating consumer preference data into the modelling. Consumer preference is an essential element for integration into the final decision-making process of sharing economy systems (Piscicelli, Cooper and Fisher, 2015). Consumer decisions also support accessing underutilised assets, such as car fleets by peer-to-peer or consumer-to-consumer market segments (Frenken, 2017). Hence, incorporating consumer preferences into the dynamic LCA is critical for effectively assessing the GHG emissions of the transition to car-based sharing economy modes (see Section 2.3). A Bass model-based structure is used to integrate the imitation and innovator behaviour of autonomous shared mobility system users (Stasinopoulos, Shiwakoti and Beining, 2021). The Bass model-based SD behaviour is an approach that incorporates consumer preferences and calculates LCA outcomes based on consumer choices. However, combining consumer preference attributes such as fare, powertrain changes, and vehicle body style that respond to temporal changes and their causality must be researched.

The dynamic LCA method provides a structured approach aligned with the LCA methodology (ISO, 2006) and the SD technique and confirms the ability to analyse sharing economy systems. The integration of consumer preference into dynamic LCA is identified as a research area to develop to connect consumer preference changes in the attributes to determine the GHG changes of the transition to car-based MaaS.

2.8 This work

Increasing car-based MaaS usage is considered a way to reduce GHG emissions from personal mobility. It is commercially available in four major forms: carsharing, carpooling, ridesourcing and taxi. MaaS use depends on consumers' socioeconomic, demographic and living location based on public transit facilities and journey type (Section 2.2). Studies have concluded that journey fare, door-to-door time, and convenience are key consumer attributes of MaaS users that differ from those of private vehicle owners. However, the focus is minimal on measuring the influence of vehicle technologies such as powertrain systems and body styles as the consumer attributes in car-based MaaS, although they significantly determine the GHG emissions. In summary, considering them as consumer attributes is uniquely important to assess the transition to MaaS environmentally.

The behaviour of MaaS users differs from that of the linear economy by shifting from ownership to usership and demanding relatively newer products. Therefore, MaaS fleets are technologically upgraded faster than traditional private vehicle fleets. Shared mobility operators are also shifting faster from dominant ICEV fleets to BEVs. In addition to powertrain changes, there has been a significant shift from sedans to SUVs. These technological changes are time-dependent (temporal) and significantly influence the personal mobility fleet composition. They also affect the GHG emission outcomes of mobility fleets. In summary, the impacts of consumer preference and temporal fleet technology causally connect and affect the transition to car-based MaaS modes and related GHG emissions.

This thesis assesses the impact of the transition from private car use to car-based sharing economy modes on GHG emissions by considering the causal interrelations between consumer preferences and temporal fleet technology changes in personal mobility. The derived main research question is as follows:

> **What is the impact of the transition from private car use to car-based sharing economy modes on GHG emissions, considering consumer preferences and fleet technology changes?**

Two associated research questions (ARQs) are derived, aligning with the key research question. They are:

- ARQ1: How can the influence of temporal fleet technology changes and their causal effect on consumer preferences in GHG emissions from MaaS be quantified?

- ARQ2: What is the significance of consumer attributes influencing the transition to car-based MaaS?

The thinking process to reach the major research problem is presented in Figure 2-8, based on the shortlisted critical factors as a part of the literature review.

The dynamic LCA is an effective method for combining causal and temporal changes to analyse GHG outcomes. The emerging dynamic LCA method is based on the standardised conventional LCA principles and framework with an extended consideration of integrating the temporal elements. Extended processes, such as dynamic process inventories, support the effective integration of temporal LCI data instead of static data. A few studies have employed a dynamic LCA to assess shared mobility modes. However, no study has integrated primary consumer preferences into dynamic LCA studies to determine the GHG emissions of the transition to car-based MaaS modes. Hence, developing a methodological framework to analyse consumer preference-integrated dynamic LCA is identified as a key delivery of this study. The primary data collection of the consumer preference attributes of car-based MaaS is recognised as key to connecting to the dynamic LCA model. Overall, the GHG emissions of the transition to car-based MaaS modes can be more realistically measured by combining consumer preference results and fleet technology changes.

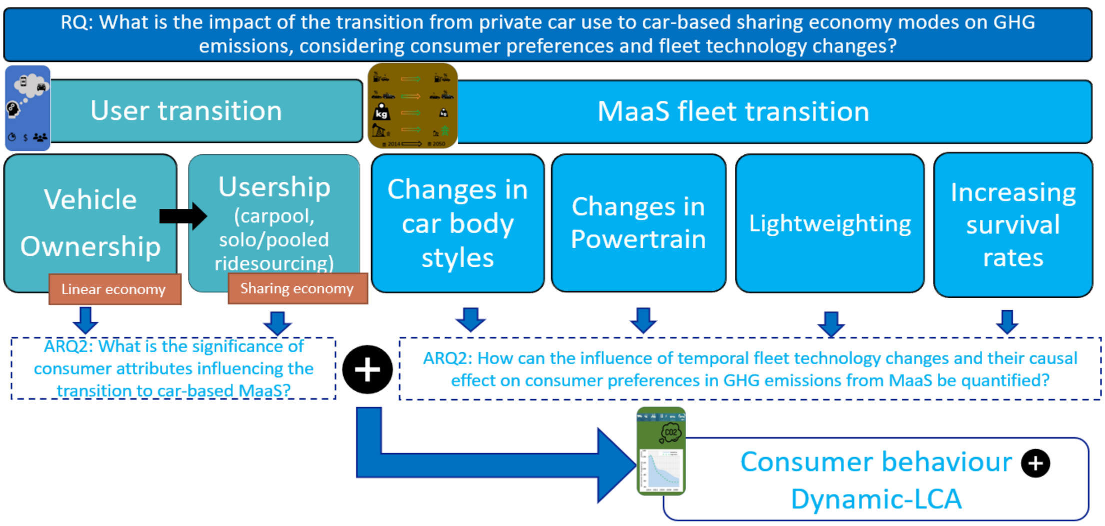

Figure 2-8 A simplified flow diagram to represent the thinking process to reach the major research problem based on the literature review findings

3 RESEARCH METHODOLOGY

Publication relevant to this chapter

Fernando, C., Soo, V. K., Compston, P., & Doolan, M. (2022). Life Cycle Environmental Impact of Mobility Servitization: The Effect of Fleet Technology Changes. *Procedia CIRP*, *105*, 829–834. https://doi.org/10.1016/j.procir.2022.02.137

Fernando, C., Buttriss, G., Yoon, H.-J., Soo, V. K., Compston, P., Kim, H. C., De Kleine, R., & Doolan, M. (Under review). Characterising the consumer preferences of car-based mobility for a round-trip to work. *Journal of Consumer Behaviour*.

Fernando, C., Buttriss, G., Yoon, H.-J., Soo, V. K., Compston, P., & Doolan, M. (Accepted). Integration of consumer behaviour into dynamic life cycle assessment for the sharing economy: Methodology and case study for shared mobility. *International Journal of Life Cycle Assessment*.

Introduction

This chapter details the research methods adopted in this study. Section 3.1 presents the scope of the study, and Section 3.2 defines the research strategy by providing an approach to resolving the identified research requirements in Chapter 2. This section also identifies the research methods used to collect the data required to respond to the research questions. Section 3.2 also introduces the chosen analytical tools and concludes with a summary.

3.1 Scope of the study

The key findings derived from the literature review were considered in determining the scope of the study. A journey type and geographical location representing significant opportunities to shift to car-based MaaS are crucial features to demonstrate GHG emission changes in the transition.

The market availability of car-based MaaS modes is also considered, along with the technological changes in the MaaS fleets.

The round-trip to work journey is chosen as the scope of this study. This study defines round-trip to work as the door-to-door journey from home to the office and return trips. It does not include work-related travel or business travel. It is also the most frequent person journey type (15%) in the US other than non-regular journey types such as shopping and recreational trips (McGuckin and Fucci, 2018, p. 36), and the most significant contributor to congestion-prone city traffic (Dixit *et al.*, 2010). An average US employee travels 20.6 km daily to/from work (McGuckin and Fucci, 2018). The number of commuting employees in the US has risen from 133.5 to 144.8 million from 2010 to 2019 (US Census Bureau, 2020a). It is also the only journey type that increased from 13.4% to 15.1% from 2009 to 2017, while total commuting trips decreased by 11% in the US (McGuckin and Fucci, 2018, p. 32,36,38). The above journey characteristics represent the significance of the round-trip to work and its contribution to light-duty vehicle GHG emissions, which represent 57% of the US transport sector GHG emissions (US EPA, 2020b).

The US was selected as the geographical area for the study based on its significant changes in the use patterns of car-based MaaS modes (McGuckin and Fucci, 2018, p. 78; US Census Bureau, 2020a; Schneider, 2021b) and government policy-based technology changes to tackle climate change, such as fleet electrification (The White House, 2021). The self-driven round-trip-to work cohort has increased from 64.4% in 1980 to 75.9% in 2019 in the US, and the shared ride usage in commuting to work, including carpooling, made up 10.3% of the total trips (US Census Bureau, 2020a). This case demonstrates current car-based MaaS practices. The round-trip to work user characteristics are also determined by the public transit levels of the location (Section 2.2). Overall, the US is chosen as the geographical scope for a location-based study that considers public transit levels.

Three car-based MaaS modes, a) carpooling, b) solo-ridesourcing[7], and c) pooled-ridesourcing, are chosen to assess the transition of personal mobility in commuting to work in the US. Carpooling (including informally organised trips) represents the highest car-based MaaS mode for commuting to work (US Census Bureau, 2020a). However, its usage has decreased from 19.7% in 1980 to 9.8% in 2019 (Office of Energy Efficiency and Renewable Energy, 2016; US Census Bureau, 2020a). On the other hand, solo-ridesourcing and pooled-ridesourcing have shown an increasing market share

[7] solo-ridesourcing term is employed to highlight the usage of the ridesourcing mode in non-shared trips

in a few US cities, such as New York and Chicago relative to taxis (Schneider, 2021b, 2021a). Also, those relatively new modes have replaced taxis in other US cities, demonstrating higher consumer choice (Rayle *et al.*, 2016). Hence, this study does not consider taxis as a car-based MaaS mode because consumer interest is relatively low in cities. The users of the three selected modes showed different consumer interests (attributes) and the utilisation of varying journey types (see Section 2.3). In addition, as discussed in Section 2.4.2, their fleets have shown differences, such as larger body type vehicles in pooled-ridesourcing and more BEVs expected in ridesourcing modes (Lyft, 2020; Uber, 2020). The occupancy rates of the three modes represent the maximum range of personal mobility (Henao, 2017; Union of Concerned Scientists, 2020b). In summary, the selection of carpooling, solo-ridesourcing, and pooled-ridesourcing represents a varied shared mode possibility in personal mobility for a round-trip to work journey in the US.

The GHG emissions changes from the cradle to the grave, considering the temporal and causal fleet technology changes in the transition from private vehicles to car-based MaaS modes (carpooling, solo and pooled-ridesourcing) in an average round-trip to work in the US is chosen as the scope of this study.

3.2 Research strategy

Implementing a clear research strategy that addresses the research question is an outcome of setting up the research problem, aim and objectives (Singh and Bajpai, 2007). Hence, the strategy formulation started by considering the defined research requirements and questions in Section 2.8. This thesis's key research question is: **What is the impact of the transition from private car use to car-based sharing economy modes on GHG emissions, considering consumer preferences and fleet technology changes?** ARQ1 highlights the importance of identifying methods that can quantify the influence of both temporal and causal features on GHG emissions, considering changes in fleet technology and consumer preferences. ARQ2 demands the investigation of the significance of consumer attributes that influence the transition to a car-based MaaS mode. Figure 3-1 presents an overview of the research process undertaken to answer the research questions.

The first phase of the research process, including problem identification, has already been presented in Chapter 1. Subsequently, a comprehensive literature review was performed on car-based MaaS GHG emissions, fleet technology changes, identifying car-based MaaS consumer attributes and shortlisting the analytical methodologies used (Chapter 2). Knowledge gaps were also identified using LCA as a static methodology and the capabilities of integrating consumer preference data into dynamic LCA modelling (Section 2.7).

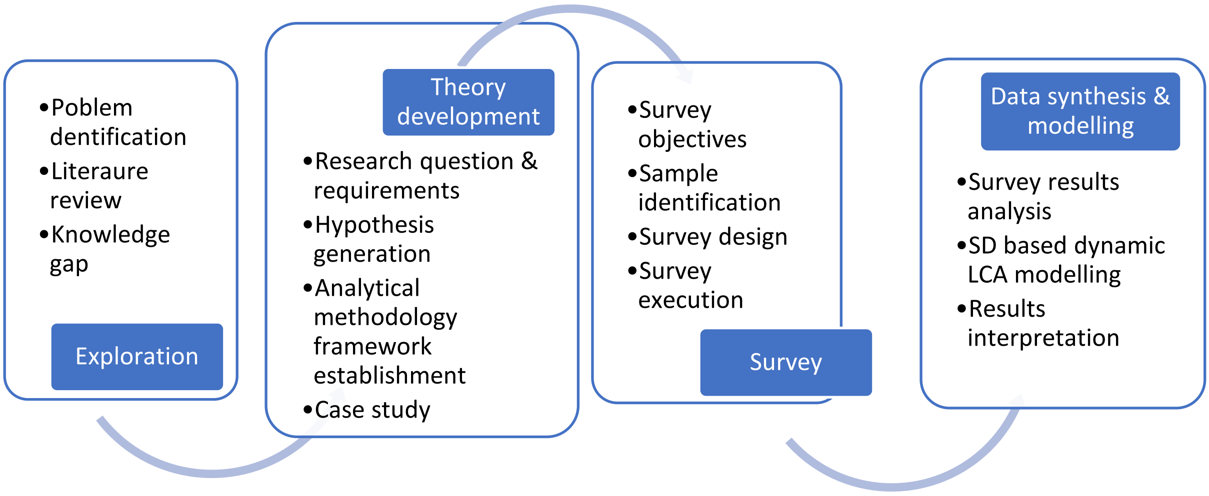

Figure 3-1 Phases of the research process employed in this study

Note: adopted from (Soo, 2018)

Section 3.3 presents the theoretical development and the second phase of the research process to fill the above-identified research gaps. Subsequently, a preliminary hypothesis and analytical methodology framework were developed. The analytical tools, capabilities and limitations are discussed in Section 3.3, followed by a chosen case study in Section 3.1. In Chapter 4, a customised methodology framework is introduced to close the gaps in analytical tool integration. Based on the selected analytical tools, a market survey was conducted to explore the case study presented in Chapter 5. In Chapter 6, the results are synthesised to explore the impact of the transition from private car use to car-based sharing economy modes on GHG, considering consumer preferences and fleet technology changes.

The analytical phase of this study is a consumer preference survey, a commonly used primary data collection process in car-based MaaS consumer studies discussed in Section 2.3. This research process starts with survey objectives, followed by sample identification and design, and ends with the execution of the survey. The research process is presented in Chapter 5.

3.2.1 Research methods

The research methods used to execute the established research process are discussed in this section.

The research types are defined based on the three research questions and their data collection requirements. They are presented in Table 3-1. Mixed methods research (mixed research approach) (Johnson and Onwuegbuzie, 2004) was chosen to address these three research questions. Creswell (1999) highlights the mixed research approach in terms of its ability "to understand complex phenomena qualitatively as well as to explain the phenomena through numbers, charts and basic statistical analyses." This approach has been used in consumer preference studies (Huang *et al.*, 2019) and in reviewing LCA studies (Seyis, 2020).

Table 3-1 The types of data, data requirements and relevant research types for collecting them

Research question	Research type	Data type	Key data requirement
What is the impact of the transition from private car use to car-based sharing economy modes on GHG, considering consumer preferences and the fleet technology changes?	Exploratory	Qualitative	Identify the factors that influence the GHG emissions of car-based MaaS: powertrain type, vehicle body style, changes in automobiles such as lightweighting, occupancy rates in MaaS modes, indirect emissions of energy sources and feedstock. Consumer preferences: ARQ2
	Explorative	Quantitative	The values and temporal behaviour of the above key influencing factors
ARQ1: How can the influence of temporal fleet technology changes and their causal effect on consumer preferences in GHG emissions from MaaS be quantified?	Explorative	Qualitative	Methods used to assess car-based life cycle GHG emissions Consumer preferences Integrate temporal and causal variables. Identify and explore the strengths and gaps of the existing analytical tools addressing the research questions.
ARQ2: What is the significance of consumer attributes influencing the transition to car-based MaaS?	Quantitative	Survey	Consumer preference data on car-based MaaS modes for the selected case study

The explorative research method was utilised in LCAs in GHG emission-based studies assessing both product systems (Ma *et al.*, 2018) and service systems (Trevisan and Bordignon, 2020). This method is also utilised to study alternative vehicle fleet technologies, such as HEV demand (Kurani, Turrentine and Sperling, 1994). Hence, this method is suitable within the scope of this study. Likewise, survey-based research has been extensively employed to understand the car-based MaaS user preferred choices discussed in Section 2.3. The method has been operationalised in many forms, including the DCE model (Carroll, Caulfield and Ahern, 2017). Overall, a mixed methods research approach combining exploratory and survey methods was utilised to collect data for the three research questions.

3.3 Research analytical tools

A combined approach of consumer preference based on the DCE model and dynamic LCA based on LCA and SD methods are identified as the analytical research tools required for the study. The combined approach delivers the research strategy step analytical methodology framework to assess the research questions identified in Section 2.8. Sections 3.3.1 to 3.3.5 discuss the above combination of methods, and their methodological requirements and essential components are identified in establishing an integrated methodology framework.

3.3.1 Life cycle assessment method

The structured and systematic LCA method (ISO, 2006) has been utilised to analyse the GHG assessments of the car-based MaaS modes. This method has been employed in life-cycle GHG assessments of shared mobility and has been extensively employed to analyse GHG emissions in car-based MaaS fleets since 2001 (Doka and Ökobilanzen, 2001; Vedrenne *et al.*, 2014; Carranza *et al.*, 2016; Amatuni *et al.*, 2020; Sun and Ertz, 2021). It has also been employed to assess powertrain changes in car-based MaaS, such as electrification (Castel-Branco, Ribau and Silva, 2015; Guyon, 2017). This study utilised the LCA method to assess the influence of vehicle body style. The LCA method has also been used to analyse vehicle technologies (Hawkins *et al.*, 2013; Lombardi *et al.*, 2017). Hence, this method has been adopted in both linear and sharing economy systems. The LCA method is more robust than carbon footprint analysis, which relies on emission factors (Alvarez *et al.*, 2016). The LCA databases are available to cater to car-based case studies, and the GREET model has developed a lightweighting scenario for extended GHG emissions scenario analysis (Wang *et al.*, 2021). The established sustainability assessment frameworks, such as the product sustainability index (Jawahir *et al.*, 2006) and life cycle sustainability assessment (Kloepffer, 2008), are not considered to align with the defined scope of the study, GHG emissions assessment in Section 3.1.

Overall, this thesis uses LCA as a GHG emission analysis tool and follows the ISO 14040 standard-based structured methodological application (ISO, 2006). The LCA model design is discussed in Section 4.2.

3.3.2 System dynamics method

The SD method is chosen to integrate the temporal and causal influences on the GHG emission results of the transition to MaaS. A technique capable of adopting the temporal characteristics of a system is essential in this study to analyse the changing fleet dynamics that influence GHG emissions. The SD method can also be used to manage causality (known as feedback loops) between consumer preferences and automobile technologies (Jiang, 2019). This technique has been used in car-based MaaS mode system modelling (see Section 2.5) and in the temporal environmental impacts of car-based shared mobility (Luna *et al.*, 2020; Stasinopoulos, Shiwakoti and Beining, 2021).

This study adopts Sterman's five-step iteration modelling process to implement SD modelling (Sterman, 2000, pp. 85–104; Jiang, 2019). As shown in Figure 3-2, the five steps—a) problem articulation, b) formulation of dynamic hypothesis, c) formulation of a simulation model, d) testing (reference modes, robustness and sensitivity), and e) policy design and evaluation—provide an iterative and systematic structure in applying SD. Hence, the results of any step can influence the insights of the other steps and enable revisions in an earlier step. Each modelling process step is important for integration into the combined analytical tool.

The Bass diffusion model was chosen to explain the transition to car-based MaaS behaviour, considering the model's adaptability from early innovation to market maturing periods (Bass, 1969; Sterman, 2000, sec. 9.3.) (see Section 2.5.1). It was employed to assess the adoption of car-based MaaS (C. Zhang *et al.*, 2020). Lee et al. (2022) utilised the Bass model in an SD model to analyse shared mobility regulation contexts, and Jiang (2019) used it to explore different powertrain types.

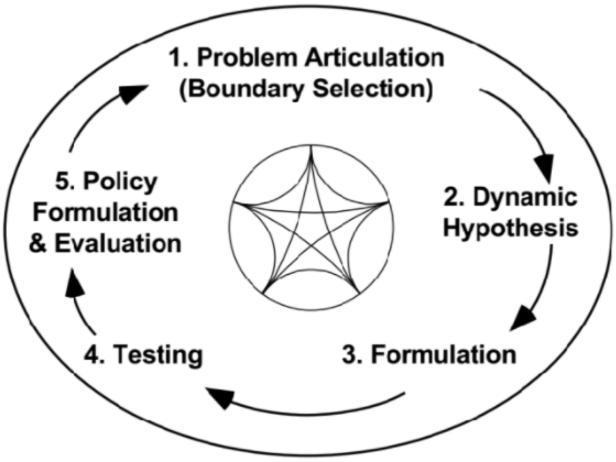

Figure 3-2 The iterative SD modelling process

Source: Business Dynamics Systems Thinking and Modeling for a Complex World, John D. Sterman (2000), Commercial Electronic and Print Use, copyright © McGraw Hill, reprinted by permission of McGraw Hill (CHA887761455-1), https://www.mheducation.com/permissions.html

Stella Architect software (version 1.9.4) is used to illustrate SD modelling by integrating consumer preferences, the transition to MaaS and their life cycle GHG impacts. The SD models are visualised using causal loop diagrams and stock and flow diagrams.

3.3.3 Stated preference analysis and discrete choice experiments

The stated preference choice method was chosen to analyse consumer preferences. This method is commonly employed in MaaS mode studies (Hunt and McMillan, 1997; Washbrook, 2002; Correia, Silva and Viegas, 2013; Malodia and Singla, 2016; Carroll, Caulfield and Ahern, 2017; Alonso-González *et al.*, 2020). The conjoint analysis technique is a widely accepted stated preference method employed in transportation studies (Green and Srinivasan, 1978) and extended to different mobility experiences, such as autonomous rides (Krueger, Rashidi and Dixit, 2019). This technique has also been employed to determine consumer preferences in shared mobility studies (Hildebrandt *et al.*, 2015; König, Bonus and Grippenkoven, 2018; An *et al.*, 2021; Keller *et al.*, 2021). In conjoint analysis, a choice is constructed with a combination of the levels of selected attributes, and the respondents state their preferred choice combination (Green and Srinivasan, 1978, 1990). The constrained choices in the conjoint analysis block provide the option to select the most suitable out of a few choice combinations and trade-offs. This method has also been adopted in fleet technology studies, such as those on preferences in different powertrain systems (Lebeau *et al.*, 2012; Jiang, 2019; Qian, Grisolía and Soopramanien, 2019; Klein, Lüpke and Günther, 2020). Taken together, this study used the conjoint analysis technique to assess consumer preferences.

A DCE model was selected to analyse the choices. It is commonly used in transportation-related choice modelling exercises. DCE is used to model a mutually exclusive set of choices (Ben-Akiva and Lerman, 1987). Starting from binary choice travel modes, the model has been extensively used in choice modelling with more than two attributes: trip frequency and car ownership (Warner, 1962; Ben-Akiva, 1973; Ben-Akiva and Lerman, 1987; Bierlaire, 1998). They further described the use of the model in choices with the characteristics of collectively exhaustive alternatives. Choice-based conjoint analysis, a type of conjoint analysis, integrates the aspects of DCE and considers brands (alternatives) (Cohen, 1997). Hence, the mobility alternatives of this study–carpooling, solo-ridesourcing, and pooled-ridesourcing with private vehicles as the baseline scenario–can be represented by employing the choice-based conjoint analysis approach. It is commonly used in consumer behaviour analysis (Sichtmann, Wilken and Diamantopoulos, 2011), in MaaS behaviour assessments (Hildebrandt *et al.*, 2015; König, Bonus and Grippenkoven, 2018; Vij *et al.*, 2020; An *et al.*, 2021; Keller *et al.*, 2021) and in car technologies (Klein, Lüpke and Günther, 2020; Berneiser *et al.*, 2021). In summary, choice-based conjoint analysis was selected as the DCE technique to incorporate into the consumer survey in this study.

3.3.4 Survey analysis

The random utility model-based DCE was chosen to analyse the choice-based conjoint analysis results. Random utility theory is employed to interpret the choice behaviour of humans, while DCE is used for simulating consumers' actual market behaviour (Louviere, Flynn and Carson, 2010). As defined in equation (3-1) adopted from Train (2009, p. 34,37), the random utility model represents a decision maker (n) that faces a choice among J alternatives. The utility that decision maker n obtained from alternative j is given by

$$U_{nj}=\beta_n' x_{nj}+\varepsilon_{nj}, \text{j=1, 2,..., J} \tag{3-1}$$

where x_{nj} is a vector of attributes relating to alternative j and person n; β_n is a vector of partworth utilities for the attributes which depict person n's tastes associated with each of the observed attributes, and ε_{nj} is an error term that is an independently and identically distributed standard normal distribution with mean 0 and standard deviation 1 (εnj ~ N (0,1)).

The standard logit/MNL model was selected as the estimation procedure to analyse the choice-based conjoint analysis results. The MNL model is commonly used in stated preference choice experiments (Ben-Akiva and Atherton, 1977, pp. 3, 60–66; Train, 2009, chap. 3). MNL has been employed in DCE and conjoint analysis models that studied MaaS consumer behaviour (Shaheen, Chan and Gaynor, 2016; Carroll, Caulfield and Ahern, 2017).

Consumer preference results are interpreted based on aggregated preferences (utility/partworth). These aggregated utility parameters (also known as Alternative-Specific Coefficients (ASCs)) (β_n) are calculated based on the individual preference scores (U_{nj}) generated by the software Conjoint.ly. The utility values are calculated for each attribute level for the four mobility modes (J = 4: carpooling, solo-ridesourcing, pooled-ridesourcing and private vehicle use). Attribute importance is calculated based on the average utility parameters for each MaaS mode.

3.3.5 Combined dynamic-life cycle assessment

The dynamic LCA method, supported by the SD modelling interface, combines the temporal variables into the life-cycle GHG calculations of the transition to MaaS. Hence, it provides an approach to combining the SD modelling outcomes of temporal fleet changes and causality elements with LCA work. As discussed in Section 2.7.1, this method has been used in a shared mobility case study (Stasinopoulos et al., 2021).

Compared to typical ISO 14040-based LCA applications (ISO, 2006), some extensions have been used to apply the dynamic LCA method. In dynamic LCA, the Dynamic Process Inventory (DPI) replaces the traditional static LCI. This feature is managed by considering temporal parameters as inputs for the LCI calculation in this study. The changes in vehicle energy economy rates and lightweighting against the modelling time horizon are examples of DPI parameters. Similarly, dynamic system changes, such as fleet composition, are introduced. However, given the research objectives, this study did not consider dynamic characterisation and dynamic normalisation factors.

As highlighted in Section 2.7.4, combining consumer preference with dynamic LCA has been identified as a constraint. Hence, this issue has been identified as a major problem in answering ARQ1 (see Table 3-1) using only dynamic LCA features. Therefore, a combined analytical methodology framework to integrate consumer preference, SD and LCA models is introduced in

Chapter 4. A summary of the selected analytical tools and their relevance to ARQ1 and other research questions are presented in Table 3-2.

Table 3-2 The utilised analytical tools and their relevance to the ARQ1:

What methods can be used to assess temporal fleet technology changes and their causal effect on consumer preferences for GHG emissions of MaaS?

	Analysis requirement	Analytical tool	Relevance to other research questions	Results Chapter
(1)	Assess consumer preference	DCE, Random Utility Model and MNL	ARQ2, key research question	5
(2)	Assess the temporal fleet technology changes and their causal effect	SD		6
(3)	Assess GHG emissions	LCA		
(4)	The combined approach of GHG assessment and causality and dynamics: (3) + (2)	Dynamic LCA	Key research question	7
(5)	The combined approach of consumer preference and dynamic LCA: (4) + (1)	Introduced in Chapter 4		7

3.4 Summary

This chapter described the research methods and analytical tools chosen to support the defined strategy for answering the identified research questions. A mixed research approach was selected, utilising explorative and survey methods to facilitate data collection for the three research questions. This chapter explored the answer to the ARQ1, 'How can the influence of temporal fleet technology changes and their causal effect on consumer preferences in GHG emissions from MaaS be quantified?'. The selected methods were applied to explore the key research question and ARQ2 in the following chapters.

The LCA technique was chosen to assess GHG emissions, considering its substantial use in MaaS and vehicle fleet technology change. The method follows the ISO 14040 structured approach, and its application is systematic. However, GHG impact analysis of the transition to car-based MaaS is impossible using only the LCA method. The SD method supported by Sterman's five-step SD iteration process and the Bass model were used to analyse the influence of the temporal characteristics of the MaaS fleets and feedback of consumer preferences. The benefit of integrating the consumer preferences based on the stated preference analysis with the temporal life cycle assessment is that it combines the market preferences into the overall environmental assessment. Hence, the results are more practical compared to the conventional LCA analysis. The SD modelling interface-based dynamic LCA method has been identified to support the combination of temporal effects and environmental impact assessment. However, its ability to incorporate consumer preferences has been identified as a challenge.

A round-trip to/from work trip was chosen as the journey case study to explain the research questions, given its significance in personal mobility and as the most frequent routine journey. The US has been chosen as the geographical location, given the increasing use of shared mobility modes in their cities. Carpooling, solo-ridesourcing and pooled-ridesourcing have been selected as the car-based MaaS modes to represent the range of occupancy rates, different adoptions of fleet technology and range of user behaviour attributes. The historical values of the transition to car-based MaaS in US roundtrip to/from work will be employed to validate the analytical method as a part of the policy formulations and evaluation step. In summary, this case study represents a significant range of consumer preference selections in the transition to MaaS possibilities, including their dynamics in personal mobility and changes in GHG emissions.

4 CONSUMER BEHAVIOUR AND DYNAMIC LCA MODEL INTEGRATION

Publication relevant to this chapter

Fernando, C., Buttriss, G., Yoon, H.-J., Soo, V. K., Compston, P., & Doolan, M. (Accepted). Integration of consumer behaviour into dynamic life cycle assessment for the sharing economy: Methodology and case study for shared mobility. *International Journal of Life Cycle Assessment*.

Fernando, C., Soo, V. K., Compston, P., & Doolan, M. (2022). Life Cycle Environmental Impact of Mobility Servitization: The Effect of Fleet Technology Changes. *Procedia CIRP*, *105*, 829–834. https://doi.org/10.1016/j.procir.2022.02.137

Fernando, C., Soo, V. K., Compston, P., Kim, H. C., De Kleine, R., Weigl, D., Keith, D. R., & Doolan, M. (2020). Life cycle environmental assessment of a transition to mobility servitization. *Procedia CIRP*, *90*, 238–243. https://doi.org/10.1016/j.procir.2020.01.098

A font colour scheme is introduced in Table 4-1 to distinguish the applications of modelling components in this thesis. They relate to the specific modelling work.

Table 4-1 Key to text and SD modelling work

Item/modelling component	Font description
DCE model components	Light blue
SD model components	Light brown
LCA model components	Green
Sub-model, sub-model component	Dark green
Stock and flows	Blue
Converters – system defined	Blue
Converters – primary data-based	Bright green
Converters – secondary data-based	Purple
Converters – DPI	Brown

Introduction

This chapter introduces a novel approach to combining consumer preferences into dynamic LCA by employing the SD technique as the modelling interface. The proposed methodological framework provides a solution to the identified research gap in incorporating market-based primary data and their causal influence on temporally influenced LCA data, as identified in Chapter 3. The causal relationship between consumer preferences and fleet technology changes is crucial in this study, considering the relatively fast changes in MaaS fleets.

This requirement is further emphasised by the facts presented in Section 2.3. It highlights the significant difference in the consumer preferences of MaaS users compared with private vehicle users. The car-based MaaS models reduce upfront capital investment and increase access to services (usership) without owning them like in the linear economy system (take-make-use-waste). This expenditure change in sharing economy models allows greater access to expensive high-tech and newer products (Ajanovic, 2015). Hence, there are changes in shared mobility mode use and fleets, such as achieving maximum longevity levels in a shorter time than in conventional linear economy systems due to high levels of utilisation. These characteristics influence the MaaS GHG emissions and are temporal and response to the feedback of consumer preference. Therefore, this thesis proposes a new approach incorporating sharing economy consumer preferences into a dynamic LCA. This approach is then applied to model the changes in GHG emission due to the adoption of car-based MaaS systems by integrating the influence of consumer preferences. Section 4.1 introduces the proposed methodological framework for overcoming this research gap. Sections 4.2 to 4.6 explain its applicability in establishing a methodology framework to answer the key research question '**What is the impact of the transition from private car use to car-based sharing economy modes on GHG emissions, considering consumer preferences and fleet technology changes?**'. This explanation relates to the case study introduced in Section 3.1.

4.1 Consumer Behaviour Integrated Dynamic LCA methodological framework

The Consumer Behaviour Integrated Dynamic LCA (C-DLCA) methodological framework is introduced to incorporate consumer preferences into the dynamic LCA of sharing economy systems, including car-based MaaS (see Figure 4-1). The methodological framework provides a sequenced, robust and structured approach to utilise SD, LCA and DCE methods to integrate consumer preferences into dynamic LCAs. The framework provides a solution to combine consumer preference-based primary data integration in LCA studies, a research gap identified by previous research work. Past work has integrated consumer behaviour into LCA calculation work (Krystofik, Babbitt and Gaustad, 2014; Polizzi di Sorrentino, Woelbert and Sala, 2016; Shahmohammadi *et al.*, 2018). Polizzi di Sorrentino et al. (2016) employed a similar approach to the stated preference technique to quantify LCA findings based on consumer preferences. However, past studies have not integrated derived primary consumer preferences, dynamic changes, and LCA work together. Hence, the influences of consumer behaviour outcomes that causally affect the outcomes have not been captured. As revealed in Chapter 2, considering temporal changes and consumer preferences is crucial to understanding life cycle environmental impacts in sharing economy modes, such as shared mobility. Overall, the C-DLCA framework provides a solution to the above critical gap by integrating the critical information collected from personal mobility consumers to understand their temporal influences in shared mobility systems and, finally, on GHG emissions.

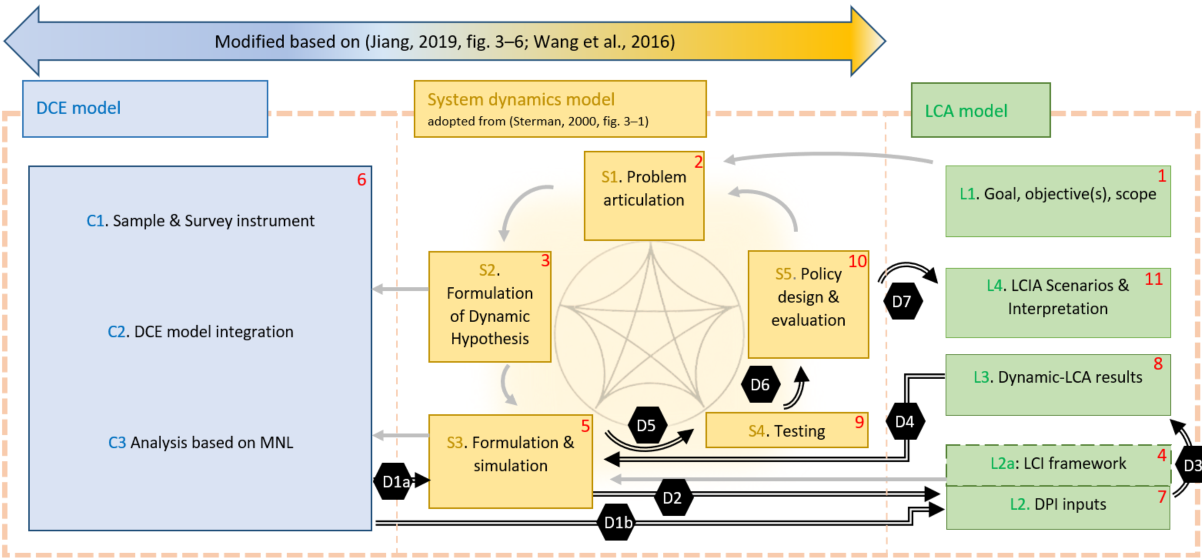

Figure 4-1: Proposed C-DLCA methodological framework of sharing economy systems

Notes: The top right number in each process box proposes the most practical sequence of the steps. Ash and black arrows (hexagons) represent the feedback and data flows, respectively. Components represent in the framework: Blue - DCE model and consumer preference data, Yellow - System Dynamic modelling interface (the star mark resembles the iteration characteristics of the chosen SD modelling framework (Sterman, 2000)), Green - LCA phases

The methodology framework comprises three components: a) DCE to integrate consumer preference data, b) SD – the modelling interface to integrate temporal fleet technology changes and their causal effects, and c) LCA calculations. They resemble constant iterations by adopting Sterman's five-step iterative process as the SD interface (Sterman, 2000, pp. 87–104). The interconnections in the centre of the diagram (star) represent the possibility of iteration, feedback process and non-linear sequence of the SD modelling steps. The three components of the approach, DCE, SD and LCA, are used to assess consumer preferences, fleet dynamics and life cycle impacts, respectively. Therefore, these steps help to understand the real world's systems and mental models.

The methodology framework starts with setting up LCA goals, objectives and scope (L1) as ISO 14001-based LCA principles are chosen as the key methodology. As discussed in Section 2.7.2, the literature revealed that the SD method had been used to integrate dynamic and causal (feedback) effects into dynamic LCA (Stasinopoulos, 2013; Stasinopoulos, Shiwakoti and Beining, 2021). Hence, the SD problem (S1) is articulated based on the derived LCA goals, objectives and scope to align LCA and SD components and enhance the clarity of the approach. In the next step, the dynamic hypothesis for the model is formulated (S2), considering step S1 and exploring the current knowledge of similar systems and plausible models. The SD model simulation and formulation (S3) is chosen as the following process for understanding the model design. This process also acts as the data information exchange centre in the C-DLCA framework. In the proposed framework, listing the LCI framework requirements (L2a) is recommended, then connecting with step S3 to understand the required inputs for DPI calculations and the dynamic hypothesis modelling (S2) outcome to understand the consumer preference survey outcomes. This step is a proactive measure to ensure that all required parameters are collected while executing the DCE component.

The DCE and SD components (S2, (C1, C2, C3), and S3) are integrated by modifying previous work (Wang, Lai and Chang, 2016; Jiang, 2019, figs 3–6). The customised integration demonstrates the capability to simulate and analyse consumer transition behaviour to car-based MaaS. The DCE model has three components defining the sample and design of the survey instrument (C1), DCE model integration employing the chosen choice-based conjoint assessment technique (C2), and analysis based on the MNL method (C3). The DCE outcome is the first quantitative data input in the model (**D1a**). The simulated data outcomes **D2** and the direct inputs from DCE results to calculate DPI (**D1b**) are fed into the DPI calculation process (L2). The DPI represents the LCI step in the conventional LCA, integrating temporal characteristics (see Section 3.3.5). The DPI results process the dynamic LCA results (L3) with the support of external LCA databases, such as GREET model (Wang *et al.*, 2021). The data outcomes **D4** to **D7** follow the testing and calibration (S4) and policy design and evaluation (S5) SD process steps via the data and process exchange step S3. The LCIA scenario analysis and interpretation (L4) is designed to align with the defined policy scenarios (S5) in the SD model iteration. The data flows represent the chosen hybrid approach of the SD and LCA methods instead of following the rigid approach from LCA to SD or vice-versa, as discussed in Section 3.3.5. Sterman's five-step iterative process facilitated this non-linear iteration process.

The C-DLCA methodology framework provides a solution by filling the gap between combining consumer preference and dynamic LCA work. It provides a structured solution to answer the key research question: 'What is the impact of the transition from private car use to car-based sharing economy modes on GHG, considering consumer preferences and fleet technology changes?'.

The application of the framework to analyse the chosen case study and determine the answers to the key research question is as follows. Sections 4.2 to 4.6 establish the model design from steps L1, S1, S2, L2a and S3. SD policy scenarios are defined in Section 6.3. The model design establishment shown in Figure 4-2 represents the above scope.

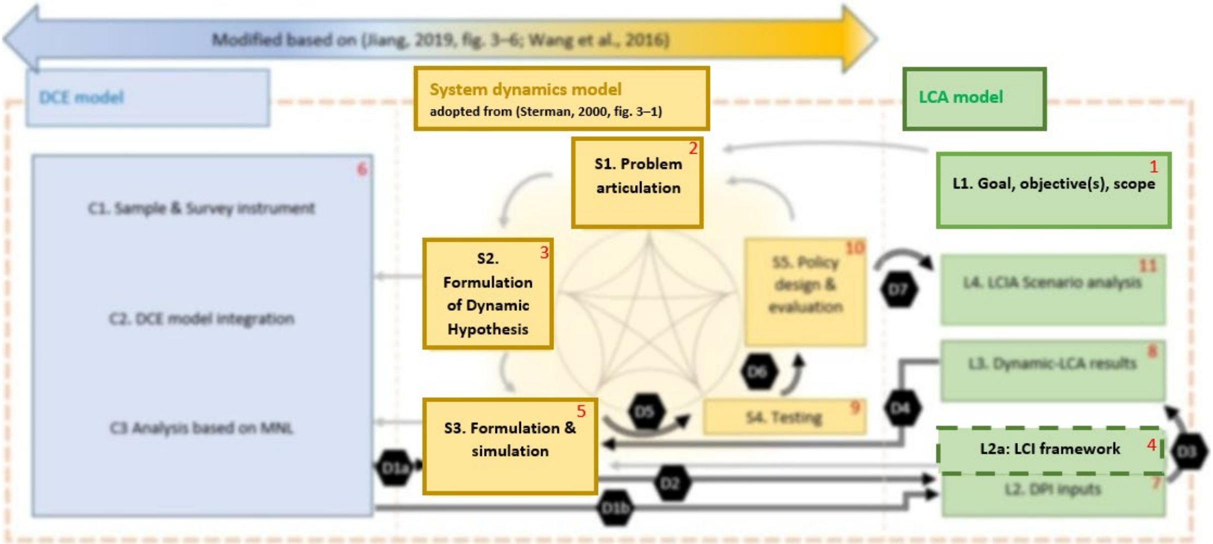

Figure 4-2 C-DLCA methodology framework components relevant to model applications from Sections 4.2 to 4.6

The results of DCE, SD and dynamic LCA modelling are presented in Chapters 5, 6 and 7, respectively.

4.2 LCA model design (L1)

The LCA model design follows ISO 14040 principles (ISO, 2006). The model design supports the first step (L1) of the C-DLCA methodology framework. It starts with defining the goals and objectives (Section 4.2.1) and then selecting the scope and functional unit (Section 4.2.2). This step also lays the base for the LCI, LCIA and interpretation phases, as discussed in Sections 4.5 and 7. The LCA model design is the key methodological step to generating life-cycle GHG emission results of the transition to car-based MaaS by employing the C-DLCA framework.

4.2.1 LCA goal & objectives (L1)

The goal of the LCA is developed based on the defined research question and chosen case study in Section 3.1 to generate the required results. Thus, the goal is defined as 'analysing the GHG impacts of the transition from private car use to car-based sharing economy modes in an average round-trip to/from work journey in the USA, considering the consumer preferences and fleet technology changes'. Carpooling, solo-ride sourcing, and pooled-ride sourcing have been chosen as the car-based sharing economy modes (Section 3.1). The use of a private vehicle for the round-trip to work forms the business-as-usual (baseline) scenario. The availability of the data sources and the required accuracy of the results to integrate into the C-DLCA model are also considered during LCA goal setting. The LCA design sets the groundwork enabling interested parties to make digestible, informed decisions during the results generation. Mobility service providers, policymakers and interested users are identified as the interested parties of this study.

4.2.2 LCA scope and functional unit (L1)

The scope of the LCA study is kept comprehensive to cover both car-based MaaS and private vehicle usage. The scope of the LCA considers the fleet (the product) utilised or impacted in the transition to MaaS. Hence, the production[8] and EoL phases are included in the LCA scope other than the conventional use phase. Incorporating the technological elements representing pre-manufacturing, manufacturing, use, and post-manufacturing is critical in considering the applicability of total life-cycle principles in fleet environmental assessments (Jawahir *et al.*, 2006; Badurdeen *et al.*, 2009; Hapuwatte and Jawahir, 2019). It also expands the analysis to integrate absolute sustainability components by considering the utilisation of scrap metals in vehicle manufacturing (cradle-to-cradle aspect) (Bjørn and Hauschild, 2013). Henceforth, the extension of production and EoL phases enables the integration of the temporal impacts when considering the nature of sharing economy assets that frequently upgrade to newer technology and achieve maximum product longevity in a more brief lifespan. The decision also supports integrating the impacts of vehicle lightweighting and increasing survival trends into LCA. Relevant external factors, such as electric grid and refinery GHG emissions have been considered to represent indirect (Scope 2) GHG emissions (Jenn, 2020). Refinery and electricity grid impacts are also considered part of the scope, including the changing electricity grid GHG factors. Therefore, a full life cycle (cradle-to-grave) is chosen as the scope for the selected case study, including the changes in powertrain systems, different car body styles in the fleets, and incorporating the sharing economy based MaaS consumer preferences compared to conventional linear economy users. However, land

[8] Term production is used in this thesis to represent the total emissions relates with raw material and vehicle manufacturing process

consumption changes, such as transportation infrastructure, are excluded on the basis that the impact of the changes in active fleet size is linear for static land consumption (Firnkorn and Müller, 2011), and the targeted impact category is GHG emissions for this study.

Figure 4-3 shows the importance of considering fleet technology and the scope, cradle-to-grave in the life cycle GHG emissions of car-based MaaS modes. The adoption of HEV and BEV sedans in carpooling, solo-ridesourcing, and pooled-ridesourcing has reduced GHG emissions compared to petrol-driven private vehicle fleets by 40% to 46% and 55% to 62%, respectively. As shown in Figure 4-3, the adoption of SUVs in carpooling, solo-ridesourcing, and pooled-ridesourcing has shown an increase in GHG emissions compared to petrol-driven, HEV and BEV private vehicle fleets: 8% to 28%, 21% to 27%, and 3% to 15%, respectively. The results highlight the importance of integrating the powertrain and body style changes in GHG assessments of the car-based shared mobility mode. These results suggest that integrating temporal changes in the fleet powertrain composition is significant in GHG emission assessments of car-based MaaS modes.

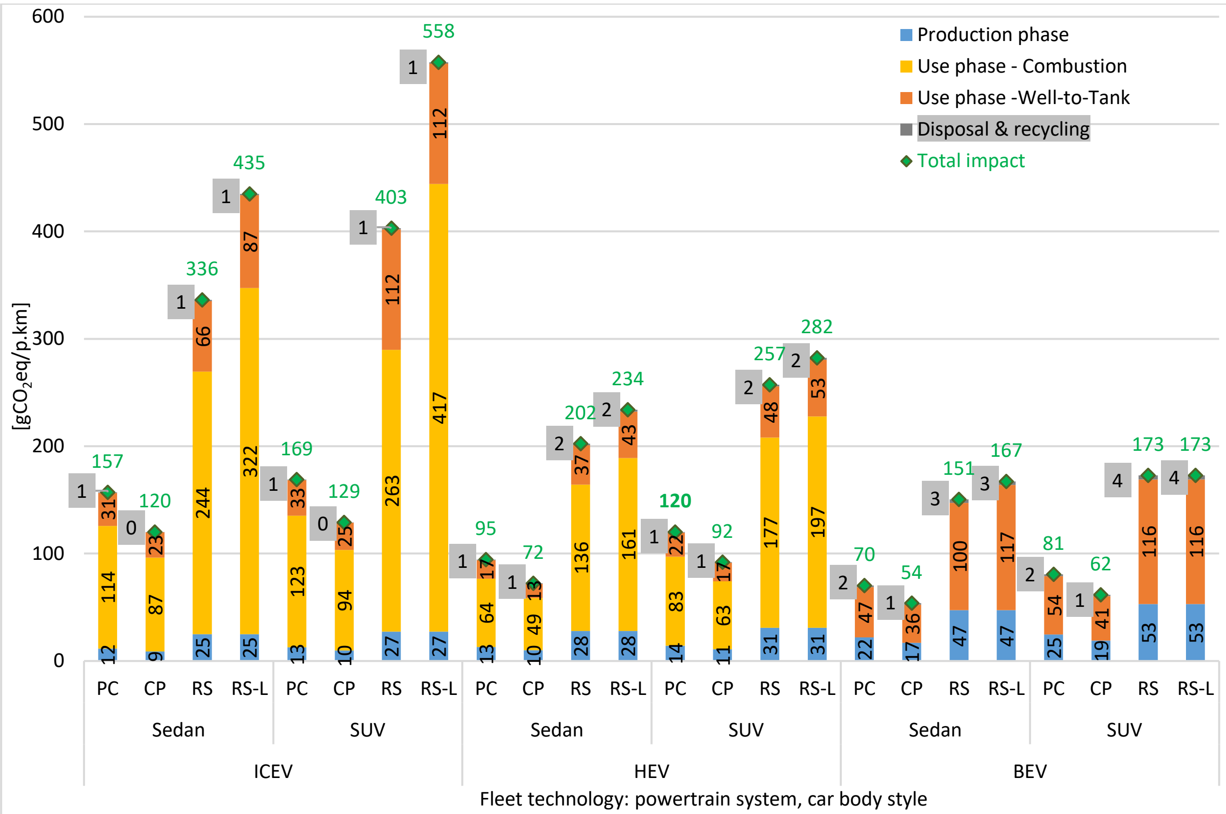

Figure 4-3 Life cycle GHG impacts of the transition to different technologies of MaaS fleets

Notes: PC – private vehicle, CP – carpooling, RS-ridesourcing, RS-L – ridesourcing using a large body type vehicle

Selecting a service-based functional unit is essential for interpreting the LCA results of the chosen sharing economy-based MaaS modes (Henao, 2017; Union of Concerned Scientists, 2020b). Hence, p.km is chosen as the functional unit for interpreting the C-DLCA results. This unit (p.km) is employed to compare car-based MaaS against private vehicles, the baseline scenario selected for this study. It represents mobility, the prime function of personal mobility modes. It allows a comparison between the MaaS modes by considering the net occupancy rates. In summary, service-based p.km is a better unit than conventional distance-based units. It links a key SD modelling outcome to the number of users (passengers) and their influence on GHG emissions.

The GHG emissions of car-based MaaS have shown 26% and 17% GHG reductions in carpooling petrol-driven and BEV fleets, respectively, by applying the lightweighting scenarios of Elgowainy et al. (2016). As shown in Figure 4-4, vehicle lightweighting provides a solution for reducing GHG emissions in MaaS fleets, specifically in conventional powertrain-driven vehicles[9]. The findings further highlight that the choice of raw materials utilised for vehicle lightweighting affects the final GHG emissions, aligned with Milovanoff et al.(2019).

The latest GREET model has been chosen as the life-cycle GHG assessment tool (Wang et al., 2021), and its database is extensively used. The GREET model values are utilised as the LCI inputs, and their calculated GHG emission values are used to derive GHG outcomes. The model also provides the lightweighting scenario identified as a technological change to integrate LCA modelling (Section 2.4.3). The timely-varied lightweighting scenario LCI outcomes were utilised as DPI inputs. The LCI formulation (L2a) is presented in Section 4.5.

[9] The full modelling data can be found in (Fernando *et al.*, 2020)

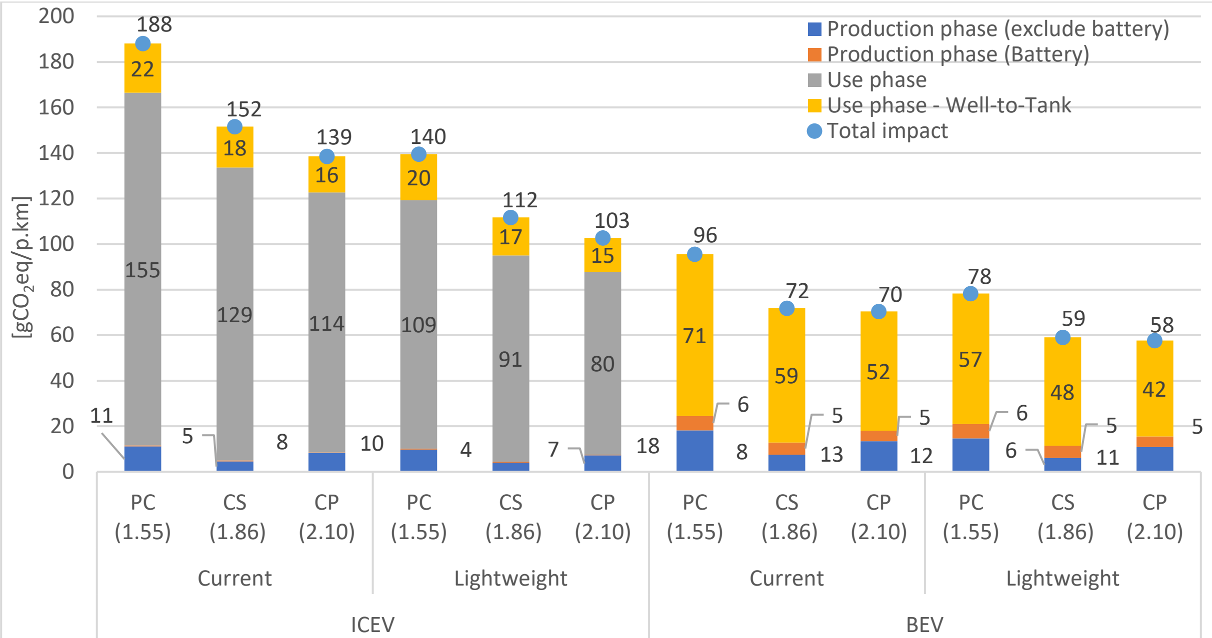

Figure 4-4 Life cycle GHG emissions of car-based MaaS modes: effects of lightweighting and electrification

Note: Occupancy rates are indicated in parentheses. PC – private vehicle, CS – carsharing (station-based), CP – carpooling. ICEV – internal combustion engine vehicles, BEV- battery electric vehicles

4.3 SD model problem articulation (S1)

The C-DLCA methodology framework employs the SD modelling approach as the model interface and enables the integration of consumer preferences and dynamic LCA. A five-step iteration process approach has been adopted to establish SD modelling (Sterman, 2000, chap. 3.4). It provides an interface to combine consumer preferences and LCA and enables revisions in earlier steps (Section 3.3.2).

SD modelling starts with problem articulation, the first of Sterman's five steps (Sterman, 2000, pp. 85–89) and Step 2 (S1) in the C-DLCA framework. Problem articulation initiates the construction of an SD model to represent the system for studying the problem. The defined key research question is articulated as an SD model problem. Employees shift from the use of private vehicles to car-based MaaS. Hence, personal mobility fleets (private vehicles and MaaS) are identified as the key variables to consider in answering the problem. Key variables can incorporate temporal and causal relationships into the SD model by aligning with the defined LCA goal (Section 4.2.1). The SD problem articulation step complements step L1 in Figure 4-1 and supports integrating the temporal and causal elements in the expected dynamic LCA results. The rest of the key components that define the system boundary of the problem articulation (Richardson and Pugh III, 1981, chap. 2.1; Sterman, 2000, pp. 89–94) are discussed in Sections 4.3.1 and 4.3.2.

4.3.1 Reference mode

The reference mode (dynamic problem definition) explains the historical and possible future behaviours of the key variables. The reference mode of the user transition to car-based MaaS choices has increased based on their historical behaviour (see Section 2.1.1). However, there are changes between the modes. The reference mode of personal mobility fleets has shown significant changes and has revealed temporal aspects, as explored in Section 2.4. Hence, the identified key variables incorporate the market dynamics through their reference modes into the SD model, so the expected dynamic LCA results include temporality and causality features. Also, those link with the defined functional unit of the LCA.

4.3.2 Time horizon

The time horizon (simulation or modelling period) is defined based on the chosen MaaS modes (alternatives), historical behaviour and dynamic problem definition related to the anticipated changes. The model starting time is defined from 2014, considering the starting year of pooled-ridesourcing, the newest out of the three chosen MaaS modes (Uber, 2022). Historical data on carpooling and past estimated values are also considered when estimating the initial values of the stocks. The year 2050 was chosen as the end of the SD simulation, considering the market dynamics in powertrain types and vehicle body styles (see Section 2.4.1 and 2.4.2). Significant changes in personal mobility fleets are expected based on policy changes (The White House, 2021), transport network company commitments (Lyft, 2020; Uber, 2020), and auto manufacture commitments (Foote, 2021) from 2030 onwards in the US. Increases in vehicle longevity (Elgowainy *et al.*, 2016; Davis and Boundy, 2021, pp. 3–20) and market demands (McGuckin and Fucci, 2018, p. 66; Cozzi and Apostolos, 2021) are dynamic and change quickly. As a whole, a longer simulation time would increase uncertainty.

The identified problem characterisation, reference mode and the chosen time horizon for understanding behaviour are addressed in Section 4.3.2.

4.4 Establishment of the dynamic hypothesis (S2)

The dynamic hypothesis guides modelling structures by understanding behaviour through current theories on the problem. Richardson and Pugh III (1981, p. 55) define it as "a statement of system structure that appears to have the potential to generate the problem behaviour", and Sterman (2000, p. 95) refers to "a working theory of how the potential problem arose". Hence, in this study, the dynamic hypothesis initiates the conceptualisation of consumer preference integration into dynamic LCA calculations based on the articulated problem in Section 4.3.

An initial dynamic hypothesis is defined based on the identified two key temporal variables, MaaS users and fleets, in Section 4.3. The Bass diffusion model was identified as a theory explaining the transition of potential adopters to active adopters in the early innovation and market maturity phases. The selection considered adopting the model in different market maturity levels of the chosen car-based MaaS modes. The literature findings in Section 2.2 provide empirical evidence for the dynamic hypothesis on key variable MaaS user behaviours. Carpooling employees have been declining since 2012 (US Census Bureau, 2020a). Meanwhile, solo- and pooled-ridesourcing users are likely to grow further (Rayle *et al.*, 2016; Schneider, 2021b, 2021a). The literature also explains consumer preference attributes that influence MaaS user adaptability (Section 2.3). In summary, the Bass diffusion model has been chosen as the initial dynamic hypothesis for the transition to shared mobility models.

Furthermore, changes in personal mobility fleets were also observed based on historical behaviour (Section 2.4). The forecasted changes in the powertrain types and vehicle body style composition provide a preliminary dynamic hypothesis for starting the SD modelling. However, it was also observed that the changes in fleet technology elements were significant within a shorter period. The influences of vehicle technology changes on MaaS users and personal mobility fleets are explained by employing the SD modelling technique in Chapter 6. The endogenous elements that ensure the causality characteristics of the identified preliminary dynamic hypothesis are discussed in Section 4.4.1.

4.4.1 Endogenous explanation and SD model boundary

The endogenous variables of the study are based on the variables that depict consumer preferences and MaaS user changes in the personal mobility fleet. The key research question demands the integration of consumer preferences and fleet technology changes into GHG emission calculations of the dynamic LCA. Hence, significant changes in fleet technology compositions (which are also temporal) and their influence on consumer preferences are captured as important endogenous feedback in the dynamic hypothesis process. However, none of the identified consumer attributes is endogenous or related to the articulated SD modelling problem in Section 4.3, the established LCA goals in Section 4.2.1 and the key research questions in Section 2.8. Therefore, the SD model boundary is defined to further understand the endogenous explanation. Table 4-2 provides the model boundary chart of the SD model to determine the dynamic LCA results for the transition to MaaS.

Table 4-2 Model boundary chart – Transition to MaaS and interrelated GHG changes

Endogenous – *arising from within*	Exogenous – *arising from without*	Excluded
Consumer preference: body style	Trip fare distribution	User transition inter MaaS models
Body style distribution in fleets*	Trip duration distribution	Second-hand vehicle sale
Fleet size*	Passenger number distribution	Macroeconomy changes
	Employment change and Car-based mobility %	Fleet operational changes (e.g., deadheading improvements)
	Required cars per trip* (to calculate fleet size)	Irregular mobility changes (e.g., COVID-19 pandemic)
	Powertrain distribution*	
	Electricity grid & Well-to-Tank GHG emissions*	
	Vehicle lightweighting trend*	
	Secondary raw material consumption*	

Note: *parameters related to LCI framework design, see Section 4.5

The endogenous variables are determined based on their contributions to the LCA calculation and mapping of causal structures. This extended step helps understand the requirements of the consumer behaviour experiment, considering the LCA model needs. This step also links the identified reference mode(s) and the key variables of the SD model. Based on the above, two out of the five consumer attributes identified in Section 2.3 support causality and contribute to LCA analysis. These are *powertrain types*[10] and *body style* compositions in personal mobility fleets. However,

[10] Attributes are typed in italic fonts to distinguish from the rest of the text

the composition of the fleet powertrain system is largely externally determined by government policies (The White House, 2021) and other requirements (see Section 2.4.1). Therefore, vehicle body style explains the key endogenous feedback loop that considers consumer preference inputs. This selection is based on the shared mobility mode app providing decision-making attributes (see Figure 1-1), the significant market changes from sedans to SUVs, and their GHG impacts (Section 2.4.2).

Key exogenous variables are also identified to complete the dynamic hypothesis process. Four consumer preference attributes, excluding the identified endogenous variable *body style* are considered exogenous variables in this study. Three technical variables affecting the LCA results are also identified as exogenous factors. These are (a) vehicle lightweighting, (b) survival rates, and (c) electric grid GHG changes. These variables provide direct inputs for calculating vehicle production and fuel/energy processing GHG emissions. The parameters that affect the number of commuting employees using private vehicles and fleet size are also included in the listed exogenous variables.

The excluded variables are listed in the last category of Table 4-2. The number of influencing variables in the personal mobility industry is significant, and incorporating them into an SD model is impractical for many reasons. Factors such as macroeconomic changes are complicated to integrate, and inter-mode user transition and second-hand vehicle sales are excluded based on data accessibility constraints. Irregular events that affect overall mobility (such as COVID-19 impacts) are also excluded.

The boundary-setting exercise supports the hypothesis of the SD model, using the Bass diffusion model to explain the overall SD model behaviour.

4.4.2 Adoption of the Bass model

The transition to MaaS is hypothesised based on the Bass model, considering the influence of consumer and fleet changes (Bass, 1969; Sterman, 2000, chap. 9.3.). The Bass model follows innovators and imitators influenced by advertisements and WoM, respectively. The behaviour of the transition from employees commuting by private vehicles to active MaaS users (adopters in the Bass model) is modelled to represent the resulting stock (see Figure 4-5). The transition to MaaS users is identified as the reference mode.

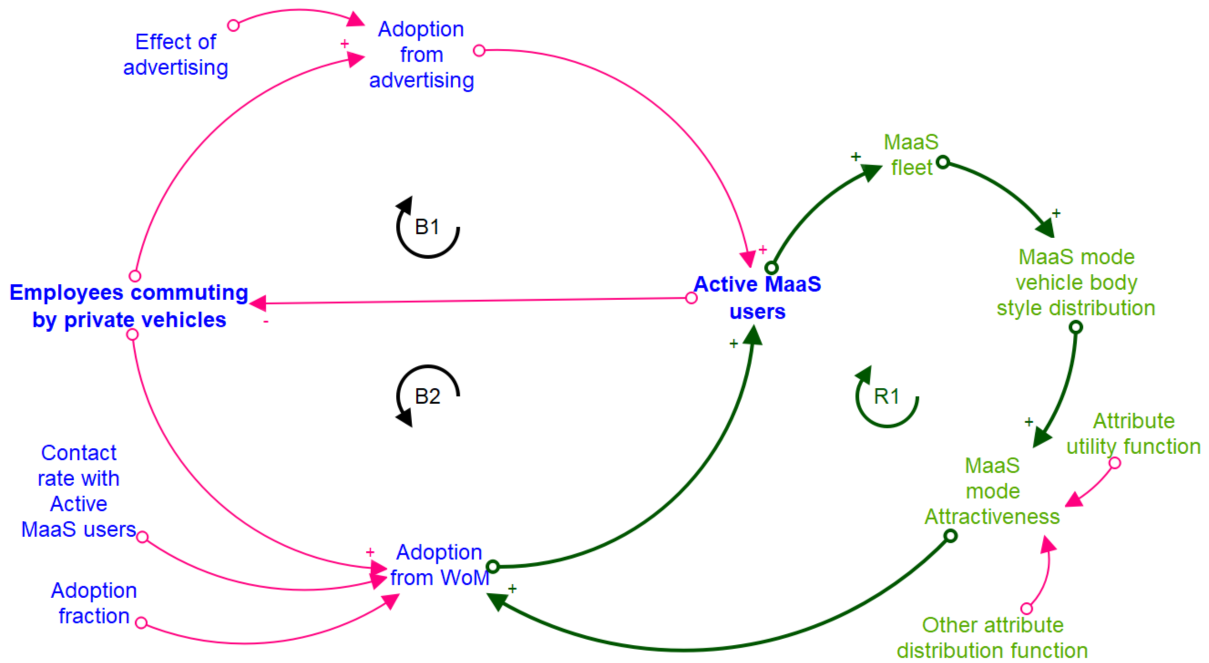

Figure 4-5 Causal loop diagram - Transition to shared mobility modes

Note: adopted from (Bass, 1969), Variables in green fonts – introduced to integrate the consumer preferences

A causal loop diagram representing this transition is shown in Figure 4-5. Causal loop diagrams, also referred to as influence diagrams or, in more mathematical circles, directed graphs, are commonly used to represent the feedback structure of a system (Richardson and Pugh III, 1981, pp. 25–30; Sterman, 2000, chap. 5). Positive and negative signs at the end of the arrow indicate the polarity of the feedback loop. A positive sign indicates that the variables at the opposite ends of the arrow tend to move in the same direction.

The causal loop diagram in Figure 4-5 supports the articulated SD model problem and the derived dynamic hypothesis. Feedback loop **B1** represents the innovators, generally the early adopters following advertisements. Loop **B2** describes imitators who shift based on the influence of WoM. Both loops represent the negative or balancing (self-control) feedback behaviour of the system.

The additional variables Mode attribute distribution and MaaS mode attractiveness are introduced to integrate consumer responses into the transition to MaaS. This creates a **reinforced (self-reinforcing) feedback loop** (**R1**). However, the polarity of this feedback loop depends on the results of the variable MaaS mode attractiveness, introduced based on the product attractiveness concept by Schmidt & Gary (2002) (Section 2.5.2). The feedback loops in the causal loop diagram in Figure 4-5 also help to understand the reference mode (the pattern, behaviour over time (Sterman, 2000, p. 90)), confirming the dynamic hypothesis of the SD model.

As a result of the above explanations, active MaaS users and fleets are recognised as the key stocks and are aligned with the identified reference modes in Section 4.3.1. These stocks also support the endogenous explanation of the system introduced in Section 4.4.1. These outcomes are employed to establish the LCI framework, as explained in Section 4.5. In Section 6.1, the Bass model is operationalised into SD modelling work to analyse the transition to MaaS.

4.5 Life cycle Inventory framework (L2a)

The LCI framework (L2a in Figure 4-1) provides the required LCI inputs for the process step of formulating the simulation model (S3). Step L2a is an extra step identified in the C-DLCA framework beyond typical dynamic LCA work. It supports the hybrid approach of integrating SD and LCA methods and begins with the defined hypothesised model (Sections 4.4.1 and 4.4.2). The hypothesis process supports identifying the required input data fields to calculate the LCI. Next, they are categorised based on the following two definitions: First is the source of the data field identified in the model boundary system in Table 4-2. The second classification is based on dynamic LCA good practices: data fields within DPI or dynamic inventory analysis and dynamic system inventory (Sohn *et al.*, 2020; Su *et al.*, 2021). Dynamic system inventory is not considered in the proposed methodology. The required variables for the LCI framework to derive the DPI profile are introduced as * in Table 4-2.

The defined model boundary and LCI framework provide inputs for constructing the formulation and sub-model structures in Section 4.6. The quantitative modelling and outcome of this step, DPI work, are presented in Section 7.1.

4.6 Formulating the simulation model (S3)

Formulation represents the connecting interface of consumer preference survey outcomes and LCI results in SD modelling. As presented in the proposed methodology framework, the formulation process enables the hybrid approach adopted in this research by connecting and functioning as a data-exchange process to incorporate SD and LCA methods. As shown in Figure 4-1, it links data from consumer preference (**D1a**), LCI input data (**D2**), LCIA outcome data flow (**D4**) and finally connects them all with the step, Testing (S4) with the data flow D5. Step S3 also facilitates information flow from the LCI framework to the consumer preference study. Hence, formulating a simulation model is complex. Overall, three sub-models are introduced to simplify the formulation step and are presented in Section 4.6.1.

4.6.1 Sub-model structure

The sub-models are utilised to explain deeper information flows (Sterman, 2000, p. 100). The problem articulation and model boundary have already determined the model requirements and composition. Figure 4-6 presents a simplified sub-model to illustrate the data and information links associated with the previously identified formulation of the simulation model. The defined research questions and goals of the LCA study and the problem articulation outcome of the SD model are considered to derive these sub-models. Hence, the three identified sub-models are the transition to MaaS, fleet behaviour, and the dynamic LCA (indicated as D-LCA in Figure 4-6) calculation. Three sub-models explain the behaviour of the transition model by incorporating consumer preferences, changes in fleet adoption based on the powertrain and body style changes and, subsequently, their overall influence on dynamic life-cycle GHG emissions. They are aligned with the key stocks identified in Section 4.4.2. Thus, the three sub-models support the execution of the formulation step aligned with the identified key stocks of the model.

Sub-models transition to MaaS and fleet behaviour are explained in Chapter 6, and the dynamic LCA calculation is described in Chapter 7.

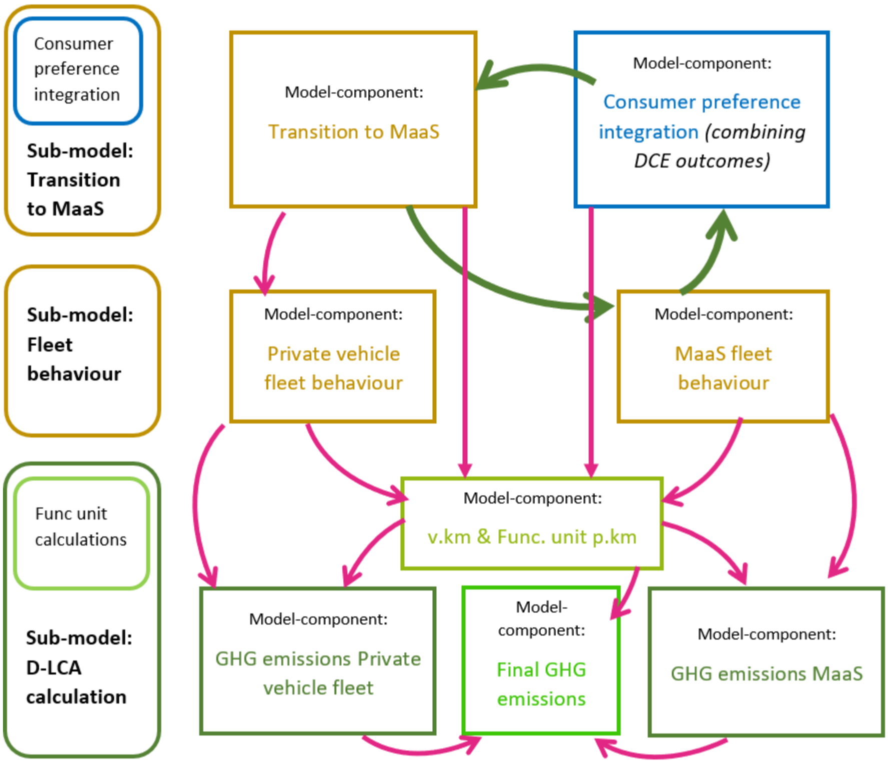

Figure 4-6 Sub-model diagram for the SD stock and flow model of the transition to car-based MaaS on GHG emissions

Note: the detailed stock and flow diagram can be found in Figure E-1 in Appendix E

4.7 Summary

This chapter introduced the novel methodological framework, C-DLCA, to overcome the barrier of incorporating consumer preferences into dynamic LCA work. The introduced framework supports the causality and temporality of fleet dynamics and consumer preferences and subsequently links the behaviour to dynamic life-cycle GHG outcomes. Therefore, the methodology framework is an approach to answer the key research question: What is the impact of the transition from private car use to car-based sharing economy modes on GHG emissions, considering consumer preferences and fleet technology changes?'.

The overall framework adhered to ISO 14040-based LCA principles and started with the LCA model establishing (L1) the LCA goal and objectives. While the LCA goal aligns with the key research question, a full life-cycle scope is identified to produce more meaningful results based on sharing economy characteristics. Chapter 7 examines the LCI, LCIA and interpretation phases.

SD modelling started with the problem articulation (S1) step that aligned with the research question and the set LCA goal. The modelling period is set from 2014 to 2050. The dynamic hypothesis was generated based on historical data and the Bass model (Bass, 1969). The endogenous explanation supports the development of a clear model boundary that identifies endogenous, exogenous and excluded variables. These are considered in the LCI framework (L2a) step before formulation (S3) to determine the required information.

Three sub-models (transition to MaaS, fleet behaviour and dynamic LCA calculation) are chosen to execute the formulation of the simulation model. They are also aligned with the identified key stocks and are examined in Chapters 6 and 7. After considering the US-based historical data and the forecasted policy and market changes, high BEV adoption is adopted as the policy scenario. It is also linked with life cycle GHG emission changes and provides different implications for the chosen MaaS modes.

5 CONSUMER PREFERENCE SURVEY RESULTS

Publication relevant to this chapter

Fernando, C., Buttriss, G., Yoon, H.-J., Soo, V. K., Compston, P., Kim, H. C., De Kleine, R., & Doolan, M. (Under review). Characterising the consumer preferences of car-based mobility for a round-trip to work. *Journal of Consumer Behaviour*.

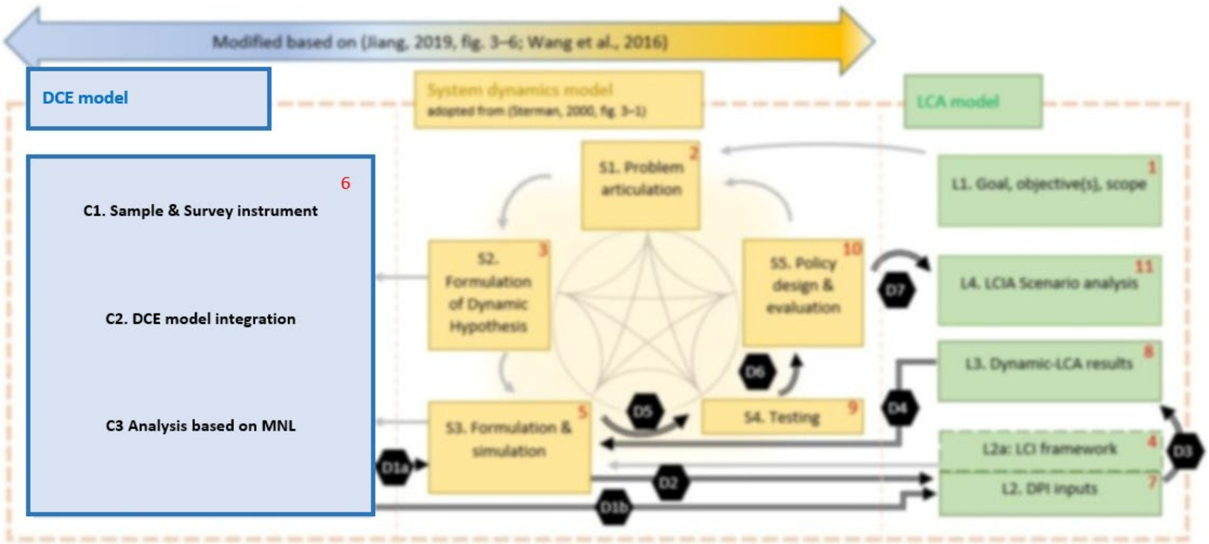

Figure 5-1 C-DLCA methodology framework components relevant to Chapter 5

Introduction

This chapter presents the primary data collected to help analyse the identified case study. The scope of this survey is an average round-trip to/from work in the US (see Section 3.1). Chapter 5 begins with the survey objectives. The survey sample selection, preparation and execution are presented in Sections 5.1 to 5.3. The analysis phase is in Sections 5.4 to 5.6. Section 5.6 further explains the utilisation of primary data outcomes in the dynamic LCA model to generate the GHG emissions of the transition to car-based MaaS. The chapter ends with a discussion (Section 5.7) and a summary.

5.1 Market survey objectives

Market survey objectives are based on the derived research objectives in Section 1.3 and ARQ2: What is the significance of consumer attributes influencing the transition to car-based MaaS? Based on the C-DLCA framework, the market survey is the only primary data source that combines consumer preferences and behaviour inputs to determine the life-cycle GHG emissions of the transition to car-based sharing economy modes. The survey question is defined to focus on the targeted market, as introduced in Section 3.1.

Survey question:

'What attributes influence US consumer preferences for car-based mobility modes for commuting to work?'

The following survey objectives were defined to answer the survey question:

1. Characterising the consumer preferences of attributes and their levels (utility values)
2. Determine the influence of demographics on attributes and utility values by achieving a national representative sample for sex and age

5.2 Survey sample selection (C1)

The sampling was developed to cover a range of demographics of employees who commute to work using private mobility modes. The sample was chosen based on the respondents' a) sex, b) age, c) educational attainment, e) gross household income, and f) household size. The representative sample approach was operationalised considering the above characteristics and not specifically from the divided sub-groups (not following the stratified sampling approach) (Acharya *et al.*, 2013). Employees who used public transport were not part of the sampling process based on the set survey objectives that aligned with the survey question. Sex and age representation focused on including appropriate employee diversity levels (Prieto, Baltas and Stan, 2017; Davlembayeva, Papagiannidis and Alamanos, 2019; Flores and Jansson, 2021). As identified in Section 2.2, household income and educational attainment were also considered in terms of their influence on the decision-making of the transition to car-based sharing economy modes of to/from work journeys (Clewlow and Mishra, 2017; Schaller, 2018). The transition to pooling modes depends on household size and vehicle ownership (McGuckin and Fucci, 2018). These factors were also captured beyond the consumer demographics. As a whole, the above demographics are considered in sampling to increase the accuracy of the survey.

The sampling plan was developed to cover a range of US cities based on geography and public transit levels. Car-based MaaS modes largely exist in cities (Carroll, Caulfield and Ahern, 2017). As discussed in Section 2.2, their usership is influenced by the population density of the location and the household vehicle availability (Firnkorn and Müller, 2011; Vasconcelos *et al.*, 2017; McGuckin and Fucci, 2018, p. 65).

Thus, cities were selected by the following two criteria:

> First, at least three cities to cover the US Census Bureau-designated regions (US Census Bureau, 2013) to represent geographical presence and population.
>
> Then, select at least one city to cover low, medium and high-public transit levels based on public transit ridership below 10%, 11-20%, and 21% above, respectively (US Census Bureau, 2019b).

The sample locations were selected on average 10.3 km radius (one-way distance of an average round-trip to work in the US) from the central business districts of the chosen cities.

The Delphi method (Dalkey and Helmer, 1963) has been employed to finalise the sample locations. Four mobility experts representing academia and industry from the US were invited to contribute to establishing consensus on the cities and priority orders. The expert group opined their views based on the above two criteria after multiple iteration processes. The experts also provided general guidance to avoid sampling conditions that deviate from the population (e.g., New York City sampling was limited to less than 5% of the total sample). The outcomes are shown in Table 5-1. The summary of the demographics of the sample is presented in Section 5.4.2.

The planned sample size for the survey was 2,851. This number was generated considering the commuting worker population of the chosen sampling locations (Metropolitan Sampling Areas) based on the high/low transit composition and geographical coverage (Statistical Regions) (US Census Bureau, 2013, 2019b, 2021), and maintaining the sampling consistency with the two largest commuting surveys in the US (Federal Highway Administration (FHWA), 2018; US Census Bureau, 2019a). The panel availability, budgets and timely survey completion were also considered while finalising the sample size. The chosen value is far above the required respondents (600) based on the DCE model combinations requisites (see Section 5.3.3).

Table 5-1 Sampling plan based on the DELPHI method outcome and achieved sample sizes

US Census Region	Cities: Planned sample size# | Achieved sample size			Status [%, planned vs achieved]
	High-public transit	Medium-public transit	Low-public transit	
Northeast	1,234 | 1,274 Boston MA: 350 | 347 Cambridge MA: 150 | 42 Philadelphia PA: 400 | 474 New York NY**: 62 | 89 Jersey City NJ: 50 | 57 Washington DC: 222 | 264	140 | 122 Buffalo NY: 80 | 83 New Haven CT: 25 | 21 Bridgeport CT: 15 | 18	94 | 98 Pittsburgh PA: 97 | 98	92%
Midwest	262 | 263 Chicago IL: 262 | 263	74 | 80 Minneapolis MN: 74 | 80	144 | 148 Cleveland OH: 144 | 148	104%
South	50 | 55 Arlington VA: 50 | 55	104 | 128 Baltimore MD: 100 | 102 Miami FL: 4 | 26	255 | 289 Atlanta GA: 185 | 212 New Orleans LA: 77 | 77	115%
West	163 | 165 San Francisco CA: 163 | 165	174 | 183 Urban Honolulu HI: 50 | 56 East Los Angelis CA* Portland OR: 40 | 92 Bellevue WA: 84 | 35 Fremont CA*	157 | 163 Los Angelis CA: 157 | 163	103%
Total	1,709 | 1,757 (102%)	492 | 549 (112%)	650 | 698 (107%)	105%
	2,851 | 2,968			

Notes: Sampling locations were finalised considering the geographical representation and public transit usage. The number calculated based on the US Census Bureau (2013, 2019, 2021), *excluded due to panel constraints, **less than 5% of the total sample. Achieved sample sizes are indicated in blue coloured fonts

After obtaining ethics clearance, the survey was conducted from 23 April to 23 May 2021. The ethical aspects of this research have been approved by the Australian National University Human Research Ethics Committee (Protocol 2020/682) under the project title 'Consumer attitudes and behaviours in the decision-making process of the transition to shared mobility modes'. Approval was granted to sample commuting workers (aged 18 years and older) from metropolitan and mid-sized cities in the USA. A de-identified panel was sourced from an ESOMAR[11]-compliant and ISO 20252:2019 certified panel company.

[11] the European Society for Opinion and Market Research

5.3 Survey instrument design (C1)

The survey instrument is designed in four parts. After a short introduction, the first part introduces the screening questions. The screening questions ensured that the respondents were employees who travelled to work before COVID-19 from the identified sample locations and were compliant with ethics approval requirements, such as the minimum age to participate. As discussed in Section 2.2, the survey was established to represent the pre-COVID-19 context, considering the significant changes in personal mobility during the pandemic and early recovery periods. The second part aims to understand the choice preferences in transition decision-making based on the combination of attribute levels (Sections 5.3.2 to 5.3.3). The third and fourth parts cover the descriptive questions to profile the respondent demographics and are discussed in Section 5.3.4. Table D-1 in Appendix D presents the complete survey questionnaire.

5.3.1 Survey design and software

The DCE model is adopted to design the consumer survey. As discussed in Section 3.3.3, the model requirements match the survey requirements. Car-based MaaS modes are mutually exclusive choices, and the number of alternatives (brands that are MaaS modes in this study) is more than two (Ben-Akiva and Lerman, 1987). Choice-based conjoint analysis, a type of conjoint analysis, is utilised to operationalise the stated preference-based consumer choice model in the survey.

Conjoint.ly software (Conjoint.ly, n.d.) integrates DCE into the consumer survey. This supports the choice-based conjoint analysis technique and uses the hierarchical Bayesian MNL estimation procedure to perform individual-level preference analysis (Conjoint.ly, n.d.).

5.3.2 Selection of MaaS consumer preference attributes (C2)

The attributes *cost* (journey fare) and *time* (door-to-door journey duration) were chosen based on existing studies (Correia, Silva and Viegas, 2013; Sarriera *et al.*, 2017; Lippke and Noyce, 2020). These are the most commonly used attributes in car-based MaaS studies, including the three selected car-based MaaS modes (see Figure 2-2). The consideration of journey fare represents the consumer's willingness to pay, which differs from solo to pooled shared mobility modes. Hence, the selection supports gauging the relationship of willingness to pay for solo rides compared to a relatively inconvenient pooled trip that characterises extra time and compromises privacy. A similar choice experience can be explored by including attribute time. As shown in Figure 2-2, the other attributes classified under the cost, convenience (Palma and Rochat, 2000; Schaller, 2018) and service quality (Nguyen-Phuoc *et al.*, 2020) categories are not common to all three MaaS modes. Therefore, they are not considered in this study.

The *number of passengers* has been chosen as an attribute to distinguish consumer preferences in the solo and pooled modes. Previous studies on pooled riding modes have used attributes such as interaction comfort (Cui *et al.*, 2020) and privacy concerns (Lavieri and Bhat, 2019) (see Section 2.3). However, they differ in the number of passengers on a journey. The term *number of passengers* excludes the driver in ridesourcing modes. It represents the gross occupancy rate that links with the chosen functional unit, p.km, to analyse the final dynamic LCA results (see Section 4.2.2).

Two non-conventional attributes, *powertrain type* and *vehicle body style* were chosen to integrate the dynamic fleet technology changes in personal mobility. As discussed in Section 2.3.1, this selection captures the MaaS consumer demographics in technology features. The *vehicle body style* attribute provides insights into consumer preference choices, such as the significant uptake of SUVs in personal mobility fleets in the US (Section 2.4). Likewise, the *powertrain type* attribute can measure the consumer preference for fleet electrification trends. Both attributes can measure the influence of consumer preferences on environmental implications. Therefore, the selection of attributes also aligns with answering the ARQ2: 'What is the significance of consumer attributes influencing the transition to car-based MaaS?' and relates this to the environmental consequences of the transition to MaaS.

In summary, *cost* (fare), *time* (door-to-door), *number of passengers, powertrain type*, and *vehicle body style* were chosen as consumer preference attributes for the choice-based conjoint analysis block in the survey.

5.3.3 Design of Choice-Based Conjoint Analysis (C2)

The choice-based conjoint analysis model was designed based on the attributes chosen in Section 5.3.2. Three car-based MaaS modes—a) carpooling, b) solo-ridesourcing, and c) pooled-ridesourcing—were used as alternatives. The attribute levels were determined using two approaches. The first approach considers available market options when deciding on attribute levels. This approach is applied to the *number of passengers, powertrain type* and *vehicle body style*. Only three body styles were assumed to be used for personal mobility, despite the use of light-duty vehicles in the US survey analysis (US EPA, 2021). They are commonly used passenger vehicle body styles: sedans, SUVs and hatches. Three common powertrain types—a) gasoline, b) HEV, and c) BEV—are chosen as the levels for the *powertrain type*. These are presented in Table 5-2 by classification, based on their characteristics. The attribute levels for the *number of passengers* were customised to represent MaaS modes.

The second approach was to find the specific attribute levels for journey *cost* and *time,* considering the actual journey characteristics. A Google map-based study was performed to understand the time range for an average round-trip to work in the US. A few cities were chosen to represent the three public transit classes from different US census regions. The survey was conducted during the morning (city-onwards) and evening (outer-city) rides. Detailed results are presented in Table C-1 and Table C-2 in Appendix C. The carpooling fares were estimated based on this. The time levels representing average to/from work trips were listed based on the literature (McGuckin and Fucci, 2018; US Census Bureau, 2020a). The total attribute level set is presented in Table 5-2.

Table 5-2 Attribute level applicability matrix applied for the Choice-Based Conjoint model

Attribute	Cost* [$][a]					Time: door-to-door [minutes][b]					Number of passengers**					Powertrain type[c]			Body style[c]		
Level	15	19	21	25	40	15	20	25	30	40	1	2	3	4	5	ICEV	HEV	BEV[d]	Sedan	SUV	Hatch
PC	✔	✔	✔	✔	✔	✔	✔	✔	✔	✔	✔	X	X	X	X	✔	✔	✔	✔	✔	✔
CP	✔	✔	✔	✔	X	✔	✔	✔	✔	✔	X	✔	✔	✔	✔	✔	✔	✔	✔	✔	✔
sRS	X	✔	✔	✔	✔	✔	✔	✔	✔	✔	✔	X	X	X	X	✔	✔	✔	✔	✔	✔
pRS	X	✔	✔	✔	✔	✔	✔	✔	✔	✔	X	✔	✔	✔	X	✔	✔	✔	✔	✔	✔

Notes: [a]sRS, pRS- (Uber, 2021b), CP-estimated based on sRS, [b](McGuckin and Fucci, 2018; US Census Bureau, 2020a), [c](US EPA, 2021), [d](Lyft, 2020; Uber, 2020; Berneiser *et al.*, 2021),*cost includes the overall expenses for a journey, including fuel and maintenance, parking, vehicle depreciation, licensing and insurance, MaaS partner profit/markup fees, Transport Network Company /mobility operator profits, etc., **excluding the driver in solo-ridesourcing (sRS) and pooled-ridesourcing (pRS), CP-carpooling

Table 5-2 outcomes programmed into the choice-based conjoint analysis design in Conjoint.ly. Figure 5-2 shows an example of a choice-based joint analysis choice set from the survey. Each respondent answered eight choice sets and had to select the most preferred choice combination out of four (see four columns headed with the alternative in Figure 5-2). Conjoint.ly generated a minimum required sample size of 600. Hence, the planned sample size of 2,851 (see Section 5.2) is well above the software suggestion. Conjoint.ly software's response quality management options are used to enhance survey accuracy. The results were interpreted using 95% confidence intervals.

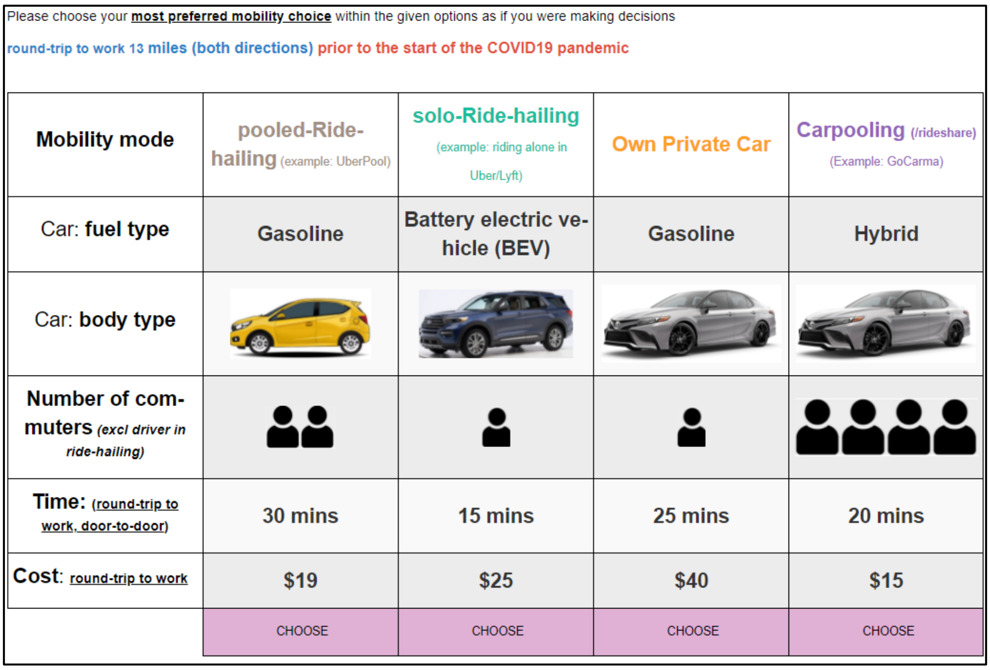

Please choose your **most preferred mobility choice** within the given options as if you were making decisions

round-trip to work 13 miles (both directions) prior to the start of the COVID19 pandemic

Mobility mode	pooled-Ride-hailing (example: UberPool)	solo-Ride-hailing (example: riding alone in Uber/Lyft)	Own Private Car	Carpooling (/rideshare) (Example: GoCarma)
Car: **fuel type**	Gasoline	Battery electric vehicle (BEV)	Gasoline	Hybrid
Car: **body type**				
Number of commuters *(excl driver in ride-hailing)*				
Time: round-trip to work, door-to-door)	30 mins	15 mins	25 mins	20 mins
Cost: round-trip to work	$19	$25	$40	$15
	CHOOSE	CHOOSE	CHOOSE	CHOOSE

Figure 5-2 An example of a Choice-Based Conjoint Analysis block as appeared in the survey

Note: Developed using Conjoint.ly.

5.3.4 Descriptive questions

The descriptive questions were multiple-choice questions in three parts of the survey. The first part examined residential location (city) and frequency of work during the pre-COVID-19 period. The next part, positioned after the choice-based conjoint analysis block, targeted the understanding of respondents' mobility practices, including their familiarity with the three MaaS modes. The last part covered demographic and socioeconomic information, such as sex, age, highest educational attainment, and income. Household details, such as household size, vehicle ownership, and powertrain types, were also included as descriptive questions. The latter question aims to explore user demographics to find behaviour patterns. Four screening questions were included in the first and third parts of the survey to ensure quality responses.

Segregated analyses of consumer demographics are based on descriptive questions. Results were analysed to understand consumer preferences based on demographic factors. In Section 5.4, the sample composition analysis provides an overview of the sample by categorising the respondents according to the above characteristics.

5.4 Survey results – Sample (C3)

The sampling achieved 105% (2,968) of the planned size with minimum deviations. As shown in Table 5-1, the 8% deviation in the locations in the Northeast Census Region was due to panel constraints. However, public transit level-based requirements introduced in Section 5.2 were met by increasing the sample size in other regions to achieve a representative US-wide public transit sample.

5.4.1 Exclusions

A significantly large number of responses (4,881) were rejected based on the survey quality management options. The most extensive removal, 2,785, was based on four screening questions (Q1, Q3, Q5 and Q23). Some of these questions were targeted to comply with the survey ethics conditions, and the rest were qualifier questions. The survey software options triggered more than 2,000 rejected responses, while the remainder were from manual exclusions. A detailed exclusion summary is shown in Table 5-3. These exclusions were reported after the questionnaire was changed based on the soft launch results, targeting 300 qualified samples. Based on the outcome of the soft launch, a few qualifying questions were changed to increase clarity, and a few were introduced to ensure quality sampling. Technical changes were also made to the survey questionnaire to rectify the connecting answers. The soft launch also supported exploring the features in the Conjoint.ly software, the platform used to administer the survey, particularly to activate various quality assurance features. Therefore, a qualified sample is a set of high-quality responses.

Table 5-3 Sampling exclusion summary

Reason	Quantity
Screened out: based on the screening questions Q1: Consent question: if chosen, *I am below 18 years and agree to participate in the survey,* or *I DO NOT agree to participate in this survey* Q3: based on the city before COVID-19 time: if chosen, the option *Other* Q5: based on travel to work – if chosen: *I did not travel to/from work* Q23: qualifier question age: if chosen *<18yrs*	2,785
Conjoint.ly software triggered and excluded:	
Opened the survey link, not continued	1,892
Incomplete	108
Low quality	43
Manually excluded	
Responded time too long or shorter (possible response time was set from 3-40 minutes)	46
Not within the geographical scope (USA)	7
Total excluded	4,881
Qualified sample	2,968
Total responses	7,849

5.4.2 Sample composition

The sample achieved the national representative goal for sex and age, with some minor deviations. Figure 5-3 shows the analysed subcategories. The deviation in the two main sex classes was only 3% compared with the national representative. The most significant variation in age classes compared with the national average was 55–64 years, with a 5% deviation. However, the national representative values were within the confidence intervals for the two most common age classes (25-34 and 35-54), representing 64% of the total sample. Overall, the sex and age characteristics represent the national averages in the sample and are statistically significant.

The household size parameter was determined with deviations from the national average. The sample was skewed towards a larger household density for three or more members. However, the maximum variation within a class was 7%, and household size was not a planned quantitative sample condition but a qualitative indicator of user behaviour. As a whole, these deviations are insignificant, considering the research objectives of the study.

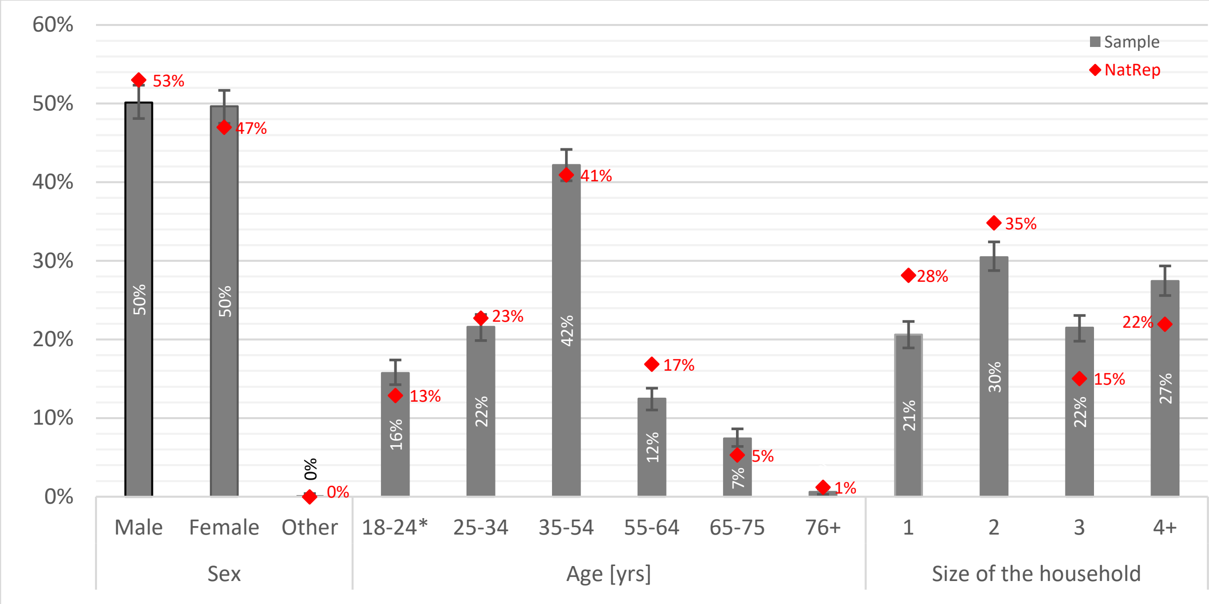

Figure 5-3 Sample composition - Sex, age and size of the household

Notes: National Gender & Age of the Labour force (US Bureau of Labor Statistics, 2020) *including 16 yrs onwards, National Representative (NatRep) Size of the Household (US Census Bureau, 2020c). Whiskers: 95% confidence intervals

The educational attainment of the sample was skewed towards a more educated cohort. A 28% deviation between national representatives and bachelor's and postgraduate qualifications was observed. As shown in Figure 5-4, the most significant variation (15%) was recorded in high school graduate and postgraduate classes compared to the national representative value. In contrast, the household income level was within acceptable tolerance levels compared to the national average. The largest household gross income class (USD 65,000 or above) was within the national representative level and also within the confidence intervals. The largest deviation (5%) was observed in the two combined classes, from USD 50,000 to USD 74,000 income per annum.

The sample behaviour of car ownership was correlated with the status of public transit in respondents' residential locations (see Figure 5-5). Only the Not owned and 3+ cars classes have shown statistically significant deviations based on the transit level. The national representative values represent overall vehicle ownership in households and are unrelated to public transit levels. Hence, it was difficult to confirm the significance of the observed sample bias towards lower household car ownership than the national average. However, the sample was more biased regarding vehicle ownership of the alternative powertrain systems. A significant deviation was observed, with a more than 10-fold increase in sample size for HEVs and BEVs compared to the national average (US Energy Information Administration - EIA, 2020). However, there were no statistically significant observations in powertrain combinations with respect to the transit levels.

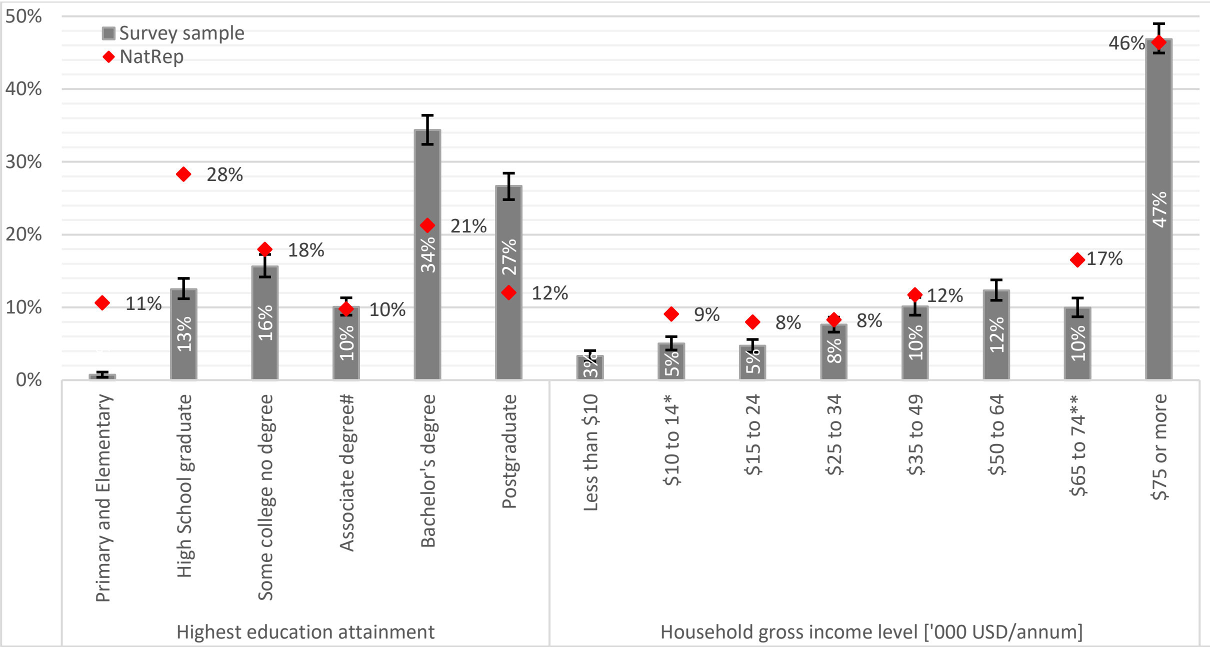

Figure 5-4 Sample composition - Educational attainment and household income

Notes: National Representative (NatRep) Highest Education Attainment (US Census Bureau, 2020b, p. 2019), #including Academic Associate degrees, NatRep Households by Total Money Income (US Census Bureau, 2020d, p. 2019), *including less than $10k, **$50-74k (no split figures available for $50-64k and $65-74). Whiskers: 95% confidence intervals

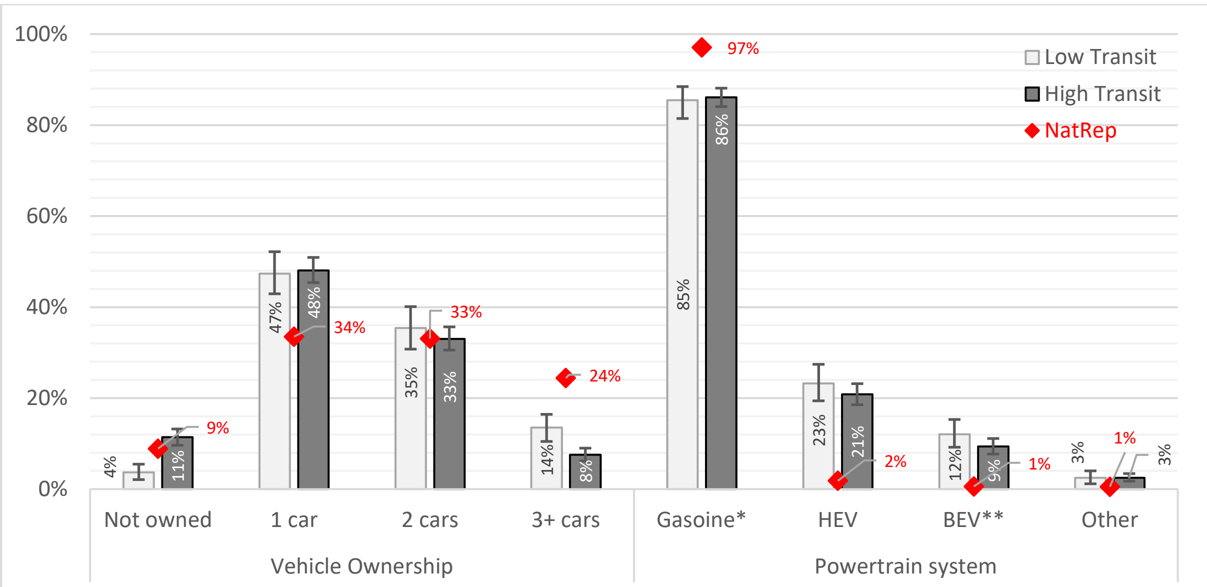

Figure 5-5 Sample composition: Household car ownership and powertrain system

Notes: National Representative (NatRep) of household car ownership based on McGuckin & Fucci (2018, p. 59), powertrain system based on US Energy Information Administration - EIA (2020). Whiskers: 95% confidence intervals

5.5 Survey results: User preferences (C3)

The survey results of consumer preferences for the transition to car-based MaaS from private vehicles for a round-trip to work in the US are presented in two forms. Section 5.5.1 shows the importance of attributes, and Section 5.5.2 considers attribute-level behaviours.

5.5.1 Importance of attributes

The respondents chose *cost* as the most critical consumer decision-making attribute when selecting a car-based sharing economy mode to/from work trips in the US, excluding carpooling. This finding is crucial for commercial ridesourcing operators considering the journey type and the survey sample to optimise their fee structures. The deviated results shown in Figure 5-6 are unsurprising as carpooling is often organised mutually. A significantly higher consumer preference was given to the attribute *cost* among solo-ridesourcing and private vehicles (60%–62%) than for carpooling and pooled-ridesourcing (29%–47%). This difference can be explained by the higher journey fare in solo rides than in cost-shareable pooled options. Private vehicle users also considered *cost* to be the most significant attribute in a to/from average work journey in the US. The expenses incurred, such as parking and toll fees, were included and indicated in the survey. Overall, they were expected to be considered in respondents' preferences.

The results demonstrated that door-to-door *journey time* was at least 27% more important when consumers decided on a shared mobility mode. Not surprisingly, it was highest for carpooling. Carpooling users were extremely concerned about their journey time. The reasons can be listed based on the nature of the mode, mutual organisation, and extra distances and time to collect passengers. Therefore, the results highlight the importance of reducing the lead time and journey optimisation in conventional MaaS modes, such as carpooling. The *journey time* was the second most important attribute for the other two MaaS modes that operate on apps.

The respondents selected the *number of passengers* as the third-highest attribute, with a 14%–24% preference weight. This attribute was relevant only to the two high-occupancy modes.

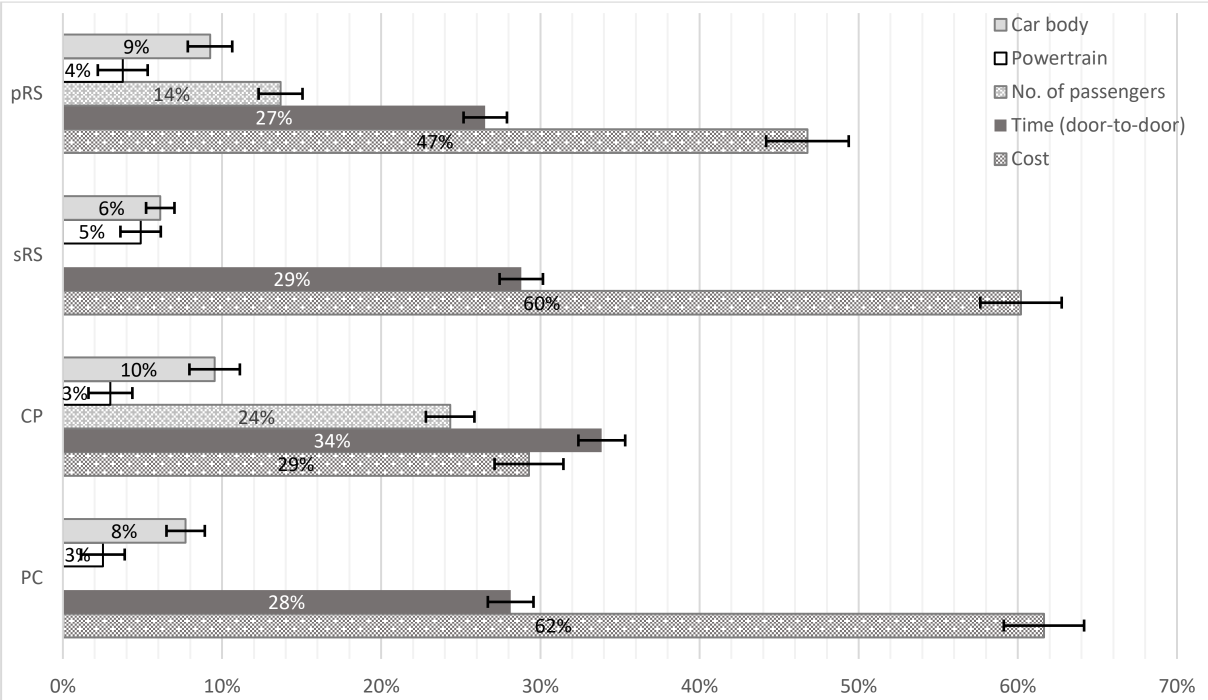

Figure 5-6 Relative importance of the attributes

Note: CP- carpooling, sRS - solo-ridesourcing, pRS - pooled-ridesourcing, PC – private vehicles. Whiskers: 95% confidence intervals

The *vehicle body style* recorded a higher consumer preference than the *powertrain type*. It had a 6%–10% influence on consumer preference compared to 3%–5% for the *powertrain type*. However, the above consumer preference is statistically insignificant in the solo-ridesourcing mode. This observation justifies the selection of *vehicle body style* as an attribute for the first time in a consumer preference study of MaaS modes. The observations highlighted the importance of *body style,* with at least 10% and 9% preference in two high-occupancy modes, carpooling and pooled-ridesourcing, respectively. This finding provides an important insight to the MaaS operators about the fleet technology value attributes. Though the vehicle manufacturers focus significantly on the powertrain type changes (see Section 2.4.1), the MaaS users' decisions are more based on the *vehicle body style*. In summary, *body style* is a suitable attribute for measuring convenience in car-based MaaS modes other than the number of passengers.

5.5.2 Importance of attribute levels (utilities)

Unsurprisingly, carpooling users demonstrated the least cost flexibility (maximum USD 19) compared with the two ridesourcing modes (up to USD 25) (see Figure 5-7). A possible reason for this behaviour was the relative trade-offs carpooling users make regarding convenience – such as time against cost. Interestingly, employees in the round-trip to work case study were willing to pay for pooled-ridesourcing trips over solo-ridesourcing if the fare was USD 19 to 25. However, users did not want to pay USD 40 or above for an average 21 km round-trip to work journey by utilising the three car-based MaaS modes. Interestingly, no overlaps were shown in the confidence intervals, highlighting the statistical significance of the utility values for the attribute cost.

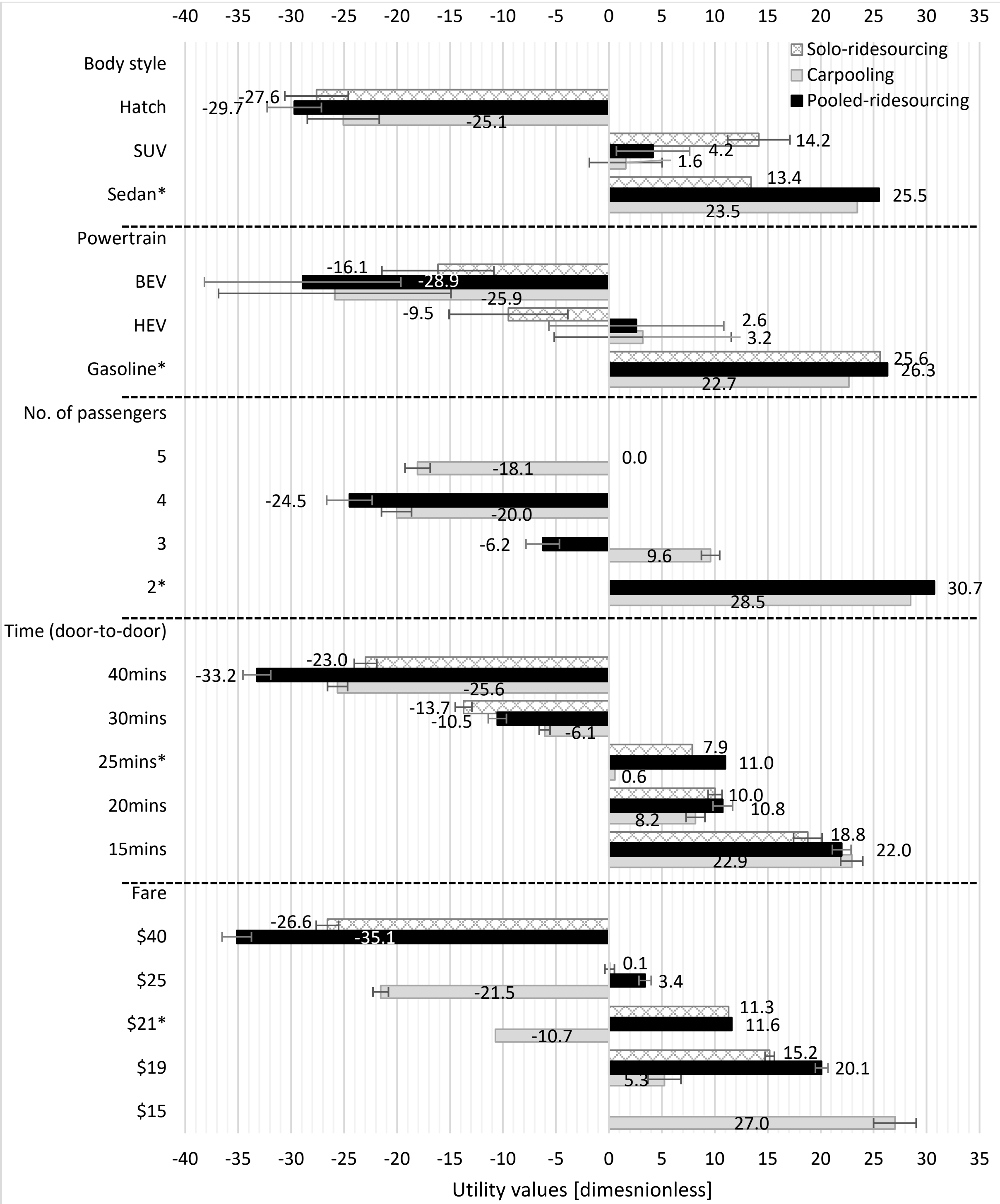

Figure 5-7 Level utility values – the key survey outcomes into attribute levels

Note: *baseline levels, no confidence intervals. Whiskers: 95% confidence intervals

A striking result from Figure 5-7 is that the pooled-ridesourcing mode has shown a higher preference value (11.0) at 25 min for the attribute *journey time,* while carpooling was far lower (0.6). These results can be explained by carpooling and pooled-ridesourcing user practices. Carpooling trips are often prearranged or routine trips compared with pooled-ridesourcing users. On the other hand, pooled-ridesourcing users are ready to walk an extra distance and spend spare waiting time. As Figure 5-7 shows, the users did not like to spend 30 min upwards on their round-trip to work journey in a car-based MaaS mode. The lowest two journey time classes (15 and 20 mins) have not shown significant deviations based on the confidence level values.

The results also show that the pooled-ridesourcing users did not prefer pooling with more than one extra passenger (two passengers per journey). However, carpooling users have shown an interest in pooling up to three passengers. These utility preferences can be explained based on the convenience aspect of high-occupant pooling modes, similar to journey fares. The higher *number of passenger* preferences for carpooling can also be explained by the sample being biased towards larger households (see Section 5.4.2). Family pooling, also known as 'fampooling', is a common journey characteristic in trips to work in the US (US Census Bureau, 2020a).

The most surprising aspect of the *vehicle body style* levels was the consumer preference for low-occupancy solo-ridesourcing mode, which has shown interest in large vehicle body style SUVs (14.2) compared to high-occupant pooled-ridesourcing (4.2) and carpooling (1.6) (see Figure 5-7: the latter two modes are not statistically comparable). In contrast to SUVs, sedans were selected as the preferred vehicle body style for carpooling and pooled-ridesourcing. These findings are unexpected based on the occupancy levels to which they cater. Hatchbacks were not preferred for any mode.

Although the survey sample favoured alternative powertrain systems (Section 5.4.2), BEVs were not accepted for car-based sharing economy modes. Nevertheless, the results show that gasoline vehicles were accepted for all modes. Hence, the *powertrain type* utility preferences did not support the state policy and transport network companies' drive towards fleet electrification, as discussed in Section 2.4.1. The results provide critical input to reconsider the effectiveness of the communications and awareness of the benefits of the transition to BEVs and address technical perceptions such as range anxiety. A comparison between HEVs and BEVs is impossible because the utility values are not statistically insignificant. The HEV option was not recognised for solo-ridesourcing modes, whereas the results are less significant for carpooling and pooled-ridesourcing.

Overall, the importance of attributes and utility values suggests an association between them and MaaS modes. The following section explores consumer characteristics that support the above results.

5.5.3 Market survey insights for the C-DLCA model

The insights from the choice model (Section 5.6) provide qualitative insights to assist in completing the dynamic hypothesis in the transition to car-based MaaS (S2 in the C-DLCA methodology framework). The derived importance of attributes and utility values are directly utilised in the formulation (S3) process step to integrate consumer preference outcomes into the SD model.

5.6 Characteristics of the round-trip to work commuters (C1)

It can be seen from the survey results that private vehicles are the most dominant commuter mode used by employees for round trips to work. As shown in Figure 5-8, its usage was correlated with the public transit level of the residential location. The results also show that low-public transit city consumers use at least 15% more private vehicles than users in high-public transit cities. In contrast, users in high-public transit cities have better access to public transport services (12.4%) to commute to work than those in low-public transit cities and 13.6% lower utilisation in car-based MaaS modes. However, these values are not comparable as they are not statistically significant. Hence, considering public transit levels in the sampling plan is justified.

Figure 5-9 shows the detailed MaaS mode utilisation based on the two public transit level locations. Conventional carpooling was the highest choice for round-trips to work journeys in low-public transit cities. On the other hand, solo-ridesourcing was more prevalent in high-public transit cities. Pooled-ridesourcing has not shown a significant statistical difference between the two public transit levels, possibly due to the smaller sample size and being the latest of the selected car-based MaaS modes. Therefore, the consumer preference behaviour of MaaS modes correlates with the location's public transit level. However, deriving a quantitative relationship is not possible as the mode utilisation values are not statistically significant.

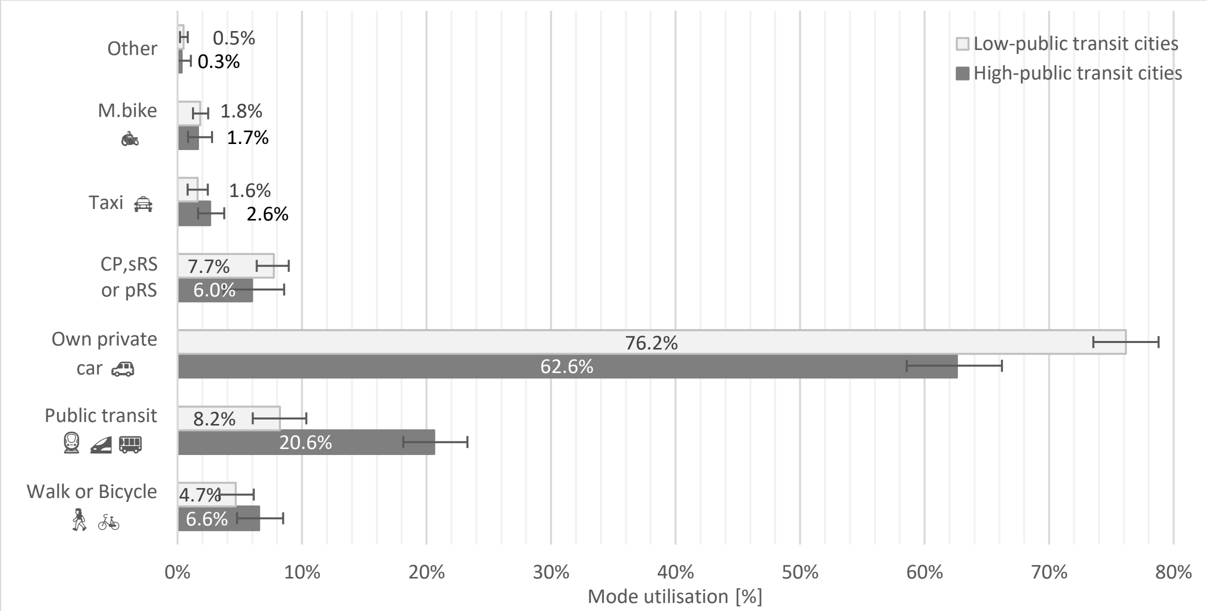

Figure 5-8 Most frequently used mobility mode for the round-trip to work – based on respondents' resident location's public transit level

Note: CP- carpooling, sRS - solo-ridesourcing, pRS - pooled-ridesourcing. Whiskers: 95% confidence intervals

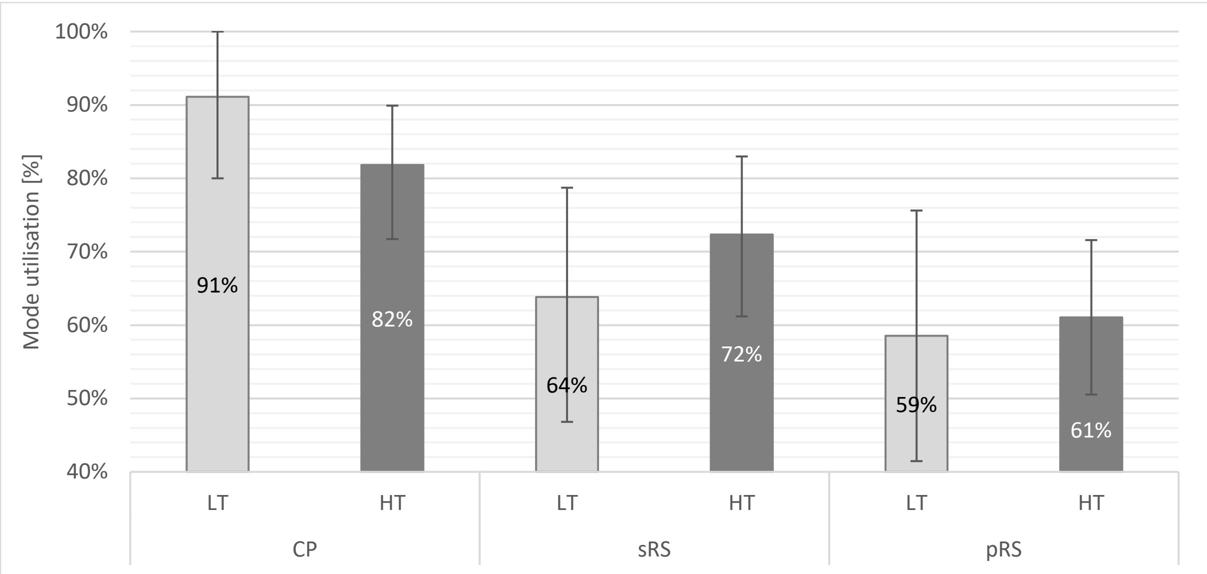

Figure 5-9 Percentage used of car-based MaaS modes for the round-trip to work based on the public transit status of the respondents' location

Notes: participants who saw the question: High-public transit (HT) 105|Low-public transit (LT) 48, CP- carpooling, sRS - solo-ridesourcing, pRS - pooled-ridesourcing. Whiskers: 95% confidence intervals

However, the frequency of work trips did not influence the MaaS mode or location based on public transit levels (see Figure 5-10). The respective values of high and low-public transit levels were not statistically different. Hence, round-trip frequency was not analysed further.

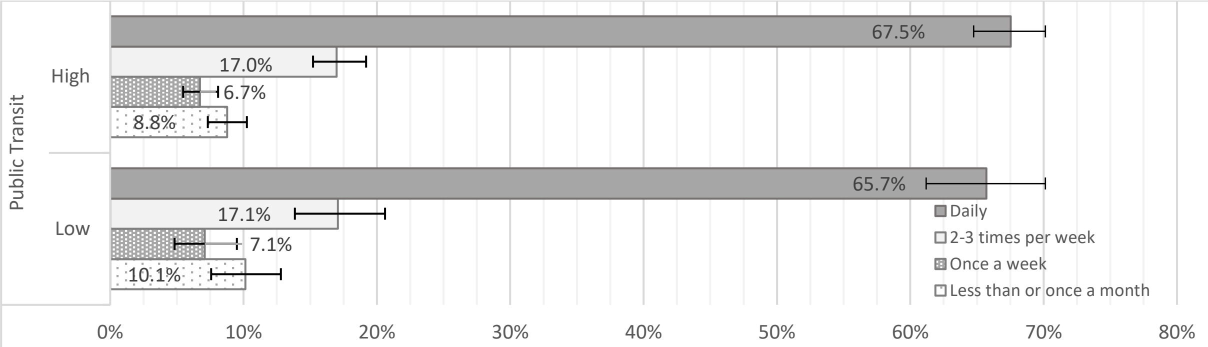

Figure 5-10 Extended analysis - Roundtrip to work - Journey frequency: based on public transit status of the location

Note: Whiskers: 95% confidence intervals

Figure 5-11 shows the correlation between the respondents' preferences and age in own private cars for the round-trip to work journey. Private vehicle utilisation in the oldest employee group (65+ yrs) was 30% more than that in the youngest (18-24 yrs), and a gradual increase has been observed from the age group 25-34 yrs onwards. In contrast, the young (below 35 yrs) labour force favoured car-based MaaS 38% higher than the older (55 yrs older). Hence, a noticeable difference was observed between the younger and older groups in the above modes. This behaviour can be explained based on the health and income levels because the sample cohort comprised current employees. The preferences for the other personal mobility modes are not statistically significant.

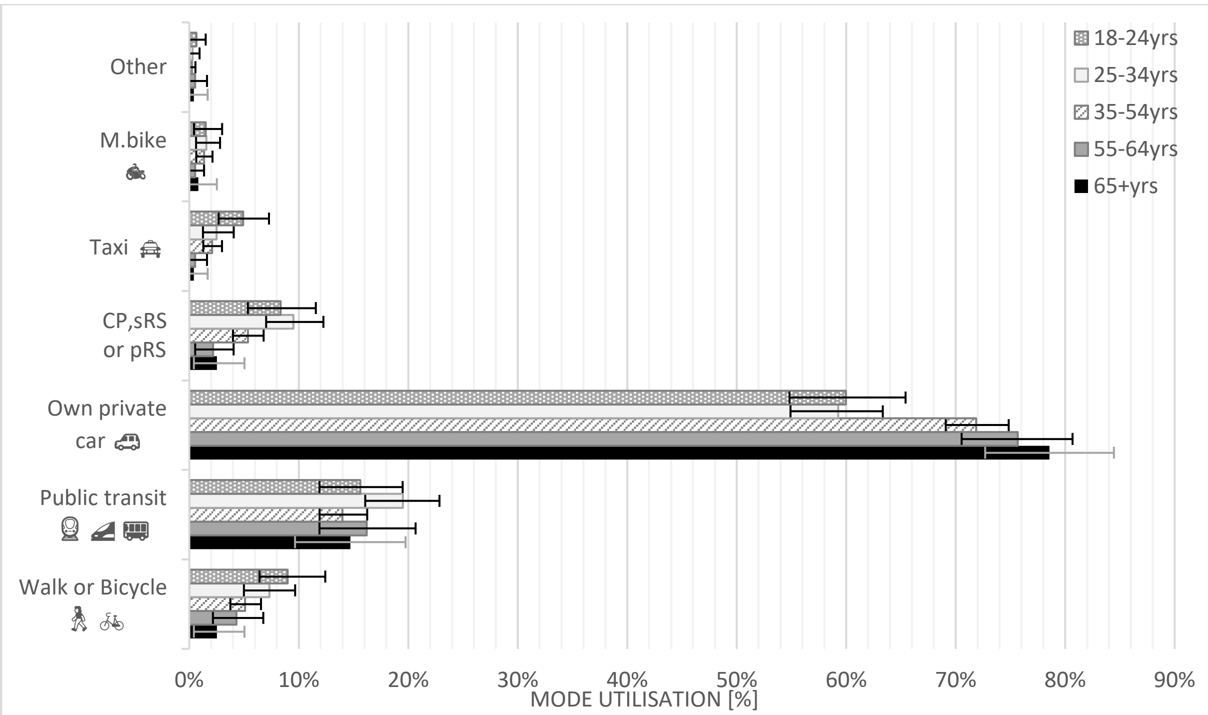

Figure 5-11 Most frequently used mobility mode for the round-trip to work – based on respondents' age

Note: CP- carpooling, sRS - solo-ridesourcing, pRS - pooled-ridesourcing. Whiskers: 95% confidence intervals

Therefore, further analysis of age classes was performed to understand the influence of age on the selection of MaaS (see Figure 5-12). The highest user preference for MaaS mode use was in the age class 35-54 yrs. Respondents older than 54 yrs demonstrated a significant reluctance to use car-based MaaS. However, there was no significant variation in consumer preferences among the different age groups and MaaS mode types, although overall MaaS usage and age were correlated.

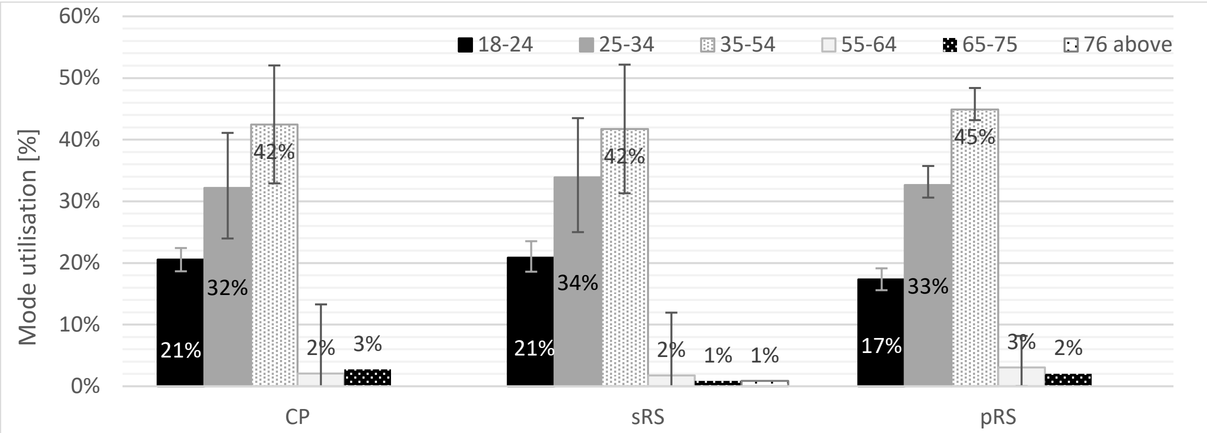

Figure 5-12 MaaS mode utilisation against the respondents' age

Notes: CP- carpooling, sRS - solo-ridesourcing, pRS - pooled-ridesourcing. Whiskers: 95% confidence intervals

The age-based findings highlighted the correlation between age and attribute importance in the car-based MaaS, targeting SD modelling work. The analysis in Table 5-4 illustrates the significance of age in the attributes that lead to different policy scenarios in the dynamic LCA work. For this, the two age groups (18 to 24yrs and 55+ yrs) that show the highest deviations were chosen, and their attribute importance values were listed for comparison. The results indicate no significant difference between the attribute importance values representing the two age groups. However, the vehicle body style slightly differed from the other attributes. Considering the above facts, the *vehicle body style* was chosen as a temporal input for the formulation and simulation (S3) step in the SD modelling (see Section 6.1.1).

Figure 5-13 provides insights into the stability of car-based MaaS usage in the US to/from work journeys. The majority (61%) confirmed their loyalty to the MaaS mode, and 8% rejoined after giving up or forgoing it. The user characteristics demonstrated a lower possibility (30%) of exiting (abandoning) MaaS. These user characteristics were integrated into the SD modelling work.

The user characteristics have shown the influence of the location, which depends on public transit levels and age group, on the car-based MaaS mode selection in a round-trip to the work journey in the US.

Table 5-4 Relative importance of attributes representing two extreme age ranges

MaaS mode		PC		Carpooling		solo-ridesourcing		Pooled-ridesourcing	
Attribute	Age [yrs]	I	CL	I	CL	I	CL	I	CL
Cost	18-24	60.2%	5.9%	28.2%	5.2%	59.9%	6.2%	45.8%	6.1%
	55+	62.9%	5.7%	29.0%	4.6%	60.2%	5.7%	46.2%	5.8%
Time	18-24	27.4%	3.5%	31.2%	3.6%	28.6%	3.3%	26.6%	3.4%
	55+	28.1%	3.1%	34.2%	3.3%	27.2%	3.1%	24.9%	3.0%
#passengers	18-24			23.0%	3.6%			11.4%	3.3%
	55+			26.4%	3.4%			16.6%	3.1%
Powertrain	18-24	1.5%	3.6%	4.1%	3.6%	4.7%	3.3%	4.0%	4.0%
	55+	3.7%	2.9%	3.8%	2.9%	7.2%	2.7%	5.6%	3.3%
Vehicle body	18-24	10.9%	3.3%	13.5%	4.4%	6.9%	2.4%	12.2%	3.9%
	55+	5.3%	2.5%	6.5%	3.1%	5.3%	1.8%	6.6%	2.6%

Notes: Sample sizes: 18-24 yrs – 467, 35-54 yrs – 608, 55+yrs age ranges integrated considering the sample size), I=importance of the attribute, CL=95% confidence interval. PC – private cars

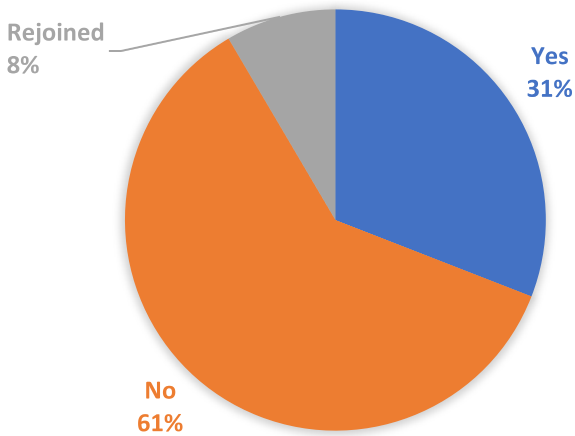

Figure 5-13 MaaS user continuity – question aimed at willingness to reuse MaaS

Note: number of participants who saw this question – 165

5.7 Discussion

The survey was completed with 2,968 qualified respondents after a stringent quality assurance process, and the sample size was significant compared to past studies. The uniqueness of the survey was applying three stringent sampling conditions. They are a) geographical representation based on the US Census Bureau-designated regions, b) representing three public transit levels, and c) demographics to achieve the US national representative values. The sample demographics achieved the national representative values with minor deviations, and the geographical and public transit-based location (cities) coverage was slightly varied due to the sampling constraints. However, it did not impact the overall planned sample number and was significantly higher than the requisites for the DCE choice combinations. Because of the substantial sample and its representative scope, it can be considered market-responsive, considering the most relevant consumer characteristics based on location and demographics. The selection of the most relevant attributes, including fleet technology-based powertrain and vehicle body style, for the car-based shared mobility consumer preference analysis, revealed significant insights. The vehicle body style was chosen as a shared mobility consumer attribute for the first time in this study.

This research reinforces previous studies showing that *cost* is the most influential attribute in consumer preferences for car-based MaaS (Washbrook, 2002; Malodia and Singla, 2016). It is a cognitive trade-off, not just the consumer's economic costs, but also the effort in utilising the service (Ostrom and Lacobucci, 1995). Hence, the parameter of willingness to pay can be utilised to explain the changes in consumer cost preferences (Ho, Mulley and Hensher, 2020). The results show that consumers are willing to pay more for ridesourcing trips than for carpooling trips. The above findings are statistically significant based on the derived confidence level intervals. Ridesourcing is a systematically organised commercial business compared to mutually organised carpooling. Hence, the performance and service level improvement of ridesourcing trips is greater than that of carpooling. Their performance and convenience of use are further improved by interactive apps (Shaheen and Cohen, 2019), a common feature in sharing economy modes (Möhlmann, 2015). Therefore, these features increase convenience and thus reduce perceived switching costs. The extra interior space in pooled-ridesourcing fleets can be a convenient feature that reduces switching costs. The results in this section indicate consumers' willingness to pay for extra convenience explains why pooled-ridesourcing users are willing to pay more than solo-ridesourcing users up to $25, contrary to previous work (Hou *et al.*, 2020). It can be assumed that the respondents' willingness to pay results represent the actual market behaviour because the sample has slightly deviated towards the higher side from the average household income distribution (Section 5.4.2).

The results for *journey time* align with those of previous studies (Washbrook, 2002; Rayle *et al.*, 2014; Malodia and Singla, 2016; Lippke and Noyce, 2020). Carroll et al., 2017 found the significance of consumer preference for access and extra wait times in their carpooling study. The derived *journey time* utility values in Section 5.5.2 show a positive value until 25 min. Therefore, the results imply that the chosen car-based MaaS modes are acceptable, considering the average door-to-door time using a private vehicle in the US (McGuckin and Fucci, 2018, p. 79). It can be assumed that there is a higher journey time flexibility in the actual market since the survey sample was more towards larger households compared to the national representative (see Figure 5-3).

The *number of passenger* results also aligns with previous studies on convenience constraints such as interaction comfort (Cui *et al.*, 2020) and privacy and convenience (Lippke and Noyce, 2020). The results can be explained based on the considerably required personal effort to switch from private vehicles to public or shared transport with entrenched habits and perceived trade-offs in terms of sacrifice of convenience (Carrus, Passafaro and Bonnes, 2008; Moser, 2015). The journey optimisation efforts of transport network companies are a potential reason for the attribute difference between carpooling and solo-ridesourcing modes (Uber, 2020). The *number of passengers* and convenience are further supported by the US light-duty vehicle market trends favouring SUVs (US EPA, 2021).

The consumer preferences of the two technical attributes (*powertrain type* and *body style*) directly affect the life cycle GHG emissions of the transition to MaaS. Consumers' lower preference for BEVs and higher preference for SUVs in solo-ridesourcing were unexpected outcomes of the survey (they are further discussed in Section 8.2). Larger body size SUVs and gasoline vehicles are the largest GHG-emitting combination in car-based MaaS fleets (see Figure 4-3). DCE outcomes have shown some unexpected results, showing that the highest preference for low-occupancy-based solo-ridesourcing users is for the above fleet technology combination. Surprisingly, the BEV option is also rejected in all three MaaS modes, contradicting previous studies (Galatoulas *et al.*, 2017; Jenn, Laberteaux and Clewlow, 2018). Overall, the two technical fleet attributes are more broadly discussed in Chapter 8, and both are identified, providing significant inputs to SD modelling in the formulation and simulation process (S3).

5.8 Summary

A market survey was conducted to generate the qualitative and quantitative inputs required for the C-DLCA model. The sample was identified with US geographical and public transit coverage and achieved 2,968 qualified responses. The survey instrument was based on the stated preference choice method. The choice-based conjoint analysis technique was adopted to integrate the DCE model. The consumer preference attributes for the Choice-Based Conjoint Analysis model are chosen based on the literature, and their levels are identified based on the literature and Google maps-based study. The results were analysed using the random utility method and MNL model. The derived importance of attributes and level utility values highlights consumer preferences relying on the MaaS mode. They are identified as significant quantitative inputs to the C-DLCA modelling work. The survey responses for the descriptive questions have provided qualitative inputs for SD modelling work. While the attributes *cost* and *time* were aligned with the existing studies, the attribute *powertrain type* has shown contradictory results against previous studies. The *vehicle body style* has also brought novel insights, as there have been no attempts to employ it as an attribute of a MaaS survey.

6 MaaS User and Fleet Behaviour

Publication relevant to this chapter

Fernando, C., Buttriss, G., Yoon, H.-J., Soo, V. K., Compston, P., & Doolan, M. (Accepted). Integration of consumer behaviour into dynamic life cycle assessment for the sharing economy: Methodology and case study for shared mobility. *International Journal of Life Cycle Assessment.*

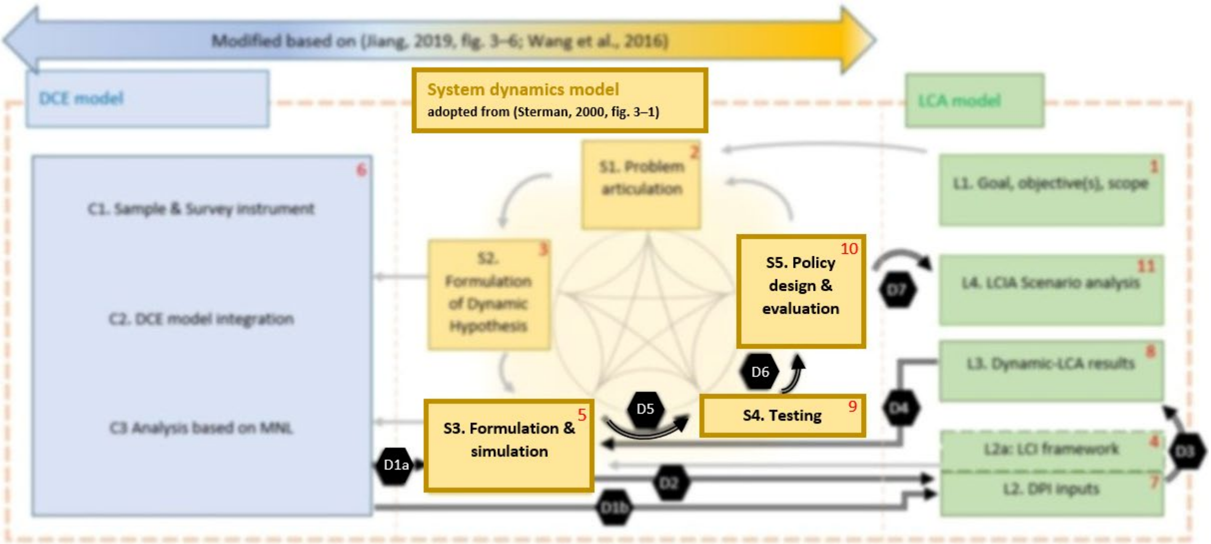

Figure 6-1 C-DLCA methodology framework components relevant to Chapter 6

Introduction

The system dynamics modelling establishment is introduced in this chapter. It includes setting up step S3 in the C-DLCA framework, simulation and formulation based on the defined LCA objectives in Section 4.2, problem articulation (S1) in Section 4.3 and the dynamic hypothesis (S2) in Section 4.4. The transition to MaaS and fleet behaviour sub-models out of the three identified in Section 4.6.1 are simulated and formulated in this chapter. The sub-model implementations are presented in Sections 6.1 and 6.5, and their outcomes are presented in Sections 6.4 and 6.6. The DCE-based survey results derived in Chapter 5 (**D1a** in Figure 4-2) are integrated into the transition to MaaS sub-model, and the causality of the consumer preferences is combined. The model calibration and testing outcome, step S4 in the C-DCLA framework, is presented in Section 6.2, and the policy scenarios (S5) are introduced in Section 6.3. This chapter ends with a discussion and summary.

6.1 Model implementation (S3): Sub-model – Transition to MaaS

This section presents the SD model implementation of the transition to MaaS, the first of three sub-models introduced in Section 4.6.1. This sub-model integrates the primary data from the consumer preference survey results generated in Chapter 5. The DCE outcomes are combined into the SD model, and this step is pivotal in the formulation and simulation work. As introduced in Section 4.3.1, the reference mode is chosen as the 'user transition to car-based MaaS modes'. The problem articulation and hypothesising by employing the Bass model to understand the transition behaviour to MaaS is operationalised into an SD model in this section based on the established causal loop diagram. Section 6.1.1 presents the formulation and simulation steps of the transition to the MaaS sub-model.

6.1.1 Integration of survey results into sub-model transition to MaaS

The sub-model transition to MaaS is created based on the Bass model (Bass, 1969; Sterman, 2000, chap. 9.3.3). As shown in Figure 6-2, two key stocks are identified in this sub-model based on the causal loop diagram presented in Figure 4-5. The stock commuting employees by private vehicles represents the conventional commuters to work using their private mobility modes. This stock depends on two secondary data-based variables: employment change and car-based mobility. The stock of active MaaS users is the result of this transition. The difference in the stocks represents private vehicle users. Overall, both stocks are critical in calculating GHG emission behaviour.

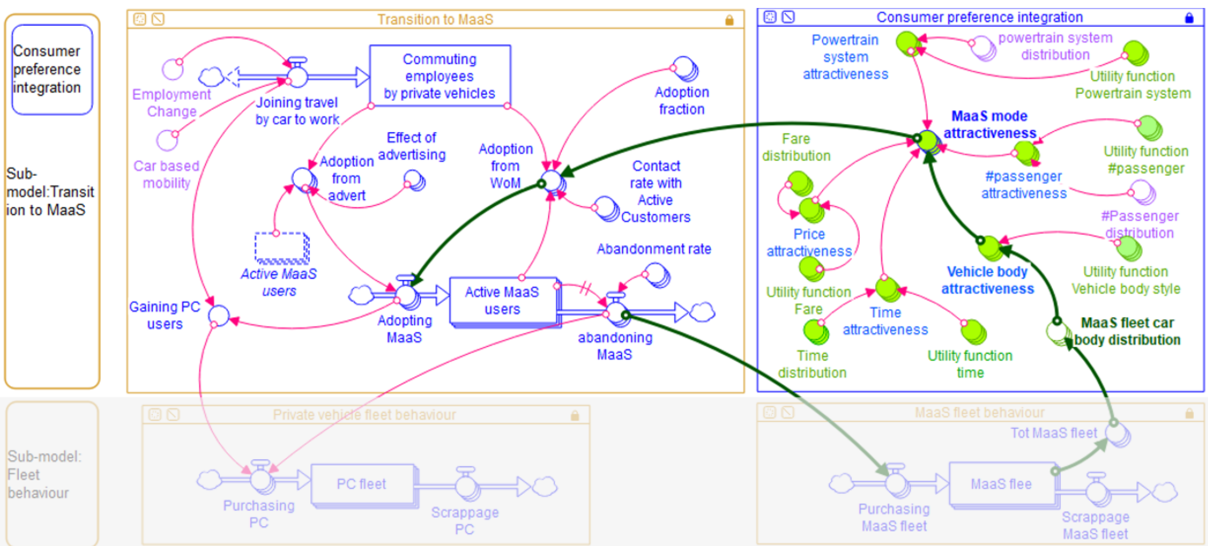

Figure 6-2 Stock and Flow Diagram of the transition to MaaS sub-model

Note: only the relevant variables are shown from the other sub-models

Based on the Bass model, the adoption rate depends on adoption from advertisements (advert) and adoption from WoM. Advertising drives imitators, and innovators are driven based on WoM or other positive feedback sources (Sterman, 2000, chap. 9.3.3). Two adoption sources, WoM and advertising are assumed to be independent, and the total adoption rate is expressed in Equation (6-1), based on (Sterman, 2000, p. 333).

$$\text{Total Adoption Rate} = \text{Contact rate} * \text{Adoption fraction} * \text{Potential adopters} * \text{Adopted population}/\text{Total population} + \text{Advertising effectiveness} * \text{Potential adopters} \quad (6\text{-}1)$$

The stock of potential adopters is determined by the total population (commuting employees by private vehicles) and adopters (active MaaS users). It can be represented as an auxiliary variable (Sterman, 2000, p. 336), and their relationship is expressed in Equation (6-2).

$$\text{Potential adopters} = \text{Total population} - \text{adopters} \quad (6\text{-}2)$$

The variable MaaS mode attractiveness introduced in Section 4.4.2 is employed to combine consumer preference outcomes from the survey into the SD model. Schmidt and Gary (2002, p. 371) have utilised the product attractiveness in SD modelling, the original concept that derived the variable MaaS mode attractiveness. Product attractiveness conceptually resembles the variable 'fraction willing to adopt' introduced by Sterman (2000, p. 336), representing MaaS mode attractiveness in this study. Sterman (2000, p. 336) argues that "potential adopters is a fraction of the total population which is less than the current number of adopters". Hence, Equation (6-2) is reworked by introducing Equation (6-3).

$$\text{Potential adopters} = \text{MaaS mode attractiveness} * \text{Commuting Employees by cars} - \text{Active MaaS users} \quad (6\text{-}3)$$

Therefore, Equation (6-1) is reworked by introducing Equation (6-4), considering the concepts of product attractiveness and fraction willing to adopt, and combining Equation (6-3).

$$\text{Adopting MaaS} = \text{Contact rate with Active customers} * \text{Adoption fraction} * (\text{MaaS mode attractiveness} * \text{Commuting Employees by cars} - \text{Active MaaS users}) * \text{Active MaaS users}/\ \text{Total population} + \text{advertising effectiveness} * (\text{Total population} - \text{Active MaaS users}) \quad (6\text{-}4)$$

Price attractiveness, Time attractiveness, number of passenger attractiveness, Vehicle body style attractiveness, and Powertrain type attractiveness are introduced to integrate the derived utility values in Section 5.5.2 and attribute level distributions. The data sources of attribute levels are presented in Table 6-1.

Table 6-1 Attribute level distribution data sources

Attribute	Cost[a]					Time: door-to-door[a]					Number of passengers[b]					Powertrain type[c]	Body style[d]
Level	15	19	21	25	40	15	20	25	30	40	1	2	3	4	5	Gasoline, HEV, BEV	Sedan, SUV, Hatch
CP	40	40	10	10	**X**	5	30	25	20	20	**X**	92	6	2		Calculated based on (U.S. Energy Information Administration - EIA, 2021, Table 39)	Calculated based on (US EPA, 2021)
sRS	**X**	49	22	26	3	40	19	25	31	22	100	**X**	**X**	**X**	**X**		
pRS	**X**	1	5	54	40	3	8	18	3	41	**X**	93	6	1	**X**		

Notes: All values are in %, **X** – not applicable. [a]Based on Google map-based study sampling in six cities in the USA for solo-ridesourcing (sRS) and pooled-ridesourcing (pRS). Results are presented in Table C-1 and Table C-2 in Appendix C, CP-estimated based on sRS, [b]calculated best fit based on: carpooling – 2.18 calculated based on US Census Bureau (2020), solo-ridesourcing – 1, pooled-ridesourcing - 2.3, a conservative estimation based on previous studies (Henao and Marshall, 2018; Uber, 2020, p. 59; Wilkes *et al.*, 2021), [c]endogenous variable, [d]exogenous variable

Random utility theory and MNL model-based logit probability are applied to calculate attribute attractiveness variables (Tran *et al.*, 2013). The connecting variable with the DCE outcomes in the transition to MaaS sub-model, MaaS mode attractiveness, is defined in Equation (6-5). The error of the utility equation is an independently and identically distributed standard normal distribution with a mean of 0 and a standard deviation of 1 (N (0,1)). The probability that individual *n* would choose alternative *j* out of *J* alternatives (carpooling, solo-ridesourcing and pooled-ridesourcing in the case study) is given by

$$Prob_{nj} = \frac{exp\beta' x_{nj}}{\sum_{j=1}^{J} exp\beta' x_{nj}} \tag{6-5}$$

where x_{nj} is a vector of attributes, representing the attribute distribution among different levels relating to alternative *j* and person n; β_n is a vector of partworth utilities for the attributes that depict a person n's tastes associated with each of the observed variables (attribute in this case). The partworth utility results for the β_n are based on the consumer preference results presented in Section 5.5.2.

These data inputs are programmed in SD modelling in the arrayed form to integrate the carpooling, solo-ridesourcing and pooled-ridesourcing values separately. The stock and flow diagram shown in Figure 6-2 illustrates the underlying physical structure of the transition to MaaS sub-model. The SD modelling software Stella Architect (version 1.9.4) is used for modelling, and the SD model formulation notes, including the utilised attribute level distributions, are listed in Appendix G.

The feedback system is limited to the attribute *vehicle body style* based on the introduced endogenous explanation, model boundaries (Table 4-2) and limitations discussed in Section 4.4.1. The input feedback loop from the stock sub-model fleet behaviour is discussed in Section 6.5.

Sections 6.2 and 6.3 are introduced to establish the calibration and policy scenarios for all three sub-models. Section 6.4 presents the results of the transition to the MaaS sub-model.

6.2 Calibration and model optimisation (S4)

The dynamic model simulation is initiated with the model calibration (testing) step. This step is critical for constants, the precise values of which are difficult to gauge because most of these parameters are intangible. Model calibration is performed to estimate the values of these model constants to ensure the robustness of policies under extreme conditions (High BEV adoption in this work) and to assess the SD model structure and model parameters based on their sensitivity to uncertainties (Sterman, 2000, chap. 3.5.5).

The calibration process supports reproducing real-world behaviour in the SD model to achieve the model goal. The historical datasets for the model calibration requirement were obtained from two key data sources. A) The employee-related data on the self-driven and employment change are based on US labour statistics and transport survey databases (Toossi, 2002; US Census Bureau, 2020a). B) Private vehicle and car-based MaaS usage for work rides in the US are mainly based on the National Household Transport Survey (McGuckin and Fucci, 2018; US Census Bureau, 2020a). A summary of the secondary data values employed in the calibration process is presented in Table E-1 in Appendix E. Because of secondary data constraints, some estimations were made, particularly in the pooled-ridesourcing calculations. The software-based optimisation process employed to calibrate the model is discussed in Section 6.2.1.

The calibration process is also utilised as a model validation step. Although all models are incorrect, model validation presents derived model behaviour. It provides a comparison with the reference modes. In this research, the model was calibrated using the historical (pre-COID19), real-world round-trip to work journeys in the USA for initial values and compared with the reference modes. Hence, the calibration step supported the establishment of a reliable baseline scenario.

6.2.1 Payoff calculation and calibration results

The Stella payoff function is used as the software environment for calculating the simulation payoff values. The comparison type 'squared error' is chosen as the payoff method. It behaves in the same manner as the negative value of the log-likelihood in terms of its response to parameter changes (Isee Systems, no date). The comparison-run data are based on historical data for the four stocks. They are active CP users, active solo-ridesourcing users, active pooled-ridesourcing users and commuting employees via private vehicles. The historical data utilised for the payoff calculation are presented in Table E-1 in Appendix E. The software provides a payoff list. The payoff number was calculated based on the iterative and repeating model simulations. It represents the smallest difference between the values for the real data and simulation results.

The Stella Run Optimisation (R-Run) function is utilised to calibrate the model. The historical data utilised for the payoff calculation are also used in the R-Run function for the model calibration process. A few variables in the transition to the MaaS sub-model were identified to rely on the calibration process, considering the constraints to acquiring reliable and case-specific secondary data. They are abandonment rate, adoption fraction, contact rate with active customers and effect of advertising. The final calibrated results for the above variables are presented in Table 6-2. The detailed payoff and calibration reports generated in Stella are presented in Table E-2 and Table E-3 in Appendix E.

Table 6-2 Model calibration results with confidence bounds (95%)

Model constant name	Mode (*j*)	Calibration results in confidence bounds 95%		
		Baseline Scenario		
		Lower	Mean	Upper
Abandonment rate	Carpooling	*	0.198682	*
	Solo-ridesourcing	*	0.194728	*
	Pooled-ridesourcing	*	0.150907	*
Adoption fraction	Carpooling	0.005782	0.005840	0.005890
	Solo-ridesourcing	0.008230	0.008678	0.009288
	Pooled-ridesourcing	0.001972	0.004422	0.006085
Contact rate with active customers	Carpooling	109.1419	109.9947	110.8509
	Solo-ridesourcing	104.7628	110.0026	115.0030
	Pooled-ridesourcing	49.3020	109.9956	160.9802
Effect of advertising	Carpooling	*	0.000749	*
	Solo-ridesourcing	0.000750	0.000789	0.000839
	Pooled-ridesourcing	0.000386	0.000468	0.000520

Note: * No significant change, The High BEV adoption values are almost similar. See Table E-3 in Appendix E

6.2.2 Sensitivity analysis

Sensitivity analysis investigates the significance of the conclusions based on the purpose of the model when the estimated inputs and assumptions vary within a plausible range of uncertainty (Sterman, 2000). It observes the influence of the model constants on the overall behaviour of the model. Hence, the sensitivity analysis provides both parametric and structural model behaviour analyses. Richardson & Pugh III (1981, p. 278) highlight the hierarchy of three different sensitivities in SD modelling. They are numerical, behavioural and policy sensitive.

This research uses 95% confidence intervals to represent numerical sensitivities. This selection aligns with consumer survey outcomes and past work (Jiang, 2019).

The sensitivity of the model behaviour should also check the policy recommendations to check the policy sensitivities (Sterman, 2000). Sensitivity checks are critical for discovering and improving the flaws of a model. A policy sensitivity analysis is performed by introducing a representation of extreme conditions in current MaaS market practices in Section 7.6.

6.3 Policy scenario specifications (S5)

High BEV adoption is identified as the most relevant policy scenario considering the goal of the LCA model and the derived dynamic hypothesis. BEVs are low-carbon transportation options for cities (Köhler, Turnheim and Hodson, 2020). The BEV composition of personal mobility in the US has shown significant historical changes and dynamics in its forecasts (see Section 2.4.1). As shown in Sections 2.3 and 2.6, the high BEV adoption scenario significantly influences fleets' life cycle GHG emissions and depends on consumer choices. Hence, the chosen policy scenario illustrates its influence on the GHG emissions of the transition to MaaS and aligns with the defined key research question: '**What is the impact of the transition from private car use to car-based sharing economy modes on GHG emissions, considering consumer preferences and fleet technology changes?'.** Policy scenario selection also provides interesting insights into making informed decisions by the identified interested parties of this study: a) mobility service providers, b) policymakers and c) interested users (see Section 4.2.1).

The percentage of fleet electrification is chosen as the policy scenario indicator to analyse the GHG emissions of fleet technology changes. The US light-duty automobile fleet market developments (U.S. Energy Information Administration - EIA, 2020) and the US president's executive order on 50% BEVs as new cars from 2030 onwards (The White House, 2021) are chosen as the baseline scenario. The 100% BEV, an extreme condition that policymakers support (Dijk, Wells and Kemp, 2016), is chosen as the high BEV adoption scenario from 2030 onwards. This selection aligns with the sustainability commitments of transport network companies (Lyft, 2020; Uber, 2020). The technology composition, temporal changes, assumptions and data sources for the two scenarios are presented in Table 6-3.

The combination of powertrain types and vehicle body styles is chosen to align with the conjoint analysis attributes in Section 5.3.3. Changes in vehicle body style, especially the trend of high SUV adoption, are also considered when parameterising the scenarios to analyse their influence. Table 6-3 presents the technological possibilities that affect the transition to MaaS. The calculated powertrain type and body style composition data are presented in Table C-3 and Table C-4 in Appendix C.

Table 6-3 Technology adoption scenarios and parameters

Technology change	Scenario	MaaS mode	Body style	2023-2030	2030-2040	2040-2050
BEV adoption (New vehicles sales BEV%)	Baseline	CP, PC	Sedan	50%[1]	100%[4]	S
			SUV	50%[1]	100%[4]	S
		sRS, pRS	Sedan	100%[2]	S	S
			SUV	50%[a3]	100%[4]	
	High BEV	CP, sRS, pRS	Sedan	100% from 2026	S	S
			SUV	100% from 2026	S	S
SUV adoption (New vehicle sales SUV%)	Both scenarios	CP	Sedan	Market trend[5]	S	S
			SUV	Market trend[5]	S	S
			Hatch	Balance	Balance	Balance
		sRS	Sedan	Balance	Balance	Balance
			SUV[5]	150% x CP, max 71%	S	S
			Hatch[6]	3%	2%	1%
		pRS[7]	Sedan	20%	S	S
			SUV	80%	S	S
			Hatch	0%	S	S
Vehicles scrappage rates[8]	Both scenarios	CP	Sedan	See Figure C-1 (a) in Appendix C		
			SUV	See Figure C-1 (b) in Appendix C		
		sRS, pRS	Sedan	See Figure C-1 (c) in Appendix C		
			SUV	See Figure C-1 (d) in Appendix C		
Vehicle lightweight	Both scenarios	All	All	Until 2023 – no change 2023 to 2043: based on (Wang *et al.*, 2021) 2043 onwards – sustained		

Sources and Notes: [1](The White House, 2021), [2](Lyft, 2020; Uber, 2020), [3]Assuming SUV electrification is behind compared to the sedan (US EPA, 2021, 2018), [4]Assuming market will follow the US President's executive orders (The White House, 2021), [5]Based on the Sedan market trend (McGuckin and Fucci, 2018, p. 66, 2018, fig. 12) and the fees structure of sRS (Uber, 2021c), [6]Estimated based on (US EPA, 2021, 2018), [7]Based on the fleet requirement of pRS (Uber, 2021d), [8]Calculated based on survival rates. The combined survival rates are calculated for sedans and SUVs based on (Lu, 2006, p. 8; Davis and Boundy, 2021, pp. 3–20)
S-sustain, a - assumption, e - estimated

The above policy specifications are integrated into the SD simulations and analysed in Section 6.4.

6.4 Results – Transition to MaaS user behaviour

The model outcomes of the user transition from private vehicles to MaaS are presented in this section. The transition to car-based MaaS supports reducing the number of employees that use private vehicles for the round-trip to work journey in the US, a steeper decline than the US Census Data (US Census Bureau, 2020a) (see Section 6.4.5). The outcome presentation begins with the aggregated MaaS behaviour in Section 6.4.1. A significant aggregated MaaS user increase is observed and discussed. However, the individual behaviour of car-based MaaS modes is unique and further explored in Sections 6.4.2 to 6.4.4. In summary, the approach taken in this study on consumer preference integration has supported deriving the unique behaviour of the chosen MaaS modes separately and analysing them individually.

The numerical sensitivities of the results are analysed employing 95% confidence intervals as introduced in Section 6.2.2.

6.4.1 Transition behaviour: Aggregated MaaS users

According to the model results, the user transition from private vehicles to car-based MaaS mode increases. MaaS adoption considerably increases from the mid-2020s, and the difference between the two scenarios is minimal. As shown in Figure 6-3, the model outcome predicts that the number of self-driven employees (private car – PC) in the US will decline from the late-2020s. The private vehicle user reduction is more significant in the high BEV adoption scenario than in the baseline scenario. In contrast, car-based MaaS users show a significant increase in the high BEV adoption scenario compared to the baseline. Therefore, the model findings suggest that the high BEV adoption scenario attracts more car-based MaaS users than the baseline scenario does. For private vehicle use, it works vice-versa. Both user segments are examined to find mode-specific user behaviours in Sections 6.4.2 to 6.4.5.

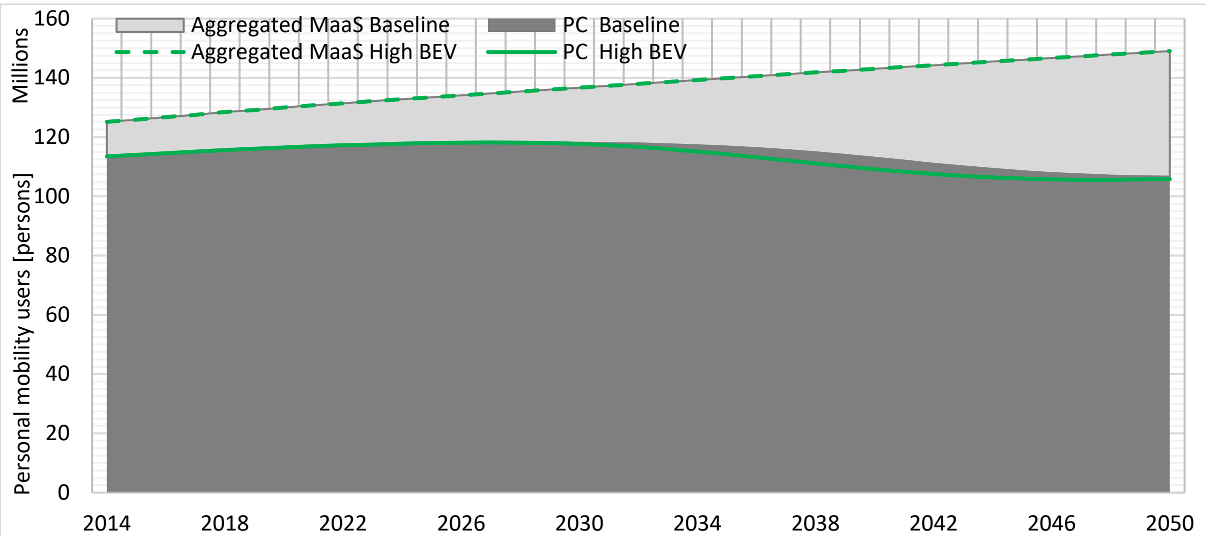

Figure 6-3 The transition to MaaS mode users from private vehicles

Note: PC – private vehicle

6.4.2 Carpooling user behaviour

The only decreasing trend in car-based MaaS users is observed among carpooling users. The model outcome suggests a higher reduction in the high BEV adoption scenarios than the baseline (see Figure 6-4). In the initial modelling period, carpooling users in the baseline scenario show a slightly increasing trend, with a few oscillating curves based on historical data (US Census Bureau, 2020a). Later, it starts to decline. The model outcomes demonstrate a more noticeable decline from the mid-2020s in the high BEV adoption scenario, followed by the baseline case from the early 2030s. As shown in Figure 6-4, the modelling outcomes of the carpooling users in the two scenarios are within 95% confidence levels at the end of the modelling period. Therefore, an inter-scenario analysis is feasible only for carpooling user behaviour before 2048. The trend generally declines in both scenarios, and users dislike the high BEV adoption scenario for carpooling more than the baseline.

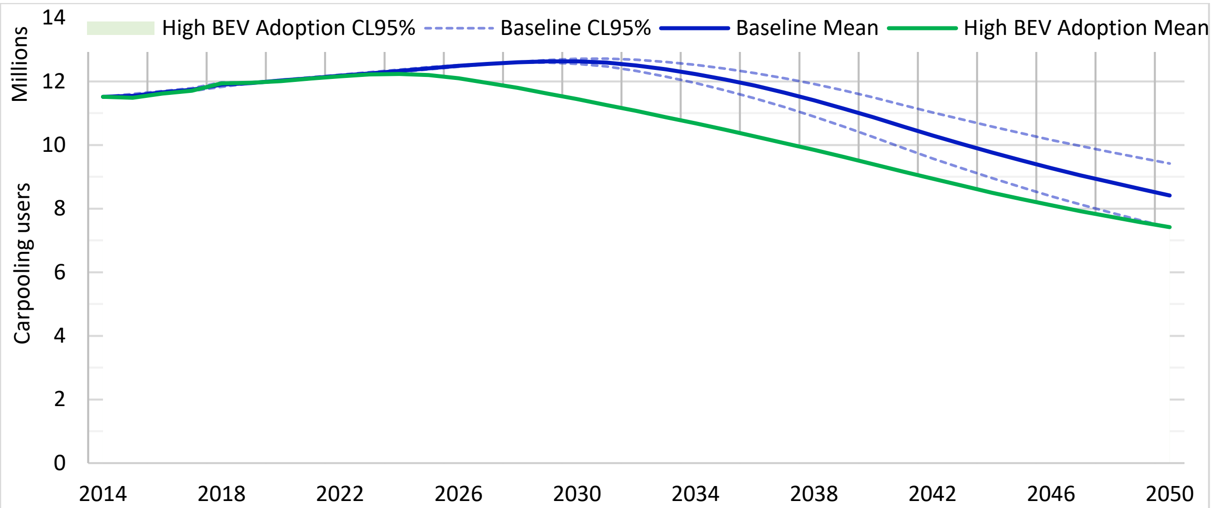

Figure 6-4 Transition to carpooling user behaviour

Note: CL–control limits, representing the confidence intervals

6.4.3 Solo-ridesourcing user behaviour

The low-occupancy-based solo-ridesourcing shows the highest adoption in the transition to MaaS for the chosen case study. As shown in Figure 6-5, the model results suggest a significant increase in solo-ridesourcing users in the round-trip to work journey in the USA over the modelling period. The results align with the current ridesourcing market trends of major cities in the US (Schneider, 2021b, 2021a). The uptake is more considerable in the high BEV adoption scenario than in the baseline scenario. This depends on the utility values of the BEVs and fleet composition. With the expedited BEV rates from 2023 targeting 100% new car sales by 2030, the high BEV scenario attracted more users than the baseline scenario, which targeted 50% new BEV sales by 2030. The increasing trend is visible until the final stage of the modelling period. However, data points are not statistically significant based on 95% confidence intervals before 2025 and from the mid-2040s onwards. In summary, the model outcomes suggest the highest user uptake in the transition to car-based MaaS in solo-ridesourcing with the high BEV adoption scenario compared to other modes presented in Sections 6.4.2 and 6.4.4. The uptake can be further increased if the BEV utility values are favourable for the ridesourcing (See Figure 5-7).

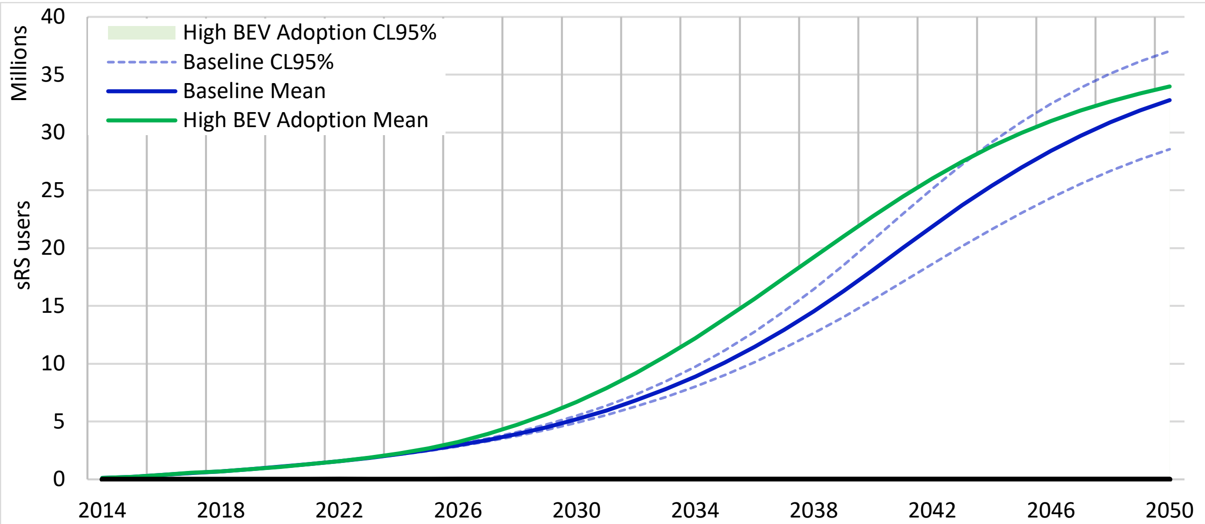

Figure 6-5 Transition to solo-ridesourcing user behaviour

Note: CL–control limits, representing the confidence intervals

6.4.4 Pooled-ridesourcing user behaviour

As shown in Figure 6-6, slight growth is observed in the pooled-ridesourcing users. However, the results are challenged by data constraints and calibrations. Pooled-ridesourcing is the most recently introduced car-based MaaS mode (Uber, 2022). Hence, its trajectory increases slowly in the round-trip to work journey compared to solo-ridesourcing. However, it is accepted against carpooling (see Figure 6-4). The 95% confidence level interval outcomes in Figure 6-6 reveal both fleet technology scenarios in pooled-ridesourcing user behaviour are within 95% confidence intervals showing no significant change in the behaviour. However, like carpooling, the high BEV adoption user trajectory of pooled-ridesourcing is lower than that of the baseline scenario. The node around

2018 is based on historical data. However, a detailed interpretation is impossible owing to the number of assumptions and data constraints in the calibration process.

Pooled-ridesourcing behaviour is not discussed separately in future sections because its contribution to the aggregated MaaS is insignificant. Its usership in round-trips to work in the US was almost 0% in 2014, and at the end of the modelling, it will be not more than 1%. However, the mode's contribution is considered in the aggregated MaaS model calculation.

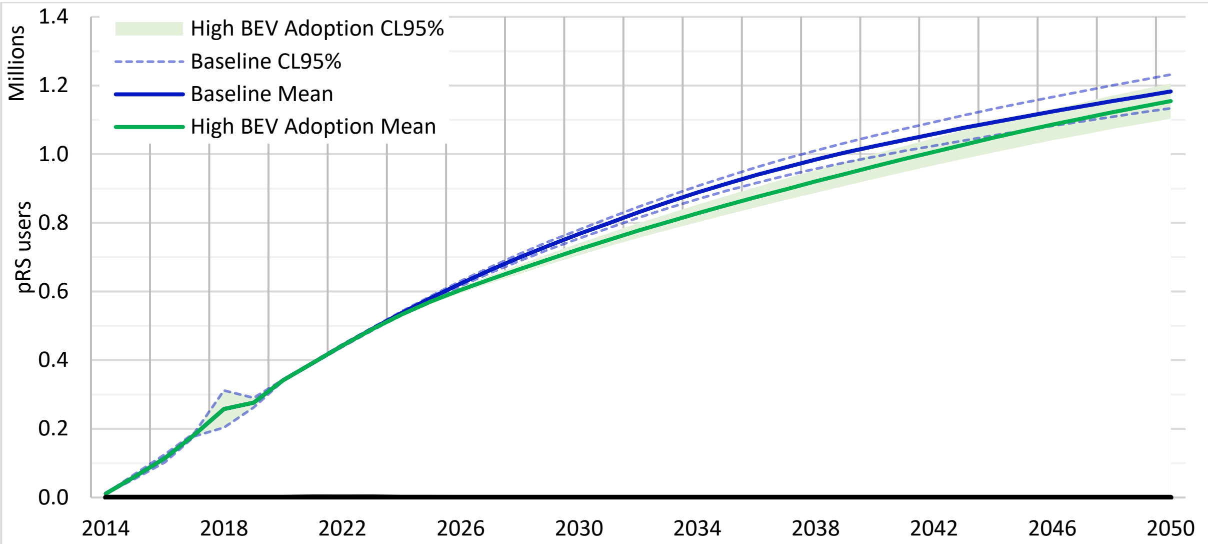

Figure 6-6 Transition to pooled-ridesourcing user behaviour

Note: CL–control limits, representing the confidence intervals

6.4.5 Private vehicle user behaviour

Private vehicle users show a slight decrease during the modelling period. It starts from the mid-2020s onwards in both scenarios. The timelines are aligned with the transition to high BEV adoption fleets. This trend demonstrates private vehicle users shifting to MaaS modes, especially adopting solo-ridesourcing. The two graphs in Figure 6-5 and Figure 6-7 complement each other. The decreasing trend of the private vehicle usage is clear and significant from the early 2030s until the mid-2040s between the two scenarios. The high BEV adoption curve has shown a flattening behaviour at the end of the modelling compared to the baseline. However, a significant comparison between the two scenarios is only possible from 2030 to 2044, during which the confidence intervals do not overlap.

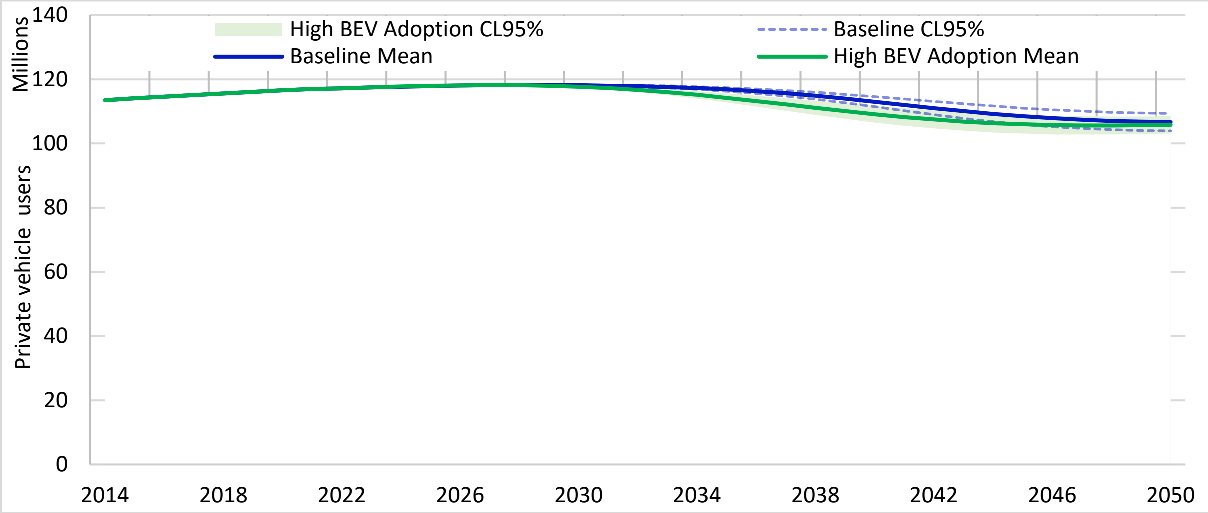

Figure 6-7 Private vehicle user behaviour

Note: CL–control limits, representing the confidence intervals

The personal mobility user behaviour outcomes demonstrate an increase and decrease in the adoption of solo-ridesourcing modes and pooling options, respectively, while observing a declining trend in private vehicle users in the chosen journey type to/from work in the US. The results show different adoption trends in the three MaaS modes and the influence of car technology adoption – high BEV. Overall, fleet behaviour is analysed by integrating the derived user trends into SD modelling, and the results are analysed in Sections 6.5 and 6.6, respectively.

6.5 Model implementation (S3): Sub-model – fleet behaviour

This section presents the SD model establishment of the private vehicle and MaaS fleet behaviour and the second of the three sub-models introduced in Section 4.6.1. The expected outcome of this sub-model is to determine the fleet behaviour of three MaaS modes extending to powertrain type and body style compositions by integrating the outcomes of the transition to MaaS sub-model. Hence, the reference mode of this sub-model is chosen as 'fleet stock'. The problem articulation work to understand personal mobility fleet behaviour is operationalised into an SD model in this section.

The two sub-model components, MaaS fleet behaviour and private vehicle fleet behaviour represent the aggregated personal mobility fleet behaviour. As shown in Figure 6-8, the multi-arrayed MaaS fleet and PC fleet are the two key stocks in this sub-model that describe the behaviour of powertrain type and vehicle body style compositions. Both stocks are modelled by spitting into two stocks only for modelling purposes. The stocks Fleet 2014 represent the initial stock in 2014 (including the historical fleet), and Fleet 2014 onwards is the ongoing stock. The variables Scrap rate PC fleet 2014, Scrap rate MaaS fleet 2014, Scrap rate PC fleet 2014 and Scrap rate MaaS fleet 2014 are formulated based on the outcomes of the curve-fitting exercises of the vehicle survival rates (Lu, 2006; Davis and Boundy, 2021) (see Figure C-1 in Appendix C). Figure 6-8 shows that inflows are the only formulation differences between MaaS and PC sub-model components. Detailed formulation descriptions, including the initial stock values, can be found in Appendix G. The behaviour of the stocks is derived based on system feedback and exogenous factors.

The stock MaaS fleet 2014 onwards connects the feedback loop between the transition to MaaS and consumer preference integration sub-model components. Subsequently, it establishes a feedback loop (causal relationship) with the variables MaaS fleet body distribution, vehicle body style attractiveness and MaaS mode attractiveness (see the **green loop** in Figure 6-8). The complete SD modelling stock and flow diagram are presented in Figure E-1 in Appendix E. The values for gross occupancy, an exogenous variable that determines the behaviour of the MaaS fleet, were sourced from the literature. They are carpooling – 2.18, calculated based on the US Census Bureau (2020), solo-ridesourcing – 1, pooled-ridesourcing–2.3, a conservative estimation based on previous studies (Henao and Marshall, 2018; Uber, 2020, p. 59; Wilkes *et al.*, 2021). The variable cars per trip is defined as the inverse of the gross occupancy rates and distinguishes the vehicle requirements of MaaS modes. It was assumed that two trips could be performed utilising a vehicle in ridesourcing fleets to cater to/from work trips that usually occur during peak hours. The temporal fleet technology changes are integrated through the variable MaaS fleet tech changes. They are based on Table 6-3. Two variables, delay function PC and delay function MaaS are introduced based on the outcomes of the scrappage rate integration curve-fitting exercises.

The steps to formulating the stock PC fleet in the private vehicle fleet behaviour sub-model component are similar to the MaaS fleet. The only exception is calculating the PC-to-user ratio variable using the inverse of the occupancy rate of private vehicles to/from work journey, 1.18 (McGuckin and Fucci, 2018, p. 58). However, the private vehicle fleet behaviour sub-model component is considered exogenous to the system by assuming that abandoning MaaS users shift to private vehicles and not vice-versa. The values for the variable PC fleet tech changes are based on Table 6-3.

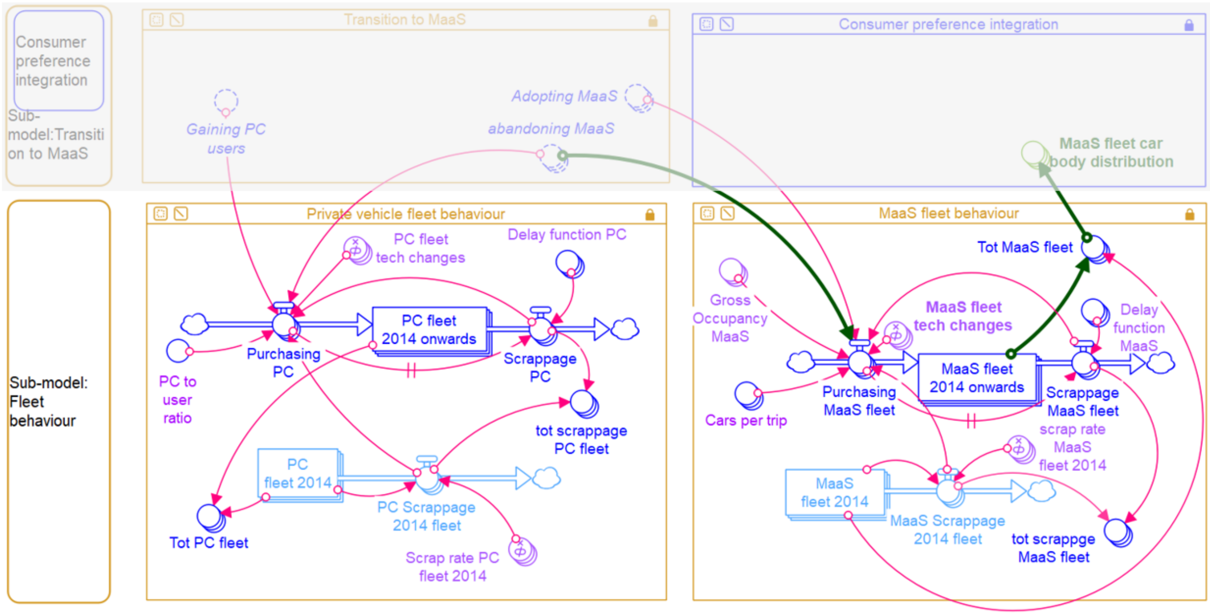

Figure 6-8 Stock and flow diagram of the fleet behaviour sub-model

Note: only the relevant variables are shown from the other sub-models

6.6 Results – fleet behaviour

This section presents the model outcomes of the dynamic fleet behaviour of the transition to MaaS from private vehicles.

An increase in the overall personal mobility fleet is shown even though the model results suggest higher transition rates to the car-based MaaS modes. The aggregated personal fleet behaviour is explored in Section 6.6.1. The fleet behaviours of the chosen car-based MaaS modes are significantly different based on user volumes derived in Section 6.4, attribute preferences for fleet technology changes (powertrain type and vehicle body style) and vehicle replacement patterns. Solo-ridesourcing has the highest fleet replacement rates to align with the transport network company requisites. The MaaS fleets are explored separately in Sections 6.6.2 and 6.6.3, and finally, the private vehicle fleet behaviour is analysed in Section 6.6.4.

Two key levels are chosen from the attributes of powertrain type and body style to analyse and discuss results based on their significance. Therefore, HEVs from powertrain types and hatch from body style are not explained separately in this thesis based on their insignificant representation. However, their results are taken into account in the overall analysis. Like in user behaviour, 95%

confidence intervals are used for the quantitative sensitivity analysis of fleet behaviours. However, they are not included in the graphs to simplify the presentation.

6.6.1 Personal mobility aggregated fleet behaviour

According to the model results, the total personal mobility fleet shows an increase. Figure 6-9 shows an almost equal total fleet growth from the mid-2020s to 2050 in the baseline and high BEV adoption scenarios. Both graphs show a steady increase in round-trips to work in the US. Unsurprisingly, the highest decline is in sedan gasoline, while the highest increase is in SUV BEVs. The SUV body style demonstrates a significant increase throughout the modelling period. The gasoline fleet, which was almost 100% in 2014, shows a substantial decline in both scenarios and a greater decrease in the high BEV adoption scenario. Shared mobility modes are separately examined to find mode-specific fleet behaviours in Sections 6.6.2 to 6.6.4.

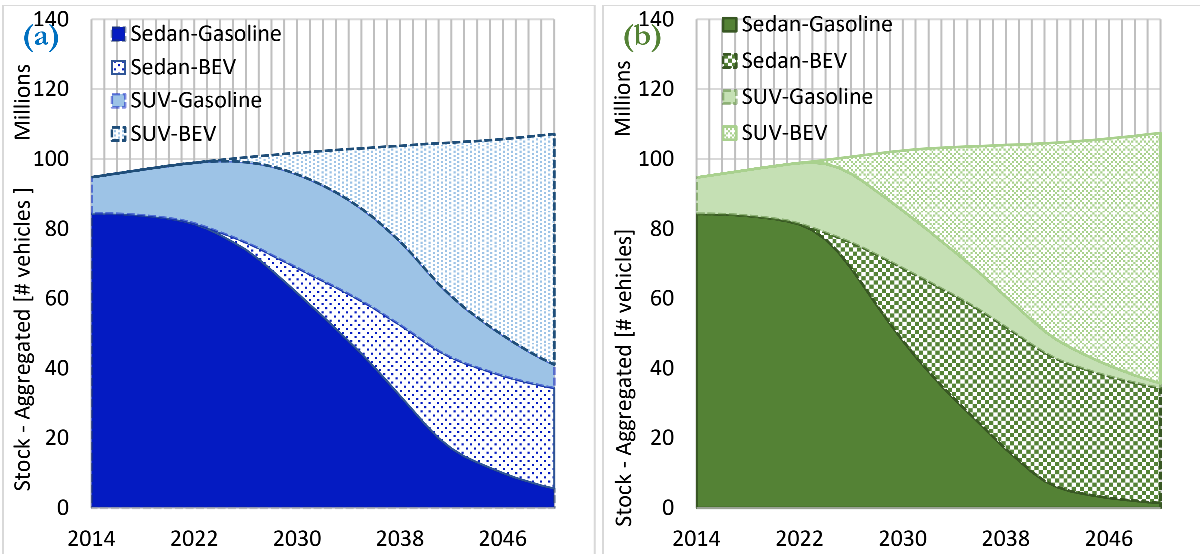

Figure 6-9 Personal mobility aggregated fleet stock behaviour

Note: (a) Baseline scenario and (b) High BEV adoption scenario

6.6.2 Carpooling fleet behaviour

Carpooling has shown the largest fleet reduction, while the slightest fleet composition changes between the baseline and high BEV adoption scenarios. Figure 6-10 shows a higher carpooling fleet stock reduction in the high BEV adoption scenario than in the baseline. The fleet drop aligns with the diminishing user trend explored in Section 6.4.2 and the users' dislike of the fleet transition to BEVs (Section 5.5.2). Although considerable gasoline vehicle reduction is shown in both scenarios, a more noticeable gasoline fleet exists at the end of the modelling time than in the other two MaaS modes. The potential reasons are increased automobile longevity based on survival rates (Lu, 2006, p. 8; Davis and Boundy, 2021, pp. 3–20), reduced user volumes, and no market mechanism to limit vehicle age as in ridesourcing modes. The highest fleet increase was observed during the transition to the SUV BEV fleet. The most interesting aspect of Figure 6-10 is the significant reduction in the number of sedans. This observation highlights the importance of considering body style in car-based MaaS fleet behaviour analysis and dynamic LCA calculations.

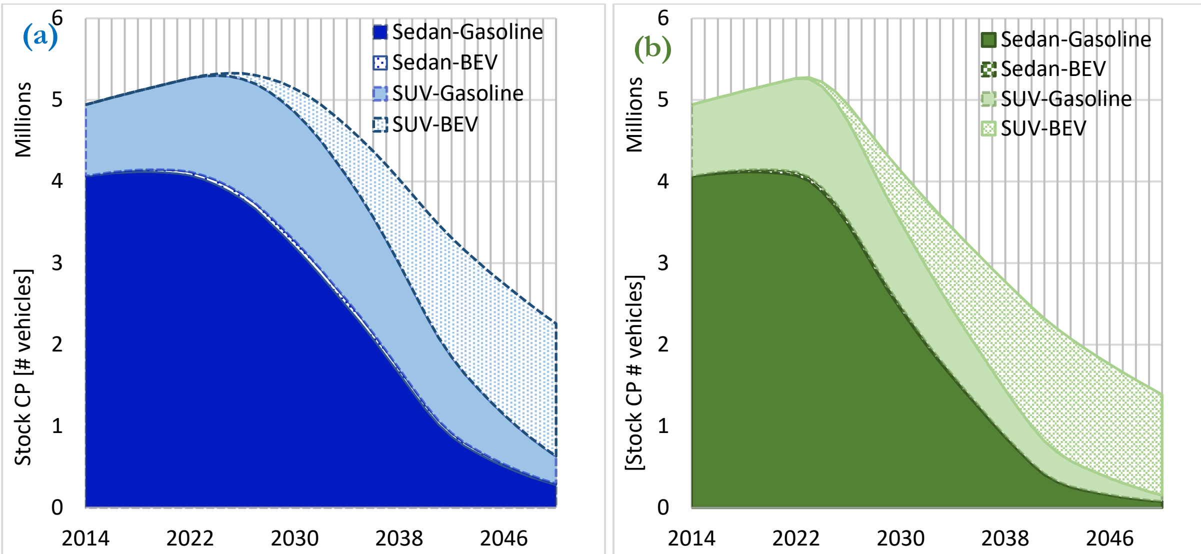

Figure 6-10 Carpooling fleet behaviour

Note: (a) Baseline scenario and (b) High BEV adoption scenario

The purchasing behaviour of the carpooling fleet also highlights the transition from conventional ICEVs to BEVs. The gasoline-driven carpooling fleet purchasing fraction will drop from almost 100% (in 2014) to 0% in 2050. It also reflects the reinforced consumer preference for SUVs. The respective body style and powertrain type curves in scrappage and purchasing reflect the delayed response of reaching the EoL of vehicle fleets (see Figure E-2 in Appendix E). A significant influence on this delay is the improved survival rate of newer vehicle fleets (Lu, 2006, p. 8; Davis and Boundy, 2021, pp. 3–20). The purchasing trajectory in the high BEV adoption scenario reflects the system feedback on the dropping of carpooling consumers in the early 2020s. This demonstrates a steeper decline in the sedan gasoline fleet fraction than in the baseline scenario. The same behaviour can also be seen in the scrappage graph (Figure E-2 in Appendix E) with a lower magnitude sedan gasoline curve compared to the baseline scenario. The lower magnitude represents the overall fleet and user reduction in the high BEV adoption scenario.

6.6.3 Solo-ridesourcing fleet behaviour

As shown in Figure 6-11, the solo-ridesourcing shows the highest fleet increase. The modelling outcome suggests the most significant fleet increase is required to cater to solo-ridesourcing users. It is more than a 200-fold increase. Interestingly, the reduction in gasoline vehicles in solo-ridesourcing fleets is very small because the initial fleet is also small. The modelling results also suggest a significantly higher BEV uptake from the mid-2020s while flattening and diminishing the gasoline fleet trajectory. The model predicts that a small number of gasoline-driven cars will remain at the end of the modelling period. However, these numbers are statistically uncertain. Unsurprisingly, SUV adoption is significant in solo-ridesourcing compared to sedans, similar to carpooling fleet behaviour. The SUV composition in 2050 is almost a three-fold increase compared to the 2014 solo-ridesourcing fleet and is only second to pooled-ridesourcing fleet behaviour.

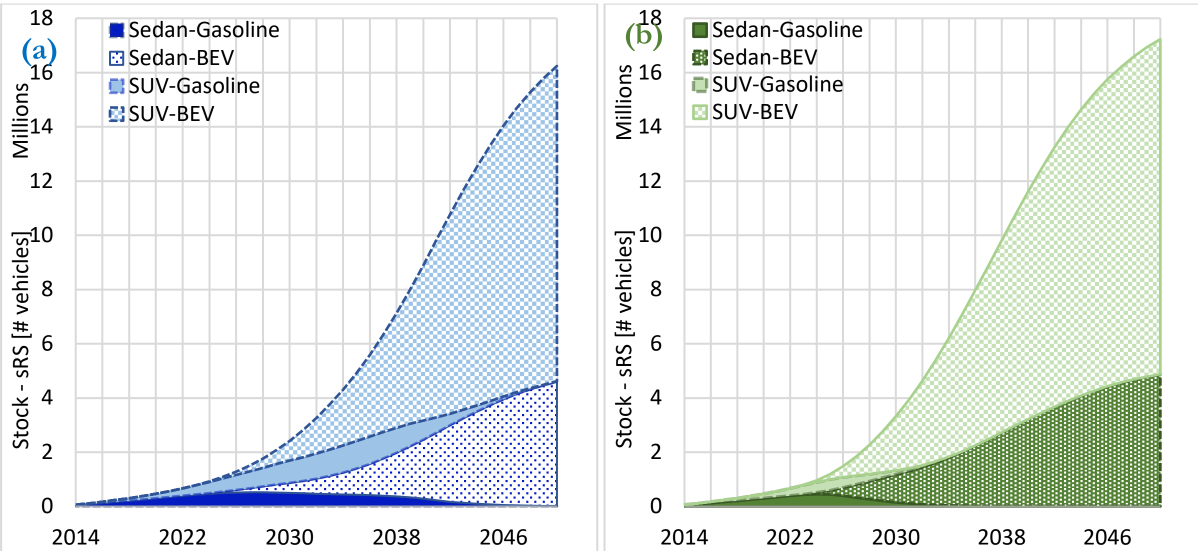

Figure 6-11 Solo-ridesourcing fleet behaviour

Note: (a) Baseline scenario and (b) High BEV adoption scenario

The purchasing and scrappage graphs (see Figure E-2 and Figure E-3 in Appendix E) reflect the delay process applied in the fleet behaviour sub-model (see Figure 6-8). However, the solo-ridesourcing fleet demonstrates a shorter delay period between the purchasing and scrappage graphs than the respective carpooling. This observation aligns with the model integration of more frequent replacements of ridesourcing fleets compared with carpooling. In the purchasing graph, a larger fleet requirement is shown to cater to the extensive solo-ridesourcing consumer in the high BEV adoption scenario than in the baseline scenario. The flattening sedan-BEV purchasing curves in both scenarios highlight the transition from sedans to SUVs in the solo-ridesourcing fleet.

However, it only appears with a lag in the scrappage graph because of the extended delay influenced by the improved survival rates for newer cars (Lu, 2006, p. 8; Davis and Boundy, 2021, pp. 3–20).

The results highlight that solo-ridesourcing fleet dynamics can significantly influence dynamic LCA calculations based on the magnitude of the fleet increase and changes in fleet composition.

The pooled-ridesourcing fleet, the smallest of the chosen three car-based MaaS modes, shows complete SUV BEV adoption from the early 2030s in the high BEV scenario and later in the baseline. In the baseline scenario, the sedan gasoline trajectory decreases and reaches 100% BEVs by 2050. As discussed in Section 6.4.4, the statistical significance of the pooled-ridesourcing values is weaker than that of the other modes.

The modelling data suggest a significant increase in car-based MaaS fleet volumes from 2014 to 2050 and significant changes in fleet technology adoption in the three MaaS modes. The total fleet size, powertrain type and body style factors are unique to the car-based MaaS mode, with the highest contribution from solo-ridesourcing. The overall MaaS fleet outcomes show a steady increase in fleet electrification, reaching almost 100% by 2050, while almost three-quarters of the fleets are SUVs.

6.6.4 Private vehicle fleet behaviour

The model outcomes predict a significantly small decrease in private vehicle fleet stock during the modelling period. As shown in Figure 6-12, the private vehicle fleet shows a slight increase in the first decade, following a flattening curve and a slight reduction. There is no major change within both scenarios. However, similar to other modes, fleet technology composition is significantly changed. The BEV and SUV adoptions are significant but less than the ridesourcing fleets. A possible reason for this is the slower fleet replacement speed compared to ridesourcing fleets. As seen in Figure 6-12, a 100% BEV is not reached by private vehicle fleets in either scenario within the modelling period. The modelling outcomes suggest that many private gasoline vehicles will exist by 2050 in the baseline and high BEV adoption scenarios. The SUV composition of private vehicle fleet stock in 2050 substantially increased at the end of the modelling period compared to the beginning.

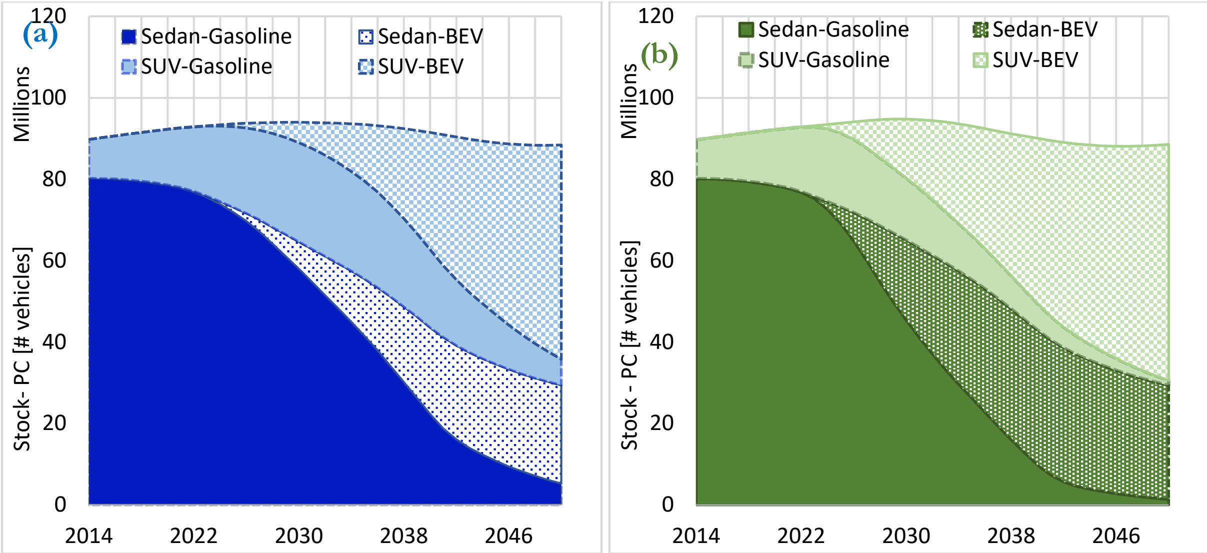

Figure 6-12 Private vehicle fleet size behaviour

Note: (a) Baseline scenario and (b) High BEV adoption scenario

6.7 Discussion

The personal mobility user and fleet behaviour were analysed based on the C-DLCA methodology framework, combining primary consumer preference data based on the constrained choices of the conjoint model-based primary data survey. Therefore, the derived results are more realistic because the same attributes used in the conjoint analysis are utilised in the Bass diffusion model-based transition to the MaaS sub-model. Hence, the derived results represent the influence of consumer preference and fleet technology changes in the transition to car-based sharing economy modes.

The model results show that the transition to car-based MaaS has reduced the number of employees that used private vehicles for the round-trip to work journey in the US by 20% from 2014 to 2050. Though the declining trend is aligned with the US Census Data-based round-trip to work journey (US Census Bureau, 2020a), the quantitative results show a steeper decline. The decline in the employment increase rate in the US can be identified as a reason for the reduction in overall self-driven values (Toossi, 2002). However, this observation commonly influences other car-based MaaS modes. Overall, the approach taken in this study on consumer preference integration has supported deriving the unique behaviour of the chosen MaaS modes separately and analysing them individually.

Surprisingly, the overall personal mobility fleet increases even though the model results suggest higher transition rates to the car-based MaaS modes. Therefore, fleet reduction is not achieved with the transition to car-based MaaS modes. A greater reason is that the highest transition is to the solo-ridesourcing mode, which requires faster vehicle replacements.

The highest user uptake by solo-ridesourcing aligns with the current car-based sharing economy market dynamics in major US cities (Uber, 2020; Schneider, 2021b, 2021a). The US census source, American Consumer Survey (ACS) data, has not considered ridesourcing a separate mobility mode for to/from work trips (US Census Bureau, 2020a). Hence, the available data does not support interpreting solo-ridesourcing uptake as a percentage. The consumer preference model inputs represent acceptance of solo-ridesourcing modes in the round-trip to work journey. However, previous studies found that the ridesourcing mode is commonly used for social, shopping and errand trips (Wolf *et al.*, 2015; Rayle *et al.*, 2016; Tirachini, 2019; Vij *et al.*, 2020). In summary, the outcomes of this study have important implications for determining GHG emission behaviour in the round-trip to work journey dominated by carpooling (Nurul Habib, Tian and Zaman, 2011; McGuckin and Fucci, 2018), which would shift to solo-ridesourcing in the future.

User preferences of powertrain type directly influence the transition to MaaS modes and fleet volumes based on the number of users. The high BEV adoption scenario has not shown a significant change compared to the baseline case in the overall user volumes and fleet size to/from work trips. The three MaaS modes behave differently by adopting the high BEV adoption scenario. Consumers have shown a significantly higher preference for gasoline vehicles in all personal mobility modes based on the utility values derived from the consumer choice-based survey (see Section 5.5.2). The highest utility value for BEVs is in solo-ridesourcing among the negative values for the three MaaS modes. This result is reflected in the SD model outcome by predicting extensive solo-ridesourcing consumers in the high BEV adoption scenario against the baseline scenario. However, the powertrain system was not identified as an exogenous variable in the Transition to MaaS sub-model. Hence, there is no feedback from consumer behaviour on the fleet other than inbuilt model data based on the derived scenarios in Section 6.3. The model outcomes of the purchasing and scrappage fleet volumes per annum can significantly influence the dynamic LCA results, especially the production and EoL phases, considering the powertrain type and car body style composition.

The model outcomes demonstrate a strong response to the temporal changes in vehicle body style composition. It is the only attribute that provides causal feedback (endogenous) and links the Bass model-based transition outcomes with consumer preferences and vice-versa. The survey outcomes of high utility values for SUVs (Section 5.5.2) connect with the increasing SUV fraction in the personal mobility fleet. Subsequently, more SUVs attract consumers. This model outcome demonstrates a causality and represents the reinforced loop (**R1**) introduced in Figure 4-5. The model supports SUV usage due to the positive utility values and the introduced feedback that combines the sub-models Transition to MaaS and fleet behaviour, employing the variable **MaaS fleet car body distribution** (see the **green loop** in Figure 6-2 and Figure 6-8). In the model inception, only the secondary data employed in the calibration process promoted SUVs based on historical trends and market projections. However, with feedback, the system itself reinforces SUV utilisation. Overall, the consideration of vehicle body style as a consumer preference attribute in the survey and the Transition to MaaS sub-model is prominent.

6.8 Summary

Transition to MaaS and fleet behaviour, the first two sub-models of the three introduced in Section 4.6.1 were established, and their outcomes were explored in this section. The transition user volumes, their characteristics, and fleet behaviour were generated by applying the C-DLCA framework by combining consumer preferences and car-based personal mobility fleet changes. The SD sub-model structure integrated the causality and temporality features of the related variables. The calibration process derived the values for the constants, the precision of which is difficult to gauge.

Results suggest that the transition to MaaS decreases private vehicle usage significantly and increases the lower occupancy-based solo-ridesourcing usership and, consequently, the total personal mobility fleet. The model outcomes demonstrate the shift to SUVs in personal mobility. Hence, the results highlight the importance of selecting the attribute vehicle body style as an endogenous variable in car-based MaaS studies by demonstrating its feedback in SD modelling and considering body style as an attribute of the DCE model. Although powertrain type is an exogenous attribute, the model outcomes demonstrate its significance in the transition to MaaS. The high BEV adoption scenario demonstrated more transition from private vehicles to MaaS but behaved differently within the MaaS modes with a broad shift to solo-ridesourcing. Hence, the environmental implications of these dynamics are complex. The complex dynamics were captured by employing the developed C-DLCA framework integrating consumer preferences, temporality and causality elements. The outcomes of this chapter provide the dynamic inputs to calculate a market-responsive dynamic LCA.

The dynamic LCA calculation is based on the outcomes of the sub-model fleet behaviour. Different behaviours of the powertrain, body style compositions and fleet quantities are direct inputs to calculate the dynamic GHG changes in the transition to car-based MaaS from private vehicles. Derived outcomes of the sub-model transition to MaaS provide the inputs to calculate p.km, the chosen functional unit of this study. In summary, all the endogenous and many exogenous inputs to calculate the dynamic LCA are employed from the results of this Section. The dynamic LCA calculation sub-model is presented in Chapter 7.

7 DYNAMIC LCA RESULTS

Publication relevant to this Chapter

Fernando, C., Buttriss, G., Yoon, H.-J., Soo, V. K., Compston, P., & Doolan, M. (Accepted). Integration of consumer behaviour into dynamic life cycle assessment for the sharing economy: Methodology and case study for shared mobility. *International Journal of Life Cycle Assessment.*

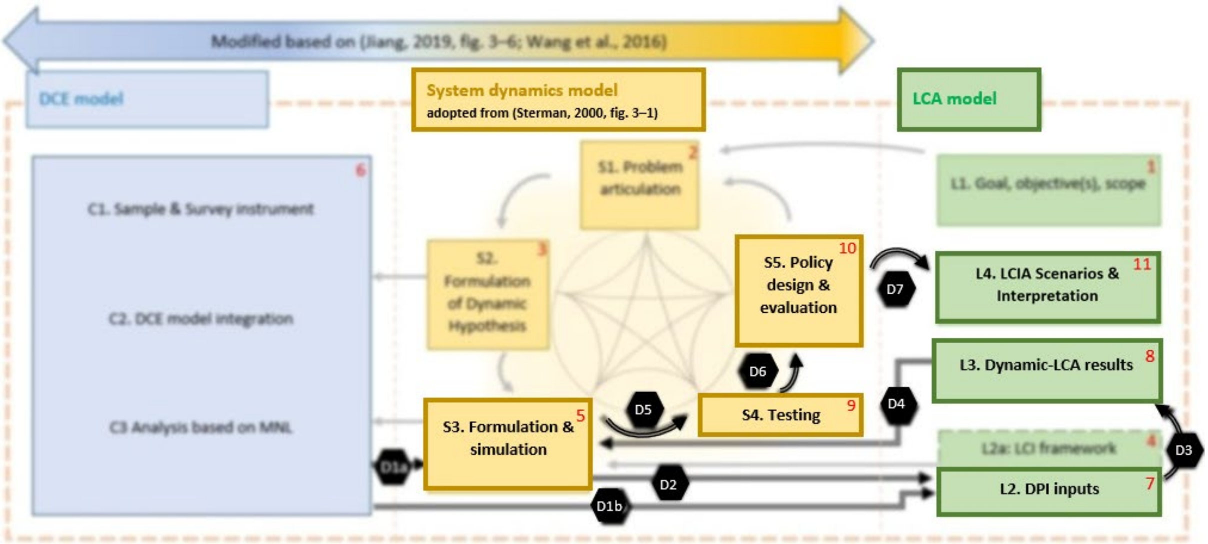

Figure 7-1 C-DLCA methodology framework components relevant to Chapter 7

Introduction

The SD model establishment of the last sub-model, dynamic LCA calculation, is presented in this chapter. Dynamic LCA calculation is the third and the last sub-model. It provides quantitative inputs to operationalise the LCA model component of the C-DLCA methodology framework (see Figure 7-1). This chapter presents an analysis to achieve research Aim 3: Determine the significance of consumer preferences and fleet technology changes on the dynamic GHG emission changes of the transition to car-based sharing economy modes over time by selecting a case study. It also answers the established key research question, **'What is the impact of the transition from private car use to car-based sharing economy modes on GHG emissions, considering consumer preferences and fleet technology changes?'.** The establishment of the sub-model dynamic LCA calculation differs somewhat from the typical LCA design process. Section 7.1 explains the connectivity of the established LCA components of the C-DLCA framework in the previous sections and the dynamic LCA calculation sub-model.

7.1 Dynamic LCA calculation readiness

The C-DLCA methodology framework starts and ends with the LCA components, ensuring that it follows ISO 14040 principles. It starts from the step goal, objectives and scope setting (L1) and ends in the step LCIA scenarios and Interpretation (L4). The LCA goal defined in Section 4.2.1: 'analysing the GHG impacts of the transition from private car use to car-based sharing economy modes in an average round-trip to/from work journey in the USA, considering the consumer preferences and the fleet technology changes', highlights the dynamical requirements of the study considering the changes in the fleets. The chosen scope of study in Section 3.1 is aligned with the set goal and combines consumer preferences. The selection of p.km as the functional unit of the study and cradle-to-grave as the LCA scope is based on the literature and the anticipated impacts of the transition to car-based sharing economy modes (see Section 4.2.2). An interim step, LCI framework setting up (L2a), which was an input for the formulation and simulation (S3) step, was discussed in Section 4.5. The LCI data and information requirements were identified before administering the survey to collect data.

The remaining two steps of the LCA components in the C-DLCA framework are explored in this chapter. A DPI is introduced in Section 7.2 instead of the conventional (static) LCI phase (step L2 in the C-DLCA framework). This step is introduced to incorporate the temporal influencing factors from the external LCA database (the GREET model is used in this research) and the derived dynamic outcomes from the previous two sub-models (transition to MaaS and fleet behaviour in Section 6). Section 7.3 introduces the model implementation steps, formulation and simulation (S3) and dynamic LCA results (L3). They are combined with the user and MaaS fleet behaviour dynamic outcomes derived in Chapter 6. The dynamic LCA results (L3) are analysed and discussed in Sections 7.4 and 7.5 (L3, S5 and L4 steps in Figure 7-1). The effect of combining consumer preference in dynamic LCA is explored in Section 7.6, and a sensitivity analysis is checked against the variable deadheading in Section 7.7. The chapter ends with a discussion on the interpretation of dynamic LCA results and a summary in Sections 7.8 and 7.9.

7.2 Dynamic process inventory (L2)

The dynamic LCA calculation sub-model integrates the derived fleet behaviour outcomes from Chapter 6 to generate the DPI. This approach produces a dynamic LCI profile instead of a conventional static approach (Sohn *et al.*, 2020). The inputs from the sub-model fleet behaviour are combined with the GREET database (Wang *et al.*, 2021) to create the DPI. The (static) LCI data inputs are sourced from the GREET model for the fleet technology types chosen in this study. Two vehicle body styles – sedan and SUV-related GREET model data–are employed, and 90% of sedan impacts are assumed for the hatch body style. Passenger car type number one from the GREET model for sedans and SUVs is chosen for this study's modelling work. Three powertrain types—a) gasoline-driven, b) HEV, and c) BEV data—are also sources of the GREET model. In addition, the GREET model-based vehicle lightweighting factors are also integrated into the DPI, as shown in Table 6-3. The DPI is created considering the three key life cycle phases, and the approach is presented in Sections 7.2.1 to 7.2.3.

7.2.1 DPI establishment – production

The DPI establishment for vehicle production comprises two components. The GHG profile is established in the first part based on the secondary data obtained from the GREET model. It contains three GHG sources: embedded raw materials, automobile production and battery production. The GREET model follows the secondary material-integrated raw material impact calculation method. Hence, recycled components are already considered in the production phase and avoided in EoL calculations. Automobile production GHG emissions represent the impact of the consumed thermal and electrical energy quantities per vehicle. Battery production-related GHG emissions are calculated based on the powertrain type. Only lead-acid battery impacts are considered for gasoline vehicles. In addition, nickel-metal hydride (NiMH) batteries have been considered for HEVs and Li-ion batteries for BEVs.

The second part of the DPI establishment for vehicle production considers the vehicle lightweighting changes introduced in Section 3.3.1. Table 7-1 presents the derived lightweighting values for the different body styles and powertrain types considered in this study. A 20-year cycle was assumed from 2020 to implement the GREET model lightweighting scenarios from 14.8% to 20.5%. In contrast, the raw material composition changes targeting lightweighting, increasing the embedded GHG and, subsequently, the production of GHG emissions. Hence, production GHG values and vehicle lightweighting are integrated into the production DPI calculation process by applying the linear spread approach from 2020 to 2039. The DPI production phase profile summary is derived based on Table 7-1 weight distribution and the respective LCI values from the

GREET model presented in Table C-5 in Appendix C. The influence of lightweighting on increasing fuel economy is considered in the DPI use phase.

Table 7-1 Vehicle weight excluding the battery

Body style	Powertrain type	Weight [kg/vehicle] 2014 to 2019[1]	Linear weight reduction [kg/vehicle, (%)] from 2020-2039[2]	Weight [kg/vehicle] 2040 onwards[1]
Sedan	Gasoline	1,385	217 (15.7%)	1,168
	HEV	1,555	268 (17.2%)	1,288
	BEV	1,742	357 (20.5%)	1,384
SUV	Gasoline	1,680	249 (14.8%)	1,431
	HEV	1,901	313 (16.5%)	1,587
	BEV	2,166	435 (20.1%)	1,733
Hatch*	Gasoline	1,241	195 (15.7%)	1,051
	HEV	1,400	241 (17.2%)	1,159
	BEV	1,567	322 (20.5%)	1,246

Notes: [1] (Wang *et al.*, 2021), [2]Calculated based on (Wang *et al.*, 2021), *assumed 90% of sedans

7.2.2 DPI establishment – use phase

The use phase of DPI changes consists of three GHG emission components. These are a) combustion emissions in gasoline and HEV fleets, b) secondary emission sources, such as refinery emissions and electric grids, and c) fleet maintenance. The combustion component contributes significantly to the use-phase GHG emissions of gasoline vehicles (see Figure 4-4). The GREET model data are employed to calculate the DPI profile for the combustion GHG emission component (Wang *et al.*, 2021). The use-phase GHG calculations are derived utilising the GREET model lightweight vehicle GHG emission factors and the energy economy benefits for the introduced vehicle lightweighting scenario in Section 6.3. From 2020 to 2039, calculations are performed by applying the linear weight reduction based on Table 6-3. Temporal changes in the well-to-tank, including refinery GHG emission factors, were not employed in this study due to data accessibility challenges. Vehicle fluid-related GHG emissions are included in the DPI process to represent maintenance GHG impacts and are considered to not change during the modelling period. These data were sourced from the GREET model. The derived DPI use phase profile summary is presented in Table C-6 in Appendix C.

The US electricity grid GHG emission changes are integrated into the use phase DPI calculations. An estimated 53% GHG emission reduction is expected from 2014 to 2050 in the US electricity grid (U.S. Energy Information Administration - EIA, 2016, 2019, 2021) (see Figure C-2 in

Appendix C). This indirect GHG emission change significantly influences the use phase GHG emissions of the BEV fleets. However, grid GHG emission changes are not utilised in the manufacturing energy-related GHG impacts discussed in Section 7.2.1 due to the uncertainties of the automobile manufacturing locations. These considerations are not directly related to the research purposes and aims.

7.2.3 DPI establishment – EoL

The energy required to treat a vehicle at the EoL and battery recycling impacts is considered in the DPI establishment for the EoL phase. Recycled material impacts are not considered because the GREET model follows the secondary material approach, and these impacts are already captured in the production phase (Wang *et al.*, 2021). The energy requirements for EoL treatments differ based on body style and were obtained from the GREET model. The adopted automobile lightweighting changes are also considered to calculate the EoL DPI profile by considering the vehicle weight prorated energy and respective GHG emissions. The derived DPI–EoL profile summary is presented in Table C-7 in Appendix C.

The SD model implementation to combine the separately calculated DPI processes with the sub-model outcomes to determine the dynamic LCA profile is presented in Section 7.3.

7.3 Model implementation (S3, L3): Sub-model – Dynamic LCA calculation

This section presents the SD model implementation of the dynamic LCA calculation and the last of the three sub-models introduced in Section 4.6.1. The sub-model fleet behaviour and DPI outcomes are combined in this sub-model to generate the final dynamic LCA results (L3). As shown in Figure 7-2, the dynamic LCA calculation sub-model contains four components. They are a) GHG emissions from private vehicles, b) GHG emissions from MaaS, c) the functional unit calculations for p.km and distance-based v.km units, and d) GHG emissions results component. Their model simulations are presented in Sections 7.3.1 to 7.3.3. The complete SD model formulation notes are listed in Appendix G.

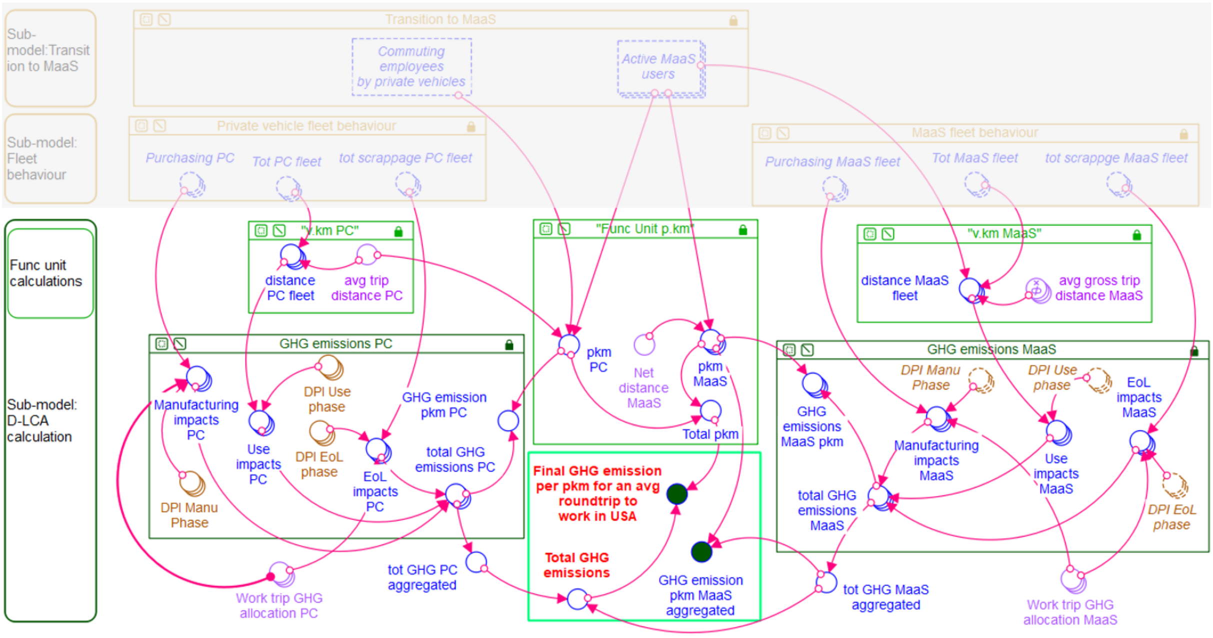

Figure 7-2 Stock and Flow Diagram of the D-LCA calculation sub-model

Note: only the relevant variables are shown from the other sub-models

7.3.1 GHG emissions calculations for private vehicles and MaaS

As shown in Figure 7-2, the two GHG emissions sub-model components (private vehicles (PC) and MaaS) incorporate the DPI outcomes and the dynamic inputs from other sub-models (transition to MaaS and fleet behaviour in Section 6) to generate the dynamic LCA results. The SD simulation of these sub-model components is combined with the dynamic LCA calculation sub-model based on the DPI outcomes derived in Section 7.2 for the three life-cycle phases.

Production phase dynamic LCA results are calculated by combining the DPI production phase outcomes (DPI Prod Phase) and related variables. As shown in Figure 7-2, purchasing PC and purchasing MaaS fleet are identified as the most relevant flows that directly influence the GHG emissions of production in private vehicles and MaaS fleets, respectively. The two variables provide the system feedback (from the sub-model fleet behaviour) to quantify the production dynamic LCA results by multiplying them with the respective DPI production profiles. The variables of work trip GHG allocation MaaS and work trip GHG allocation PC are introduced to allocate the GHG contribution of the round-trip to/from the work journey into the production and EoL impacts of MaaS and private vehicle fleets, respectively. The calculated allocation factors are presented in Table C-8 of Appendix C. These variables are incorporated into the production and EoL dynamic LCA calculation formulation as multipliers.

The use phase dynamic LCA impacts are calculated by multiplying the variable distance (v.km) by the respective DPI use phase elements. The use impacts PC and use impact MaaS are calculated by multiplying the DPI use phase elements (DPI Use Phase) derived in Section 7.2.2 by the distance PC fleet and distance MaaS fleet, respectively. The fleet stocks provide system feedback to calculate the total distances by combining the total gross journey distances. The private car trip distance is computed by multiplying the average (avg) trip distance for round-trip work in the US (20.6 km per day) by the size of the private vehicle fleet (Tot PC fleet). The variable average gross distances of the MaaS for each mode are calculated considering the respective deadheading values presented in Table 7-2. The derived journey distance value is also multiplied by the average working days (260) to calculate the average annual journey distance (U.S. Bureau of Labor Statistics, no date).

Table 7-2 Input data and sources - calculating the gross distance and p.km

Parameter		Value	Source/remarks
Gross distance private vehicle and Net distance MaaS [km]		20.6	(McGuckin and Fucci, 2018, p. 20)
Distance-based v.km calculation			
Deadheading [%]	CP	12%	Assumed 25% of pooled-ridesourcing
	sRS	40%	Calculated based on (Henao and Marshall, 2018)
	pRS	48%	Assumed 20% higher than solo-ridesourcing

The EoL dynamic LCA impact calculation follows a similar approach to the production impact calculations. The only difference is that in the EoL process, scrappage outflows (tot scrappage PC fleet and tot scrappage MaaS fleet) are used instead of purchasing inflows in the production phase. Detailed GHG emission calculations of the SD model can be found in Appendix G.

7.3.2 Functional unit calculations

The functional unit p.km is the product of the net distance and number of passengers (Henao, 2017; Union of Concerned Scientists, 2020b). The net distance of 20.6 km/round-trip to work is based on the latest US National Household Transport Survey (McGuckin and Fucci, 2018, p. 20). The p.km calculation is based on two stocks. They are a) active MaaS user representing the number of car-based MaaS passengers and b) 'private vehicle users', the difference between the stocks of commuting employees by private vehicles and active MaaS users.

7.3.3 Dynamic LCA – results interpretation (L4)

The final dynamic LCA results (L4 in Figure 4-1) are presented in two forms. The results are generated from separate MaaS modes and aggregated personal mobility fleets and interpreted based on two forms. These are the absolute GHG emissions expressed in tonnes of carbon dioxide equivalent (tCO_2eq) and are referred to as the functional unit illustrated in gCO_2eq/p. km. Both cases express GHG emissions as carbon dioxide equivalent (CO_2eq).

The dynamic LCA results are interpreted to understand the system behaviour and to highlight the responses to the temporal and causal interrelations. Hence, the dynamic LCA results in Section 7.4 are presented as a qualitative and quantitative mixed approach. This approach prioritises more SD model behaviour-based interpretations without highlighting only the quantitative modelling outcomes. These interpretations are based on the reference modes (see Section 6.2.1). Therefore, this approach avoids possible misinterpretations based on the quantitative outcomes of the SD model, which depend on several assumptions that lead to uncertainties. A sensitivity check is performed to check the robustness of the system (see Section 7.6).

7.4 Results – Dynamic LCA (L3 and L4)

This section presents the model outcomes of the dynamic LCA of the transition from private vehicles to MaaS. GHG is chosen as the life cycle impact category to interpret results based on the selected life cycle database, the GREET model (Wang *et al.*, 2021), and aligns with the previous research practices (see Table A-2, Table A-4, Table A-5 in Appendix A). The results are presented in three forms: a) absolute GHG emissions, c) specific GHG emissions related to the functional unit p.km, and c) the number of p.km and interpreted as explained in Section 7.3.3. Like in user and fleet behaviour analysis, 95% confidence intervals are used for the quantitative sensitivity analysis of dynamic GHG results. However, they are not included in the main graphs to simplify the presentation and are attached in Appendix E (Figure E-6 to Figure E-9).

The dynamic GHG results show that the transition from private vehicles to car-based MaaS is not providing a complete solution to the personal mobility GHG emissions of round-trips to work in the US by providing a specific answer for the key research question: '**What is the impact of the transition from private car use to car-based sharing economy modes on GHG emissions, considering consumer preferences and fleet technology changes?**' However, the high BEV adoption scenario reduces the life cycle GHG emissions compared to the baseline scenario. The dynamic GHG emissions behaviour of the aggregated personal mobility fleets is explored in Section 7.4.1. Section 7.4.4 explores the private vehicle fleet-related dynamic GHG results. It is also the mobility mode that recorded the highest GHG emission reduction. Dynamic GHG behaviours of car-based MaaS modes show significant differences, which are presented in Sections 7.4.2, 7.4.3 and 7.4.5.

7.4.1 Dynamic GHG emission behaviour – Aggregated personal mobility

The model outcomes show a significant reduction in aggregated personal mobility-related GHG emissions for round-trips to work in the US by transitioning to car-based MaaS at the end of modelling compared to the beginning. This observation is common for both scenarios. The GHG emission reduction trend is aligned with the higher user transition to MaaS (see Figure 6-3) and the fleet transition to lower GHG-emitting BEVs (see Figure 6-9). As shown in Figure 7-3 (a), a steep reduction in absolute GHG emissions begins in the mid-2020s and continues in the baseline scenario. Thus, the reduction rate decreases and flattens at the end of the modelling period. However, the high BEV adoption scenario shows an increase starting in 2022 and only starts to reduce from the mid-2020s. This trajectory represents the contribution of higher manufacturing emissions during aggressive fleet electrification to achieve 100% BEV sales by 2030 (the life cycle phase implications are discussed in detail in Section 7.5). As a whole, this observation proves that the model responds to the scenarios introduced in Section 6.3.

The absolute GHG emission reduction difference between the baseline and high BEV adoption scenarios is insignificant considering the entire modelling period (Figure 7-3 (a)). Hence, considering the high BEV adoption, the transition to car-based MaaS does not provide a complete solution to personal mobility-related GHG emissions for the chosen case study. Therefore, it is worthwhile to analyse specific GHG emission behaviours.

The specific GHG emission reductions of the aggregated car-based personal mobility modes also align with the absolute GHG emission trajectory since the personal mobility p.km values do not show differences (Figure 7-3 (c)). The above behaviour can be further observed in Figure E-6 in Appendix E, with the confidence intervals. The p.km behaviour is based on a similar number of users in both scenarios (see Figure 6-3). As shown in Figure 7-3 (b), a larger GHG reduction per p.km can be seen in the high BEV adoption scenario compared to the baseline case. This difference is expected based on generating lower GHG emissions in the high BEV adoption scenario fleet compared to the baseline. At the end of the modelling period, the high BEV adoption scenario shows a lower and more stabilising curve than the baseline. Compared with the baseline, this behaviour can be explained by the complete fleet transition to BEVs in the high BEV adoption scenario (see Figure 6-9). Similar behaviour for the baseline is expected beyond the modelling period because the fleet transition to BEVs is slower than the high BEV adoption scenario. These values represent the policy scenarios introduced in Section 6.3.

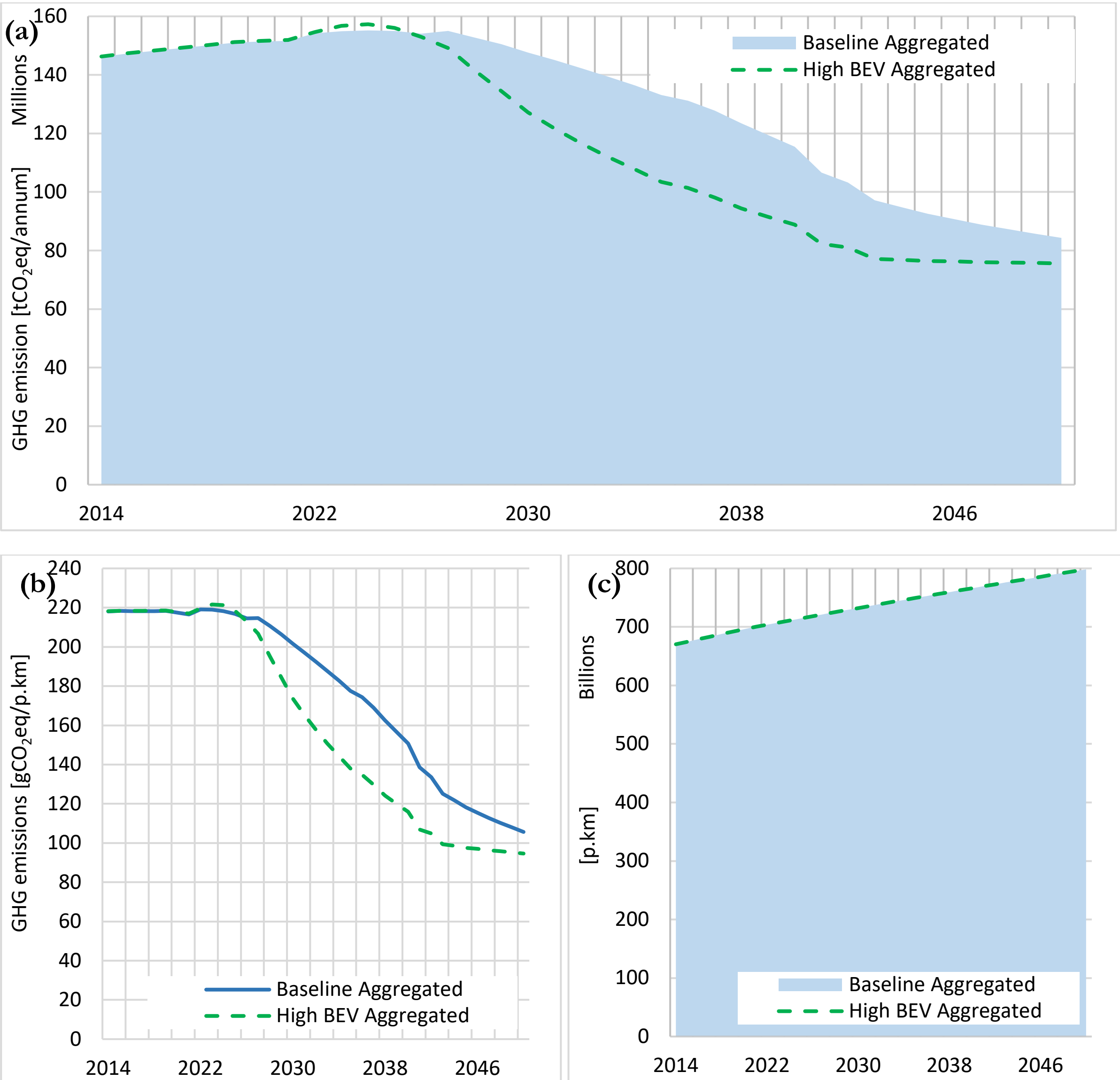

Figure 7-3 Dynamic GHG results – Aggregated car-based personal mobility modes

Notes: (a) Absolute GHG emissions, (b) Specific GHG emissions compared to p.km, (c) Passenger kilometres. See Figure E-6 in Appendix E for the graph with confidence intervals

The aggregated dynamic GHG outcomes result from the four personal mobility modes considered in this section. In summary, analysing the contribution of specific mobility modes is critical for understanding the particular contribution of each mode. Sections 7.4.2 to 7.4.4 explore the mobility mode contribution of GHG emissions in the transition to MaaS modes, and Section 7.4.5 analyses the aggregated MaaS GHG emission behaviour.

7.4.2 Carpooling – Dynamic GHG emission behaviour

The carpooling mode predicts significant GHG emission savings at the end of modelling compared with starting. It also shows that the savings in the high BEV adoption scenario are greater than those in the baseline (see Figure 7-4 (a)). Both scenarios show a slight increase in GHG emissions in the first few years. This behaviour is based on historical data. The sudden increase from 2022 to 2024 is based on the higher manufacturing GHG emissions generated by aggressive BEV replacement to achieve the high BEV adoption scenario requirements. This observation is common in all mobility modes, and only the magnitude differs. The high BEV adoption scenario shows a steady GHG emission reduction from 2024 onwards compared to the baseline scenario. This reduction is due to the significant decrease in use-phase GHG emissions owing to the faster transition to the BEV fleet and is further supported by the US grid electricity GHG reductions (see Section 7.2.2). As discussed in Section 6.4.2, user behaviour is more favourable for the baseline in the carpooling mode. Hence, it is essential to understand the specific GHG emission behaviour measured against the passenger occupancy integrated p.km, carpooling being the high-occupancy-based MaaS mode.

Unsurprisingly, the high BEV adoption scenario of carpooling shows the least GHG emissions in the transition to car-based MaaS modes (see Figure 7-4 (b)). The largest GHG emissions difference between the baseline and BEV adoption scenarios is recorded in the carpooling mode and is also statistically significant (see Figure E-7 in Appendix E, with the confidence intervals). The trend started in 2022 because of the lower GHG emissions generated by electrified fleets. The results also indicate a steady GHG emission reduction in the baseline scenario when expressed against the functional unit p.km. Both scenarios show the highest GHG emissions in carpooling mode in 2022-2024, aligning with the absolute GHG emission explanation for the same period. Interestingly, GHG emissions in the high BEV adoption scenario have shown a slightly higher behaviour than the baseline until 2023. The results are aligned with the absolute GHG emission trends and are based on historical data. Another explanation is the influence of indirect factors on the systems, such as electric grid GHG emissions. This observation is also common in the solo-ridesourcing mode. The GHG emission per p.km results align with the carpooling consumer preference and fleet behaviours discussed in Sections 6.4.2 and 6.6.2.

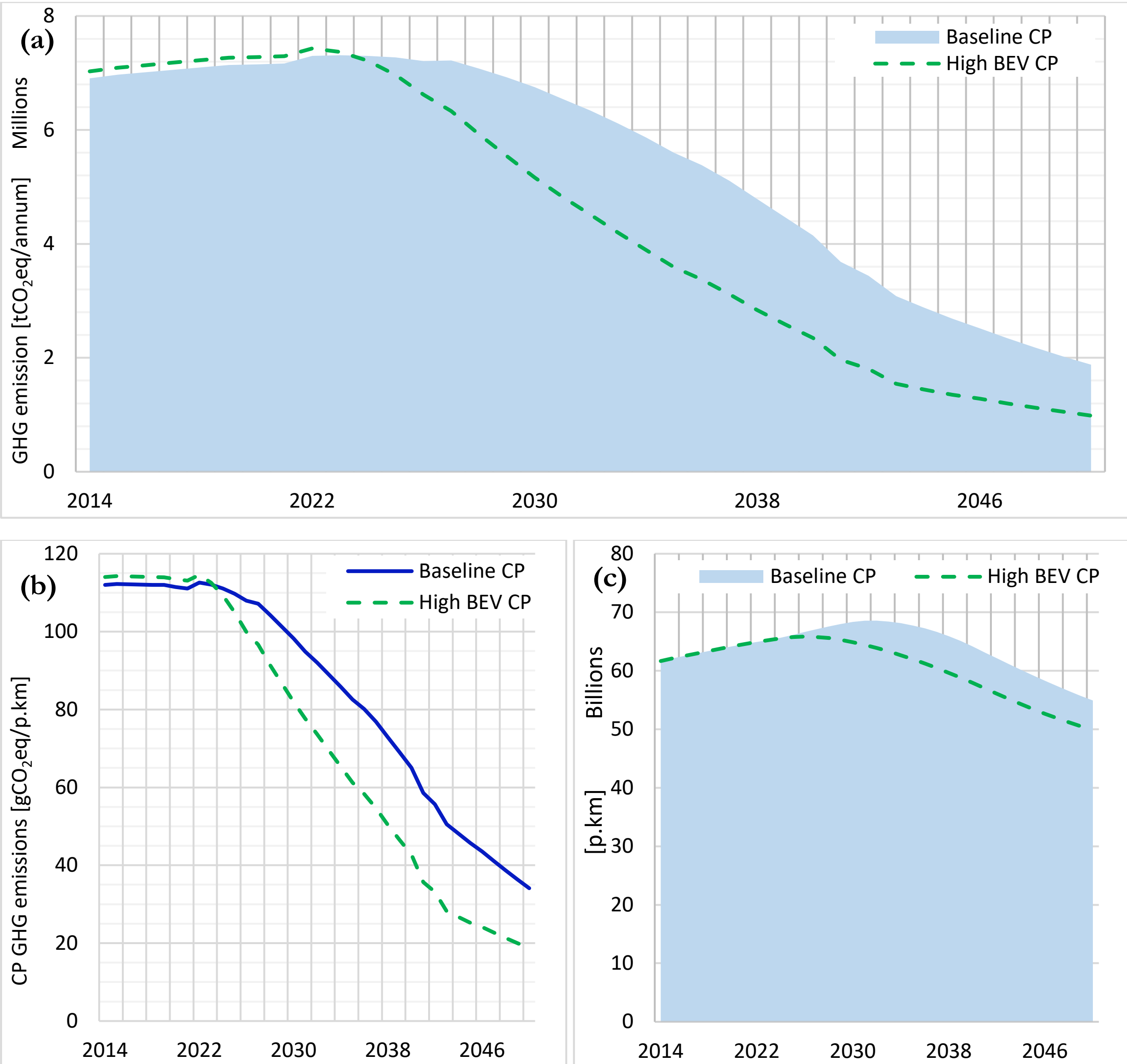

Figure 7-4 Dynamic GHG results – Carpooling

Notes: (a) Absolute GHG emissions, (b) Specific GHG emissions compared to p.km, (c) Passenger kilometres. See Figure E-7 in Appendix E for the graph with confidence intervals

As per the model results, the overall carpooling p.km units decreased at the end of the modelling period compared to the beginning. The high BEV adoption scenario showed a higher p.km reduction than the baseline scenario. This trend can be explained the behaviour of lower user preference for carpooling in the high BEV adoption scenario compared to the baseline, as shown in Figure 6-4. Interestingly, the GHG emissions per p.km for carpooling in high BEV adoption are smaller than the baseline from 2025, although the p.km behaviour decreases. This result demonstrates the importance of the contribution of fleet electrification even in high-occupancy car-based MaaS modes.

7.4.3 Solo-ridesourcing – Dynamic GHG emission behaviour

The model results suggest a significant increase in absolute GHG emissions in the solo-ridesourcing mode in both scenarios. As shown in Figure 7-5 (a), in the baseline scenario, GHG emissions showed a significant increase, with an average of 20-fold. This emission trend is influenced by multiple factors representing the nature of the mode and fleet technology elements. The solo-ridesourcing mode represents the lowest occupancy rate among the three car-based MaaS modes chosen for this work. Hence, its net service distance is significantly lower than that of the other modes by generating non-productive distances, also known as deadheading in the mobility industry (see Table 7-2). Hence, the extra distance generates more emissions than in the other MaaS modes. The larger high GHG emitting SUV composition in the solo-ridesourcing fleet also complements the generation of more GHG emissions compared with other modes (see Figure 6-11).

Unlike carpooling, the solo-ridesourcing fleet in the high BEV adoption scenario emits more GHG emissions than the baseline scenario. This emission behaviour is aligned with the higher user transition to solo-ridesourcing in the high BEV adoption scenario (see Section 6.4.3). The emission behaviour of both scenarios is closely similar until 2022, which shows similar behaviour to all mobility modes. However, the node from 2022 to 2026 is more prominent in the high BEV adoption scenario than in other mobility modes. This observation represents the increasing production phase GHG emissions due to the aggressive fleet electrification shift led by transport network companies in ridesourcing compared to conventional carpooling and private vehicle fleets. Hence, the model responds to the policy scenarios introduced in Section 6.3. From there onwards, the trend is maintained below the baseline emission trajectory until the mid-2030s. The increase in GHG emissions in the high BEV scenario in the latter part of the modelling period is supported by the user transition trend, as shown in Figure 6-5. In 2050, this mode will contribute closer to one-quarter of the overall personal mobility GHG emissions, with slight changes in the baseline and high BEV adoption scenarios.

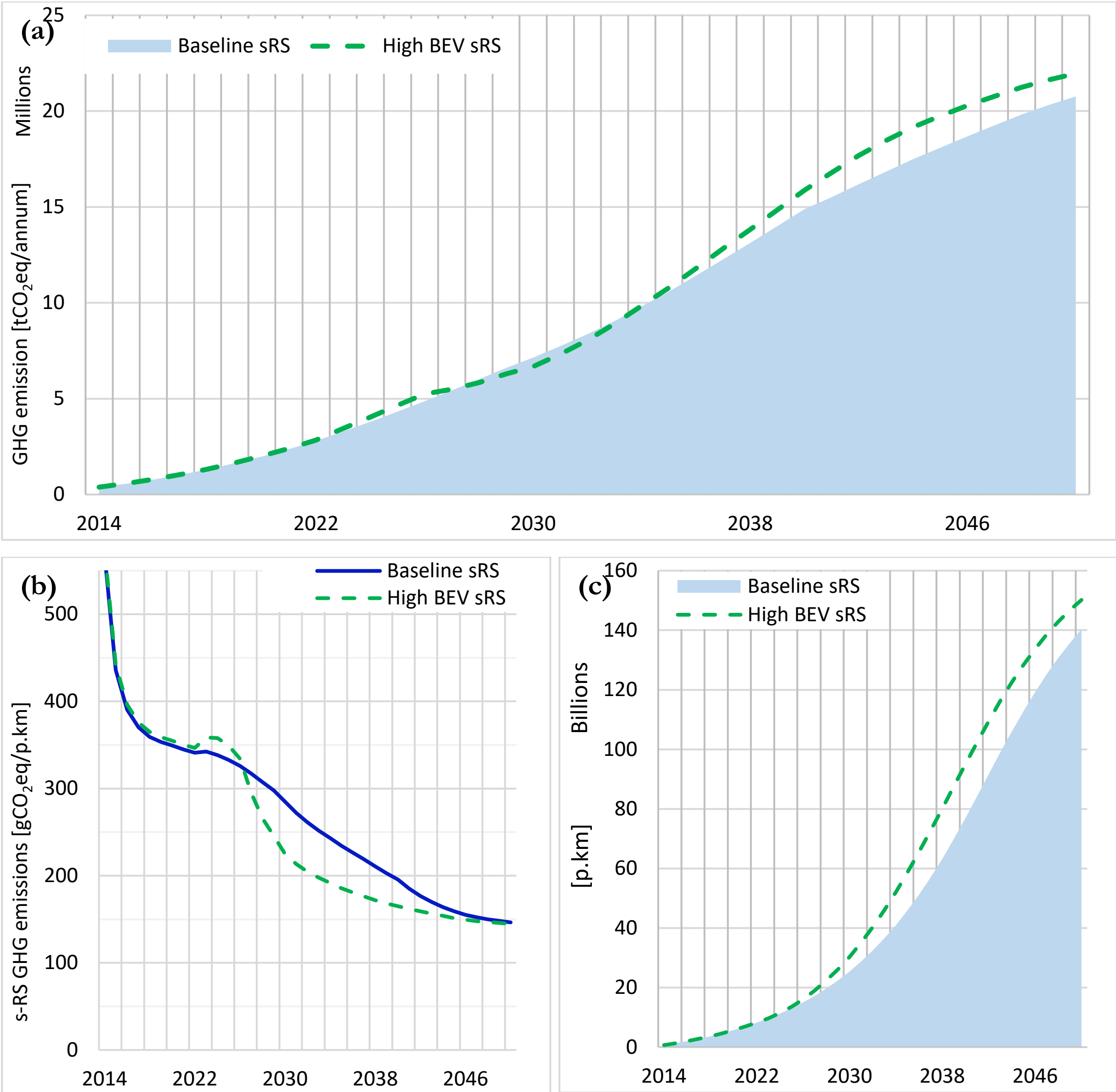

Figure 7-5 Dynamic GHG results – Solo-ridesourcing

Notes: (a) Absolute GHG emissions, (b) Specific GHG emissions compared to p.km, (c) Passenger kilometres. See Figure E-8 in Appendix E for the graph with confidence intervals

The solo-ridesourcing dynamic GHG emissions are also dominated by more frequently replacing fleet stock compared to carpooling and private vehicles due to the fleet prerequisites enforced by transport network companies (Uber, 2021d). The replacements significantly contribute to GHG emissions in the production phase while shifting to BEVs. These dynamics are discussed further in Section 7.5.

The specific GHG emission trajectory of solo-ridesourcing shows a reduction in both modes (see Figure 7-5 (b)). However, the reduction is significantly lower than the carpooling-specific GHG results shown in Figure 7-4 (b). Two technology scenarios have demonstrated statistical significance until the mid-2040s (see Figure E-8 in Appendix E, with the confidence intervals). The occupancy rates substantially influence this deviation. The solo-ridesourcing mode represents the lowest occupancy rate of the chosen personal mobility modes (Henao, 2017). Similar to the absolute emission behaviour, a slightly higher GHG emission per p.km is shown until 2022 in the high BEV adoption scenario; then, a sudden increase is demonstrated from 2022 to 2026 due to the increased BEV fleet production GHG emission impacts. Henceforth, the high BEV scenario demonstrates a higher GHG reduction behaviour than the baseline scenario until the end of the modelling time. Nevertheless, the difference between the two scenarios at the end of the modelling period is insignificant.

A significant p.km increase is observed in solo-ridesourcing mode, contributing nearly three-quarters of p.km in the car-based MaaS modes for the chosen journey at the end of the modelling period. The increase in BEV adoption aligns with the consumer preference-driven user transition (see Figure 6-5 and Figure 7-5 (c)). These results demonstrate the significant consumer preferences for solo-ridesourcing in the US round-trip to work trips supported by the consumer preferences and the respective fleet behaviour, both in powertrain types and body styles (see Sections 6.4.3 and 6.6.3). The vehicle kilometre results also reveal significant contributions from the solo-ridesourcing mode compared to the total distance against the aggregated MaaS, providing significant insights into the deadheading characteristics of the mode. Overall, the deadheading is chosen as a sensitivity check parameter in this research (see Section 7.7.3).

Pooled-ridesourcing also shows similar behaviour to solo-ridesourcing with a significantly lower magnitude (see Figure E-4 in Appendix E). The pooled-ridesourcing fleet is the largest high GHG emitting SUV-dominant car-based MaaS mode among the three chosen types. However, higher occupancy rates significantly lower the specific GHG emissions of pooled-ridesourcing compared with solo-ridesourcing. Aggressive fleet electrification driven by transport network companies beyond policy pressure is another reason for lowering GHG emissions. However, a specific interpretation is not provided because of the calibration data constraints explained in Section 6.4.4, which is the newest of the three chosen car-based MaaS modes. However, its contribution is considered in overall GHG assessments, although it is insignificant.

7.4.4 Private vehicle fleet – Dynamic GHG emission behaviour

The most significant absolute GHG reduction is shown in private vehicle fleets. The results are shown in Figure 7-6 (a) and indicate that GHG emissions will be halved by 2050 compared with 2014 in the baseline scenario. The savings are higher if the transition is in the high BEV adoption scenario. This trend is qualitatively similar to the carpooling GHG emissions shown in Figure 7-4 (a) and the overall personal mobility presented in Figure 7-3 (a).

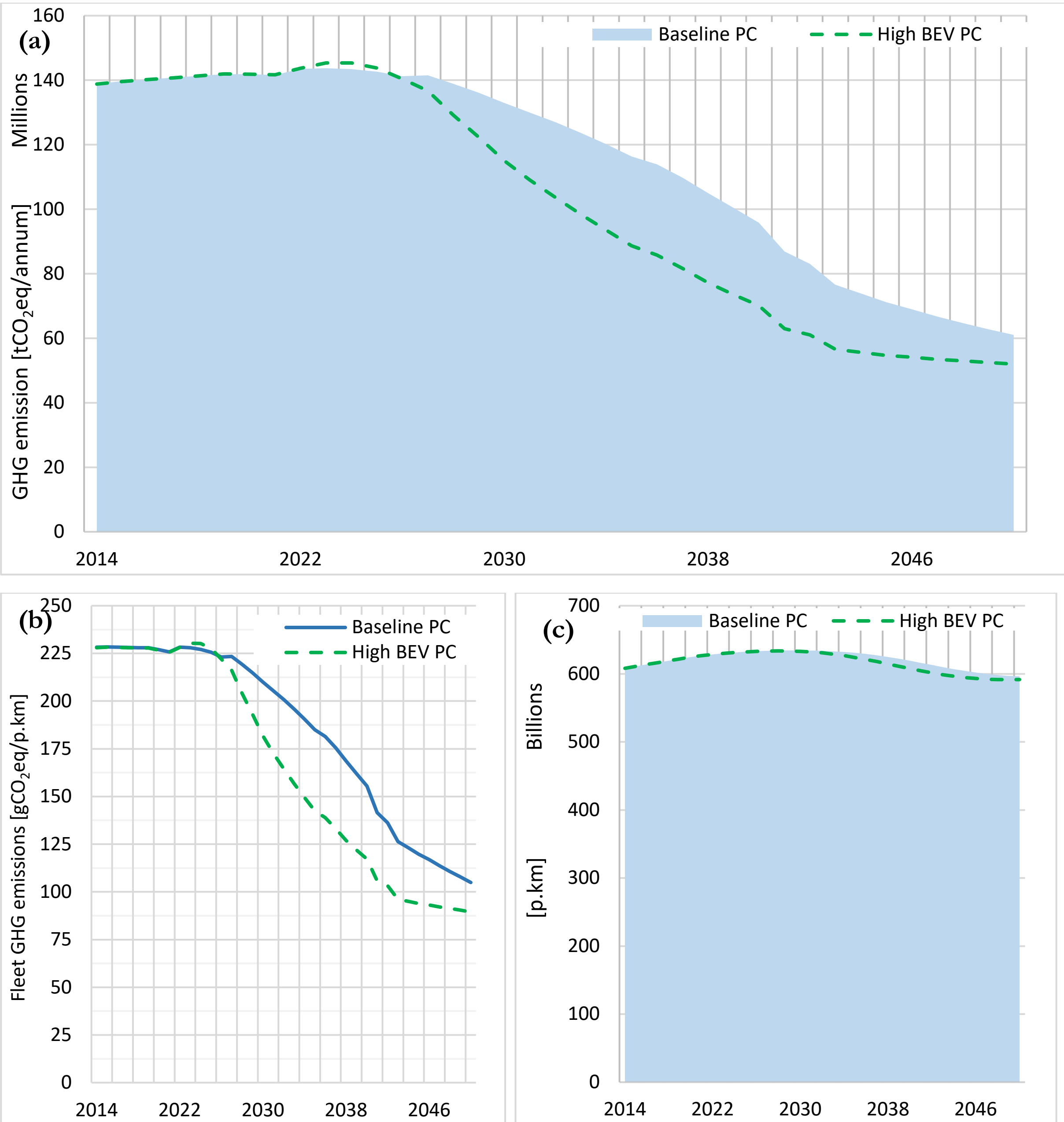

Figure 7-6 Dynamic GHG results – Private Vehicle fleet

Notes: (a) Absolute GHG emissions, (b) Specific GHG emissions compared to p.km, (c) Passenger kilometres. See Figure E-9 in Appendix E for the graph with confidence intervals

In both scenarios, the private vehicle fleet shows a significant GHG reduction per p.km from 2016 onwards (see Figure 7-6 (b)). At the end of the modelling time, the overall GHG reductions align with the absolute GHG emission behaviour because there is no deadheading for private vehicle use on a round-trip to work. Hence, a sensitivity check based on deadheading is irrelevant for private vehicle use. The specific GHG emissions of the private vehicle fleet show a trajectory similar to the absolute GHG emissions of carpooling, including the uncertainty analysis (see Figure E-9 in Appendix E, with the confidence intervals). This behaviour is due to the use of identical fleet technology modelling inputs, considering that the carpooling fleet is a subset of the private vehicle fleet (see Section 6.3). Hence, the explanation of carpooling-related GHG emission behaviour in Section 7.4.2 is valid for private fleet behaviour. However, in the carpooling mode, the occupancy rate was higher than that of private vehicles. In summary, the influence of the functional unit, p.km, is different.

As shown in Figure 7-6 (c), private vehicles' p.km reduced slightly in 2050 compared to 2014. It is a function of the stocks: commuting employees by private vehicles and active MaaS users because the average round-trip distance is a constant. These stocks depend on two variables: employment changes and car-based mobility. The final p.km results are also determined by causality responses based on consumer preferences. The declining p.km values reflect the integration of consumer preference and user behaviour in the high BEV adoption scenario than the baseline scenario. This observation complements more users shifting to solo-ridesourcing by this time (see Section 6.4.3), reducing p.km in private vehicle use (see Section 6.4.5).

7.4.5 Aggregated MaaS modes – Dynamic GHG emission behaviour

In this section, the dynamic GHG behaviour of the aggregated MaaS is analysed. Consumer preference was sought for three different MaaS modes in Chapter 5, and user and fleet behaviour were analysed separately in Chapter 6. Their dynamic LCA results are analysed in Sections 7.4.2 and 7.4.3. The key research question of this study demands an overall analysis of the transition from private vehicles to car-based sharing economy modes for the chosen scope of the study. This section explores an aggregated analysis of the three car-based MaaS modes.

Figure 7-7 (a) shows that the absolute GHG emissions of the aggregated MaaS modes rise at least three-fold from 2014 to 2050. The aggregated MaaS GHG emissions per p.km in 2050 do not show a reduction in either scenario compared to 2014. The change in GHG emissions per p.km is a function of the MaaS modes' emission behaviour and their p.kms. This is more broadly explained in the latter part of this section, considering the two variables, emissions and p.km (see Figure 7-8). Figure 7-7 (b) shows an increasing trend of the aggregated MaaS mode GHG emissions per p.km in the first 15 years and a decline in the baseline scenario. The shift to the higher specific GHG-emitting solo-ridesourcing mode and the reduction of lower-specific GHG-emitting carpooling users contribute to the increasing GHG emission per p.km. The occupancy rates of the two modes also contributed to the emission changes. The gap between the two scenarios is small until 2022; the year starts transitioning to fleet electrification per set policy scenario in Section 6.3. In summary, the specific GHG results show the importance of fleet electrification in the overall transition from private vehicles to car-based MaaS.

Surprisingly, the high BEV adoption scenario does not bring significant absolute GHG benefits, considering the transition to aggregated MaaS based on consumer choices. The specific GHG emissions in the high BEV adoption scenario showed a considerable increase from 2022 to 2026, followed by a steep decline and a flattening curve at the end of the modelling period. This observation can be explained based on the transport network companies' fleet electrification plans for the solo-ridesourcing fleets, with the largest contribution to the aggregated MaaS (more than 90%; see Section 7.4.3) (Lyft, 2020; Uber, 2020). Their production impacts are represented by an increasing trend in GHG emissions from 2022 to 2026. The explanation for the above GHG changes is similar to that for the personal mobility modes discussed in Sections 7.4.2 to 7.4.4.

Figure 7-7 (b) shows that the high BEV adoption scenario attracts more p.km than the baseline scenario. It also shows a steady increase in p.km units of the aggregated MaaS modes. The specific GHG results represent the above aggregated p.km behaviour.

The overall GHG emission per p.km changes between the private and aggregated MaaS fleets are significant (nearly 20%) at the end of the modelling time (see Figure 7-6 and Figure 7-7). Also, the gap between the two scenarios is small in the aggregated MaaS GHG emission results and private vehicle fleet emissions. The model results also predict that the aggregated MaaS GHG per p.km results are higher than those for private vehicles from 2030 onwards in the high BEV adoption scenario (see Figure 7-6 (b) and Figure 7-7 (c)). Hence, an analysis based on a detailed comparison is performed to understand the specific contributions of the three MaaS modes.

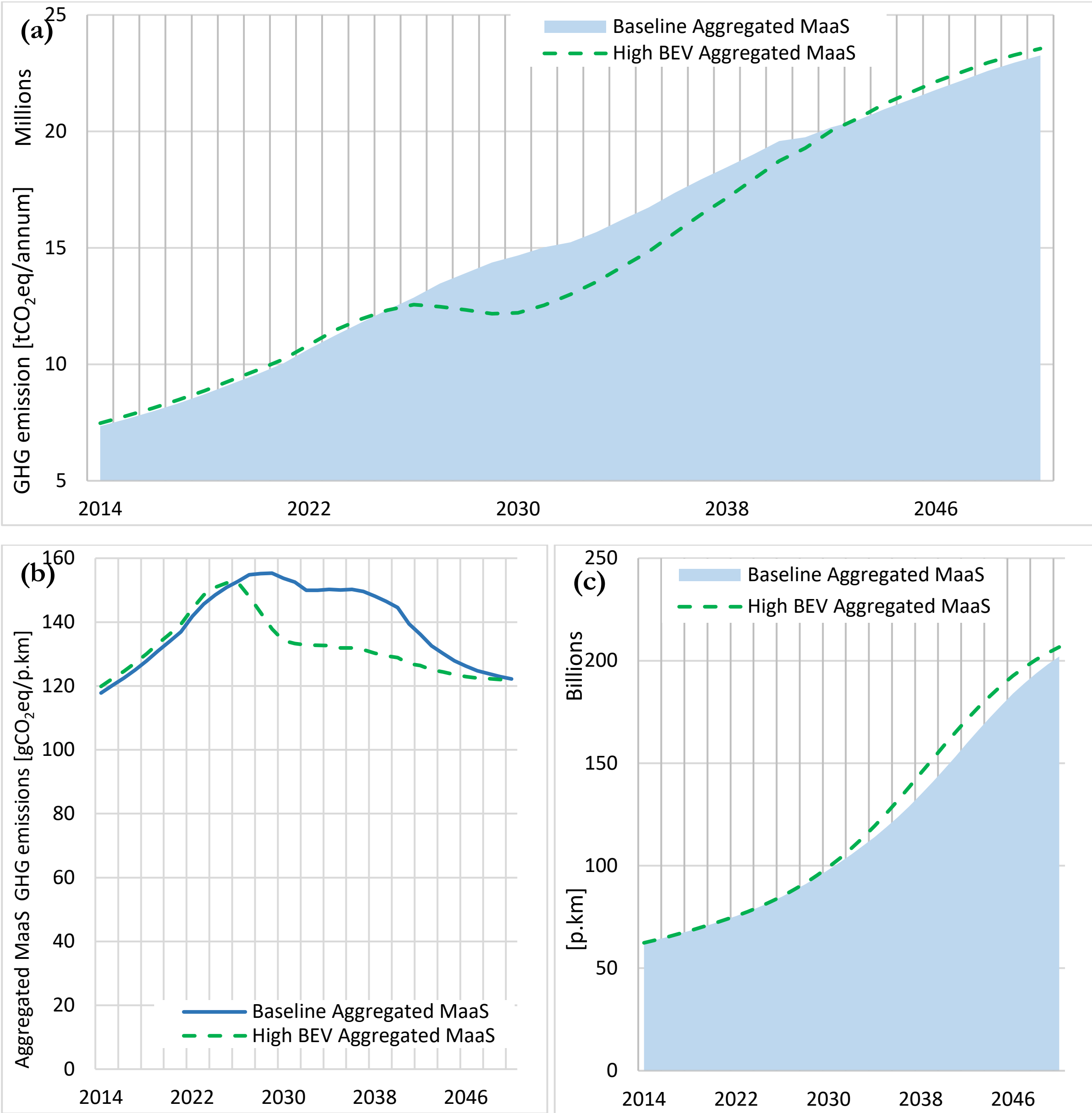

Figure 7-7 Dynamic GHG results - Aggregated car-based MaaS modes

Notes: (a) Absolute GHG emissions, (b) Specific GHG emissions compared p.km, (c) Passenger kilometres

The graphical summary in Figure 7-8 shows GHG emissions and the p.km disproportionate among carpooling and ridesourcing modes that contribute to the aggregated MaaS emission behaviour discussed in the above paragraphs. In the initial modelling period, the highest GHG emissions contribution was from carpooling, and the mode represented almost 100%. As discussed in Section 6.4.3, the transition to solo-ridesourcing intensifies by the end of modelling, resulting in a more significant GHG contribution than the initial modelling time (see Figure 7-4 and Figure 7-5). Graphs (a) and (b) in Figure 7-8 show that the absolute GHG emissions of carpooling contribute nearly one-tenth while the p.km is closer to one-third. However, high GHG emitting low-occupancy-based solo-ridesourcing represents a lower p.km value than the p.km values of high-occupancy (pooling) modes with lower absolute GHG emissions. Therefore, the two graphs in Figure 7-8 represent the contradictory behaviour of the absolute GHG emissions and the respective travelled p.km of car-based MaaS modes. Their behaviour also justifies the selection of p.km as the functional unit of this study to express the dynamic LCA results.

Results presented in Figure 7-8 also highlight the importance of promoting higher occupancy and pooling modes instead of low-occupancy modes within the transition to car-based MaaS with high deadheading rates. Another explanation is the fleet-based GHG contributions, which are identical for each MaaS mode. For example, the solo-ridesourcing fleet includes significantly more BEVs than carpooling; however, it also has a substantially higher SUV composition. Overall, the contribution of dynamic fleet technology changes and occupancy-based MaaS mode analysis is crucial for determining GHG emissions during the transition to MaaS.

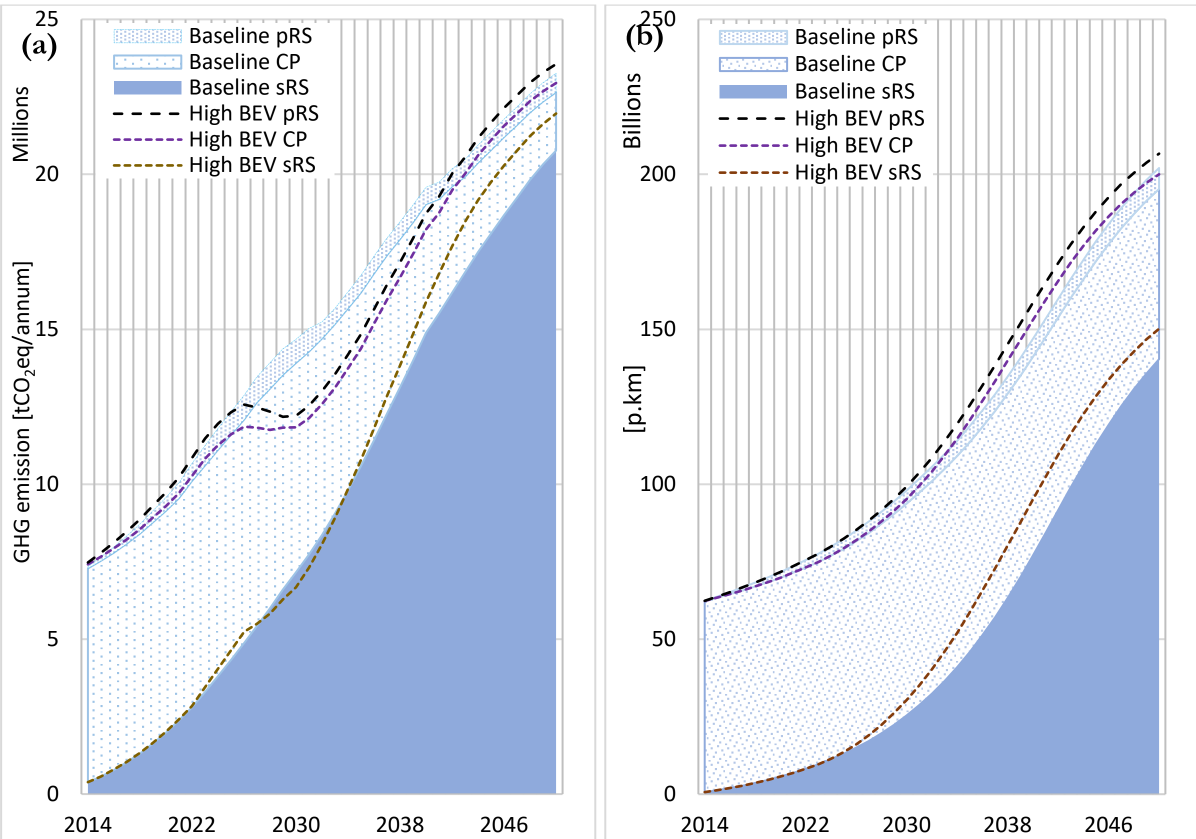

Figure 7-8 Dynamic GHG results of the transition to MaaS of three car-based MaaS modes

Notes: (a) Absolute GHG emissions, (b) Passenger kilometres

The above analysis also implies the importance of fleet technology changes and deadheading in the final dynamic GHG results for the MaaS modes. Deadheading is a key contributor to solo-ridesourcing becoming the highest specific GHG-emitting MaaS mode among the three types chosen (see Table 7-2). The sensitivity checks in Section 7.6 are based on both influencing factors. Performing an extended analysis to determine the emission behaviour within the life cycle phases of these modes is identified as a step to explore the results further and is discussed in Section 7.5.

7.5 Implications of the results – life cycle phases (L3 and L4)

The model outcomes show that GHG emissions only reduce in the use phase in the transition to car-based MaaS. As shown in Figure 7-9 (b), the model predicts a significant GHG reduction in the use phase and a little more in the high BEV adoption scenario compared to the baseline at the end of the modelling period compared to 2014. Based on the historical data, both scenarios showed a steady increase in use-phase GHG emissions in the initial modelling phase. However, from the mid-2020s onwards, the high BEV adoption scenario shows a steeper decline in the use phase GHG emissions compared to the baseline scenario. This trend is largely supported by fleet electrification. Vehicle lightweighting also complements the GHG emission reduction trend and is further supported by greener electric grid GHG emission profiles. At the end of the modelling period, the curve of the high BEV adoption scenario flattens compared to the baseline. This demonstrates the significantly high BEV transition and that it can reach the lowest possible GHG emissions per the set policy scenarios in Section 6.3. The use phase accounts for over three-quarters of the overall GHG emissions throughout the modelling period. However, in 2050, the use-phase GHG emission contribution will be around half of the overall GHG emissions. The shift to BEVs is the key reason for the use phase emission reduction, which is supported by the decreasing GHG emission contribution of the US electricity grid.

The GHG emissions of the production phase show an increasing trend contributing to the GHG emissions throughout the modelling period (Figure 7-9 (a)). In the high BEV adoption scenario, the production GHG emissions show an increase from 2022, when gasoline vehicles are replaced, to achieve 100% BEV purchase by 2030 (see Section 6.3). The sudden increase in GHG emissions in the production phase from 2022 is due to the increasing BEV composition in the fleet (see Figure 6-9) and higher GHG emissions from BEV production compared with gasoline vehicles (Wang *et al.*, 2021). The graphical behaviour of the two scenarios affirms this argument. The flat curves in the initial modelling period represent the gasoline-dominant fleet, based on historical data with relatively lower production phase GHG emissions. The nodes in the early 2040s represent the higher fleet replacement behaviour of private vehicles and carpooling fleets that are dominated by the BEV SUVs (see graphs (a) and (b) in Figure E-2 in Appendix E for carpooling purchasing behaviour, which is similar to private vehicles). BEV SUVs represent the highest production GHG emitting fleet combination option (Wang *et al.*, 2021). At the end of the modelling period, the production phase reaches nearly half of the total GHG emissions. This observation highlights the importance of the future environmental sustainability performance of the automobile manufacturing phase while shifting to fleet electrification. The contribution of the EoL phase is insignificant compared to both the production and use phases (see Figure E-5 in Appendix E).

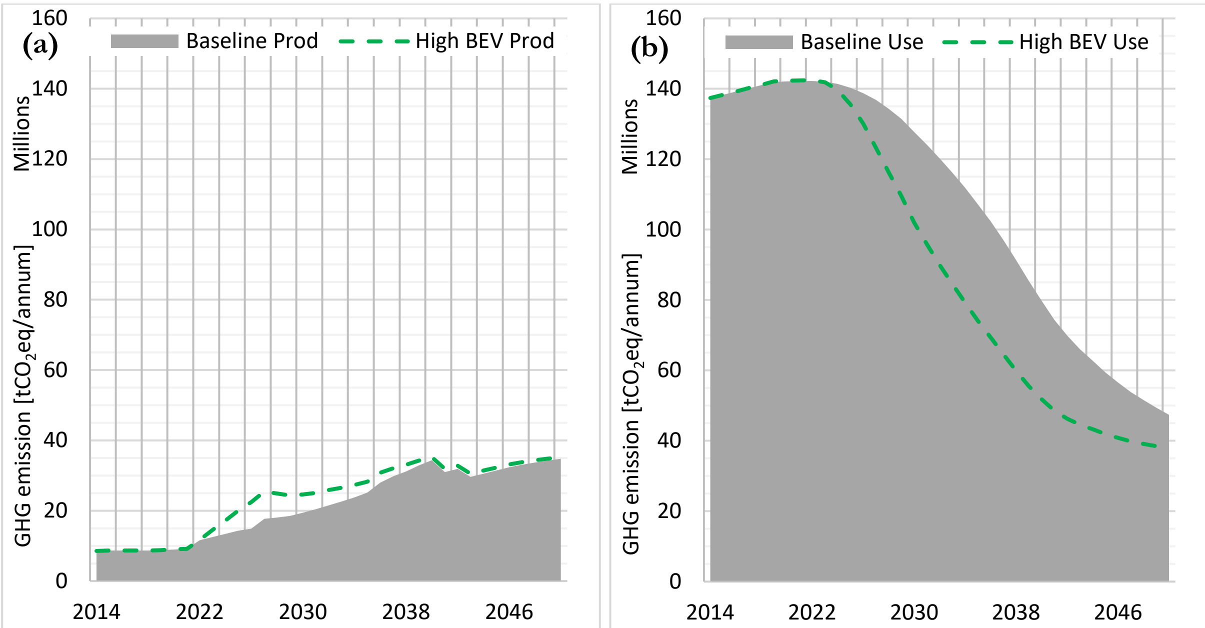

Figure 7-9 Dynamic GHG emission results of aggregated car-based personal mobility

Notes: (a) Production phase, (b) Use phase

Figure 7-10 shows a detailed analysis of the contribution of the selected MaaS modes to the two key life cycle phases. The private vehicle fleet contributes the highest GHG emissions in the use phase ((c) and (d) graphs). In the modelling period, it contributes nearly 90% of GHG emissions. Besides the most extensive fleet size, a potential reason is that the private vehicle fleet BEV composition is smaller than that of the MaaS modes. Another critical factor is its slower replacement rate than car-based MaaS modes such as ridesourcing. Hence, the private vehicle fleet composition is older than the ridesourcing fleet and less energy efficient. However, a significant observation towards the end of the modelling period is the reduction of the private vehicle fleet in the use phase GHG dominance. It is further reduced in the high BEV adoption scenario. In contrast, the solo-ridesourcing use phase GHG fraction is increased significantly, reaching nearly one-fifth at the end of the modelling period, which is initially insignificant. Overall, the aggregated car-based MaaS modes contribute to higher use phase GHG emission fractions at the end of the modelling time, mainly dominated by the solo-ridesourcing mode. This observation is supported by the significant user shift to the solo-ridesourcing mode (see Section 6.4.3) and the larger deadheading component of the mode (see Table 7-2).

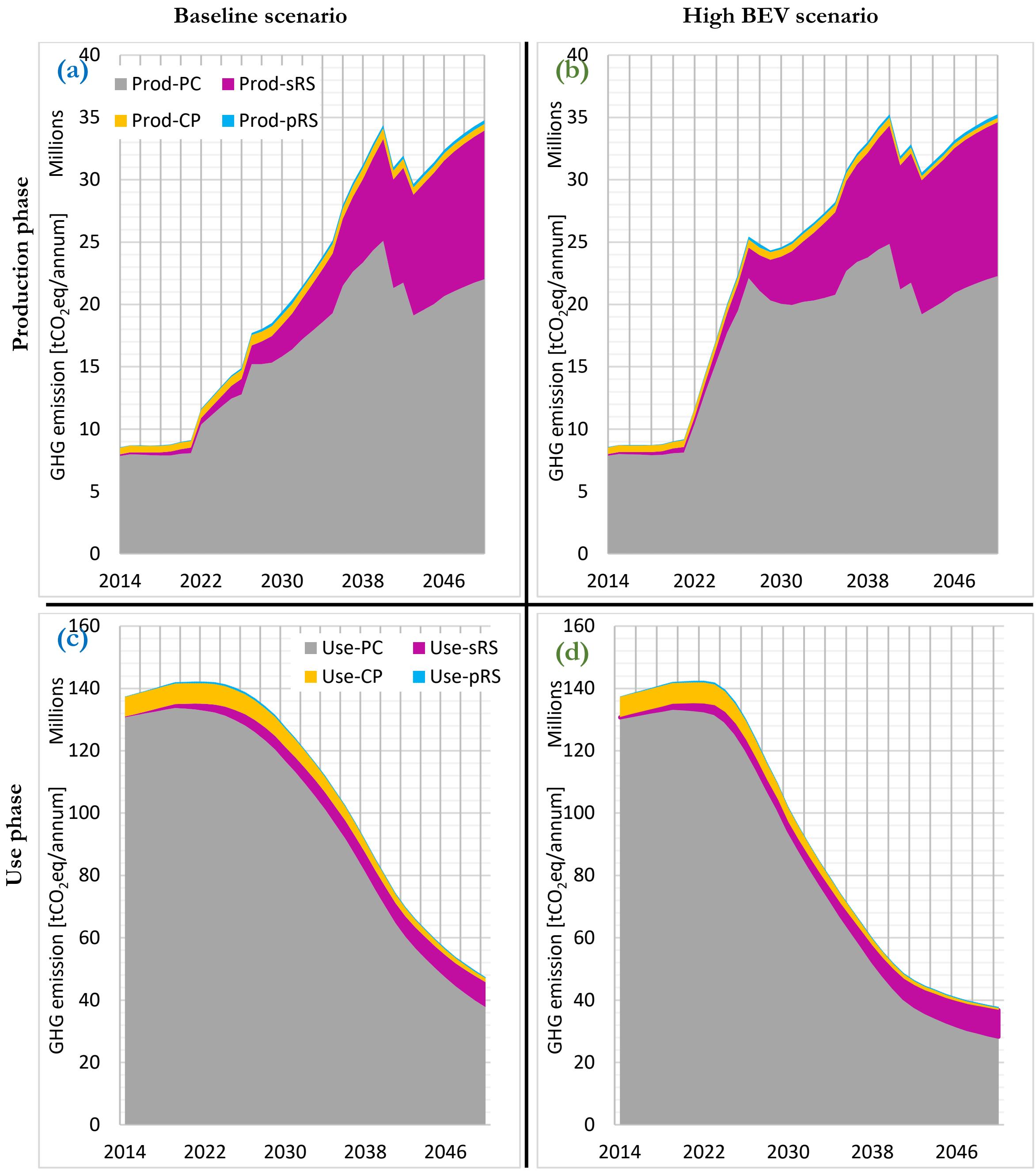

Figure 7-10 Dynamic GHG results - Car-based personal mobility modes – life cycle phases

Notes: (a) Production phase – Baseline scenario, (b) Production phase – High BEV adoption scenario, (c) Use phase – Baseline scenario, (d) Use phase – High BEV adoption scenario

Surprisingly, solo-ridesourcing records more than one-third of the production GHG emissions in both scenarios (see Figure 7-10 (a) and (b)). A possible reason for the higher GHG emissions in the solo-ridesourcing production phase is the higher purchasing and scrappage rates required to maintain the vehicle age restrictions enforced by the transport network companies (Uber, 2021a). The combination of larger BEV and SUV fractions in the ridesourcing modes explains the rise in production phase GHG emissions. Both BEVs and SUVs generate larger production phase GHG emissions than ICEVs and body styles such as sedans (Wang *et al.*, 2021). The transition to MaaS modes and consumer preferences regarding the powertrain type and body style contribute to these GHG emission behaviours. The results in this chapter suggest that GHG emissions other than the use phase are higher in car-based MaaS modes compared to the private vehicle fleet.

The most significant changes in the production phase GHG emissions are from private vehicles, representing three-quarters of the overall production emissions. The fleet purchasing behaviour and the vehicle production GHG emission rates determine the production of GHG emissions. The composition of private vehicle purchases significantly changes from gasoline sedans and SUVs to more BEV-driven vehicles, particularly SUVs, in the late 2030s (see Figure 7-11 (b)). The higher GHG emissions in the production phase due to fleet electrification can be seen by comparing graphs (a) and (b) in Figure 7-11. The highest production phase GHG emissions are recorded when the complete transition to BEVs with a higher composition of SUVs demonstrates a node by the end of the 2030s. Consumer preferences determine the vehicle purchasing composition (based on the derived utility values in Section 5.5.2), and the results of the SD sub-model transition to MaaS and replacements for the scrappages are also determining factors in fleet purchasing. Then, the production phase GHG emissions are generated by combining the derived DPI values in Section 7.2.1. Henceforth, the fluctuations of the graph in Figure 7-11 are determined by many factors. The private vehicle purchasing and production phase GHG emission reduction trends from the end of the 2030s onwards can be explained based on the private vehicle user reduction trends (see Figure 6-7).

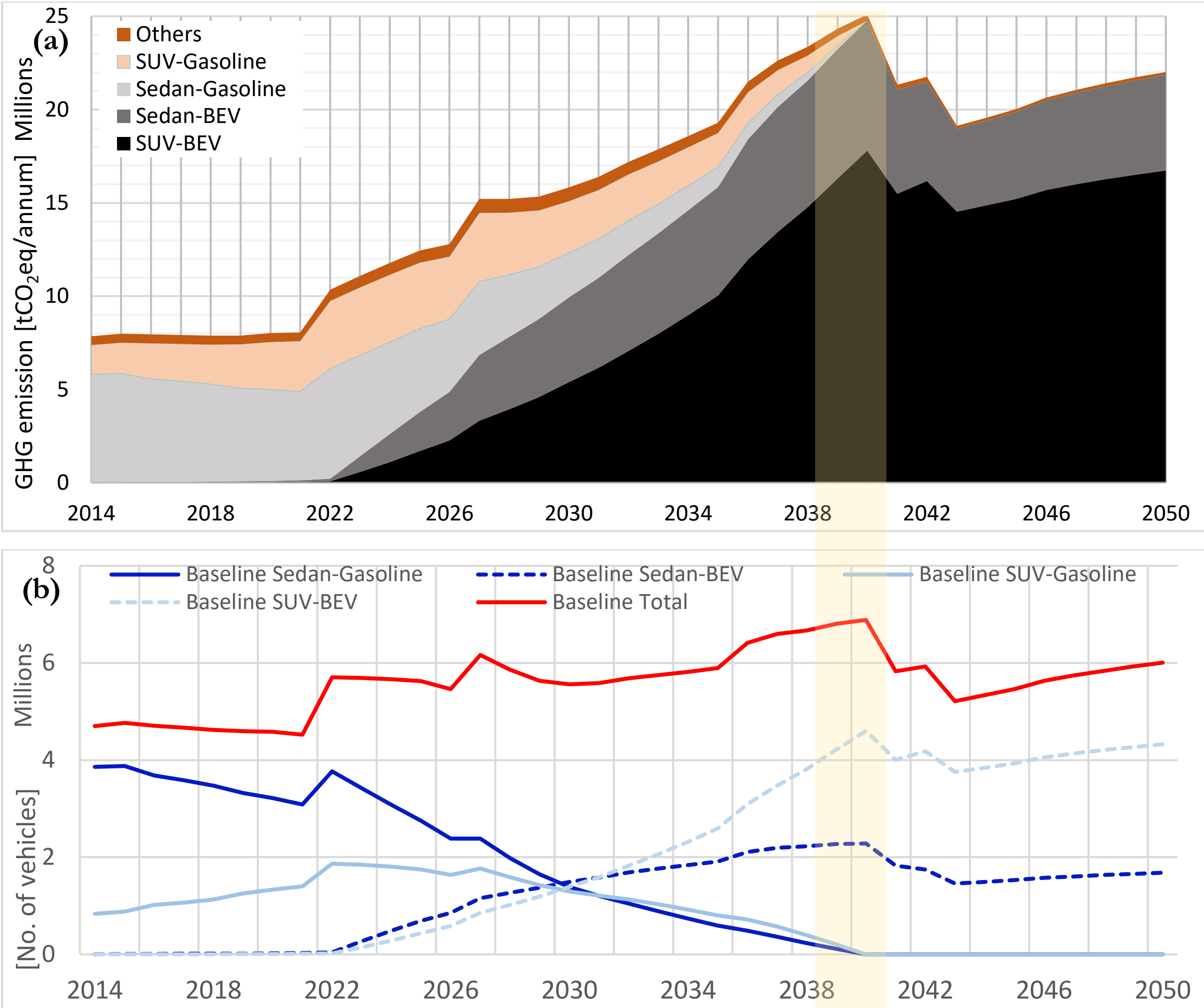

Figure 7-11 Private vehicles – production phase

Notes: (a) Dynamic GHG emission results based on fleet technology composition – baseline scenario; (b) Private vehicle purchasing trends based on the key fleet technology composition – baseline scenario. The yellow highlighted area represents the complete transition to BEVs.

7.6 Effect of consumer preferences

A significant gap can be seen in the dynamic GHG results for the two conditions of combining and not considering consumer preference. In typical dynamic LCA work, only the temporal changes influence the results compared to a conventional, static LCA (Sohn *et al.*, 2020). Figure 7-12 shows the generated results combining consumer preference in dynamic GHG emissions (as discussed in Section 7.4) and the conventional dynamic LCA approach (without considering consumer preference). The graphical representation of 'not considering consumer preference' is generated by simplifying the sub-model transition to MaaS introduced in Section 6.1.1. A simple, linear formulation is introduced to car-based MaaS modes instead of the Bass diffusion model-driven causality explanation, as in Sections 4.4.1 and 6.1. Hence, the results 'not considering consumer preference' shown in Figure 7-12 only characterise the fleet technological attributes (powertrain type and vehicle body style compositions, lightweighting and longevity improvements, and the US electric grid GHG changes) as introduced in Section 6.3. At the end of the modelling, the GHG emission trajectory that considered the consumer preference is one-third higher than the typical dynamic GHG emission analysis. In summary, a significant GHG emission gap is determined between the integrated DCE results (i.e., consumer preference combined, as in this work) versus the typical approach of not considering them.

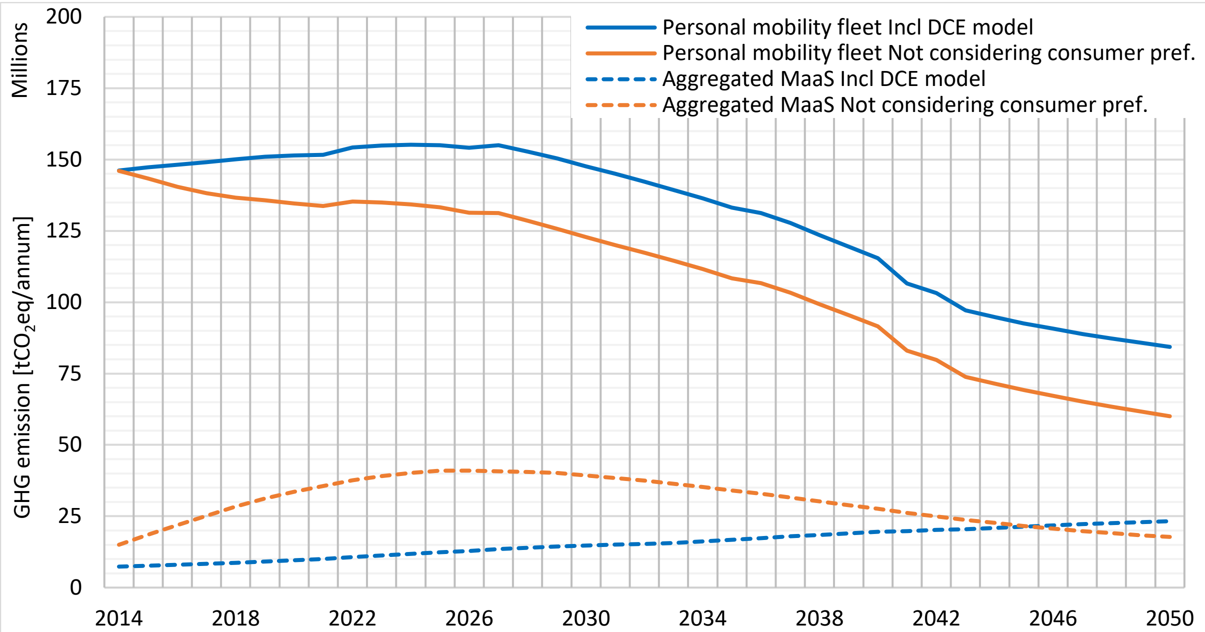

Figure 7-12 Consumer preference integrated dynamic LCA results versus not combining it

Note: The baseline scenario results

As shown in Figure 7-12, the results align with the initial hypothesis of this work; consumer preference influences the dynamic LCA of the transition to car-based sharing economy modes (see Section 2.8). A GHG emission reduction is expected without consumer preference integration, considering the anticipated fleet technology changes introduced in Section 6.3. However, the expected GHG emission reduction, considering only fleet technology changes shows a significantly higher reduction compared to the results shown in Section 7.4. Figure 7-12 demonstrates that the expected higher GHG reduction by applying only the technology changes is not in accordance with the market response. Consumer preference integration significantly changes the car-based MaaS composition, considering fleet technology offerings. These findings also align with the outcomes of Sections 6.4, 6.6 and 7.6, particularly the behaviour of consumer preferences in different MaaS modes. In this work, the vehicle body style was chosen only as the endogenous explanation (see Section 6.1). Overall, the above results highlight the significance of combining consumer preference in dynamic LCA analysis in the transition to a car-based sharing economy for the chosen US work trip case study.

Figure 7-12 represents the aggregated outcome of several mobility modes with different occupancy rates. The influence of consumer preference in the dynamic GHG results differs for each MaaS mode based on consumer attributes, such as powertrain type. Hence, specific interpretations can be made for each MaaS mode, and the results can be further influenced by their respective occupancy rates. However, such an analysis is not performed based on the scope of the research question: 'overall transition to car-based sharing economy' (see Section 2.8). Another observation is that only the technology-based uncertainties would have been analysed if consumer preferences were not integrated into the analysis. The sensitivity of the uncertainty associated with consumer preference and other sensitivity elements are further discussed in Section 7.7.

7.7 Sensitivity check (S4)

The sensitivity check focuses on the model's behavioural sensitivity (also known as structural sensitivity). As introduced in Section 6.2.2, it is one out of three hierarchical sensitivity kinds (the other two are addressed using 95% confidence intervals (numerical) and policy scenario analysis (policy sensitivity)). The sensitivity check is a part of the testing process (S4) in the C-DLCA methodology framework. This step re-evaluates a careful analysis of the real systems and the SD modelling works. First, a sensitivity analysis is performed to understand the uncertainty of the survey and the associated consumer preferences in Section 7.7.1. Then, two more specific sensitivity checks are performed, as explained in the next paragraphs.

The two fleet technology-based attributes—powertrain type and body style—are identified as the key variables subjected to direct changes in the SD model as the first step. This selection was made by considering the connection of the chosen sensitivity parameters with the primary data collection process and policy scenarios. Powertrain type and body style are two attributes in the market survey, and the policy scenarios are evaluated based on the powertrain type changes, particularly in high BEV adoption. Hence, the sensitivity parameter selection for behavioural sensitivity complements numerical sensitivity by considering the uncertainties of the attributes and policy sensitivity. The importance of the vehicle body style and powertrain system in the final dynamic GHG emissions results of the transition to car-based sharing economy work was highlighted in Section 7.4. Their significance to the implications of different life cycle phases was discussed in Section 7.5. The two chosen sensitivity parameters are significant in the structural sensitivity analysis and are presented in Section 7.7.2.

The results also revealed the significance of solo-ridesourcing out of the three car-based sharing economy modes. It has shown the highest user volumes, the largest fleet size and the most significant GHG emissions among the three car-based MaaS modes (Sections 6.4.3, 6.6.3, 7.4.3). Therefore, a key variable that connects with solo-ridesourcing and model behaviour was explored other than the chosen two parameters: powertrain type and body style. As discussed in Sections 7.4 and 7.5, deadheading is a common factor influencing car-based shared mobility GHG emissions, particularly when interpreted using an occupancy-based functional unit such as p.km. However, solo-ridesourcing represents more than two-fold deadheading values compared to carpooling[12] (see Table 7-2). The deadheading values are also employed to calculate the variables Work trip allocation MaaS and Avg gross trip distance MaaS in the fleet behaviour and dynamic LCA calculation sub-models. As a whole, the deadheading of solo-ridesourcing is chosen as a model behavioural check parameter and is presented in Section 7.7.3.

7.7.1 Sensitivity associated with consumer preferences

This section analyses the uncertainties associated with consumer preference from the survey (the DCE model) outcomes and their influence on the dynamic GHG results. The utility levels and their associated uncertainties were discussed in Section 5.5.2. The 95% confidence levels of the utility values derived from the DCE model are employed to calculate the dynamic GHG results of the transition to MaaS. As discussed in Section 7.6, the uncertainties of the market responses are also integrated into the dynamic GHG emission results by integrating consumer preferences. Figure 7-13 represents the sensitivity of the results to the uncertainty in the survey and the associated consumer preferences in both scenarios.

[12] Pooled-ridesourcing is not considered based on its significance (see Section 6.4.4)

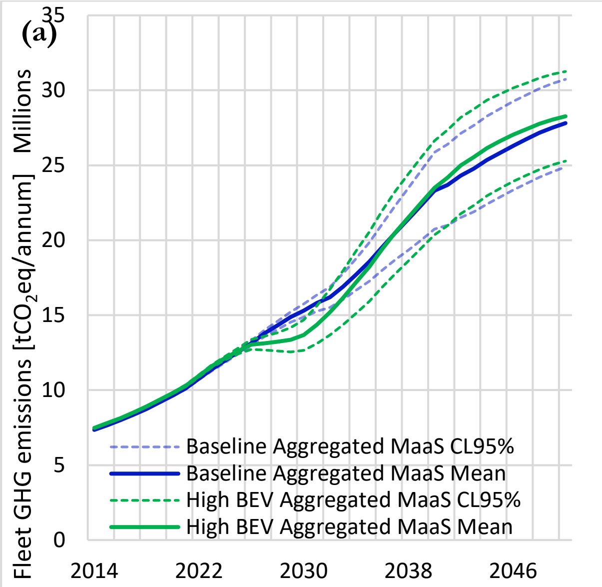

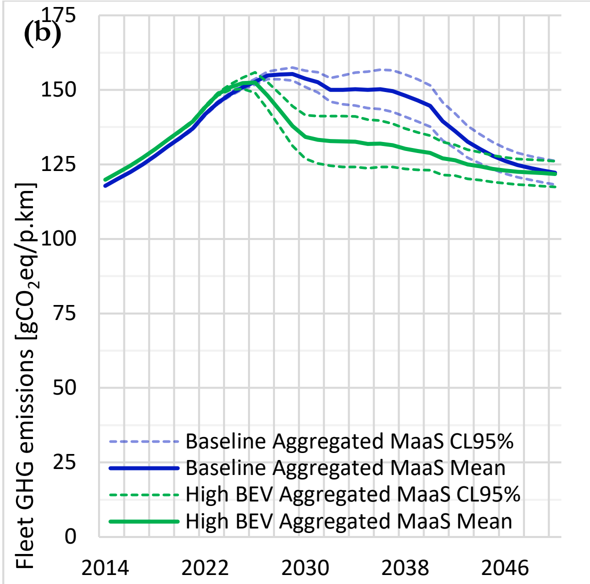

Figure 7-13 Sensitivity analysis - consumer preference impact in aggregated MaaS

Note: CL – control level. (a) Absolute GHG emissions in tCO_2eq, (b) Specific emissions in $gCO_2eq/p.km$

The absolute GHG emission of aggregated MaaS does not show significance between the two scenarios, considering the consumer preference integrated uncertainty assessment. Both graphs in Figure 7-13 show a smaller range of uncertainty in both scenarios until the mid-2020s and increasing after that. This observation resembles the influence of consumer preference based on the rapid fleet technology shifts starting in the mid-2020s, as discussed in Sections 6.4 and 6.6. It also highlights the importance of considering technology-based attributes in shared mobility-based market surveys, aiming to generate results as inputs for the dynamic LCA work.

Graph (b) in Figure 7-13 highlights the significant changes in the specific GHG emission values in both scenarios from the mid-2020s until the mid-2040s. These findings also align with the outcomes of Sections 6.4, 6.6 and 7.6, particularly the behaviour of consumer preferences in different MaaS modes and their aggregated results. Therefore, the graphs in Figure 7-13 represent the difference between the baseline and high BEV scenarios in the dynamic GHG emissions results of aggregated MaaS are not significant. The sensitivities of cumulative fleet technology changes are explored in Section 7.7.2. Both graphs in Figure 7-13 highlight the importance of integrating the sensitivity of the uncertainty associated with consumer preference analysis to demonstrate market-responsive behaviours.

7.7.2 Sensitivity check – fleet technology changes

The model behaviour for the two fleet technology changes is separately evaluated. The evaluation is based on the numerical sensitivity values derived in Section 5.5.2. Those values are integrated into the SD modelling work, and the outcomes are presented in Figure 7-14. The trajectory of the mean and control limit range also suggests the model stability in the two extreme conditions of the body style and powertrain type based on the market survey results. Employing a range of extreme arbitrary values is not operationalised to the SD model, considering the DCE method principles and constrained choices applied in the survey instrument.

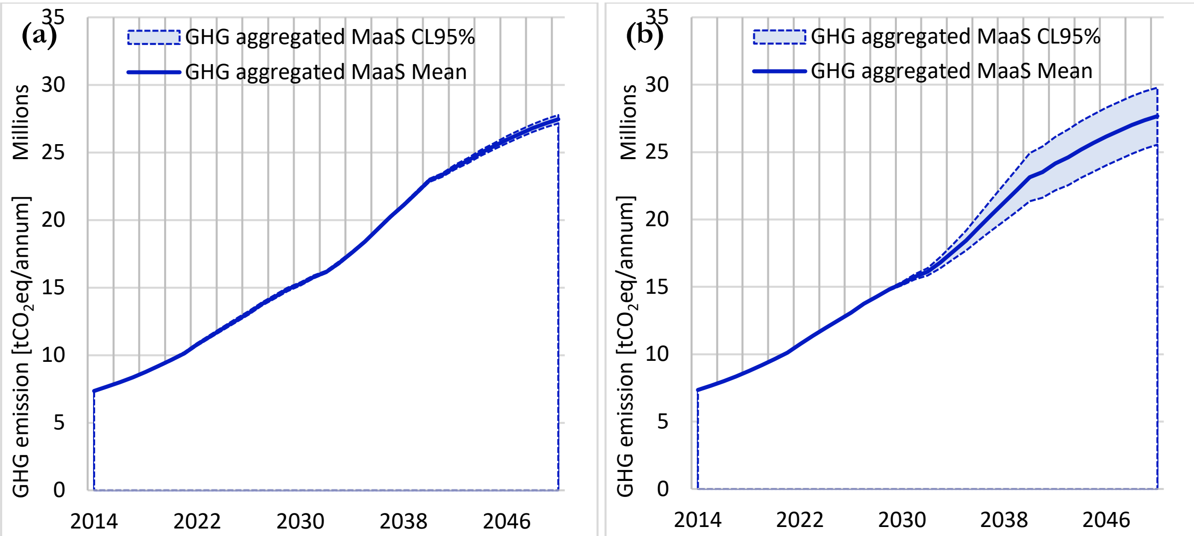

Figure 7-14 Sensitivity check - fleet technology – Dynamic GHG emission results aggregated MaaS

Note: Baseline scenario; (a) sensitivity test with control level 95% for body style only; (b) sensitivity test with control level 95% for powertrain type only

It is apparent from the two graphs in Figure 7-14 that the powertrain type is more significant in the sensitivity checking compared to the body style. The graphical behaviour is aligned with the derived confidence intervals of the utility values, as shown in Figure 5-7. Sensitivity analysis can be simplified by varying the parameters one at a time (Hamby, 1994). The results suggest more than 4 million tCO_2eq of absolute GHG emissions range based on the respondents' choice of the powertrain system in selecting a car-based MaaS mode in 2050. The high BEV scenario has also shown a similar trend (see Figure F-1 in Appendix F). Hence, the powertrain type is selected only as the sensitivity parameter for the following sensitivity checks.

The powertrain type control level 95% values are integrated into the SD model and operationalised. The outcomes are presented in Figure 7-15. Graphs representing the dynamic GHG emissions of the overall personal mobility fleet utilised in the round-trip to work in the US (graph (a)) and the aggregated MaaS (graph (b)) represent stable trajectories consistent with the outcomes presented in Sections 7.4.1 and 7.4.5. They also show that the overall effect of the powertrain type on GHG emissions per p.km is more prominent in the aggregated MaaS modes than in the overall personal mobility fleet. It shows a 5% uncertainty range by considering the powertrain type as the sensitivity parameter. However, the per p.km range of uncertainty for the aggregated MaaS is smaller than the absolute emissions. This observation can be further explained based on the smaller range of the p.km when checked against the sensitivity parameter powertrain type (see Figure F-2 in Appendix F). In summary, the sensitivity checks on the powertrain type demonstrate the significance of the chosen sensitivity parameter in the final results, particularly the absolute GHG emissions in aggregated MaaS, without affecting the model's structural stability.

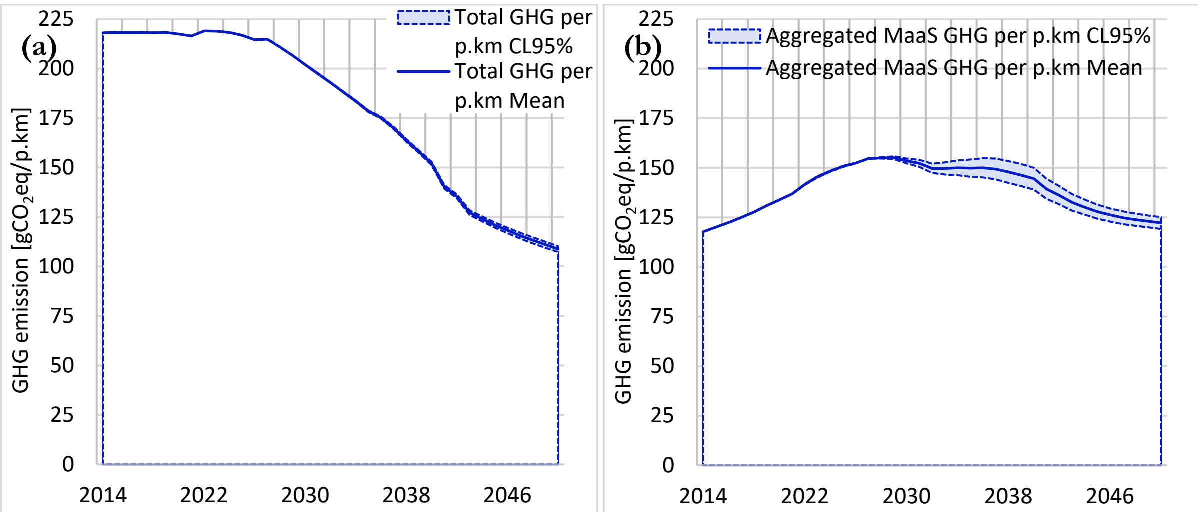

Figure 7-15 Sensitivity check - powertrain type in Dynamic GHG emission results

Notes: sensitivity test with control level 95% for powertrain type only; (a) GHG emissions per p.km of overall personal mobility, (b) GHG emissions per p.km of aggregated MaaS

7.7.3 Sensitivity check – solo-ridesourcing deadheading

The solo-ridesourcing deadheading sensitivity parameters are operationalised into the SD model. Two uncertainty levels are selected based on the Transport Network Company forecasts (Uber, 2020, p. 47). A 15% average range of deadheading and 25% targeted deadhead reduction in major city markets are chosen as the two ranges to check the sensitivity of the model. Figure 7-16 represents the outcome of the solo-ridesourcing deadheading sensitivity check.

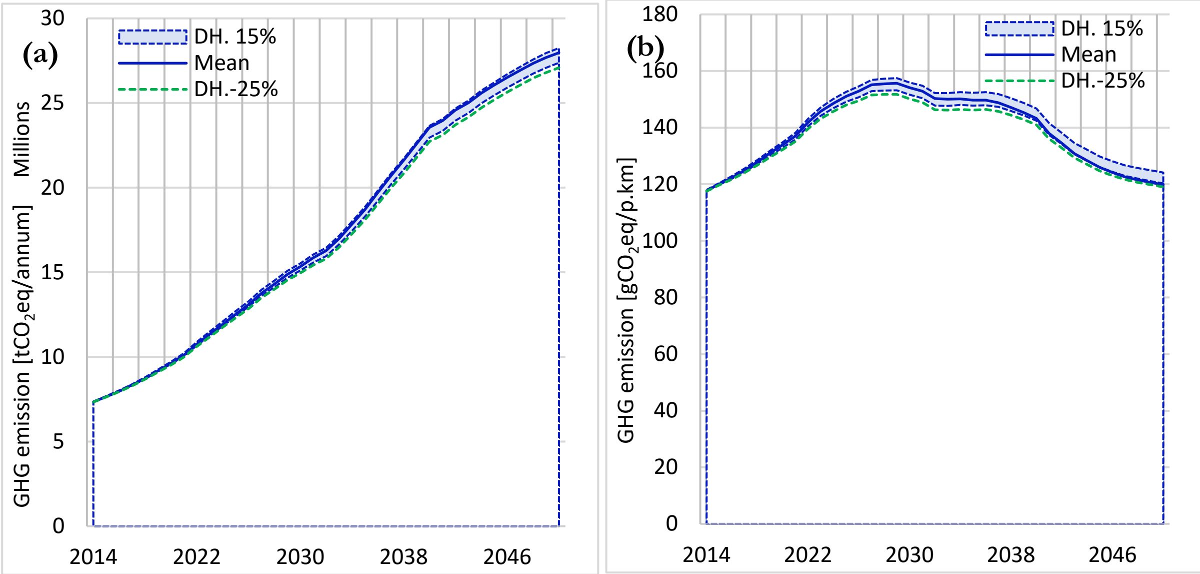

Figure 7-16 Sensitivity check - solo-ridesourcing deadheading – Dynamic GHG emission results aggregated MaaS

Note: sensitivity test with solo-ridesourcing deadheading: 15% range and 25% reduction; (a) absolute GHG emissions of aggregated MaaS, (b) GHG emissions per p.km of aggregated MaaS

The model demonstrates stability in both sensitivity ranges. The absolute (see Figure 7-16 (a)) and per p.km (graph (b)) based GHG emissions demonstrate that the sensitivity of the solo-ridesourcing deadhead changes is insignificant. It only shows a 3% uncertainty of the absolute GHG emissions of the aggregated MaaS in 2050 when the deadheading is reduced by 25%. The significance is smaller in the 15% deadheading range. The SD model adjustment for integrating solo-ridesourcing deadheading is based only on reducing the non-productive driver travel distances (Avg gross trip distance MaaS) and related emissions. However, parameters such as cars per trip are also considered in the actual deadheading optimisation process. These changes could not be integrated into SD modelling due to a lack of case-specific data availability. Overall, the actual deadheading GHG reduction benefits are larger than the generated results.

7.8 Discussion

The dynamic LCA calculation sub-model combined the temporality into the final results by integrating the derived dynamic fleet behaviour to generate dynamic LCA results. The model applications combined the flows, purchasing and scrappage to determine the dynamic production and EoL LCA outcomes by integrating the temporal changes in powertrain type and body style. The model formulation work was also established for LCA calculations of the use phase. The calculated DPI with temporally varied GHG emission factors were also integrated into the production, use and EoL phases of the LCA modelling work. Therefore, the combination of SD modelling outcomes and DPI values changed the results into a dynamic representation against the typical static LCA calculation approach. This approach supports better-informed decision-making for sensitive systems with time-varied parameters. Also, it highlights the contributing factors in terms of demand (production), use and disposal of the fleet, and the impacts of fleet technology by integrating the DPI factors.

The derived absolute GHG results highlight the importance of integrating consumer preference, behaviour and fleet changes in the LCA calculations. Results highlighted at least one-third of the GHG emission gap at the end of the modelling period between the outcomes that considered consumer preferences and not. Hence, the C-DLCA based dynamic GHG emission results are more meaningful. The results have shown the influence of consumer preference by reducing carpooling GHG emissions and significantly increasing solo-ridesourcing. In summary, the dynamic LCA calculation sub-model is market-responsive.

The variable gross occupancy MaaS has significantly influenced the dynamic- GHG emission results. The variable is considered exogenous and static in SD modelling and also represents the occupancy rate of different MaaS modes for the selected journey. The chosen occupancy rates are based on conservative estimations without considering the deadheading eliminated net occupancy rates (Henao and Marshall, 2018). The variable is employed to calculate the inflow of the purchasing MaaS fleet (from Sections 6.5 and 6.6) and influences the fleet size (stock - MaaS fleet) and, subsequently, the GHG emissions in the dynamic LCA results sub-model. The employed functional unit, p.km, depends on net occupancy and is considered the most practical and meaningful approach for interpreting shared mobility-based environmental impacts (Union of Concerned Scientists, 2020b). Therefore, the integration of occupancy rates explains the outcomes of MaaS modes and private vehicle fleet aggregated GHG results expressed in gCO_2eq per p.km. Although solo-ridesourcing comprises the most extensive electrified fleet than other modes, the higher deadheading influences the net occupancy rates and, subsequently, the GHG emission footprint. The solo-ridesourcing mode records an average of 40% deadheading due to the nature of the mode (Henao and Marshall, 2018). Low occupancy-based solo-ridesourcing contributes 90% to the GHG emissions of the aggregated MaaS, which increased two-fold at the end of the modelling period compared to the beginning. The sensitivity analysis targeted solo-ridesourcing deadheading demonstrates a smaller range to optimise by only considering the non-productive distance benefits. Tu et al. (2019) highlighted that a substantial increase in the pooling (pooled-ridesourcing and carpooling) could significantly increase the time savings in their Chengdu (China) based case study. These interrelationships (feedback) are not considered in SD modelling as they are not generic, and case study findings are unavailable.

The sensitivity analysis results based on the parameter powertrain type reveal opportunities for further reduction of GHG emissions in the transition to MaaS by promoting BEVs. The findings can be linked to justify the efforts to close the value-action gaps found in the market survey outcomes in Section 5.5. The sensitivity of the results to the uncertainty in the survey and the associated consumer preferences highlights the importance of integrating consumer preference in analysing the transition to MaaS dynamic LCAs.

The influence of the transition to MaaS GHG emissions by powertrain types, body styles and improvements in the automobile sector are further discussed in Chapter 8.

7.9 Summary

The transition to car-based MaaS, including the changes in fleet technologies and electric grid GHG, does not provide a complete solution to mitigating GHG emissions in the chosen case study. The model results suggest a maximum of half of the absolute GHG emissions reduction of personal mobility at the end of the modelling time compared to the beginning. The consumer preferences towards the high BEV adoption scenario reduce the life cycle GHG emission of the personal mobility in the round-trip to work journey in the US but are not completely mitigating.

The highest reduction during the transition to MaaS is from private vehicles. However, the contribution of solo-ridesourcing, the most preferred car-based MaaS mode, shows a smaller GHG emission reduction when measured against p.km. Hence, the p.km-based aggregated GHG emissions of the car-based MaaS are higher than private vehicle usage in both scenarios in the last phase of the modelling. The unique powertrain type and body style fleet compositions of each MaaS mode contribute differently to the aggregated GHG emissions of the transition to MaaS. Automobile improvements, such as lightweighting and indirect GHG emissions from grid electricity, also influence the three life cycle phases differently. While both adoption scenarios reduce the overall GHG emissions during the entire modelling period, their production emissions predict closer to use phase emission values at the end of the modelling time. The derived results of the sub-model dynamic LCA calculations highlight the significance of combining consumer preference and fleet technology changes on the dynamic GHG emissions of the transition to car-based sharing economy modes. Results also emphasise the significant changes in the GHG emission profiles in life cycle phases due to the above changes.

8 DISCUSSION

Introduction

This chapter summarises the research outcomes based on applying the C-DLCA framework components: consumer preference survey, SD model insights and dynamic LCA outcomes. These are discussed in Sections 8.1 to 8.5. The discussion connects theory and practice to draw out the implications of the critical findings of the current research work. Finally, the novel insights and applicable options are discussed in Section 8.6.

8.1 Features of the C-DLCA framework

8.1.1 Combining consumer behaviour into the dynamic LCA

This research introduces a new methodology framework to integrate consumer behaviour into the dynamic LCA of sharing economy systems. Hence, this is the first attempt to incorporate the causal effect of consumer preference into a dynamic LCA work with a functional endogenous relationship. The C-DLCA methodology framework is applied to evaluate the impact on GHG emissions of the transition to MaaS. This application incorporated the influence of consumer behaviour in MaaS, which is significant compared to linear economy systems due to fleet dynamics and their causal influences on the life cycle GHG results. As a result, a significantly higher acceptance of solo-ridesourcing for the chosen round-trip to work journey in the US is identified. The model outcome predicted a more than 260-time increase of solo-ridesourcing users at the end of the modelling period compared to 2014 (see Section 6.4.3). It would not have been captured without integrating consumer preferences in a typical dynamic LCA study. Alternatively, the results can be generated by relying on a linear extrapolation of the MaaS mode composition or scenario analysis. However, these approaches do not provide a causality explanation to the system. In summary, combining consumer preferences adds significant value to the results, particularly in the car-based MaaS mode composition.

As discussed in Section 7.6, the integration of consumer preferences into the dynamic GHG emissions analysis shows a vast difference compared to typical dynamic LCA work. The fleet features, such as the adoption of newer technologies (e.g., powertrain changes, body style changes), increased product (vehicle) longevity (based on survival rates), and different production and disposal patterns in car-based MaaS modes are integrated into the dynamic LCA analysis. However, incorporating consumer preferences adds more meaning to the generated dynamic GHG emissions results by capturing the market response to technology features. In this work, *powertrain type* and *body style* are chosen as the consumer preference attributes and *body style* is selected as the endogenous explanation. This selection combines the changing fleet technology dynamics, different market responses to them when applied in different car-based MaaS modes and, importantly, integrating the generated feedback by the interrelation of market response and fleet changes. Therefore, the novelty feature of the C-DLCA framework, incorporating consumer preferences and producing market-responsive dynamic GHG results, is paramount in stakeholder decision-making without confining to the technology-based emission estimates.

The above outcomes also provide important inputs to the transport network companies and other shared mobility service providers in customising their awareness, market and communication campaigns to optimise the environmental benefits of the transition to MaaS. An example is the unexpected market preferences for the attribute *body style* in shared mobility modes (see Section 5.5.2). It has shown at least a 5% preference over the powertrain (excluding solo-ridesourcing, see Figure 5-6). Integrating these findings into the dynamic LCA work generates surprising GHG emission results (see Section 7.4.5). Otherwise, the GHG emission trajectory is smaller by applying simple market projections (see Figure 7-12). Overall, integrating consumer preferences in the dynamic LCA work provides more market-responsive inputs to interested parties that can be utilised in awareness or other decision-making processes to optimise the environmental benefits of shifting to car-based MaaS modes.

8.1.2 System Dynamic iterative process steps in modelling

The established iterative process is the most prominent modelling feature of the C-DLCA methodology framework. This development is inspired by previous work (Sterman, 2000; Wang, Lai and Chang, 2016; Jiang, 2019) and by applying Sterman's five-step process iteration model (Sterman, 2000, pp. 85–104). However, it differs from the two rigid approaches combining SD and LCA modelling work in the previous studies (Section 2.7.2 and Figure 2-7). As shown in Figure 4-1, multiple data communications channels are introduced between SD and LCA modelling integration in the C-DLCA framework compared to typical LCA to SD or vice-versa as in previous dynamic LCA applications (Changsirivathanatahathamrong, Moore and Linard, 2001; Halog and Manik, 2011; Stasinopoulos, 2013; Onat *et al.*, 2016; Pinto, Sverdrup and Diemer, 2019). The framework has taken the liberty of switching between the three models: LCA, SD and DCE, for effective results generation. Hence, it identifies a mechanism for exchanging data effectively in different phases of the DCE model, SD model and three LCA phases.

8.1.3 Structure and clarity

Another highlight of the C-DLCA framework is its clarity and structured approach. The model clearly articulated the combined three methods and their components. It proposes the most practical process steps targeting sharing economy models (e.g., shared mobility) as the application and indicates them in the process steps. The C-DLCA framework in Figure 4-1 has also highlighted the data flow. Understanding the process steps and data flows are crucial steps in the simulation phase and formulation in SD modelling. It can be seen from the multiple data flows handled within the formulation and simulation process (S3) step in the framework. Hence, the framework provides a practical process flow with greater clarity. Its robust applicability in complex sharing economy systems and combining consumer preference into the dynamic LCA work has been successfully demonstrated based on the results generated for the chosen scope of the work.

The remaining sections of this chapter further explain the implications of the model outcomes by integrating consumer preference into the dynamic LCA by employing the C-DLCA framework.

8.2 Implications of technical attributes and the value-action gap

The DCE results conflict with the pro-environmental consumer attitudes established by previous research (Alemi *et al.*, 2018; Hamzah and Tanwir, 2021). A relatively lower consumer preference for HEVs and BEVs was not expected from a sample with higher educational attainment (Section 5.5.2). The level utility values for BEVs are at least -16 (see Figure 5-7). This rejection contradicts previous studies (Galatoulas et al., 2017; Jenn et al., 2018) and the prospect that increasing know-how and environmental interest would translate into the need to reduce vehicle emissions (Hamzah and Tanwir, 2021). The findings are also contrary to the anticipated environmental benefits of fleet electrification by differing from the transport network companies' roadmaps on BEV-driven fleets (Lyft, 2020; Uber, 2020), auto production shares (US EPA, 2021) and the US executive directions (The White House, 2021). The findings are aligned with L. Qian & Soopramanien (2011) and against the generic sharing behaviour determined by Say et al. (2021). In summary, the results imply that current consumer preferences for car-based MaaS for round-trips to work in the US do not support the expected environmental benefits through fleet technology changes.

The BEV and HEV compositions in transport network company fleets are still insignificant (Uber, 2020). Rettie et al. (2014) highlight that the consumer prospect to participate in 'green' behaviours is based on what they think is normal and what is regarded as normal changes over time. Overall, considering BEV and HEV as attribute levels along with their time-varied fleet composition changes and combining them into the dynamic LCA is critical when considering that consumer preference is integrated with environmental pollution interpretations in MaaS modes.

The consumer preference for *vehicle body style* significantly contradicts previous findings on pro-environmental attributes (Alemi *et al.*, 2018). Transport network company fleet upgrades with newer vehicles, vehicle maximum age restrictions (Uber, 2021a), and a larger composition of SUVs in the ridesourcing fleet align with increasing SUVs in US auto production (US EPA, 2021) are possible reasons for the consumer influences towards larger body style vehicles. A larger gasoline SUV used in solo-ridesourcing emits 332% more GHG emissions per p.km than an average SUV used in carpooling (see Figure 4-3). The rejection of the lowest GHG-emitting hatch *body style* in MaaS can also be linked to its lower share in the market (US EPA, 2021) and relatively smaller interior space.

The study presents insight into the value-action gap (Kollmuss and Agyeman, 2002), the process whereby an individual's behavioural choice is influenced by their beliefs, which are strongly influenced by their values (Ajzen, 1991). The chosen stated preferences within a constrained choice capture a strong indicator of the actual behaviour of individuals' intentions to act (Dietz, Dan and Shwom, 2005). Therefore, despite the growing concern for mitigating environmental pollution (i.e., pro-environmental attitudes), consumers frequently make choices detrimental to the environment due to the trade-offs they are forced to make. Collins & Chambers (2005) highlights the transport mode shift to public transport is based on the relative importance of situational and subjective psychological factors. These factors are further discussed in Section 8.2.1 by focusing on car-based MaaS users.

8.2.1 Influence of switching costs and user characteristics on mobility mode decision-making

The transition to MaaS is considered a constraint due to the high switching costs in both economic/situational (price etc.) and non-economic switching factors (travel time, convenience, status, etc.) (Farrell and Klemperer, 2007; Lane and Potter, 2007; Dubé, Hitsch and Rossi, 2009). Consumers' pro-environmental attitudes and values remain outweighed by the switching costs (Collins and Chambers, 2005), such as brand loyalty, a psychological cost of switching or other non-economic factors such as convenience (Farrell and Klemperer, 2007; Lane and Potter, 2007). These are further discussed to understand consumer preference attributes based on their characteristics and related elements in the transition decision-making to car-based MaaS.

Consumers' location is a notable characteristic that decides the transition to car-based mobility mode selection for the round-trip to work (Section 5.6). It is a situational switching factor. Unsurprisingly, higher private vehicle use is observed in lower public transit cities and, conversely, in high-public transit cities (Vasudevan, Agarwala and Dash, 2021) (see Figure 5-8). As shown in Figure 5-9, carpooling usage is at least 9% higher in low-public transit cities compared to high-public transit cities. The results align with the US commuter trends to work (US Census Bureau, 2020a). Factors such as toll-free high-occupancy rapid lanes during rush hours, a solution for first- and last-mile transit connections, and expensive parking fees are the potential reasons for MaaS use in high-public transit cities (Washbrook, 2002, p. 62; Shaheen and Chan, 2016). These results suggest that the price motivation in the transition to MaaS is a situational (economic) switching cost factor and a plausible reason for car-based MaaS use in high-public transit cities.

Higher pro-environmental purchasing behaviour is observed among young consumers (Delistavrou et al., 2021). Younger generations are permanently interested in shifting to shared mobility modes (Fischer, Böhme and Geiger, 2017). The relationship between MaaS usage and age groups in this study aligns with those reported by Bansal et al. (2020) and Huynh et al. (2020). Bansal et al. (2020) found an increase in ridesourcing use up to 44 years of age before declining, similar to the trends in this study (see Figure 5-11). Hence, it can be assumed that there will be an increase in the likelihood of growing the diffusion of car-based MaaS utilisation. This behaviour can be intensified if the environmental awareness of vehicle emissions increases (Hamzah and Tanwir, 2021). Increased awareness of BEVs can be identified as an easy way to increase the GHG reduction highlighted in the sensitivity analysis check in Section 7.7.2 by leveraging the existing consumer preference range.

Lifestyle, personality and awareness of environmental issues are examples of psychological or non-economic switching cost factors. Lack of awareness of technology, such as powertrain systems' environmental benefits can be identified as a potential constraint for the transition to MaaS, a psychological switching cost. Hence, range anxiety (Jiang, 2019), perceived product attractiveness (Mahmoodi *et al.*, 2021), and perceived inconvenience associated with powertrain shifts (Qian, Grisolía and Soopramanien, 2019) are possible reasons for the lower preferences for electrified fleets in MaaS. Addressing these perceived inconveniences will increase positive communications on shared mobility use and positive word-of-mouth, resulting in the adoption from WoM component in the Bass model (see Figure 6-2).

The results demonstrate that consumer choices do not support anticipated fleet technology changes in car-based MaaS. They show lower preferences for fleet electrification and higher preferences for larger body styles leading to higher GHG emissions. In summary, incorporating these findings into the dynamic LCA of MaaS can generate critical insights.

8.3 Influence of increasing fleet electrification on GHG emissions

The high BEV adoption scenario significantly influenced GHG reduction in personal mobility fleets. Hence, the results support using BEVs as low-carbon transportation pathways in cities (Köhler, Turnheim and Hodson, 2020). Specific GHG profiles (GHG emissions per p.km) of the high BEV adoption scenario have lower emissions than the baseline scenario in all modes from the mid-2020s onwards. The overall reductions are 10% above the baseline scenario that employed the US policy-based fleet electrification trends. The 100% BEV status is an extreme condition that policymakers support as a scenario to consider. However, the current disruptive niche of the full-electric vehicle scenario is insufficient to completely displace ICEVs (Dijk, Wells and Kemp, 2016). Therefore, consumer awareness of the technical characteristics of BEVs, such as range anxiety, charging stations, and lack of knowledge and complex informed decision tools, are a few factors that must be addressed to promote fleet electrification (Jiang, 2019; Folkvord *et al.*, 2020; Rizki *et al.*, 2021). Ball et al. (2021) highlight the importance of higher user awareness of BEVs and policy interventions to mitigate these gaps. Hence, consumer-informed decision awareness could promote fleet electrification, which reduces the GHG emissions of personal mobility fleets instead of relying solely on policy mechanics and technology. The development of a simple ecolabel for car-based sharing economy modes is an initiative that starts with informed decision-making tools.

The results show that BEV production and EoL GHG impacts are higher than those of ICEVs. This observation aligns with the static LCA findings shown in Figure 4-4 and in previous studies (Elgowainy *et al.*, 2016; Wang *et al.*, 2021). The increase in GHG emissions from 2022 to 2026 represents the impact of BEV production during rapid uptake. This increase is common in both scenarios and is relatively more prominent in the high BEV adoption scenario (see Figure 7-4 to Figure 7-6). The production impacts of the BEVs have shown a 102% to 106% increase compared with their respective gasoline-type models, with a significant contribution from their batteries (Wang *et al.*, 2021). As introduced in the policy scenarios in Section 6.3, a substantial uptake of BEVs is represented in the modelling to reach the 2030 US policy-driven BEV fleet composition in the baseline scenario. The uptake started in 2022. The increase in the high BEV adoption scenario is more intense, and ridesourcing fleets are further augmented to achieve the BEV aspirations of the transport network company fleet (Lyft, 2020; Uber, 2020). Hence, the model results show that GHG increased for a shorter period, which was reduced over time with the reduced use phase emissions from fleet electrification (Section 7.4.3). The increased energy economy performance and the increasing BEVs in the ridesourcing fleets support the declining GHG results from 2026 onwards in both scenarios. Similar behaviour has been shown in the model outcomes of the lower fuel economy-based vehicles produced during the 2020-2026 corporate average fuel economy freeze (commonly known as CAFE) in the US automobile market (Keith, Houston and Naumov, 2019).

Reducing US grid electricity GHG emissions is a significant indirect factor contributing to decreasing GHG emissions from BEV fleets. A 53% reduction is forecasted from 2014 to 2050 in the US grid GHG factor (U.S. Energy Information Administration - EIA, 2016, 2019, 2021), which is integrated into the modelling as an exogenous variable. The indirect grid electricity GHG emissions account for 66% to 70% of the BEV fleet emissions (Wang *et al.*, 2021). Therefore, compared to starting, the US grid GHG reduction alone reduces 33% to 35% GHG reduction in BEVs at the end of the modelling time. The US grid electricity GHG savings on vehicle manufacturing, EoL and the refinery processes are not considered in the LCA model, considering the uncertainties of the automobile manufacturing locations, assuming their contribution is insignificant and not within the scope of this research.

8.4 Influence of increasing SUVs on GHG emissions

The higher user preferences for larger vehicle bodies, such as SUVs have increased personal mobility fleets' life cycle GHG emissions. The larger body style vehicles used in carpooling or private vehicle fleets generate 8% and 15% additional GHG emissions per p.km in gasoline and BEV fleets, respectively (see Figure 4-3). Large body style vehicles are commonly used in pooled-ridesourcing fleets (Uber, 2021c, 2021d). However, the journey occupancy rates of pooled-ridesourcing are not fully optimised to harness the net benefits of larger vehicles. Previous studies assume a 1.5 occupancy rate for pooled-ridesourcing (California Air Resource Board, 2019; Union of Concerned Scientists, 2020a), while Uber reports 4.12 and 4.4 occupancy rates for their UberXL and Uber Black SUVs, respectively (Uber, 2020, p. 59). This study chooses the gross occupancy rate with the deadheading component for pooled-ridesourcing as 2.3 (Wilkes *et al.*, 2021). Hence, realistically, GHG emissions for personal mobility modes can be higher than the modelling results.

The option of utilising SUVs in solo-ridesourcing is available at a higher price (Uber, 2021c, 2021d). The significant SUV preference among solo-ridesourcing users (see Section 5.5.2) and high SUVs in the personal mobility fleet in the US have created a reinforced loop as the attribute *body style* chosen as an endogenous variable. The SUVs generate at least 11% and 29% higher GHG emissions than the average sedan vehicle used in solo-ridesourcing gasoline and BEV fleets, respectively (Figure 4-3). Hence, higher GHG emissions from larger body style and SUV fleets, and their increased fleet size in MaaS modes, contributed to the higher aggregated GHG emissions (expressed in p.km) than the private fleet (see Figure 7-7). In contrast, the higher lifetime distance values of the SUVs used in the GREET model inversely affected the overall GHG emission increase. The model assumes a 6% longer lifetime distance for SUVs than sedan models (Wang *et al.*, 2021) and also increases survival rates (Lu, 2006, p. 8; Davis and Boundy, 2021, pp. 3–20).

The results highlight the importance of considering the attribute *body style* in consumer preference studies of MaaS, its causality and the dynamics in fleets in car-based MaaS GHG studies.

8.5 The implications of automobile improvements in the dynamic LCA results

8.5.1 The effect of vehicle lightweighting

Vehicle fleet lightweighting impacts are integrated into the established DPI process (L2) in the C-DLCA framework. This has significantly reduced use-phase GHG emissions in personal mobility fleets. The model estimates 16% and 19% weight reduction in gasoline and BEV sedan fleets, respectively and 15% and 18% for SUVs based on the GREET lightweighting scenario (Wang et al., 2021). These lightweight improvements have enhanced the energy efficiency levels of vehicles from 111% to 113% in sedans and from 110% to 112% in SUVs. These improvements result in 9% to 11% use phase GHG reduction, including the well-to-pump emissions and the electricity generation and distribution impacts (Wang *et al.*, 2021). These developments are integrated into the modelling of the DPI process.

In contrast, vehicle lightweighting has increased the production of GHG. This behaviour aligns with the static LCA outcomes of the vehicle lightweighting scenarios shown in Figure 4-4 and previous studies (Kim and Wallington, 2016). The rise in vehicle material embodied GHG emissions due to lightweighting per vehicle lifetime for gasoline and BEVs are 53% to 56% and 60% to 63%, respectively (Wang *et al.*, 2021). The raw material GHG contribution of BEVs is higher than that of gasoline vehicles. Vehicle lightweighting was applied from 2023 to 2043 (see Table 6-3). This behaviour also explains the increase in GHG emissions from 2022 to 2026 for ridesourcing fleets in the high BEV scenario than in the baseline scenario (see Figure 7-5). The GREET model uses a secondary material approach in production impact calculations (Wang *et al.*, 2021). Hence, only the energy consumed for vehicle treatment is considered in the EoL operation-related LCA calculations, which is insignificant for comparison.

8.5.2 The effect of extended survival rates

Integrating the vehicle survival rate through scrappage outflow increased the accuracy of dynamic GHG emissions. Specific survival rates based on vehicle body style are employed in the modelling (Keith, Houston and Naumov, 2019; Ambrose *et al.*, 2020). In the high BEV adoption scenario, Figure 6-10 and Figure 6-11 demonstrate the remaining gasoline fleet at the end of the modelling period. This observation represents the effect of increased survival rates (Lu, 2006, p. 8; Davis and

Boundy, 2021, pp. 3–20). Despite policy pressure, it also highlights slowing the transition to BEVs due to increased vehicle longevity. Overall, the improved survival rates of modern gasoline vehicles have slowed the expected fleet electrification rate and its GHG benefits. These outcomes were not visible unless the temporal and causal relationships were integrated into the dynamic LCA modelling. In summary, these observations highlight the suitability of the developed C-DLCA framework.

The SD model outcomes demonstrated higher survivability of SUVs than sedan body styles. As shown in Figure 6-11, the delayed discrepancy in purchasing and scrappage fleet volume shows a fleet-stagnating effect supported by improved survival rates. The results are aligned with historical and extrapolated data (Lu, 2006, p. 8; Jacobsen and van Benthem, 2015; Davis and Boundy, 2021, pp. 3–20). This trend can adversely impact GHG reductions based on a slower transition to technologically improved SUV models because of the higher longevity of SUVs, especially in fleets other than ridesourcing modes. US light truck survival data were utilised as a proxy for SUVs because of a lack of data accessibility. Hence, there can be uncertainties in the influence of the survival rate of SUVs on GHG emissions. However, the identified qualitative behaviour remains unchanged.

The second life of the fleets is outside the scope of this study. Hence, the model estimates the complete scrappage of ridesourcing fleets at 15 years. This assumption is aligned with the taxi survival rates (Bishop *et al.*, 2016, p. 8) utilised as a proxy for ridesourcing-driven vehicles and transport network company conditions of vehicle eligibility in the US (Uber, 2021d). However, integrating the second life into the model can improve the model's accuracy (Amasawa *et al.*, 2020), which is practically difficult due to a lack of data.

8.6 Novel insights and applicability

This study provides the first comprehensive assessment combining consumer preferences and fleet dynamics to assess dynamic GHG changes in the transition to MaaS. The novelty of this research is the consumer preference integration into the dynamic LCA work by introducing the C-DLCA method that incorporates the MaaS consumer preference characteristics measured against the attributes and their utilities and dynamic fleet changes. However, by applying the new approach, the C-DLCA methodology framework provides more meaningful results by integrating the consumer preferences into the dynamic LCA work, beyond the typical static GHG emission changes due to powertrain changes and body style (see Figure 4-3). The robustness of the C-DLCA framework is proven by its effective application in a selected case study. The clear information, data flows, and well-defined process steps in Figure 5-1 demonstrate its structured approach.

In this study, the vehicle body style was chosen as an attribute in car-based shared mobility for the first time. The attribute body style is also considered for the endogenous explanation and combines consumer decisions and fleet behaviour. Hence, the findings contribute to determining the dynamic environmental influences of the rapidly expanding car-based MaaS business by considering the fleet characteristics and consumers' responses to them in car-based sharing economy modes. Integrating consumer preferences and dynamic fleet technology changes into LCA outcomes provides insights beyond conventional (static) LCA applications. In summary, this study establishes a framework that diverse stakeholders can use to determine the environmental consequences of sharing economy modes by incorporating dynamic and causal changes.

This study assesses the overall GHG emission impacts in the car-based shared mobility industry, including fleet dynamics and automobile changes, such as vehicle lightweighting and longevity improvements, without limiting to the use phase in typical studies (see Table A-2, Table A-4, Table A-5 and Table A-7 in Appendix A). The findings of this study contribute in several ways to the understanding of the GHG emission behaviour of the three life-cycle phases and influential fleet technology factors in the transition to MaaS. As shown in Section 7.5, the results demonstrate a lower production GHG contribution in the initial modelling time. In both the production and EoL phases, GHG emissions increase compared with the use phase. In the end, they record more emissions than the use phase. The results represent the cumulative outcomes of several fleet-related temporal and technological factors. These include changes in powertrain type, body style, vehicle lightweighting, and survival rates. The integrated modelling work also considers the indirect but significant influence of US electricity grid GHG changes. Hence, this study provides fresh insights by incorporating the most influential factors of MaaS, considering their temporal behaviour to derive life-cycle GHG results. If this is not the case, the significance of the production phase in potential personal mobility scenarios will not be explored up to this detailed level. The results in this section and their implications provide insights for auto manufacturers on market-responsive GHG results based on consumer preferences by integrating potential fleet-based technology changes.

This study reveals gaps in market readiness to accept fleet electrification in car-based sharing economies. This study is one of the first attempts to study ridesourcing modes as a choice for round-trips to work journeys, a mode committed to completing the BEV transition by 2030. As highlighted in Sections 5.5 and 8.2, a significant value-action gap exists in the consumer behaviour of ridesourcing modes. These findings reveal a contradiction between what transportation network companies offer and what consumers want. As a whole, the results are critical for transport network companies, automakers and local and national policymakers, highlighting the importance of evaluating switching cost elements to close value-action gaps. The findings are also helpful in characterising and designing informed decision tools, such as ecolabels for the sharing economy, which is essential for the market sustainability values of the sharing economy (Vestergaard, Minor and Turan, 2020).

9 Conclusion and Future Work

Introduction

The final chapter of this thesis concludes with the research findings with respect to the aims of this study. Based on the research aims defined in Chapter 1 and the research questions derived in Chapter 2, a summary of the key findings of the work is presented. The critical applications of the C-DLCA methodology framework, the outcomes from the consumer preference survey, and the implications of SD modelling, dynamic LCA results and applications are discussed. Finally, limitations and directions for future work are presented. The chapter ends with concluding remarks.

9.1 Key findings

As presented in the previous chapters, the key findings of this study are concluded in accordance with the defined research aims. Recalling from Section 1.3, the purpose of this study was:

> To determine the life cycle GHG emissions of the transition to car-based shared mobility from private vehicles by combining consumer preferences and changes in MaaS fleet technology.

Consistent with the three aims of this research, the following explanation achieves the purpose of the study answering the research questions derived in Section 2.8.

Aim 1: <u>Establish a methodological framework to combine consumer preferences and fleet technology changes considering their causality and temporal effects to assess the life cycle GHG impacts of the transition to car-based sharing economy modes</u>**.**

According to the results of the study, the C-DLCA methodology provides a structured approach to integrating the sharing economy consumer behaviour into a dynamic LCA. The methodological framework was derived from exploring the ARQ1:

> How can the influence of temporal fleet technology changes and their causal effect on consumer preferences in GHG emissions from MaaS be quantified?

It was revealed that SD modelling work and LCA analysis integration had delivered the dynamic LCA methodology, which also follows the established ISO 14040 LCA principles. The dynamic

LCA method has also been used to integrate the temporal and causal effects of technology transitions into the environmental assessment of sharing economy systems, including shared mobility-based case studies. Halog and Manik (2011) used the SD method as an interface to integrate dynamic and causal (feedback) effects into dynamic LCA. Although there are some studies that combined consumer preference in SD modelling (Wang, Lai and Chang, 2016; Jiang, 2019, figs 3–6), no studies that integrated consumer preferences and their causal effects into a dynamic LCA, which is necessary to elaborate on ARQ1, could be found in the literature. Therefore, the C-DLCA methodology framework was introduced to combine three methodological components: a) consumer preference measured by a constrained choice-based consumer survey, b) SD as the modelling interface and c) LCA calculations.

This study is the first to combine consumer preferences with dynamic LCA. Another speciality here is the model's capability to consider sharing economy modes, which behave differently from product modes based on conventional linear economy. The overall framework was established to adhere to ISO 14040-based LCA principles, starting with LCA goal setting and ending with LCIA scenarios and interpretations.

The framework introduced in the present study supports the causality and temporality of consumer preferences and fleet dynamics, while linking their behaviour to life cycle GHG outcomes. Therefore, the C-DLCA methodology framework can be viewed as an approach to answering the identified ARQ1. The key features of the framework are as follows:

- A robust structure combining consumer preferences and LCA by employing the SD method as the modelling interface by ensuring multiple iterations, as shown in Figure 3-2
- A hybrid approach combining LCA and SD models than the conventional rigid approach
- Applicability to other sharing economy models
- Uses the Dynamic Process Inventory instead of the static LCI
- Excludes Dynamic Characterisation and Dynamic Normalisation Factors

The LCA goal setting (L1) of the C-DLCA framework was aligned with the key research question of this study. The full life cycle scope was chosen considering the anticipated influence of dynamic fleet changes in the production, usage and EoL phases. The p.km is chosen as the functional unit, aligned with previous studies (Henao, 2017; Union of Concerned Scientists, 2020b). User transition to MaaS and fleet volumes was selected as the reference modes for the time horizon from 2014 to 2050, in the SD mode problem articulation (S1) step.

In this study, an initial dynamic hypothesis (S2) was defined based on the two key reference modes. Vehicle body style was identified as the endogenous explanation considering the consumers' ability to choose when they place the order for a car-based MaaS journey in the sharing economy or when they buy a car in the linear economy.

Aim 2: Assess the attributes of consumer preference and the characteristics of car-based sharing economy modes

As the case study of this research work, an average round-trip to/from work in the US was chosen. The average round-trip to work was chosen as it represents the most significant routine journey type while the US was chosen due to its significant size in the global context and the maturity of car-based MaaS modes in the US market. The case study selection and the market survey were performed to answer ARQ2:

> What is the significance of consumer attributes influencing the transition to car-based MaaS?

A market survey was conducted with 2,968 qualified samples from 24 US cities, representing geography and public transit levels. The survey instrument (C1) comprised of the choice-based conjoint analysis model and sample characterising questions. The choice-based conjoint analysis was chosen to combine the stated preference technique and DCE method (C2) features and was employed in the survey instrument in order to capture consumer behaviour. Carpooling, solo-ridesourcing, and pooled-ridesourcing were chosen as alternatives for the choice-based conjoint analysis choice sets based on their increasing popularity in US cities. The constraint-based conjoint analysis outcomes determined the importance of the attributes and level preferences to combine with the transition to the MaaS SD modelling component. The DCE-based survey findings (C3) were analysed using the random utility theory and MNL model.

This study concluded that *cost* (journey fare) and *time* (door-to-door journey time) are the most significant attributes of consumer preferences in selecting a car-based mobility mode for an average work trip in the US, which is expected.

Carpooling users demonstrated the least *cost* flexibility compared to solo-ridesourcing and pooled-ridesourcing modes. The utility values of *time* for all three modes were positive until 25 minutes, showing the results aligned with the average commute travel time in private vehicles in the US.

The attribute *number of passengers* was chosen as the third significant attribute, representing convenience characteristics such as privacy and interaction concerns. The three attributes above had significantly influenced consumer decision-making on MaaS and, subsequently, the dynamic LCA results based on their mobility preferences.

The two fleet technological attributes in this study provide a new understanding of consumer preferences. The attribute *vehicle body style* has gained higher consumer preference than the *powertrain type*. Surprisingly, the consumer preference for the low-occupancy solo-ridesourcing mode has shown interest in the large vehicle body style, SUVs, compared to pooled-ridesourcing and carpooling. Greater interest in *body style* has been observed among respondents aged 18–24 yrs than others. The most unexpected outcome was the rejection of BEVs in car-based MaaS fleets while accepting gasoline vehicles. This observation also demonstrates a gap in market readiness to accept transport network companies and government-driven fleet electrification goals. Consumer decision-making regarding these fleet technology attributes influences GHG emissions from personal mobility.

On reflection, this study offers insights into the value-action gap (Kollmuss and Agyeman, 2002). The respondents' intentions to act, depicted in this study by stated preferences within a constrained choice, strongly reflected their actual behaviour. Two technical attributes, *powertrain type* and *vehicle body style* act as proxies for preference for environmental value. However, anticipated pro-environmental behaviours were not observed.

In summary, the use of car-based MaaS can be considered a high-constraint behavioural change due to the high switching costs in either economic/situational (i.e., price, etc.) or non-economic switching (i.e., travel time, convenience, status) factors.

Respondents' location and age influenced the survey results. It has been shown that private vehicles are the most common mobility mode, with higher usage in cities with low-public transit. The results also suggested that carpooling is the preferred mode of round-trip to work by more employees who live in cities with low-public transit than those cities having high-public transit. At the same time, solo-ridesourcing is more prevalent in high-public transit cities. The young labour force (below 35 yrs) favoured car-based MaaS 38% higher than the older labour force (55 yrs above). However, age-based MaaS preferences were not considered in the SD modelling because they were beyond the scope of the present study and anticipated modelling complexities with the constrained choice approach. Nevertheless, they can be utilised to understand future trends in car-based MaaS and offer an opportunity for future study.

In conclusion, the market survey findings show that *cost, time* and *number of passengers* are significant attributes of consumer decision-making in the transition to MaaS. The higher preference for SUVs and the rejection of BEVs have shown a value-action gap against the expected pro-environmental behaviour of potential MaaS users.

Aim 3: Determine the significance of consumer preference and fleet technology changes on the dynamic GHG emission changes of the transition to car-based sharing economy modes over time by selecting a case study

The DCE-based market survey findings were incorporated into the SD model to integrate market responses into the dynamic LCA study. An SD model structure was operationalised with three sub-models to explore the influence of consumer preferences and fleet changes on the transition to MaaS users, fleet behaviour and finally, the dynamic LCA calculations. The goal of the dynamic LCA model was to answer the key research question.

What is the impact of the transition from private vehicle use to car-based sharing economy modes on GHG emissions, considering consumer preferences and fleet technology changes?

The SD-based dynamic LCA model comprises three SD sub-models to answer the key research question.

The first sub-model, i.e., transition to MaaS, was created based on the Bass model (Bass, 1969). Integration of DCE outcome by introducing the variable MaaS mode attractiveness has been one of the fresh attempts to combine the consumer preference findings into the attributes by adopting the product attractiveness concept by Schmidt and Gary (2002). It established a **feedback loop** based on the endogenous explanation of the attribute *vehicle body style*. Model calibration and testing (S4) were performed using payoff calculations. Four variables were identified as relying on the calibration process, considering the constraints to acquiring reliable and case-specific secondary data. Policy scenario specifications were introduced based on the trends and the chosen high BEV adoption scenario.

The model used in this study concluded that the user transition from private vehicles to car-based MaaS modes has increased, while the number of private vehicle users has also decreased. The high BEV adoption scenario attracted more car-based MaaS users than the baseline scenario. The most significant contribution to the increase was from the low-occupancy-based solo-ridesourcing, showing nearly 2 million extra users in the high BEV adoption mode at the end of the modelling period. The only user decreasing trend was observed in the high-occupancy-based popular carpooling mode. The pooled-ridesourcing mode demonstrated slower growth than solo-ridesourcing but was accepted against carpooling. Therefore, results of the transition to MaaS sub-model implied that the acceptance of car-based sharing economy mode was towards solo-ridesourcing.
In the second sub-model, fleet behaviour, fleet-based changes and feedback from the derived transition to the MaaS sub-model were simulated and formulated(S3). The fleet behaviour was observed based on the mobility mode, powertrain type and body style. The attribute *vehicle body style* combines the first and second sub-models through its endogenous connection. The incorporation of derived utility values from the DCE outcomes encapsulated market responses into fleet behaviour, which was analysed separately for the private vehicle and the MaaS fleets considering the different feedbacks and factors.

The study provided the first comprehensive assessment of car-based MaaS fleet behaviour changes in response to the market. The model results showed that the aggregated personal mobility fleet is increasing. However, there were many changes in fleet composition. The most significant finding is the massive increase of the aggregated MaaS fleets while private vehicles record a slight increase by 2050 compared with 2014. The highest decline is from sedan gasoline, while the highest increase is observed for SUV BEVs. The solo-ridesourcing fleet has increased significantly by adding a significant number of BEVs within 36 years of modelling time, reaching almost three-quarters of SUVs in its fleet. Private and carpooling fleets were slower in the electrification journey than in the ridesourcing mode. These behaviours show the significance of consumer preference for fleet behaviour.

The third sub-model was the D-LCA calculation, which incorporated consumer preferences through dynamic fleet behaviour. The derived DPI inputs were based on the GREET model (Wang *et al.*, 2021). It started with establishing the DPI for production, usage and EoL phases separately for different powertrain types and vehicle body styles, followed by customising them to three MaaS mode fleets. Dynamic LCA analyses were carried out for private and MaaS modes.

In conclusion, consumer preferences and the fleet changes incorporated dynamic LCA on the transition to MaaS have shown that the car-based sharing economy is a pathway to reduce GHG emissions in personal mobility only with specific fleet and consumer preference combinations. The consumer preferences towards the high BEV adoption scenario reduce the life cycle GHG emission of the personal mobility in the round-trip to work journey in the US but without complete mitigation. This trend is significantly supported by the greening of US electric grid targets. Vehicle lightweighting and improved survival rates are also supported in reducing the life cycle GHG emissions of the fleet. BEV-driven carpooling is the best car-based MaaS option for reducing GHG emissions. Although the pooled-ridesourcing mode is another high-occupancy mode, the larger SUV-based fleet composition and deadheading challenge it to achieve better GHG reduction than carpooling. The most preferred solo-ridesourcing has demonstrated the highest specific GHG emissions when measured against p.km, the functional unit used in this study. Its absolute GHG emissions have shown the importance of optimising deadheading. Though solo-ridesourcing fleet BEV share was higher than carpooling, the net occupancy is even below that of private vehicles. Hence, more use-phase emissions are generated. In 2050, the production phase GHG emissions will reach more than two third of the life-cycle GHG emissions, which was nearly 5% in 2014. The solo-ridesourcing faster fleet replacement rate has contributed significantly to GHG emissions at the end of the modelling period. This was because of the higher contribution of BEV production to GHG emissions. Overall, the aggregated MaaS-mode GHG emissions unexpectedly increased, even with higher consumer transition rates and faster fleet electrification plans.

Furthermore, the aggregated MaaS cumulative GHG emissions did not significantly differ between the baseline and high BEV adoption scenarios. Overall, based on the results, it can be concluded that the impact of the transition from private car use to car-based sharing economy modes on GHG significantly depends on fleet changes and consumer preferences. The BEV-driven pooling modes are the best option subject to closing the value-action gap by changing consumer acceptance and behaviour on fleet electrification and pooling.

9.2 Contributions and key implications of the research

Contributions and implications of this research can be expressed in three directions. These highlights will be useful for governments and mobility operators, including transport network companies, automakers and, importantly, potential consumers of car-based MaaS.

9.2.1 Implications of consumer preference

The consumer preference survey outcomes concluded that the consumer choices of trips to work in the US do not support the anticipated fleet technology-related environmental benefits of car-based MaaS. Therefore, closing the value-action gap by identifying the specific switching cost is highlighted as the key to optimising the GHG savings of shifting to car-based sharing economy modes. Effective awareness of the environmental benefits of fleet electrification is a possible pathway for increasing the utility of BEVs led by governments and environmental lobby groups. Currently, the choice of powertrain type in solo-ridesourcing apps is a limited option, only in selected locations. Transport network companies can enable customers by providing the option to choose the powertrain type while ordering a ride. However, programs to close the value-action gap related to fleet electrification and higher preferences for SUVs for solo rides can be identified as prerequisites before enabling informed decision tools. An indication of the vehicle's fuel economy and the consequences of GHG emissions for different powertrain types and body style choices can be identified as a starting step until the BEVs are amply available in solo-ridesourcing fleets. Such tools facilitate pro-environmental decision-making.

9.2.2 Implications of fleet changes

As per the model results, the high BEV adoption scenario can be concluded as a personal transportation pathway with low-carbon, in the cities complemented by the shifting to lower GHG-emitting grid electricity supplies. However, the BEV fleet uptake increased production and EoL GHG emissions. This study also highlights the GHG emissions contribution of frequent fleet replacement in solo-ridesourcing, considering the increasing production and EoL impacts of fleet electrification. The maximum operational age of a car in a ridesourcing fleet is lower than the latest survival rates (Lu, 2006, p. 8; Davis and Boundy, 2021, pp. 3–20; Uber, 2021d). Hence, a scheme to promote vehicle second life for solo-ridesourcing fleets is an alternative to reducing production and EoL GHG emissions (Amasawa *et al.*, 2020). However, the second life of the solo-ridesourcing fleet is not considered in the LCA scope of this study.

This study is the first of its kind that considered the attribute of *vehicle body style* as an endogenous variable in a choice-based study to analyse car-based MaaS mode consumer preferences and dynamic LCA work. The higher user preferences for SUVs and market dynamics have created a reinforced loop, increasing the adoption of SUVs in personal mobility and generating additional

GHG emissions. An SUV or a larger vehicle can be ordered on shared mobility apps for a journey, irrespective of the number of passengers at a higher journey fare. A transport network company-led program to discourage the use of SUVs for low-occupancy trips is an option to reduce GHG emissions. However, this proposal could be challenged in the context of high SUV adoption.

The results from the model have concluded that the highest GHG emissions were achieved by solo-ridesourcing while incorporating the transport network companies' highest commitments to a 100% BEV fleet by 2030. Deadheading is a significant element contributing to solo-ridesourcing GHG emissions. An average extra 20.6 km of non-productive distance is driven if a solo-ridesourcing vehicle accepts catering to two to/from work journeys in the US. The sensitivity results shown in Section 7.7.3 only represent the reduction of the non-productive ride due to a lack of case-specific data and illustrate the minimum emission reduction. Transport network companies boast plans to improve deadheading in the future (Uber, 2020). An industry-centric approach with a transparent market mechanism would be better than individual mobility operator-based solutions for deadheading management. Such an approach can reduce solo-ridesourcing fleets and eventually city traffic and parking congestion.

Based on powertrain type and body style explanations along with the focus on deadheading, it can be concluded that lack of control, operational optimisations and customer empowerment with a proper awareness of the selection of fleet options will hinder the transition to car-based MaaS GHG benefits.

9.2.3 Implications of auto industry led changes

Conventionally, vehicle lightweighting is an improved pathway for reducing mobility GHG emissions. However, this study highlights a decrease in the contribution of lightweighting towards overall GHG emission reduction with fleet electrification. In the BEV use phase, lightweighting benefits are complemented by increasing renewables in electricity grids. In contrast, embodied GHG emissions increase in the production phase depending on the raw material composition. Hence, the results suggest more research on lightweighting compositions in high BEV adoption scenarios and trade-offs. However, lightweighting improves range and may promote BEV usage by reducing range anxiety.

An improved survival rate is another automobile enhancement that contributes to the lifetime GHG emission reduction of a vehicle. Higher survival rates can reduce the lifetime GHG emissions of SUVs (Davis and Boundy, 2021, pp. 3–20; Wang *et al.*, 2021). However, longer survival rates can slow the accessibility of newer vehicle models. This study showed gasoline vehicle traces in fleets by the end of the modelling period in the high BEV adoption scenario. Hence, introducing policy mechanisms to incentivise fleet replacements at a significantly efficient loss stage is an alternative to managing higher survival rate trade-offs.

9.3 Research limitations and proposed future work

The key limitation of the study is the selection of a single journey type as the scope of the study (Section 3.1). The selection of a round-trip to work in the US is based on its significance in a car-based sharing economy market. Hence, the results represent this scope of work and are not representative of all types of trips. Further studies should be conducted to investigate other trip purposes and associated consumer preferences.

This study provides fresh insight regarding the importance of closing the value-action gaps in the MaaS domain. As highlighted in Section 9.2.1, further research is required to close them by identifying the specific switching costs needed to improve GHG emissions in MaaS. Hence, a market survey to understand the switching costs of fleet electrifications and high-occupancy MaaS modes is beneficial to achieving the expected environmental benefits of the car-based MaaS. These findings can be the input for environmental awareness tools, such as an ecolabel for a MaaS journey that would enable consumers to make an informed choice (Young *et al.*, 2010; Nguyen-Viet, 2022).

This study introduced and applied a new methodology framework, C-DLCA, to integrate consumer preferences into the transition to MaaS dynamic LCA calculations by employing a comprehensive consumer survey. Although a rigorous sampling plan was implemented to achieve national representation, the outcomes did not reflect choice preferences in the context of a time-varying manner in which fleet and environmental factors changed. Rettie et al. (2014) show that the consumer likelihood to engage in 'green' behaviours is based on what they think is normal and what is regarded as normal change over time. Therefore, the consumer preference results utilised for the full modelling period in this study can change based on significant changes, such as high BEV adoption scenarios. Integration of dynamic or scenario-based consumer preferences (dynamic-consumer preferences) would increase the accuracy of the transition to the MaaS sub-model and, subsequently, the dynamic LCA.

The *powertrain type* attribute was not considered endogenous because consumers do not have the option to select it in the current shared mobility apps. However, with BEV promotion in the ridesourcing fleets, the option to select the powertrain type would be generic in the future. Overall, the *powertrain type* can be considered an endogenous attribute identified as a potential future work. It can add increased research value with the speed of changes in the electrification of the personal mobility fleet.

The derived purchasing and scrappage fleet volumes provide critical improvements in vehicle durability despite increasing solo-ridesourcing fleet replacements. These dynamics can significantly impact the quantities of raw and secondary materials required in the automobile industry. A future study focusing on the circularity impacts of the transition to MaaS can provide important research implications and insights for the automobile industry. Also, this study was limited by the absence of second life data of the car-based MaaS fleets. In summary, incorporating the second life into the life cycle scope can increase the accuracy of the MaaS fleets' life cycle GHG emission results.

9.4 Concluding remarks

In conclusion, consumer preferences and fleet changes incorporated dynamic LCA on the transition to MaaS in trips to work in the US have shown that the car-based sharing economy is a pathway to reduce GHG emissions in personal mobility with specific fleets and consumer preference combinations. However, it does not provide a complete solution for mitigating GHG emissions in the chosen case study. Based on the introduced C-DLCA methodology, this work has demonstrated the importance of considering consumer preferences and combining them with fleet dynamics by establishing causal and temporal relationships for understanding car-based MaaS dynamic GHG changes. The results highlight that BEV-driven sedans in pooling modes are the best in terms of GHG savings from the transition to MaaS. Other modes were found to contribute to increased aggregated MasS GHG emissions beyond those of private vehicles. Improving environmental awareness among MaaS users to close the value-action gap to promote BEV choice and conscious SUV preference within the most popular solo-ridesourcing is highlighted to reduce car-based aggregated MaaS GHG emissions.

REFERENCES

Aamas, B. and Andrew, R. (2020) *Estimating effects on emissions of sharing*. 2020:03. Oslo: CICERO Center for International Climate Research. Available at: https://pub.cicero.oslo.no/cicero-xmlui/bitstream/handle/11250/2654398/Rapport%202020%2003%20web.pdf?sequence=1&isAllowed=y (Accessed: 22 December 2021).

Acharya, A. *et al.* (2013) ‘Sampling: Why and How of it?’, *Indian Journal of Medical Specilaities*, 4(2), pp. 330–333. Available at: https://doi.org/10.7713/ijms.2013.0032.

Ajanovic, A. (2015) ‘The future of electric vehicles: prospects and impediments’, *WIREs Energy and Environment*, 4(6), pp. 521–536. Available at: https://doi.org/10.1002/wene.160.

Ajzen, I. (1991) ‘The Theory of Planned Behavior-Organizational Behavior and Human Decision Processes 50’, *Ajzen, I.(2002) Perceived Behavioural Control, Self-efficacy, Locus of Control and the Theory of Planned Behaviour. Journal of Applied Social Psychology*, 32(4), pp. 665–683.

Akimoto, K., Sano, F. and Oda, J. (2022) ‘Impacts of ride and car-sharing associated with fully autonomous cars on global energy consumptions and carbon dioxide emissions’, *Technological Forecasting and Social Change*, 174, p. 121311. Available at: https://doi.org/10.1016/j.techfore.2021.121311.

Alemi, F. *et al.* (2018) ‘What influences travelers to use Uber? Exploring the factors affecting the adoption of on-demand ride services in California’, *Travel Behaviour and Society*, 13, pp. 88–104. Available at: https://doi.org/10.1016/j.tbs.2018.06.002.

Alonso-González, M.J. *et al.* (2020) ‘What are the determinants of the willingness to share rides in pooled on-demand services?’, *Transportation* [Preprint]. Available at: https://doi.org/10.1007/s11116-020-10110-2.

Alvarez, S. *et al.* (2016) ‘Strengths-Weaknesses-Opportunities-Threats analysis of carbon footprint indicator and derived recommendations’, *Journal of Cleaner Production*, 121, pp. 238–247. Available at: https://doi.org/10.1016/j.jclepro.2016.02.028.

Amasawa, E. *et al.* (2020) ‘Environmental potential of reusing, renting, and sharing consumer products: Systematic analysis approach’, *Journal of Cleaner Production*, 242, p. 118487. Available at: https://doi.org/10.1016/j.jclepro.2019.118487.

Amatuni, L. *et al.* (2020) ‘Does car sharing reduce greenhouse gas emissions? Assessing the modal shift and lifetime shift rebound effects from a life cycle perspective’, *Journal of Cleaner Production*, 266, p. 121869. Available at: https://doi.org/10.1016/j.jclepro.2020.121869.

Ambrose, H. *et al.* (2020) ‘Trends in life cycle greenhouse gas emissions of future light duty electric vehicles’, *Transportation Research Part D: Transport and Environment*, 81, p. 102287. Available at: https://doi.org/10.1016/j.trd.2020.102287.

Amirkiaee, S.Y. and Evangelopoulos, N. (2018) ‘Why do people rideshare? An experimental study’, *Transportation Research Part F: Traffic Psychology and Behaviour*, 55, pp. 9–24. Available at: https://doi.org/10.1016/j.trf.2018.02.025.

An, S. *et al.* (2021) ‘A Study of the Factors Affecting Multimodal Ridesharing with Choice-Based Conjoint Analysis’, *Sustainability*, 13(20), p. 11517. Available at: https://doi.org/10.3390/su132011517.

Arbeláez Vélez, A.M. and Plepys, A. (2021) ‘Car Sharing as a Strategy to Address GHG Emissions in the Transport System: Evaluation of Effects of Car Sharing in Amsterdam’, *Sustainability*, 13(4), p. 2418. Available at: https://doi.org/10.3390/su13042418.

Astegiano, P., Fermi, F. and Martino, A. (2019) ‘Investigating the impact of e-bikes on modal share and greenhouse emissions: a system dynamic approach’, *Transportation Research Procedia*, 37, pp. 163–170. Available at: https://doi.org/10.1016/j.trpro.2018.12.179.

Awad-Núñez, S. *et al.* (2021) ‘Post-COVID-19 travel behaviour patterns: impact on the willingness to pay of users of public transport and shared mobility services in Spain’, *European Transport Research Review*, 13(1), p. 20. Available at: https://doi.org/10.1186/s12544-021-00476-4.

Badurdeen, F. *et al.* (2009) ‘Extending total life-cycle thinking to sustainable supply chain design’, *International Journal of Product Lifecycle Management*, 4(1–3), pp. 49–67. Available at: https://doi.org/10.1504/IJPLM.2009.031666.

Ball, C.S. *et al.* (2021) ‘E-mobility from a multi-actor point of view: Uncertainties and their impacts’, *Technological Forecasting and Social Change*, 170, p. 120925. Available at: https://doi.org/10.1016/j.techfore.2021.120925.

Bansal, P. *et al.* (2020) ‘Eliciting preferences of TNC users and drivers: Evidence from the United States’, *Travel Behaviour and Society*, 20, pp. 225–236. Available at: https://doi.org/10.1016/j.tbs.2020.04.002.

Baptista, P. *et al.* (2011) ‘Fuel cell hybrid taxi life cycle analysis’, *Energy Policy*, 39(9), pp. 4683–4691. Available at: https://doi.org/10.1016/j.enpol.2011.06.064.

Baptista, P., Melo, S. and Rolim, C. (2014) ‘Energy, Environmental and Mobility Impacts of Car-sharing Systems. Empirical Results from Lisbon, Portugal’, *Procedia - Social and Behavioral Sciences*, 111, pp. 28–37. Available at: https://doi.org/10.1016/j.sbspro.2014.01.035.

Bass, F.M. (1969) ‘A New Product Growth for Model Consumer Durables’, *Management Science*, 15(5), pp. 215–227. Available at: https://doi.org/10.1287/mnsc.15.5.215.

Bauer, C. *et al.* (2015) ‘The environmental performance of current and future passenger vehicles: Life cycle assessment based on a novel scenario analysis framework’, *Applied Energy*, 157(Journal Article), pp. 871–883. Available at: https://doi.org/10.1016/j.apenergy.2015.01.019.

Ben-Akiva, M. (1973) *Structure of passenger travel demand models*. Maasachusetts Institute of Technology.

Ben-Akiva, M. and Atherton, T.J. (1977) ‘Methodology for Short-Range Travel Demand Predictions: Analysis of Carpooling Incentives’, *Journal of Transport Economics and Policy*, 11(3), pp. 224–261. Available at: https://www.jstor.org/stable/20052477 (Accessed: 17 June 2020).

Ben-Akiva, M. and Lerman, S.R. (1987) *Discrete Choice Analysis*. Massachusetts: The MIT Press (Theory and Application to Travel Demand).

Berjisian, E. (2021) *Environmental Impacts of Shared Mobility Services in Metro Vancouver*, p. 39. Available at: https://www.sustain.ubc.ca/sites/default/files/2021-002_Environmental%20Impacts%20of%20Shared%20Mobility_Berjisian.pdf.

Berneiser, J. *et al.* (2021) ‘The role of norms and collective efficacy for the importance of techno-economic vehicle attributes in Germany’, *Journal of Consumer Behaviour*, 20(5), pp. 1113–1128. Available at: https://doi.org/10.1002/cb.1919.

Bierlaire, M. (1998) ‘Discrete Choice Models’, in M. Labbé et al. (eds) *Operations Research and Decision Aid Methodologies in Traffic and Transportation Management*. Berlin, Heidelberg: Springer (NATO ASI Series), pp. 203–227. Available at: https://doi.org/10.1007/978-3-662-03514-6_9.

Bishop, G.A. *et al.* (2016) ‘High-Mileage Light-Duty Fleet Vehicle Emissions: Their Potentially Overlooked Importance’, *Environmental Science & Technology*, 50(10), pp. 5405–5411. Available at: https://doi.org/10.1021/acs.est.6b00717.

Bjørn, A. and Hauschild, M.Z. (2013) ‘Absolute versus Relative Environmental Sustainability’, *Journal of Industrial Ecology*, 17(2), pp. 321–332. Available at: https://doi.org/10.1111/j.1530-9290.2012.00520.x.

Botsman, R. (2015) *Defining The Sharing Economy: What Is Collaborative Consumption–And What Isn’t?*, *Fast Company*. Available at: https://www.fastcompany.com/3046119/defining-the-sharing-economy-what-is-collaborative-consumption-and-what-isnt (Accessed: 14 July 2021).

Boyden, A., Soo, V.K. and Doolan, M. (2016) ‘The environmental impacts of recycling portable lithium-ion batteries’, *Procedia Cirp*, 48, pp. 188–193.

Briceno, T. *et al.* (2005) *Using Life Cycle Approaches To Evaluate Sustainable Consumption Programs: Car-sharing*. Working Papers no.2/2005 ISSN 1504-3681. Trondheim. Available at: https://brage.bibsys.no/xmlui/handle/11250/242569 (Accessed: 12 March 2019).

Cai, H. *et al.* (2019) ‘Environmental benefits of taxi ride sharing in Beijing’, *Energy*, 174, pp. 503–508. Available at: https://doi.org/10.1016/j.energy.2019.02.166.

Cai, Y. *et al.* (2017) ‘A hybrid life cycle and multi-criteria decision analysis approach for identifying sustainable development strategies of Beijing’s taxi fleet’, *Energy Policy*, 100, pp. 314–325. Available at: https://doi.org/10.1016/j.enpol.2016.09.047.

California Air Resource Board (2019) *SB 1014 Clean Miles Standard 2018 Base-year Emissions Inventory Report*. SB 1014. Available at: https://ww2.arb.ca.gov/sites/default/files/2019-12/SB%201014%20-%20Base%20year%20Emissions%20Inventory_December_2019.pdf?utm_medium=email&utm_source=govdelivery.

Campíñez-Romero, S. *et al.* (2018) 'A hydrogen refuelling stations infrastructure deployment for cities supported on fuel cell taxi roll-out', *Energy*, 148, pp. 1018–1031. Available at: https://doi.org/10.1016/j.energy.2018.02.009.

Carissimi, M.C. and Creazza, A. (2022) 'The role of the enabler in sharing economy service triads: A logistics perspective', *Cleaner Logistics and Supply Chain*, 5, p. 100077. Available at: https://doi.org/10.1016/j.clscn.2022.100077.

Carranza, V. *et al.* (2016) 'Life Cycle Analysis: Uber vs. Car Ownership'. Institute of The Environment and Sustainability, UCLA. Available at: https://www.ioes.ucla.edu/wp-content/uploads/uber-vs-car-ownership.pdf.

Carrese, S. *et al.* (2017) 'Real time ridesharing: Understanding user behavior and policies impact: Carpooling service case study in Lazio Region, Italy', in *2017 5th IEEE International Conference on Models and Technologies for Intelligent Transportation Systems (MT-ITS)*. *2017 5th IEEE International Conference on Models and Technologies for Intelligent Transportation Systems (MT-ITS)*, pp. 721–726. Available at: https://doi.org/10.1109/MTITS.2017.8005607.

Carroll, P., Caulfield, B. (Brian) and Ahern, A. (2017) 'Encouraging sustainable commuting behaviour through smart policy provision: a stated preference mode-choice experiment in the Greater Dublin Area', in. *Irish Transport Research Network Conference 2017, University College Dublin, Ireland, 31 August -1 September 2017*, Irish Transport Research Network. Available at: https://researchrepository.ucd.ie/handle/10197/9434 (Accessed: 17 June 2020).

Carrus, G., Passafaro, P. and Bonnes, M. (2008) 'Emotions, habits and rational choices in ecological behaviours: The case of recycling and use of public transportation', *Journal of Environmental Psychology*, 28(1), pp. 51–62. Available at: https://doi.org/10.1016/j.jenvp.2007.09.003.

Castel-Branco, A.P., Ribau, J.P. and Silva, C.M. (2015) 'Taxi Fleet Renewal in Cities with Improved Hybrid Powertrains: Life Cycle and Sensitivity Analysis in Lisbon Case Study', *Energies; Basel*, 8(9), pp. 9509–9540. Available at: http://dx.doi.org.virtual.anu.edu.au/10.3390/en8099509.

Caulfield, B. (2009) 'Estimating the environmental benefits of ride-sharing: A case study of Dublin', *Transportation Research Part D: Transport and Environment*, 14(7), pp. 527–531. Available at: https://doi.org/10.1016/j.trd.2009.07.008.

Cervero, R. and Tsai, Y. (2004) ‘City CarShare in San Francisco, California: Second-Year Travel Demand and Car Ownership Impacts’, *Transportation Research Record*, 1887(1), pp. 117–127. Available at: https://doi.org/10.3141/1887-14.

Changsirivathanatahathamrong, A., Moore, S. and Linard, K. (2001) ‘Integrating System Dynamics with Life Cycle Assessment : A Framework for Improved Policy Formulation and Analysis’, *Int. Congress on Modelling and Simulation, 2001*, 3, pp. 1213–1218. Available at: https://ci.nii.ac.jp/naid/10012931338/ (Accessed: 28 May 2019).

Chen, M. (2017) ‘Welcome to the New Interdisciplinary Journal Combining Big Data and Cognitive Computing’, *Big Data and Cognitive Computing*, 1(1), p. 1. Available at: https://doi.org/10.3390/bdcc1010001.

Chen, T.D. and Kockelman, K.M. (2016) ‘Carsharing’s life-cycle impacts on energy use and greenhouse gas emissions’, *Transportation Research Part D: Transport and Environment*, 47, pp. 276–284. Available at: https://doi.org/10.1016/j.trd.2016.05.012.

Chuah, S.H.-W. *et al.* (2021) ‘Factors influencing the adoption of sharing economy in B2B context in China: Findings from PLS-SEM and fsQCA’, *Resources, Conservation and Recycling*, 175, p. 105892. Available at: https://doi.org/10.1016/j.resconrec.2021.105892.

Clewlow, R.R. and Mishra, G.S. (2017) ‘Disruptive Transportation: The Adoption, Utilization, and Impacts of Ride-Hailing in the United States’. Available at: https://escholarship.org/uc/item/82w2z91j (Accessed: 23 January 2020).

Cohen, S.H. (1997) ‘Perfect union’, *Marketing Research*, 9(1), pp. 12–17. Available at: https://www.proquest.com/docview/202714375/abstract/762807C054F042AEPQ/1 (Accessed: 20 July 2021).

Collins, C.M. and Chambers, S.M. (2005) ‘Psychological and Situational Influences on Commuter-Transport-Mode Choice’, *Environment and Behavior*, 37(5), pp. 640–661. Available at: https://doi.org/10.1177/0013916504265440.

Corby, S. (2018) *Why SUVs are becoming so popular*, *CarsGuide*. Available at: https://www.carsguide.com.au/car-advice/why-suvs-are-becoming-so-popular-34463 (Accessed: 17 February 2022).

Correia, G.H. de A., Silva, J. de A. e and Viegas, J.M. (2013) ‘Using latent attitudinal variables estimated through a structural equations model for understanding carpooling propensity', *Transportation Planning and Technology*, 36(6), pp. 499–519. Available at: https://doi.org/10.1080/03081060.2013.830894.

Coulombel, N. *et al.* (2018) 'Substantial rebound effects in urban ridesharing: Simulating travel decisions in Paris, France', *Transportation Research Part D: Transport and Environment* [Preprint]. Available at: https://doi.org/10.1016/j.trd.2018.12.006.

Cozzi, L. and Apostolos, P. (2021) *Global SUV sales set another record in 2021, setting back efforts to reduce emissions – Analysis*, *IEA*. Available at: https://www.iea.org/commentaries/global-suv-sales-set-another-record-in-2021-setting-back-efforts-to-reduce-emissions (Accessed: 14 February 2022).

Creswell, J.W. (1999) 'Chapter 18 - Mixed-Method Research: Introduction and Application', in G.J. Cizek (ed.) *Handbook of Educational Policy*. San Diego: Academic Press (Educational Psychology), pp. 455–472. Available at: https://doi.org/10.1016/B978-012174698-8/50045-X.

Cui, Y. *et al.* (2020) 'Understanding and Modeling the Social Preferences for Riders in Rideshare Matching', *Transportation* [Preprint]. Available at: https://doi.org/10.1007/s11116-020-10112-0.

Curtis, S.K. and Lehner, M. (2019) 'Defining the Sharing Economy for Sustainability', *Sustainability*, 11(3), p. 567. Available at: https://doi.org/10.3390/su11030567.

Curtis, S.K. and Mont, O. (2020) 'Sharing economy business models for sustainability', *Journal of Cleaner Production*, 266, p. 121519. Available at: https://doi.org/10.1016/j.jclepro.2020.121519.

Dalkey, N. and Helmer, O. (1963) 'An Experimental Application of the DELPHI Method to the Use of Experts', *Management science*, 9(3), pp. 458–467. Available at: https://doi.org/10.1287/mnsc.9.3.458.

Dang, L., von Arx, W. and Frölicher, J. (2021) 'The Impact of On-Demand Collective Transport Services on Sustainability: A Comparison of Various Service Options in a Rural and an Urban Area of Switzerland', *Sustainability*, 13(6), p. 3091. Available at: https://doi.org/10.3390/su13063091.

Davis, S.C. and Boundy, R.G. (2021) *Transportation Energy Data Book*. Edition 39 ORNL/TM-2020/1770 (Edition 39 of ORNL-5198). Oak Ridge, USA: Office of Energy Efficiency and Renewable Energy U.S. Department of Energy, p. 455. Available at: https://tedb.ornl.gov/wp-content/uploads/2021/02/TEDB_Ed_39.pdf (Accessed: 16 May 2021).

Davlembayeva, D., Papagiannidis, S. and Alamanos, E. (2019) 'Mapping the economics, social and technological attributes of the sharing economy', *Information Technology and People* [Preprint]. Available at: https://doi.org/10.1108/ITP-02-2018-0085.

Delistavrou, A., Tilikidou, I. and Krystallis, A. (2021) 'Nested relationships in pro-environmental purchasing: A moderated mediation model', *Journal of Consumer Behaviour*, 20(6), pp. 1648–1663. Available at: https://doi.org/10.1002/cb.1958.

Dewalska-Opitek, A. (2017) 'Generation Y consumer preferences and mobility c… — Library of Science', *Archives of Transport System Telematics*, 10, pp. 17–23. Available at: https://bibliotekanauki.pl/articles/393978 (Accessed: 21 February 2022).

Dhawan, S. and Yadav, P. (2018) 'E-Cab hailing: A study on consumer behaviour.', *ELK Asia Pacific Journal of Marketing and Retail Management*, 9(3), pp. 1–17. Available at: https://doi.org/10.31511/EAPJMRM.2018v09i03001.

Dietz, T., Dan, A. and Shwom, R. (2005) 'Social psychological and social structural influences on climate change mitigation policy support', in *Social Science Quarterly. 100th annual meeting of the American Sociological Association*, Philadelphia, USA.

Dijk, M., Wells, P. and Kemp, R. (2016) 'Will the momentum of the electric car last? Testing an hypothesis on disruptive innovation', *Technological Forecasting and Social Change*, 105, pp. 77–88. Available at: https://doi.org/10.1016/j.techfore.2016.01.013.

Ding, N. *et al.* (2019) 'Life cycle assessment of car sharing models and the effect on GWP of urban transportation: A case study of Beijing', *Science of The Total Environment*, 688, pp. 1137–1144. Available at: https://doi.org/10.1016/j.scitotenv.2019.06.111.

Dixit, V.V. *et al.* (2010) *Review of congestion pricing experiences*. Louisiana State University, Georgia State University, University of Central Florida. Available at: https://www.diva-portal.org/smash/get/diva2:1247496/FULLTEXT01.pdf (Accessed: 21 October 2021).

Doka, G. and Ökobilanzen, D. (2001) 'Complete Life Cycle Assessment for Vehicle Models of the Mobility CarSharing Fleet Switzerland', p. 14. Available at: https://www.doka.ch/DokaMobilitySTRCproc01.pdf.

Dubé, J.-P., Hitsch, G.J. and Rossi, P.E. (2009) 'Do Switching Costs Make Markets Less Competitive?', *Journal of Marketing Research*, 46(4), pp. 435–445. Available at: https://doi.org/10.1509/jmkr.46.4.435.

Dumas, J.S. and Dobson, R. (1979) ‘Linking consumer attitudes to bus and carpool usage’, *Transportation Research Part A: General*, 13(6), pp. 417–423. Available at: https://doi.org/10.1016/0191-2607(79)90005-0.

El Zarwi, F., Vij, A. and Walker, J.L. (2017) ‘A discrete choice framework for modeling and forecasting the adoption and diffusion of new transportation services’, *Transportation Research Part C: Emerging Technologies*, 79, pp. 207–223. Available at: https://doi.org/10.1016/j.trc.2017.03.004.

Elgowainy, A. *et al.* (2016) *Cradle-to-Grave Lifecycle Analysis of U.S. Light-Duty Vehicle-Fuel Pathways: A Greenhouse Gas Emissions and Economic Assessment of Current (2015) and Future (2025-2030) Technologies*. ANL/ESD-16/7 Rev.1. Illinois: Argonne National Laboratory, p. 210. Available at: https://greet.es.anl.gov/files/c2g-2016-report (Accessed: 4 March 2019).

Ertz, M., Durif, F. and Arcand, M. (2016) ‘Collaborative Consumption: Conceptual Snapshot at a Buzzword’. Rochester, NY. Available at: https://doi.org/10.2139/ssrn.2799884.

European Environment Agency (EEA) (2018) *Average age of the vehicle fleet*, *European Environment Agency*. Available at: https://www.eea.europa.eu/data-and-maps/indicators/average-age-of-the-vehicle-fleet/average-age-of-the-vehicle-8 (Accessed: 19 April 2019).

Farrant, L., Olsen, S.I. and Wangel, A. (2010) ‘Environmental benefits from reusing clothes’, *The International Journal of Life Cycle Assessment*, 15(7), pp. 726–736. Available at: https://doi.org/10.1007/s11367-010-0197-y.

Farrell, J. and Klemperer, P. (2007) ‘Chapter 31 Coordination and Lock-In: Competition with Switching Costs and Network Effects’, in M. Armstrong and R. Porter (eds) *Handbook of Industrial Organization*. Elsevier, pp. 1967–2072. Available at: https://doi.org/10.1016/S1573-448X(06)03031-7.

Federal Highway Administration (FHWA) (2018) *National Household Travel Survey*. Available at: https://nhts.ornl.gov/ (Accessed: 7 January 2021).

Federal Highway Administration (FHWA) (2019) *U.S. households are holding on to their vehicles longer - Today in Energy - U.S. Energy Information Administration (EIA)*, *National Household Travel Survey*. Available at: http://nhts.ornl.gov (Accessed: 21 January 2019).

Fernando, C. *et al.* (2020) ‘Life cycle environmental assessment of a transition to mobility servitization’, *Procedia CIRP*, 90, pp. 238–243. Available at: https://doi.org/10.1016/j.procir.2020.01.098.

Fernando, C., Soo, V.K. and Doolan, M. (2020) ‘Life Cycle Assessment for Servitization: A Case Study on Current Mobility Services’, *Procedia Manufacturing*, 43, pp. 72–79. Available at: https://doi.org/10.1016/j.promfg.2020.02.112.

Firnkorn, J. and Müller, M. (2011) ‘What will be the environmental effects of new free-floating car-sharing systems? The case of car2go in Ulm’, *Ecological Economics*, 70(8), pp. 1519–1528. Available at: https://doi.org/10.1016/j.ecolecon.2011.03.014.

Fischer, D., Böhme, T. and Geiger, S.M. (2017) ‘Measuring young consumers’ sustainable consumption behavior: development and validation of the YCSCB scale’, *Young Consumers*, 18(3), pp. 312–326. Available at: https://doi.org/10.1108/YC-03-2017-00671.

Flores, P.J. and Jansson, J. (2021) ‘The role of consumer innovativeness and green perceptions on green innovation use: The case of shared e-bikes and e-scooters’, *Journal of Consumer Behaviour*, n/a(n/a). Available at: https://doi.org/10.1002/cb.1957.

Folkvord, F. *et al.* (2020) ‘The effects of ecolabels on environmentally- and health-friendly cars: an online survey and two experimental studies’, *The International Journal of Life Cycle Assessment*, 25(5), pp. 883–899. Available at: https://doi.org/10.1007/s11367-019-01644-4.

Foote, B. (2021) ‘Ford Signs Pledge To Phase Out Fossil Fuel Vehicles By 2040’, *Ford Authority*, 10 November. Available at: https://fordauthority.com/2021/11/ford-signs-pledge-to-phase-out-fossil-fuel-vehicles-by-2040/ (Accessed: 17 February 2022).

Franco, M.A. (2019) ‘A system dynamics approach to product design and business model strategies for the circular economy’, *Journal of Cleaner Production*, 241, p. 118327. Available at: https://doi.org/10.1016/j.jclepro.2019.118327.

Frenken, K. (2017) ‘Political economies and environmental futures for the sharing economy’, *Philosophical Transactions of the Royal Society A: Mathematical, Physical and Engineering Sciences*, 375(2095), p. 20160367. Available at: https://doi.org/10.1098/rsta.2016.0367.

Fromm, H. *et al.* (2019) *A study on free-floating carsharing in Europe: Impacts of car2go and DriveNow on modal shift, vehicle ownership, vehicle kilometers traveled, and*

CO2 emissions in 11 European cities. Working Paper 36. Working Paper Series in Production and Energy. Available at: https://doi.org/10.5445/IR/1000104216.

Galatoulas, F. *et al.* (2017) ‘A Comparative Study on User Characteristics of an E-car Pooling Service in Universities in Europe’:, in *Proceedings of the 6th International Conference on Smart Cities and Green ICT Systems*. *6th International Conference on Smart Cities and Green ICT Systems*, Porto, Portugal: SCITEPRESS - Science and Technology Publications, pp. 200–207. Available at: https://doi.org/10.5220/0006302202000207.

Garaus, M. and Garaus, C. (2021) ‘The Impact of the Covid-19 Pandemic on Consumers’ Intention to Use Shared-Mobility Services in German Cities’, *Frontiers in Psychology*, 12. Available at: https://www.frontiersin.org/article/10.3389/fpsyg.2021.646593 (Accessed: 20 February 2022).

Garcia, R., Gregory, J. and Freire, F. (2015) ‘Dynamic fleet-based life-cycle greenhouse gas assessment of the introduction of electric vehicles in the Portuguese light-duty fleet’, *The International Journal of Life Cycle Assessment*, 20(9), pp. 1287–1299. Available at: https://doi.org/10.1007/s11367-015-0921-8.

Gawron, J.H. *et al.* (2019) ‘Deep decarbonization from electrified autonomous taxi fleets: Life cycle assessment and case study in Austin, TX’, *Transportation Research Part D: Transport and Environment*, 73, pp. 130–141. Available at: https://doi.org/10.1016/j.trd.2019.06.007.

Geum, Y., Lee, S. and Park, Y. (2014) ‘Combining technology roadmap and system dynamics simulation to support scenario-planning: A case of car-sharing service’, *Computers & Industrial Engineering*, 71(Journal Article), pp. 37–49. Available at: https://doi.org/10.1016/j.cie.2014.02.007.

Girard, A. *et al.* (2019) ‘Solar electricity production and taxi electrical vehicle conversion in Chile’, *Journal of Cleaner Production*, 210, pp. 1261–1269. Available at: https://doi.org/10.1016/j.jclepro.2018.11.092.

Gobble, M.M. (2017) ‘Defining the Sharing Economy’, *Research-Technology Management*, 60(2), pp. 59–63. Available at: https://doi.org/10.1080/08956308.2017.1276393.

Goedkoop, M.J. *et al.* (1999) *Product Service systems, Ecological and Economic Basics*. Ministry of Housing, Spatial Planning and the Environment, p. 132. Available at: https://presustainability.com/legacy/download/Product_Service_Systems_main_report.pdf (Accessed: 7 January 2022).

Green, P.E. and Srinivasan, V. (1978) ‘Conjoint Analysis in Consumer Research: Issues and Outlook’, *Journal of Consumer Research*, 5(2), pp. 103–123. Available at: https://www-jstor-org.virtual.anu.edu.au/stable/2489001?pq-origsite=summon&seq=1#metadata_info_tab_contents (Accessed: 22 January 2021).

Green, P.E. and Srinivasan, V. (1990) ‘Conjoint Analysis in Marketing Research: New Developments and Directions’, *Journal of Marketing*, 54(4), pp. 3–19. Available at: https://search.proquest.com/docview/1296569594/citation/B0279B3B497D4A20PQ/1 (Accessed: 25 January 2021).

Greenblatt, J.B. and Shaheen, S. (2015) ‘Automated Vehicles, On-Demand Mobility, and Environmental Impacts’, *Current Sustainable/Renewable Energy Reports*, 2(3), pp. 74–81. Available at: https://doi.org/10.1007/s40518-015-0038-5.

Grischkat, S. *et al.* (2014) ‘Potential for the reduction of greenhouse gas emissions through the use of mobility services’, *Transport Policy*, 35, pp. 295–303. Available at: https://doi.org/10.1016/j.tranpol.2014.06.007.

Guidotti, R. *et al.* (2017) ‘Never drive alone: Boosting carpooling with network analysis’, *Information Systems*, 64, pp. 237–257. Available at: https://doi.org/10.1016/j.is.2016.03.006.

Guyon, O. (2017) *Methodology for the Life Cycle Assessment of a Car-sharing Service*. KTH Royal Institute of Technology. Available at: https://www.diva-portal.org/smash/get/diva2:1183366/FULLTEXT01.pdf (Accessed: 23 October 2020).

Halog, A. and Manik, Y. (2011) ‘Advancing Integrated Systems Modelling Framework for Life Cycle Sustainability Assessment’, *Sustainability*, 3(2), pp. 469–499. Available at: https://doi.org/10.3390/su3020469.

Hamby, D.M. (1994) ‘A review of techniques for parameter sensitivity analysis of environmental models’, *Environmental Monitoring and Assessment*, 32(2), pp. 135–154. Available at: https://doi.org/10.1007/BF00547132.

Hamzah, M.I. and Tanwir, N.S. (2021) ‘Do pro-environmental factors lead to purchase intention of hybrid vehicles? The moderating effects of environmental knowledge’, *Journal of Cleaner Production*, 279, p. 123643. Available at: https://doi.org/10.1016/j.jclepro.2020.123643.

Hapuwatte, B.M. and Jawahir, I.S. (2019) ‘A total life cycle approach for developing predictive design methodologies to optimize product performance’, *Procedia Manufacturing*, 33, pp. 11–18. Available at: https://doi.org/10.1016/j.promfg.2019.04.003.

Hawkins, T.R. *et al.* (2013) ‘Comparative Environmental Life Cycle Assessment of Conventional and Electric Vehicles’, *Journal of Industrial Ecology*, 17(1), pp. 53–64. Available at: https://doi.org/10.1111/j.1530-9290.2012.00532.x.

Henao, A. (2017) *Impacts of ridesourcing – Lyft and Uber – on transportation including vmt, mode replacement, parking, and travel behavior*. University of Colorado. Available at: https://pdfs.semanticscholar.org/e2cf/15b3a462917337062834c69213bf8ed41144.pdf (Accessed: 19 June 2020).

Henao, A. and Marshall, W.E. (2018) ‘The impact of ride-hailing on vehicle miles traveled’, *Transportation* [Preprint]. Available at: https://doi.org/10.1007/s11116-018-9923-2.

Herrchen, M. (1998) ‘Perspective of the systematic and extended use of temporal and spatial aspects in LCA of long-lived products’, *Chemosphere*, 37(2), pp. 265–270. Available at: https://doi.org/10.1016/S0045-6535(98)00045-9.

Heubl, B. (2020) ‘SUVs at war with EVs: Progress in selling more electric cars is offset by the growth in sales of larger and more polluting sports utility vehicles. SUVs present greater threats to both safety and climate change. E amp;T consulted experts and examined the data about the future of the bulky vehicle class’, *Engineering Technology*, November, pp. 48–51.

Higgins, A. *et al.* (2012) ‘Combining choice modelling and multi-criteria analysis for technology diffusion: An application to the uptake of electric vehicles’, *Technological Forecasting and Social Change*, 79(8), pp. 1399–1412. Available at: https://doi.org/10.1016/j.techfore.2012.04.008.

Hildebrandt, B. *et al.* (2015) ‘The Value of IS in Business Model Innovation for Sustainable Mobility Services - The Case of Carsharing’, *Wirtschaftsinformatik Proceedings 2015* [Preprint]. Available at: https://aisel.aisnet.org/wi2015/68.

Ho, C.Q., Mulley, C. and Hensher, D.A. (2020) ‘Public preferences for mobility as a service: Insights from stated preference surveys’, *Transportation Research Part A: Policy and Practice*, 131, pp. 70–90. Available at: https://doi.org/10.1016/j.tra.2019.09.031.

Hoerler, R. *et al.* (2020) 'Are carsharing users more likely to buy a battery electric, plug-in hybrid electric or hybrid electric vehicle? Powertrain choice and shared mobility in Switzerland', in *2020 Forum on Integrated and Sustainable Transportation Systems (FISTS). 2020 Forum on Integrated and Sustainable Transportation Systems (FISTS)*, pp. 70–76. Available at: https://doi.org/10.1109/FISTS46898.2020.9264903.

Hou, Y. *et al.* (2020) 'Factors Influencing Willingness to Pool in Ride-Hailing Trips':, *Transportation Research Record* [Preprint]. Available at: https://doi.org/10.1177/0361198120915886.

Hu, M. (2018) 'Dynamic life cycle assessment integrating value choice and temporal factors—A case study of an elementary school', *Energy and Buildings*, 158, pp. 1087–1096. Available at: https://doi.org/10.1016/j.enbuild.2017.10.043.

Huang, L. *et al.* (2019) 'Consumer perceived value preferences for mobile marketing in China: A mixed method approach', *Journal of Retailing and Consumer Services*, 48, pp. 70–86. Available at: https://doi.org/10.1016/j.jretconser.2019.02.007.

Hunt, J.D. and McMillan, J.D.P. (1997) 'Stated-Preference Examination of Attitudes Toward Carpooling to Work in Calgary', *Transportation Research Record*, 1598(1), pp. 9–17. Available at: https://doi.org/10.3141/1598-02.

Huynh, T.L.D. *et al.* (2020) 'What makes us use the shared mobility model? Evidence from Vietnam', *Economic Analysis and Policy*, 66, pp. 1–13. Available at: https://doi.org/10.1016/j.eap.2020.02.007.

Ilhamsah, H.A., Prasetyo, T. and Mustajib, M.I. (2017) 'An Integrated Framework of System Dynamics and Life Cycle Assessment for Managing Sustainable Creative Industries', 12(23), p. 6.

International Energy Agency (IEA) (2021a) *Global CO2 emissions in transport by mode in the Sustainable Development Scenario, 2000-2070 – Charts – Data & Statistics*, *IEA*. Available at: https://www.iea.org/data-and-statistics/charts/global-co2-emissions-in-transport-by-mode-in-the-sustainable-development-scenario-2000-2070 (Accessed: 5 January 2022).

International Energy Agency (IEA) (2021b) *Global electric vehicle stock by transport mode, 2010-2020 – Charts – Data & Statistics*, *IEA*. Available at: https://www.iea.org/data-and-statistics/charts/global-electric-vehicle-stock-by-transport-mode-2010-2020 (Accessed: 14 February 2022).

Isee Systems (no date) *Calibration*, *Stella and iThink Version 2.0.3 with Loops that MatterTM*. Available at: https://www.iseesystems.com/resources/help/v2/Content/05%20-Running_Models/OptimizationAndCalibration/Calibration/OverviewCalibration.htm (Accessed: 14 May 2022).

iSeeCars (2022) *How Many Miles Can a Car Last? - iSeeCars.com*. Available at: https://www.iseecars.com/car-lifespan-study (Accessed: 4 February 2023).

ISO (2006) *Environmental management -Life cycle assessment - Principles and framework.* ISO 14040:2006. Zurich: International Organization for Standardization. Available at: http://www.iso.org/cms/render/live/en/sites/isoorg/contents/data/standard/03/74/37456.html (Accessed: 2 May 2019).

Jacobsen, M.R. and van Benthem, A.A. (2015) 'Vehicle Scrappage and Gasoline Policy', *American Economic Review*, 105(3), pp. 1312–1338. Available at: https://doi.org/10.1257/aer.20130935.

Jalali, R. *et al.* (2017) 'Investigating the Potential of Ridesharing to Reduce Vehicle Emissions', *Urban Planning; Lisbon*, 2(2), pp. 26–40. Available at: http://dx.doi.org.virtual.anu.edu.au/10.17645/up.v2i2.937.

Javid, R.J. (2016) 'P16 - Greenhouse Gas and Air Pollution Emission Reduction from Incentivized Carpooling', *Journal of Transport & Health*, 3(2, Supplement), p. S71. Available at: https://doi.org/10.1016/j.jth.2016.05.019.

Jawahir, I.S. *et al.* (2006) 'Total Life-Cycle Considerations in Product Design for Sustainability: A Framework for Comprehensive Evaluation', in *Trends in the Development of Machinery and Associated Technology. 10th International Research/Expert Conference*, Barcelona-Lloret de Mar, Spain.

Jenn, A. (2020) 'Emissions benefits of electric vehicles in Uber and Lyft ride-hailing services', *Nature Energy*, 5(7), pp. 520–525. Available at: https://doi.org/10.1038/s41560-020-0632-7.

Jenn, A., Laberteaux, K. and Clewlow, R. (2018) 'New mobility service users' perceptions on electric vehicle adoption', *International Journal of Sustainable Transportation*, 12(7), pp. 526–540. Available at: https://doi.org/10.1080/15568318.2017.1402973.

Jiang, Y. (2019) *Implications of Changes in Consumer Attitudes and Preferences on Alternative Fuel Vehicle Adoption: A System Dynamics and Choice Modelling*

Approach. Australian National University. Available at: http://hdl.handle.net/1885/163720.

Jin, S.T. *et al.* (2018) ‘Ridesourcing, the sharing economy, and the future of cities’, *Cities*, 76, pp. 96–104. Available at: https://doi.org/10.1016/j.cities.2018.01.012.

Johnson, R.B. and Onwuegbuzie, A.J. (2004) ‘Mixed Methods Research: A Research Paradigm Whose Time Has Come’, *Educational Researcher*, 33(7), pp. 14–26. Available at: https://doi.org/10.3102/0013189X033007014.

Jung, J. and Koo, Y. (2018) ‘Analyzing the Effects of Car Sharing Services on the Reduction of Greenhouse Gas (GHG) Emissions’, *Sustainability; Basel*, 10(2), p. 539. Available at: http://dx.doi.org.virtual.anu.edu.au/10.3390/su10020539.

Kang, S.-C. and Lee, H. (2019) ‘Economic appraisal of implementing electric vehicle taxis in Seoul’, *Research in Transportation Economics*, 73, pp. 45–52. Available at: https://doi.org/10.1016/j.retrec.2018.11.007.

Keith, D.R., Houston, S. and Naumov, S. (2019) ‘Vehicle fleet turnover and the future of fuel economy’, *Environmental Research Letters*, 14(2), p. 021001. Available at: https://doi.org/10.1088/1748-9326/aaf4d2.

Keller, K. *et al.* (2021) ‘Trust is Good, Control is Better - Customer Preferences Regarding Control in Teleoperated and Autonomous Taxis’, in *Proceedings of the 54th Hawaii International Conference on System Sciences*. *54th Hawaii International Conference on System Sciences*, Hawaii, p. 1849. Available at: https://doi.org/10.24251/HICSS.2021.225.

Kim, D., Ko, J. and Park, Y. (2015) ‘Factors affecting electric vehicle sharing program participants’ attitudes about car ownership and program participation’, *Transportation Research Part D: Transport and Environment*, 36, pp. 96–106. Available at: https://doi.org/10.1016/j.trd.2015.02.009.

Kim, H.C. (2003) *Shaping sustainable vehicle fleet conversion policies based on life cycle optimization and risk analysis*. The University of Michigan. Available at: https://css.umich.edu/sites/default/files/css_doc/CSS03-18.pdf.

Kim, H.C. and Wallington, T.J. (2016) ‘Life Cycle Assessment of Vehicle Lightweighting: A Physics-Based Model To Estimate Use-Phase Fuel Consumption of Electrified Vehicles’, *Environmental Science & Technology*, 50(20), pp. 11226–11233. Available at: https://doi.org/10.1021/acs.est.6b02059.

Klein, M., Lüpke, L. and Günther, M. (2020) 'Home charging and electric vehicle diffusion: Agent-based simulation using choice-based conjoint data', *Transportation Research Part D: Transport and Environment*, 88, p. 102475. Available at: https://doi.org/10.1016/j.trd.2020.102475.

Klint, E. and Peters, G. (2021) 'Sharing is caring - the importance of capital goods when assessing environmental impacts from private and shared laundry systems in Sweden', *The International Journal of Life Cycle Assessment*, 26(6), pp. 1085–1099. Available at: https://doi.org/10.1007/s11367-021-01890-5.

Kloepffer, W. (2008) 'Life cycle sustainability assessment of products', *The International Journal of Life Cycle Assessment*, 13(2), p. 89. Available at: https://doi.org/10.1065/lca2008.02.376.

Köhler, J., Turnheim, B. and Hodson, M. (2020) 'Low carbon transitions pathways in mobility: Applying the MLP in a combined case study and simulation bridging analysis of passenger transport in the Netherlands', *Technological Forecasting and Social Change*, 151, p. 119314. Available at: https://doi.org/10.1016/j.techfore.2018.06.003.

Kollmuss, A. and Agyeman, J. (2002) 'Mind the Gap: Why do people act environmentally and what are the barriers to pro-environmental behavior?', *Environmental Education Research*, 8(3), pp. 239–260. Available at: https://doi.org/10.1080/13504620220145401.

Komanduri, A. *et al.* (2018) 'Assessing the Impact of App-Based Ride Share Systems in an Urban Context: Findings from Austin', *Transportation Research Record*, 2672(7), pp. 34–46. Available at: https://doi.org/10.1177/0361198118796025.

König, A., Bonus, T. and Grippenkoven, J. (2018) 'Analyzing Urban Residents' Appraisal of Ridepooling Service Attributes with Conjoint Analysis', *Sustainability*, 10(10), p. 3711. Available at: https://doi.org/10.3390/su10103711.

Krueger, R., Rashidi, T.H. and Dixit, V.V. (2019) 'Autonomous driving and residential location preferences: Evidence from a stated choice survey', *Transportation Research Part C: Emerging Technologies*, 108, pp. 255–268.

Krystofik, M., Babbitt, C.W. and Gaustad, G. (2014) 'When consumer behavior dictates life cycle performance beyond the use phase: case study of inkjet cartridge end-of-life management', *The International Journal of Life Cycle Assessment*, 19(5), pp. 1129–1145. Available at: https://doi.org/10.1007/s11367-014-0713-6.

Kudoh, Y. and Motose, R. (2010) ‘Changes of Japanese Consumer Preference for Electric Vehicles’, *World Electric Vehicle Journal*, 4(4), pp. 880–889. Available at: https://doi.org/10.3390/wevj4040880.

Kumar, R. *et al.* (2020) ‘Addressing the challenges to electric vehicle adoption via sharing economy: an Indian perspective’, *Management of Environmental Quality: An International Journal*, 32(1), pp. 82–99. Available at: https://doi.org/10.1108/MEQ-03-2020-0058.

Kumar, V.V., Hoadley, A. and Shastri, Y. (2019) ‘Dynamic impact assessment of resource depletion: A case study of natural gas in New Zealand’, *Sustainable Production and Consumption*, 18, pp. 165–178. Available at: https://doi.org/10.1016/j.spc.2019.01.002.

Kurani, K.S., Turrentine, T. and Sperling, D. (1994) ‘Demand for electric vehicles in hybrid households: an exploratory analysis’, *Transport Policy*, 1(4), pp. 244–256. Available at: https://doi.org/10.1016/0967-070X(94)90005-1.

Lane, B. and Potter, S. (2007) ‘The adoption of cleaner vehicles in the UK: exploring the consumer attitude–action gap’, *Journal of Cleaner Production*, 15(11), pp. 1085–1092. Available at: https://doi.org/10.1016/j.jclepro.2006.05.026.

Lavieri, P.S. and Bhat, C.R. (2019) ‘Investigating objective and subjective factors influencing the adoption, frequency, and characteristics of ride-hailing trips’, *Transportation Research Part C: Emerging Technologies*, 105, pp. 100–125. Available at: https://doi.org/10.1016/j.trc.2019.05.037.

Lebeau, K. *et al.* (2012) ‘The market potential for plug-in hybrid and battery electric vehicles in Flanders: A choice-based conjoint analysis’, *Transportation Research Part D: Transport and Environment*, 17(8), pp. 592–597. Available at: https://doi.org/10.1016/j.trd.2012.07.004.

Lee, J. *et al.* (2022) ‘The relationship between shared mobility and regulation in South Korea: A system dynamics approach from the socio-technical transitions perspective’, *Technovation*, 109, p. 102327. Available at: https://doi.org/10.1016/j.technovation.2021.102327.

Levasseur, A. *et al.* (2010) ‘Considering Time in LCA: Dynamic LCA and Its Application to Global Warming Impact Assessments’, *Environmental Science & Technology*, 44(8), pp. 3169–3174. Available at: https://doi.org/10.1021/es9030003.

Li, X. and Yu, B. (2019) ‘Peaking CO2 emissions for China’s urban passenger transport sector’, *Energy Policy*, 133, p. 110913. Available at: https://doi.org/10.1016/j.enpol.2019.110913.

Liao, F., Molin, E. and van Wee, B. (2017) ‘Consumer preferences for electric vehicles: a literature review’, *Transport Reviews*, 37(3), pp. 252–275. Available at: https://doi.org/10.1080/01441647.2016.1230794.

Lim, S.A.H., Antony, J. and Albliwi, S. (2014) ‘Statistical Process Control (SPC) in the food industry – A systematic review and future research agenda’, *Trends in Food Science & Technology*, 37(2), pp. 137–151. Available at: https://doi.org/10.1016/j.tifs.2014.03.010.

Lippke, K. and Noyce, C. (2020) *Public Acceptance and Adoption of Shared-Ride Services in the Ride-Hailing Industry*. University of Michigan. Available at: https://deepblue.lib.umich.edu/handle/2027.42/154994 (Accessed: 20 June 2020).

Lokhandwala, M. and Cai, H. (2018) ‘Dynamic ride sharing using traditional taxis and shared autonomous taxis: A case study of NYC’, *Transportation Research Part C: Emerging Technologies*, 97, pp. 45–60. Available at: https://doi.org/10.1016/j.trc.2018.10.007.

Lombardi, L. *et al.* (2017) ‘Comparative environmental assessment of conventional, electric, hybrid, and fuel cell powertrains based on LCA’, *The International Journal of Life Cycle Assessment*, 22(12), pp. 1989–2006. Available at: https://doi.org/10.1007/s11367-017-1294-y.

Loose, W. (2010) ‘The State of European Car-Sharing’. Available at: https://www.motiva.fi/files/4138/WP2_Final_Report.pdf (Accessed: 3 July 2019).

Louviere, J.J., Flynn, T.N. and Carson, R.T. (2010) ‘Discrete Choice Experiments Are Not Conjoint Analysis’, *Journal of Choice Modelling*, 3(3), pp. 57–72. Available at: https://doi.org/10.1016/S1755-5345(13)70014-9.

Lu, M. *et al.* (2018) ‘Multiagent Spatial Simulation of Autonomous Taxis for Urban Commute: Travel Economics and Environmental Impacts’, *Journal of Urban Planning and Development*, 144, p. 04018033. Available at: https://doi.org/10.1061/(ASCE)UP.1943-5444.0000469.

Lu, S. (2006) *Vehicle Survivability and Travel Mileage Schedules*. DOT HS 809 952. Washington DC: National Center for Statistics and Analysis Regulatory Analysis and Evaluation Division National Highway Traffic Safety Administration. Available at:

https://crashstats.nhtsa.dot.gov/Api/Public/ViewPublication/809952 (Accessed: 23 February 2022).

Lueddeckens, S., Saling, P. and Guenther, E. (2020) 'Temporal issues in life cycle assessment—a systematic review', *The International Journal of Life Cycle Assessment*, 25(8), pp. 1385–1401. Available at: https://doi.org/10.1007/s11367-020-01757-1.

Luna, T.F. *et al.* (2020) 'The influence of e-carsharing schemes on electric vehicle adoption and carbon emissions: An emerging economy study', *Transportation Research Part D: Transport and Environment*, 79, p. 102226. Available at: https://doi.org/10.1016/j.trd.2020.102226.

Lyft (2020) *Leading the Transition to Zero Emissions: Our Commitment to 100% Electric Vehicles by 2030*, *Lyft*. Available at: https://www.lyft.com/blog/posts/leading-the-transition-to-zero-emissions (Accessed: 6 January 2021).

Ma, J. *et al.* (2018) 'An exploratory investigation of Additively Manufactured Product life cycle sustainability assessment', *Journal of Cleaner Production*, 192, pp. 55–70. Available at: https://doi.org/10.1016/j.jclepro.2018.04.249.

Ma, S. and Wolfson, O. (2013) 'Analysis and evaluation of the slugging form of ridesharing', in *Proceedings of the 21st ACM SIGSPATIAL International Conference on Advances in Geographic Information Systems*. Orlando, Florida: Association for Computing Machinery (SIGSPATIAL'13), pp. 64–73. Available at: https://doi.org/10.1145/2525314.2525365.

Maciel Fuentes, D.A. and González, E.G. (2021) 'Technoeconomic Analysis and Environmental Impact of Electric Vehicle Introduction in Taxis: A Case Study of Mexico City', *World Electric Vehicle Journal*, 12(3), p. 93. Available at: https://doi.org/10.3390/wevj12030093.

Mahmoodi, J. *et al.* (2021) 'Using rewards and penalties to promote sustainability: Who chooses incentive-based electricity products and why?', *Journal of Consumer Behaviour*, 20(2), pp. 381–398. Available at: https://doi.org/10.1002/cb.1870.

Malodia, S. and Singla, H. (2016) 'A study of carpooling behaviour using a stated preference web survey in selected cities of India', *Transportation Planning and Technology*, 39(5), pp. 538–550. Available at: https://doi.org/10.1080/03081060.2016.1174368.

Martin, E. and Shaheen, S. (2016) 'The Impacts of Car2go on Vehicle Ownership, Modal Shift, Vehicle Miles Traveled, and Greenhouse Gas Emissions: An Analysis of Five

North American Cities', p. 26. Available at: https://tsrc.berkeley.edu/publications/impacts-car2go-vehicle-ownership-modal-shift-vehicle-miles-traveled-and-greenhouse-gas.

Martin, E.W. and Shaheen, S.A. (2011) 'Greenhouse Gas Emission Impacts of Carsharing in North America', *IEEE Transactions on Intelligent Transportation Systems*, 12(4), pp. 1074–1086. Available at: https://doi.org/10.1109/TITS.2011.2158539.

Mathez, A. *et al.* (2013) 'How can we alter our carbon footprint? Estimating GHG emissions based on travel survey information', *Transportation; New York*, 40(1), pp. 131–149. Available at: http://dx.doi.org.virtual.anu.edu.au/10.1007/s11116-012-9415-8.

McAnulty, T., Jeswiet, J. and Doolan, M. (2017) 'Formability in single point incremental forming: A comparative analysis of the state of the art', *CIRP Journal of Manufacturing Science and Technology*, 16, pp. 43–54. Available at: https://doi.org/10.1016/j.cirpj.2016.07.003.

McAvoy, S. *et al.* (2021) 'Combining Life Cycle Assessment and System Dynamics to improve impact assessment: A systematic review', *Journal of Cleaner Production*, 315, p. 128060. Available at: https://doi.org/10.1016/j.jclepro.2021.128060.

Mccarthy, J.F. (2017) 'Sustainability of Self-Driving Mobility: An Analysis of Carbon Emissions Between Autonomous Vehicles and Conventional Modes of Transportation'. Available at: https://dash.harvard.edu/handle/1/33813411 (Accessed: 24 October 2020).

McGuckin, N. and Fucci, A. (2018) *Summary of Travel Trends 2017 National Household Travel Survey*. FHWA-PL-18-019. Washington, DC: Federal Highway Administration, p. 58. Available at: https://doi.org/10.2172/885762.

Meadows, D.H. (2008) *Thinking in Systems*. Vermont: Chelsea Green Publishing.

Metropolitan Transportation Commission (2019a) *'Five Free Rides' Incentive Program Launches on February 1, 2019 | Metropolitan Transportation Commission*. Available at: https://mtc.ca.gov/news/five-free-rides-incentive-program-launches-february-1-2019 (Accessed: 4 February 2023).

Metropolitan Transportation Commission (2019b) *New Bus/Carpool Lane Opens On West Grand Avenue Approach to Bay Bridge | Metropolitan Transportation Commission*. Available at: https://mtc.ca.gov/news/new-buscarpool-lane-opens-west-grand-avenue-approach-bay-bridge (Accessed: 4 February 2023).

Migliore, M., D'Orso, G. and Caminiti, D. (2020) 'The environmental benefits of carsharing: the case study of Palermo.', *Transportation Research Procedia*, 48, pp. 2127–2139. Available at: https://doi.org/10.1016/j.trpro.2020.08.271.

Milovanoff, A. *et al.* (2019) 'A Dynamic Fleet Model of U.S Light-Duty Vehicle Lightweighting and Associated Greenhouse Gas Emissions from 2016 to 2050', *Environmental Science & Technology*, 53(4), pp. 2199–2208. Available at: https://doi.org/10.1021/acs.est.8b04249.

Minett, P. and Pearce, J. (2011) 'Estimating the Energy Consumption Impact of Casual Carpooling', *Energies; Basel*, 4(1), pp. 126–139. Available at: http://dx.doi.org.virtual.anu.edu.au/10.3390/en4010126.

Mitropoulos, L.K. and Prevedouros, P.D. (2014) 'Multicriterion Sustainability Assessment in Transportation: Private Cars, Carsharing, and Transit Buses', *Transportation Research Record*, 2403(1), pp. 52–61. Available at: https://doi.org/10.3141/2403-07.

Möhlmann, M. (2015) 'Collaborative consumption: determinants of satisfaction and the likelihood of using a sharing economy option again', *Journal of Consumer Behaviour*, 14(3), pp. 193–207. Available at: https://doi.org/10.1002/cb.1512.

Moser, A.K. (2015) 'Thinking green, buying green? Drivers of pro-environmental purchasing behavior', *Journal of Consumer Marketing*, 32(3), pp. 167–175. Available at: https://doi.org/10.1108/JCM-10-2014-1179.

Myers, D. and Cairns, S. (2009) *Carplus annual survey of car clubs 2008/09.* PPR399. Berkshire: TRL. Available at: https://trl.co.uk/sites/default/files/PPR399.pdf (Accessed: 21 April 2020).

Namazu, M. and Dowlatabadi, H. (2015) 'Characterizing the GHG emission impacts of carsharing: a case of Vancouver', *Environmental Research Letters*, 10(12), p. 124017. Available at: https://doi.org/10.1088/1748-9326/10/12/124017.

Neate, R. (2021) 'Ford plans for all cars sold in Europe to be electric by 2030', *The Guardian*, 17 February. Available at: https://www.theguardian.com/business/2021/feb/17/ford-plans-for-all-cars-sold-in-europe-to-be-electric-by-2030 (Accessed: 21 February 2022).

Nguyen-Phuoc, D.Q. *et al.* (2020) 'Factors influencing customer's loyalty towards ride-hailing taxi services – A case study of Vietnam', *Transportation Research Part A: Policy and Practice*, 134, pp. 96–112. Available at: https://doi.org/10.1016/j.tra.2020.02.008.

Nguyen-Viet, B. (2022) ‘Understanding the Influence of Eco-label, and Green Advertising on Green Purchase Intention: The Mediating Role of Green Brand Equity’, *Journal of Food Products Marketing*, 28(2), pp. 87–103. Available at: https://doi.org/10.1080/10454446.2022.2043212.

Nijland, H. and van Meerkerk, J. (2017) ‘Mobility and environmental impacts of car sharing in the Netherlands’, *Environmental Innovation and Societal Transitions*, 23, pp. 84–91. Available at: https://doi.org/10.1016/j.eist.2017.02.001.

Nijland, H., van Meerkerk, J. and Hoen, A. (2015) *Impact of car sharing on mobility and CO2 emissions*. 1842. PBL Netherlands Environmental Assessment Agency, p. 12. Available at: https://www.pbl.nl/sites/default/files/cms/publicaties/PBL_2015_Note%20Impact%20of%20car%20sharing_1842.pdf (Accessed: 27 June 2019).

Nilrit, S., Sampanpanish, P. and Bualert, S. (2018) ‘Carbon dioxide and methane emission rates from taxi vehicles in Thailand’, *Carbon Management*, 9(1), pp. 37–43. Available at: https://doi.org/10.1080/17583004.2017.1412232.

Nordelöf, A. *et al.* (2014) ‘Environmental impacts of hybrid, plug-in hybrid, and battery electric vehicles—what can we learn from life cycle assessment?’, *The International Journal of Life Cycle Assessment*, 19(11), pp. 1866–1890. Available at: https://doi.org/10.1007/s11367-014-0788-0.

Novikova, O. (2017) ‘The Sharing Economy and the Future of Personal Mobility: New Models Based on Car Sharing’, *Technology Innovation Management Review*, 7(8), pp. 27–31. Available at: http://search.proquest.com/docview/1963138125/abstract/7871B1D16F99453FPQ/1 (Accessed: 15 January 2021).

Nurhadi, L. *et al.* (2017) ‘Competitiveness and sustainability effects of cars and their business models in Swedish small town regions’, *Journal of Cleaner Production*, 140, pp. 333–348. Available at: https://doi.org/10.1016/j.jclepro.2016.04.045.

Nurul Habib, K.M., Tian, Y. and Zaman, H. (2011) ‘Modelling commuting mode choice with explicit consideration of carpool in the choice set formation’, *Transportation*, 38(4), pp. 587–604. Available at: https://doi.org/10.1007/s11116-011-9333-1.

Office of Energy Efficiency and Renewable Energy (2016) *Fact #946: October 10, 2016 Driving Alone in a Private Vehicle is the Most Common Means of Transportation to Work*, *Energy.gov*. Available at: https://www.energy.gov/eere/vehicles/fact-946-

october-10-2016-driving-alone-private-vehicle-most-common-means (Accessed: 23 September 2021).

Onat, N.C. *et al.* (2016) ‘Combined application of multi-criteria optimization and life-cycle sustainability assessment for optimal distribution of alternative passenger cars in U.S.’, *Journal of Cleaner Production*, 112, pp. 291–307. Available at: https://doi.org/10.1016/j.jclepro.2015.09.021.

Ostrom, A. and Lacobucci, D. (1995) ‘Consumer Trade-Offs and the Evaluation of Services’, *Journal of Marketing*, 59(1), pp. 17–28. Available at: https://doi.org/10.1177/002224299505900102.

Palma, A. de and Rochat, D. (2000) ‘Mode choices for trips to work in Geneva: an empirical analysis’, *Journal of Transport Geography*, 8(1), pp. 43–51. Available at: https://doi.org/10.1016/S0966-6923(99)00026-5.

Pickering, C. and Byrne, J. (2014) ‘The benefits of publishing systematic quantitative literature reviews for PhD candidates and other early-career researchers’, *Higher Education Research & Development*, 33(3), pp. 534–548. Available at: https://doi.org/10.1080/07294360.2013.841651.

Pinsonnault, A. *et al.* (2014) ‘Temporal differentiation of background systems in LCA: relevance of adding temporal information in LCI databases’, *The International Journal of Life Cycle Assessment*, 19(11), pp. 1843–1853. Available at: https://doi.org/10.1007/s11367-014-0783-5.

Pinto, B.-M. and Rossetti, R.J.F. (2020) ‘A Graph-Based Study of the Impact of Carpooling on CO2 Emissions’, in *2020 Forum on Integrated and Sustainable Transportation Systems (FISTS)*. *2020 Forum on Integrated and Sustainable Transportation Systems (FISTS)*, pp. 359–364. Available at: https://doi.org/10.1109/FISTS46898.2020.9264850.

Pinto, J.T.M., Sverdrup, H.U. and Diemer, A. (2019) ‘Integrating life cycle analysis into system dynamics: the case of steel in Europe’, *Environmental Systems Research*, 8(1), p. 15. Available at: https://doi.org/10.1186/s40068-019-0144-2.

Piscicelli, L., Cooper, T. and Fisher, T. (2015) ‘The role of values in collaborative consumption: insights from a product-service system for lending and borrowing in the UK’, *Journal of Cleaner Production*, 97, pp. 21–29. Available at: https://doi.org/10.1016/j.jclepro.2014.07.032.

Polizzi di Sorrentino, E., Woelbert, E. and Sala, S. (2016) ‘Consumers and their behavior: state of the art in behavioral science supporting use phase modeling in LCA and ecodesign’, *The International Journal of Life Cycle Assessment*, 21(2), pp. 237–251. Available at: https://doi.org/10.1007/s11367-015-1016-2.

Prieto, M., Baltas, G. and Stan, V. (2017) ‘Car sharing adoption intention in urban areas: What are the key sociodemographic drivers?’, *Transportation Research Part A: Policy and Practice*, 101, pp. 218–227. Available at: https://doi.org/10.1016/j.tra.2017.05.012.

Qian, F. and Li, T.Z. (2014) ‘Emission Characteristics of CNG/Gasoline Dual-Fuel Taxi’, *Applied Mechanics and Materials; Zurich*, 505–506, pp. 365–369. Available at: https://doi.org/10.4028/www.scientific.net/AMM.505-506.365.

Qian, L., Grisolía, J.M. and Soopramanien, D. (2019) ‘The impact of service and government-policy attributes on consumer preferences for electric vehicles in China’, *Transportation Research Part A: Policy and Practice*, 122, pp. 70–84. Available at: https://doi.org/10.1016/j.tra.2019.02.008.

Qian, L. and Soopramanien, D. (2011) ‘Heterogeneous consumer preferences for alternative fuel cars in China’, *Transportation Research Part D: Transport and Environment*, 16(8), pp. 607–613. Available at: https://doi.org/10.1016/j.trd.2011.08.005.

Qian, L. and Soopramanien, D. (2015) ‘Incorporating heterogeneity to forecast the demand of new products in emerging markets: Green cars in China’, *Technological Forecasting and Social Change*, 91, pp. 33–46. Available at: https://doi.org/10.1016/j.techfore.2014.01.008.

Rabbitt, N. and Ghosh, B. (2013) ‘A study of feasibility and potential benefits of organised car sharing in Ireland’, *Transportation Research Part D: Transport and Environment*, 25, pp. 49–58. Available at: https://doi.org/10.1016/j.trd.2013.07.004.

Rabbitt, N. and Ghosh, B. (2016) ‘Economic and environmental impacts of organised Car Sharing Services: A case study of Ireland’, *Research in Transportation Economics*, 57, pp. 3–12. Available at: https://doi.org/10.1016/j.retrec.2016.10.001.

Rahimi, E. *et al.* (2021) ‘Perceived risk of using shared mobility services during the COVID-19 pandemic’, *Transportation Research Part F: Traffic Psychology and Behaviour*, 81, pp. 271–281. Available at: https://doi.org/10.1016/j.trf.2021.06.012.

Rayle, L. *et al.* (2014) *App-Based, On-Demand Ride Services: Comparing Taxi and Ridesourcing Trips and User Characteristics in San Francisco*. UCTC-FR-2014-08. University of California Transportation Center.

Rayle, L. *et al.* (2016) 'Just a better taxi? A survey-based comparison of taxis, transit, and ridesourcing services in San Francisco', *Transport Policy*, 45, pp. 168–178. Available at: https://doi.org/10.1016/j.tranpol.2015.10.004.

Retamal, M. (2019) 'Collaborative consumption practices in Southeast Asian cities: Prospects for growth and sustainability', *Journal of Cleaner Production*, 222, pp. 143–152. Available at: https://doi.org/10.1016/j.jclepro.2019.02.267.

Rettie, R., Burchell, K. and Barnham, C. (2014) 'Social normalisation: Using marketing to make green normal', *Journal of Consumer Behaviour*, 13(1), pp. 9–17. Available at: https://doi.org/10.1002/cb.1439.

Richardson, G.P. and Pugh III, A.L. (1981) *Introduction to System Dynamics Modeling with DYNAMO*. MIT Press.

Ritter, M. and Schanz, H. (2019) 'The sharing economy: A comprehensive business model framework', *Journal of Cleaner Production*, 213, pp. 320–331. Available at: https://doi.org/10.1016/j.jclepro.2018.12.154.

Rizki, M. *et al.* (2021) 'Electrifying Tourist Mobility in Bali, Indonesia: Setting the Target and Estimating the CO2 Reduction Based on Stated Choice Experiment', *Sustainability*, 13(21), p. 11656. Available at: https://doi.org/10.3390/su132111656.

Ryden, C. and Morin, E. (2005) *Mobility Services for Urban Systems (MOSES) Environment Assessment*. WP 6. Available at: http://www.communauto.com/images/Moses_environnement.pdf.

SAE International (2018) *Taxonomy and Definitions for Terms Related to Shared Mobility and Enabling Technologies*. J3163. SAE International, Shared and Digital Mobility Committee. Available at: https://doi.org/10.4271/J3163_201809.

Sarriera, J.M. *et al.* (2017) 'To Share or Not to Share: Investigating the Social Aspects of Dynamic Ridesharing', *Transportation Research Record*, 2605(1), pp. 109–117. Available at: https://doi.org/10.3141/2605-11.

Say, A.L., Guo, R.-S.A. and Chen, C. (2021) 'Altruism and social utility in consumer sharing behavior', *Journal of Consumer Behaviour*, n/a(n/a). Available at: https://doi.org/10.1002/cb.1967.

Schaller, B. (2018) *The New Automobility: Lyft, Uber and the Future of American Cities*. Brooklyn: SCHALLER CONSULTING. Available at: http://www.schallerconsult.com/rideservices/automobility.pdf (Accessed: 19 June 2020).

Schmidt, M.J. and Gary, M.S. (2002) ‘Combining system dynamics and conjoint analysis for strategic decision making with an automotive high-tech SME’, *System Dynamics Review*, 18(3), pp. 359–379. Available at: https://doi.org/10.1002/sdr.257.

Schneider, T. (2021a) *Taxi and Ridehailing App Usage in Chicago*, *toddwschneider.com*. Available at: https://toddwschneider.com/dashboards/chicago-taxi-ridehailing/ (Accessed: 23 September 2021).

Schneider, T. (2021b) *Taxi and Ridehailing App Usage in New York City*, *toddwschneider.com*. Available at: https://toddwschneider.com/dashboards/nyc-taxi-ridehailing-uber-lyft-data/ (Accessed: 23 September 2021).

Schulte, F. and Voß, S. (2015) ‘Decision Support for Environmental-friendly Vehicle Relocations in Free- Floating Car Sharing Systems: The Case of Car2go’, *Procedia CIRP*, 30, pp. 275–280. Available at: https://doi.org/10.1016/j.procir.2015.02.090.

Seyis, S. (2020) ‘Mixed method review for integrating building information modeling and life-cycle assessments’, *Building and Environment*, 173, p. 106703. Available at: https://doi.org/10.1016/j.buildenv.2020.106703.

Shaheen, S. and Chan, N. (2015) *Mobility and the Sharing Economy: Impacts Synopsis – Spring 2015 | Transportation Sustainability Research Center*. Available at: https://tsrc.berkeley.edu/publications/mobility-and-sharing-economy-impacts-synopsis-%E2%80%93-spring-2015 (Accessed: 28 January 2020).

Shaheen, S. and Chan, N. (2016) ‘Mobility and the Sharing Economy: Potential to Facilitate the First- and Last-Mile Public Transit Connections’, *Built Environment*, 42(4), pp. 573-588(16). Available at: https://doi.org/10.2148/benv.42.4.573.

Shaheen, S. and Cohen, A. (2019) ‘Shared ride services in North America: definitions, impacts, and the future of pooling’, *Transport Reviews*, 39(4), pp. 427–442. Available at: https://doi.org/10.1080/01441647.2018.1497728.

Shaheen, S., Sperling, D. and Wagner, C. (1998) *Carsharing in Europe and North American: Past, Present, and Future*. UCTC No 467. Berkeley: The University of CatiformaTransportation CenterUl~iversiEr of California. Available at: https://escholarship.org/uc/item/4gx4m05b (Accessed: 21 January 2019).

Shaheen, S.A., Chan, N.D. and Gaynor, T. (2016) 'Casual carpooling in the San Francisco Bay Area: Understanding user characteristics, behaviors, and motivations', *Transport Policy*, 51, pp. 165–173. Available at: https://doi.org/10.1016/j.tranpol.2016.01.003.

Shahmohammadi, S. *et al.* (2018) 'Quantifying drivers of variability in life cycle greenhouse gas emissions of consumer products—a case study on laundry washing in Europe', *The International Journal of Life Cycle Assessment*, 23(10), pp. 1940–1949. Available at: https://doi.org/10.1007/s11367-017-1426-4.

Shi, X. *et al.* (2016a) 'Electric vehicle transformation in Beijing and the comparative eco-environmental impacts: A case study of electric and gasoline powered taxis', *Journal of Cleaner Production*, 137, pp. 449–460. Available at: https://doi.org/10.1016/j.jclepro.2016.07.096.

Shi, X. *et al.* (2016b) 'Electric vehicle transformation in Beijing and the comparative eco-environmental impacts: A case study of electric and gasoline powered taxis', *Journal of Cleaner Production*, 137, pp. 449–460. Available at: https://doi.org/10.1016/j.jclepro.2016.07.096.

Shinde, A.M., Dikshit, A.K. and Singh, R.K. (2019) 'Comparison of life cycle environmental performance of public road transport modes in metropolitan regions', *Clean Technologies and Environmental Policy*, 21(3), pp. 605–624. Available at: https://doi.org/10.1007/s10098-018-01661-1.

Shokouhyar, S. *et al.* (2021) 'Shared mobility in post-COVID era: New challenges and opportunities', *Sustainable Cities and Society*, 67, p. 102714. Available at: https://doi.org/10.1016/j.scs.2021.102714.

Si, S. *et al.* (2020) 'Disruptive innovation, business model and sharing economy: the bike-sharing cases in China', *Management Decision*, 59(11), pp. 2674–2692. Available at: https://doi.org/10.1108/MD-06-2019-0818.

Sichtmann, C., Wilken, R. and Diamantopoulos, A. (2011) 'Estimating Willingness-to-pay with Choice-based Conjoint Analysis – Can Consumer Characteristics Explain Variations in Accuracy?', *British Journal of Management*, 22(4), pp. 628–645. Available at: https://doi.org/10.1111/j.1467-8551.2010.00696.x.

Sigüenza, C.P., Cucurachi, S. and Tukker, A. (2021) 'Circular business models of washing machines in the Netherlands: Material and climate change implications toward 2050', *Sustainable Production and Consumption*, 26, pp. 1084–1098. Available at: https://doi.org/10.1016/j.spc.2021.01.011.

Singh, Y.K. and Bajpai, R. (2007) *Research methodology: Techniques and trends*. APH Pub.

Sinha, M. and Tyagi, R.K. (2019) 'Exploratory analysis of vehicular light weighting with the application of carpooling system vs. synthesis and utilisation of E-glass-based composites and its effects over emissions and energy saving in the city of Delhi', *International Journal of Ambient Energy*, 0(0), pp. 1–8. Available at: https://doi.org/10.1080/01430750.2019.1573755.

Sohn, J. *et al.* (2020) 'Defining Temporally Dynamic Life Cycle Assessment: A Review', *Integrated Environmental Assessment and Management*, 16(3), pp. 314–323. Available at: https://doi.org/10.1002/ieam.4235.

Soo, V.K. (2018) *Life Cycle Impact of Different Joining Decisions on Vehicle Recycling*. Available at: https://openresearch-repository.anu.edu.au/handle/1885/143902 (Accessed: 6 December 2019).

Soo, V.K., Compston, P. and Doolan, M. (2015) 'Interaction between New Car Design and Recycling Impact on Life Cycle Assessment', *Procedia CIRP*, 29(Journal Article), pp. 426–431. Available at: https://doi.org/10.1016/j.procir.2015.02.055.

Spurlock, C.A. *et al.* (2019) 'Describing the users: Understanding adoption of and interest in shared, electrified, and automated transportation in the San Francisco Bay Area', *Transportation Research Part D: Transport and Environment*, 71, pp. 283–301. Available at: https://doi.org/10.1016/j.trd.2019.01.014.

Stasinopoulos, P. (2013) *A system dynamics approach to life cycle assessment*. Available at: https://openresearch-repository.anu.edu.au/handle/1885/150676 (Accessed: 30 October 2019).

Stasinopoulos, P., Shiwakoti, N. and Beining, M. (2021) 'Use-stage life cycle greenhouse gas emissions of the transition to an autonomous vehicle fleet: A System Dynamics approach', *Journal of Cleaner Production*, 278, p. 123447. Available at: https://doi.org/10.1016/j.jclepro.2020.123447.

Steininger, K.W. and Bachner, G. (2014) 'Extending car-sharing to serve commuters: An implementation in Austria', *Ecological Economics*, 101, pp. 64–66. Available at: https://doi.org/10.1016/j.ecolecon.2014.03.001.

Sterman, J.D. (2000) *Business dynamics: Systems thinking and modeling for a complex world*. Boston: Irwin/McGraw-Hill.

Su, S. *et al.* (2021) ‘Dynamic Life Cycle Assessment: A Review of Research for Temporal Variations in Life Cycle Assessment Studies’, *Environmental Engineering Science* [Preprint]. Available at: https://doi.org/10.1089/ees.2021.0052.

Sun, S. and Ertz, M. (2021) ‘Environmental impact of mutualized mobility: Evidence from a life cycle perspective’, *Science of The Total Environment*, 772, p. 145014. Available at: https://doi.org/10.1016/j.scitotenv.2021.145014.

Tarne, P., Traverso, M. and Finkbeiner, M. (2017) ‘Review of Life Cycle Sustainability Assessment and Potential for Its Adoption at an Automotive Company’, *Sustainability*, 9(4), p. 670. Available at: https://doi.org/10.3390/su9040670.

Te, Q. and Lianghua, C. (2020) ‘Carsharing: mitigation strategy for transport-related carbon footprint’, *Mitigation and Adaptation Strategies for Global Change*, 25(5), pp. 791–818. Available at: https://doi.org/10.1007/s11027-019-09893-2.

Teixeira, A.C.R. and Sodré, J.R. (2016) ‘Simulation of the impacts on carbon dioxide emissions from replacement of a conventional Brazilian taxi fleet by electric vehicles’, *Energy*, 115, pp. 1617–1622. Available at: https://doi.org/10.1016/j.energy.2016.07.095.

The White House (2021) *Fact sheet: President Biden Announces Steps to Drive American Leadership Forward on Clean Cars and Trucks*, *The White House*. Available at: https://www.whitehouse.gov/briefing-room/statements-releases/2021/08/05/fact-sheet-president-biden-announces-steps-to-drive-american-leadership-forward-on-clean-cars-and-trucks/ (Accessed: 25 August 2021).

Tirachini, A. (2019) ‘Ride-hailing, travel behaviour and sustainable mobility: an international review’, *Transportation* [Preprint]. Available at: https://doi.org/10.1007/s11116-019-10070-2.

Tirachini, A. and Gomez-Lobo, A. (2020) ‘Does ride-hailing increase or decrease vehicle kilometers traveled (VKT)? A simulation approach for Santiago de Chile’, *International Journal of Sustainable Transportation*, 14(3), pp. 187–204. Available at: https://doi.org/10.1080/15568318.2018.1539146.

Tirachini, A. and del Río, M. (2019) ‘Ride-hailing in Santiago de Chile: Users’ characterisation and effects on travel behaviour’, *Transport Policy*, 82, pp. 46–57. Available at: https://doi.org/10.1016/j.tranpol.2019.07.008.

Tischer, M.L. and Dobson, R. (1979) ‘An empirical analysis of behavioral intentions of single-occupant auto drivers to shift to high occupancy vehicles’, *Transportation*

Research Part A: General, 13(3), pp. 143–158. Available at: https://doi.org/10.1016/0191-2607(79)90066-9.

Toossi, M. (2002) ‘A Century of Change: The U.S. Labor Force, 1950-2050’, *Monthly Labor Review*, 125(5), pp. 15–28. Available at: https://heinonline.org/HOL/P?h=hein.journals/month125&i=531 (Accessed: 19 August 2021).

Train, K.E. (2009) *Discrete Choice Methods with Simulation*. Cambridge University Press.

Tran, M. *et al.* (2013) ‘Simulating early adoption of alternative fuel vehicles for sustainability’, *Technological Forecasting and Social Change*, 80(5), pp. 865–875. Available at: https://doi.org/10.1016/j.techfore.2012.09.009.

Trevisan, L. and Bordignon, M. (2020) ‘Screening Life Cycle Assessment to compare CO2 and Greenhouse Gases emissions of air, road, and rail transport: An exploratory study’, *Procedia CIRP*, 90, pp. 303–309. Available at: https://doi.org/10.1016/j.procir.2020.01.100.

Tu, Meiting *et al.* (2019) ‘Improving ridesplitting services using optimization procedures on a shareability network: A case study of Chengdu’, *Technological Forecasting and Social Change*, 149, p. 119733. Available at: https://doi.org/10.1016/j.techfore.2019.119733.

Uber (2020) *Climate Assessment and Performance Report*. Available at: https://d1nyezh1ys8wfo.cloudfront.net/static/PDFs/Uber_ClimateAssessmentandPerformanceReport_10_05_2020.pdf?uclick_id=2426de48-b6f4-4870-ab4b-7a2e12b13a62 (Accessed: 5 January 2021).

Uber (2021a) *Eligible-Vehicles | Drive | Uber New York City*, *Uber*. Available at: https://www.uber.com/us/en/drive/new-york/get-started/eligible-vehicles/ (Accessed: 29 September 2021).

Uber (2021b) *How are fares calculated?*, *Uber*. Available at: https://help.uber.com/riders/article/how-are-fares-calculated/ (Accessed: 12 January 2021).

Uber (2021c) *Uber Services and Types of Rides*, *Uber*. Available at: https://www.uber.com/us/en/ride/ride-options/ (Accessed: 6 January 2021).

Uber (2021d) *Vehicle Requirements | Uber Los Angeles*, *Uber*. Available at: https://www.uber.com/us/en/drive/los-angeles/vehicle-requirements/ (Accessed: 26 August 2021).

Uber (2022) *The History of Uber - Uber's Timeline*, *Uber Newsroom*. Available at: https://www.uber.com/da-DK/newsroom/history/ (Accessed: 29 January 2022).

Udo de Haes, H.A. *et al.* (2004) 'Three Strategies to Overcome the Limitations of Life-Cycle Assessment', *Journal of Industrial Ecology*, 8(3), pp. 19–32. Available at: https://doi.org/10.1162/1088198042442351.

Union of Concerned Scientists (2020a) *Ride-Hailing Climate Risks*. Cambridge MA: Union of Concerned Scientists. Available at: https://www.ucsusa.org/resources/ride-hailing-climate-risks (Accessed: 25 April 2020).

Union of Concerned Scientists (2020b) *Ride-Hailing Climate Risks (Methodology)*. Cambridge MA: Union of Concerned Scientists. Available at: https://www.ucsusa.org/sites/default/files/2020-02/Ride-Hailings-Climate-Risks-Methodology_0.pdf (Accessed: 5 January 2021).

U.S. Bureau of Labor Statistics (2020) *Databases, Tables & Calculators by Subject*. Available at: https://www.bls.gov/data/#employment (Accessed: 12 September 2021).

U.S. Bureau of Labor Statistics (no date) *Table 5. Average paid holidays and days of vacation and sick leave for full-time employees*, *Economic News Release | Table 5. Average paid holidays and days of vacation and sick leave for full-time employees*. Available at: https://www.bls.gov/news.release/ebs.t05.htm (Accessed: 6 March 2022).

US Census Bureau (2013) 'Census Regions and Divisions of the United States'. US Census Bureau. Available at: https://www2.census.gov/geo/pdfs/maps-data/maps/reference/us_regdiv.pdf (Accessed: 24 September 2021).

US Census Bureau (2019a) *American Community Survey and Puerto Rico Community Survey 2019 Subject Definitions*, p. 165. Available at: https://www2.census.gov/programs-surveys/acs/tech_docs/subject_definitions/2019_ACSSubjectDefinitions.pdf.

US Census Bureau (2019b) *Average Travel Time to Work in the United States by Metro Area*, *The United States Census Bureau*. Available at: https://www.census.gov/library/visualizations/interactive/work-travel-time.html (Accessed: 30 September 2021).

US Census Bureau (2020a) *Census - Table Results*, *Commuting Charateristics by Sex S0801*. Available at: https://data.census.gov/cedsci/table?q=s0801&tid=ACSST1Y2019.S0801&hidePreview=false (Accessed: 21 April 2021).

US Census Bureau (2020b) *Educational Attainment in the United States: 2019*, *The United States Census Bureau*. Available at: https://www.census.gov/data/tables/2019/demo/educational-attainment/cps-detailed-tables.html (Accessed: 12 September 2021).

US Census Bureau (2020c) *Historical Households Tables*, *The United States Census Bureau*. Available at: https://www.census.gov/data/tables/time-series/demo/families/households.html (Accessed: 12 September 2021).

US Census Bureau (2020d) *Income and Poverty in the United States: 2019*, *The United States Census Bureau*. Available at: https://www.census.gov/library/publications/2020/demo/p60-270.html (Accessed: 12 September 2021).

US Census Bureau (2021) *Metropolitan and Micropolitan Statistical Areas Totals: 2010-2019*, *The United States Census Bureau*. Available at: https://www.census.gov/data/tables/time-series/demo/popest/2010s-total-metro-and-micro-statistical-areas.html (Accessed: 25 September 2021).

U.S. Department of Transportation (2014) *Corporate Average Fuel Economy (CAFE) Standards | US Department of Transportation*. Available at: https://www.transportation.gov/mission/sustainability/corporate-average-fuel-economy-cafe-standards (Accessed: 5 February 2023).

U.S. Department of Transportation (2018) *Average Age of Automobiles and Trucks in Operation in the United States | Bureau of Transportation Statistics*. Available at: https://www.bts.gov/content/average-age-automobiles-and-trucks-operation-united-states (Accessed: 24 April 2019).

U.S. Energy Information Administration - EIA (2016) *Annual Energy Outlook 2016*, *U.S. Energy Information Administration - EIA - Independent Statistics and Analysis*. Available at: https://www.eia.gov/outlooks/aeo/data/browser/#/?id=8-AEO2016&region=0-0&cases=ref2016&start=2013&end=2040&f=A&linechart=ref2016-d032416a.21-8-AEO2016&map=&ctype=linechart&sourcekey=0 (Accessed: 29 January 2022).

U.S. Energy Information Administration - EIA (2019) *Annual Energy Outlook 2019*, *U.S. Energy Information Administration - EIA - Independent Statistics and Analysis*. Available at: https://www.eia.gov/outlooks/aeo/data/browser/#/?id=17-AEO2019&region=1-

0&cases=ref2019&start=2017&end=2019&f=A&linechart=ref2019-d111618a.33-17-AEO2019.1-0&map=ref2019-d111618a.4-17-AEO2019.1-0&ctype=linechart&sourcekey=0 (Accessed: 29 January 2022).

U.S. Energy Information Administration - EIA (2020) *Annual Energy Outlook 2020 Table 39. Light-Duty Vehicle Stock by Technology Type*. Available at: https://www.eia.gov/outlooks/aeo/data/browser/#/?id=49-AEO2020&cases=ref2020&sourcekey=0 (Accessed: 12 September 2021).

U.S. Energy Information Administration - EIA (2021) *Annual Energy Outlook 2021*, *Independent Statistics & Analysis U.S. Energy Information Administration*. Available at: https://www.eia.gov/outlooks/aeo/data/browser/#/?id=17-AEO2021&cases=ref2021&sourcekey=0 (Accessed: 29 January 2022).

US EPA (2018) *Explore the Automotive Trends Data*. Available at: https://www.epa.gov/automotive-trends/explore-automotive-trends-data (Accessed: 23 August 2021).

US EPA (2020a) *Fast Facts U.S.Transportation Sector | Greenhouse Gas Emissions 1990 – 2018*. EPA-420-F-20-037. Available at: https://nepis.epa.gov/Exe/ZyPDF.cgi?Dockey=P100ZK4P.pdf.

US EPA (2020b) *Sources of Greenhouse Gas Emissions*. Available at: https://www.epa.gov/ghgemissions/sources-greenhouse-gas-emissions (Accessed: 19 June 2022).

US EPA (2021) *The 2020 EPA Automotive Trends Report*. EPA-420-R-21-003. Available at: https://nepis.epa.gov/Exe/ZyPDF.cgi?Dockey=P1010U68.pdf (Accessed: 12 August 2021).

US EPA (2022) *Fast FactsU.S. Transport Sector Greenhouse Gas Emissions 1990-2020*. EPA-420-F-22-018. United States Environmental Protection Agency. Available at: https://nepis.epa.gov/Exe/ZyPDF.cgi?Dockey=P10153PC.pdf (Accessed: 20 April 2023).

Vasconcelos, A.S. *et al.* (2017) 'Environmental and financial impacts of adopting alternative vehicle technologies and relocation strategies in station-based one-way carsharing: An application in the city of Lisbon, Portugal', *Transportation Research Part D: Transport and Environment*, 57, pp. 350–362. Available at: https://doi.org/10.1016/j.trd.2017.08.019.

Vasudevan, V., Agarwala, R. and Dash, S. (2021) 'Is vehicle ownership in urban india influenced by the availability of high quality dedicated public transit systems?', *IATSS Research*, 45(3), pp. 286–292. Available at: https://doi.org/10.1016/j.iatssr.2020.12.005.

Vedrenne, M. *et al.* (2014) 'Life cycle assessment as a policy-support tool: The case of taxis in the city of Madrid', *Energy Policy*, 66(Journal Article), pp. 185–197. Available at: https://doi.org/10.1016/j.enpol.2013.10.073.

Vestergaard, M.V., Minor, J. and Turan, D. (2020) *Ecolabel potentials of Sharing Economy Services in the Nordics*. Nordic Council of Ministers. Available at: https://doi.org/10.6027/NA2020-906.

Vij, A. *et al.* (2020) 'Consumer preferences for on-demand transport in Australia', *Transportation Research Part A: Policy and Practice*, 132, pp. 823–839. Available at: https://doi.org/10.1016/j.tra.2019.12.026.

Wang, H. *et al.* (2018) 'System dynamics model of taxi management in metropolises: Economic and environmental implications for Beijing', *Journal of Environmental Management*, 213, pp. 555–565. Available at: https://doi.org/10.1016/j.jenvman.2018.02.026.

Wang, J., Lai, J.-Y. and Chang, C.-H. (2016) 'Modeling and analysis for mobile application services: The perspective of mobile network operators', *Technological Forecasting and Social Change*, 111, pp. 146–163. Available at: https://doi.org/10.1016/j.techfore.2016.06.020.

Wang, M. *et al.* (2021) *Summary of Expansions and Updates in GREET® 2020*. ANL/ESD-20/9. Oak Ridge, TN 37831-0062: Systems Assessment Center, Energy Systems Division, Argonne National Laboratory. Available at: https://greet.es.anl.gov/publication-greet-2020-summary (Accessed: 16 July 2021).

Wang, N., Tang, L. and Pan, H. (2018) 'Analysis of public acceptance of electric vehicles: An empirical study in Shanghai', *Technological Forecasting and Social Change*, 126, pp. 284–291. Available at: https://doi.org/10.1016/j.techfore.2017.09.011.

Wang, W. *et al.* (2022) 'The impact of COVID-19 on the ride-sharing industry and its recovery: Causal evidence from China', *Transportation Research. Part A, Policy and Practice*, 155, pp. 128–141. Available at: https://doi.org/10.1016/j.tra.2021.10.005.

WardsAuto (2014) *Automakers Focus on Lightweighting to Meet CAFE Standards*, *WardsAuto*. Available at: https://www.wardsauto.com/technology/automakers-focus-lightweighting-meet-cafe-standards (Accessed: 5 February 2023).

Warner, S.L. (1962) 'Stochastic choice of mode in urban travel: A study in binary choice', *METROPOLITAN TRANSPORTATION SERIES* [Preprint]. Available at: https://trid.trb.org/view/242448 (Accessed: 25 January 2021).

Washbrook, K.F. (2002) *The Requirements for the Degree of Master of Natural Resources Management*. Simon Fraser University. Available at: http://citeseerx.ist.psu.edu/viewdoc/download?doi=10.1.1.572.7990&rep=rep1&type=pdf (Accessed: 17 June 2020).

Wasserbaur, R. *et al.* (2020) 'What if everyone becomes a sharer? A quantification of the environmental impact of access-based consumption for household laundry activities', *Resources, Conservation and Recycling*, 158, p. 104780. Available at: https://doi.org/10.1016/j.resconrec.2020.104780.

Wenzel, T. *et al.* (2019) 'Travel and energy implications of ridesourcing service in Austin, Texas', *Transportation Research Part D: Transport and Environment*, 70, pp. 18–34. Available at: https://doi.org/10.1016/j.trd.2019.03.005.

Wilkes, G. *et al.* (2021) 'Determining service provider and transport system related effects of ridesourcing services by simulation within the travel demand model mobiTopp', *European Transport Research Review*, 13(1), p. 34. Available at: https://doi.org/10.1186/s12544-021-00493-3.

Wolf, I. *et al.* (2015) 'Changing minds about electric cars: An empirically grounded agent-based modeling approach', *Technological Forecasting and Social Change*, 94, pp. 269–285. Available at: https://doi.org/10.1016/j.techfore.2014.10.010.

Wu, T. *et al.* (2018) 'Development and application of an energy use and CO2 emissions reduction evaluation model for China's online car hailing services', *Energy*, 154, pp. 298–307.

Yan, X., Levine, J. and Zhao, X. (2019) 'Integrating ridesourcing services with public transit: An evaluation of traveler responses combining revealed and stated preference data', *Transportation Research Part C: Emerging Technologies*, 105, pp. 683–696. Available at: https://doi.org/10.1016/j.trc.2018.07.029.

Yang, Y. *et al.* (2012) 'Recycling of composite materials', *Chemical Engineering and Processing: Process Intensification*, 51, pp. 53–68. Available at: https://doi.org/10.1016/j.cep.2011.09.007.

Yin, B. *et al.* (2018) 'Appraising the environmental benefits of ride-sharing: The Paris region case study', *Journal of Cleaner Production*, 177, pp. 888–898. Available at: https://doi.org/10.1016/j.jclepro.2017.12.186.

Young, W. *et al.* (2010) 'Sustainable consumption: green consumer behaviour when purchasing products', *Sustainable Development*, 18(1), pp. 20–31. Available at: https://doi.org/10.1002/sd.394.

Yu, B. *et al.* (2017a) 'Environmental benefits from ridesharing: A case of Beijing', *Applied Energy*, 191, pp. 141–152. Available at: https://doi.org/10.1016/j.apenergy.2017.01.052.

Yu, B. *et al.* (2017b) 'Environmental benefits from ridesharing: A case of Beijing', *Applied Energy*, 191, pp. 141–152. Available at: https://doi.org/10.1016/j.apenergy.2017.01.052.

Zhang, C. *et al.* (2020) 'A diffusion model for estimating adoption patterns of a one-way carsharing system in its initial years', *Transportation Research Part A: Policy and Practice*, 136, pp. 135–150. Available at: https://doi.org/10.1016/j.tra.2020.03.027.

Zhang, H. *et al.* (2020) 'Mobile phone GPS data in urban ride-sharing: An assessment method for emission reduction potential', *Applied Energy*, 269, p. 115038. Available at: https://doi.org/10.1016/j.apenergy.2020.115038.

Zulhelmi, A.S.M. *et al.* (2018) *Service attributes, customer satisfaction and return usage: a case of Uber Malaysia.*, *undefined*. Available at: /paper/Service-attributes%2C-customer-satisfaction-and-a-of-Zulhelmi-Talib/91b1f0abcbbfb966746e6e7a90bc46b72ad43d09 (Accessed: 20 June 2020).

A Appendix – Systematic Quantitative Literature Review Results

Table A-1 SQLR data fields (SQLR step 6 – Structure database)

Field	Subfields
General	Authors(s), year of publication, type of the publication, name of the journal or conference
Research objectives	Powertrain and fuel-related, environmental impact assessments, user behaviour, travel mode shift, finance or economic evaluation, energy-related, service or operational
MaaS mode	4 MaaS modes, including their subcategories CS: peer-to-peer (P2P), business to business (B2B), Free-floating (FF), Station based (SB), Roundtrip, two nodes (t-n) RS: regular, pooled CP Taxi: regular, shared/pooled
Powertrain systems	ICEV, BEV, HEV
Energy sources	Petrol, diesel, electricity, liquid petrol gas (LPG), compressed natural gas (CNG), biofuel (BF)
Location (region)	North American (NA), South American (SA), Europe (EU), Asia Pacific (APAC), *Global (GL)
Research method	LCA, GHG assessment, CFP, secondary data or emission factors
Scope	Tank-to-Tailpipe (TTW) – only the use phase emissions Well-to-Wheel (WTW) – TTW + energy processing impacts Production – raw material acquisition and manufacturing impacts Full life cycle – WTW+Production+EoL Extended – indirect impacts such as infrastructure, rebound effect Scope not clear
Data sources	Primary: Surveys (including travel diaries), monitoring instruments, vehicle system based, the general public, users, drivers, MaaS providers, manufacturers Secondary: literature, LCA databases, software packages, Local databases
Type of publication*	Peer-reviewed (journals, thesis, book chapters, conference papers, reports) Non-peer-reviewed (conference papers, reports)
Research extent	Up to the LCI phase, extend to the LCIA phase
LCIA elements	LCIA method, midpoint categories, endpoint categories
Functional unit	Distance-based, passenger distance-based, time duration, fleet-based, per individual, other and not clear
Results	Compared to own private car [%], specific results, absolute results
Remarks	Additional notes

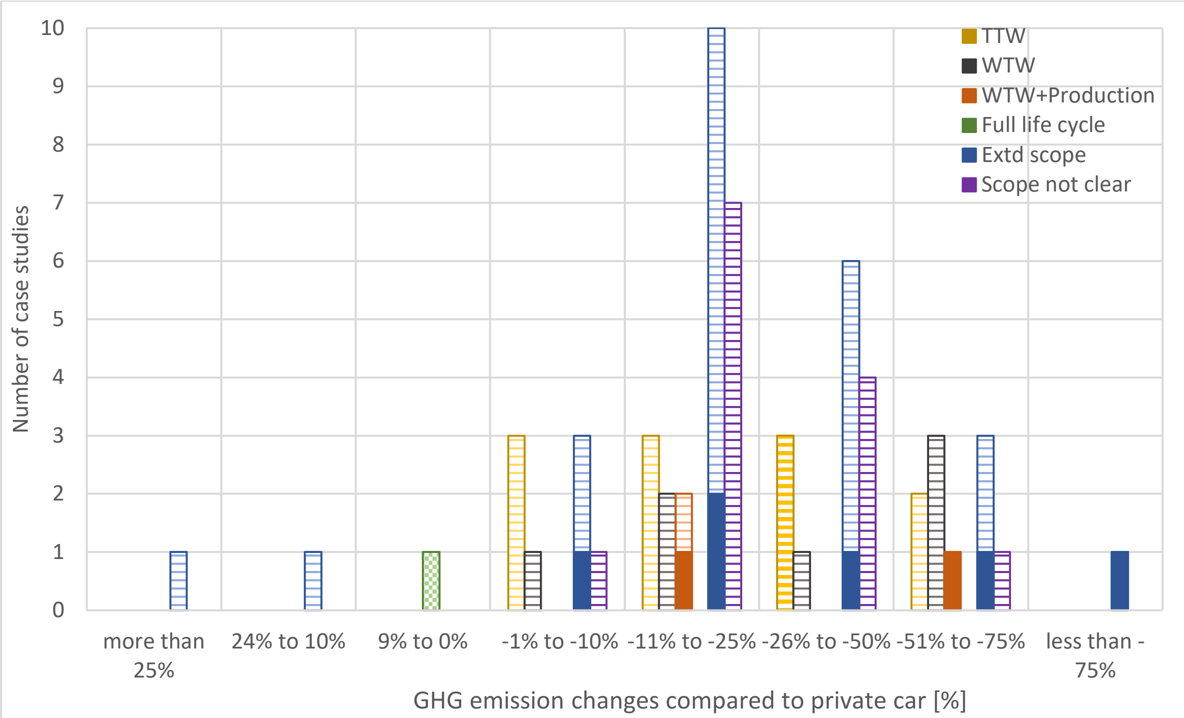

Figure A-1 Case studies of Carsharing: GHG emission changes compared to private car use based on powertrain system

Note: solid fill – BEVs, pattern fill- ICEVs, dotted fill-mix fleet of ICEVs and BEVs. WTW – well-to-wheel, TTW-tank-to-wheel, The complete SQLR can be found in Table A-2 and Table A-3

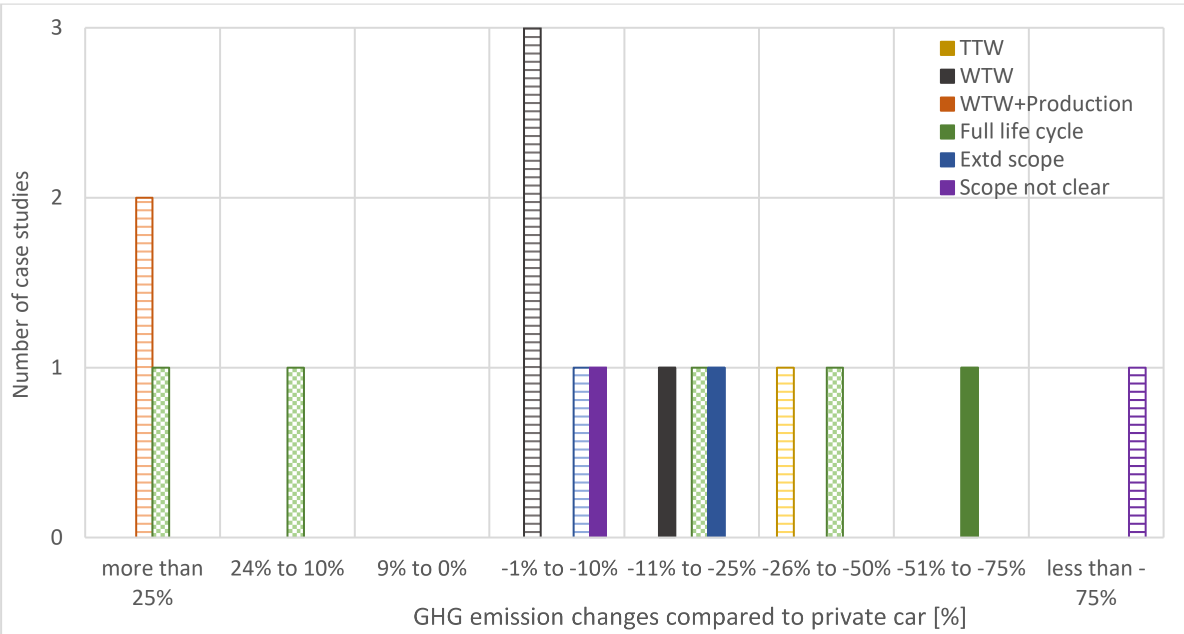

Figure A-2 Case studies of taxi: GHG emission changes compared with private car use based on powertrain system

Note: solid fill – BEVs, pattern fill- ICEVs, dotted fill-mix fleet of ICEVs and BEVs. WTW – well-to-wheel, TTW-tank-to-wheel, The complete SQLR can be found in Table A-7 and Table A-8.

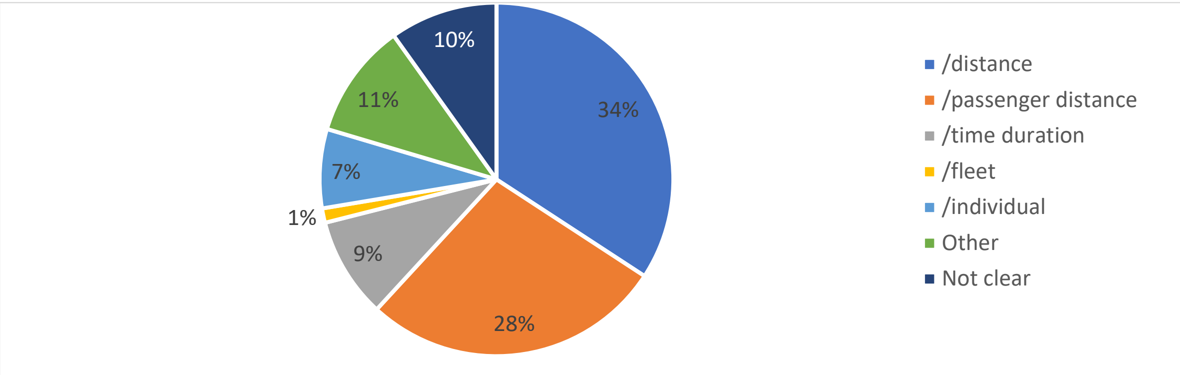

Figure A-3 Summary of interpretation of results: employed functional units.

Table A-2 Shortlisted sources – changes in GHG results Carsharing vs private vehicle

Source	Location (sub-mode)	Scope	Fuel type	GHG reduction compared to PC	Functional unit
(Doka and Ökobilanzen, 2001)*	Swiss	Ex	G,D	-39%	km
(Ryden and Morin, 2005)	Bremen	NC	NC	-39%	NC
	Belgium			-54%	
(Myers and Cairns, 2009)	Britain	NC	NC	-36%	km
(Loose, 2010)	Swiss	NC	NC	-17.5%	km
	German	NC	NC	-16%	
	German	NC	NC	-21.2%	
	Flanders	NC	NC	-21.3% to -24.5%	
	Europe	NC	NC	-7.6%	
	Europe	NC	NC	-15.6%	
	Europe	NC	NC	-16.5%	
	Austria	NC	NC	-20.3%	
	Great Britain			-36%	
(Baptista, Melo and Rolim, 2014)*	Lisbon	U+F	HEV	-35%	year
			El	-65%	
(Namazu and Dowlatabadi, 2015)*	Vancouver	U	G	-54%	year
				-64% to -74%	
(Nijland, van Meerkerk and Hoen, 2015)	Netherlands	Ex	G,D,El	-8* to -13%	user, year
(Shaheen and Chan, 2015)	USA, Canada	NC	NC	-34% to -41%	house, year
(Chen and Kockelman, 2016)*	NC	Ex	NC	Avg. -51% (-33.1% to -67.3%)	equivalent p.km in a private vehicle
(Martin and Shaheen, 2016)	Calgary	U	G	-4%	vehicle (car2go car), year
	San Diego	F	El	-6%	
	Seattle	U	G	-10%	
	Vancouver	U	G	-15%	

Source	Location (sub-mode)	Scope	Fuel type	GHG reduction compared to PC	Functional unit
	Washington DC	U	G	-18%	
(Nijland and van Meerkerk, 2017)*	Germany	U+F	NC	-13% to -18%	user, year
(Guyon, 2017)*	Madrid	U+F +P +E, Battery-P+E	El	-60%	transporting people and goods over 150,000 km for 10 years
			E	-78%	
(Ding *et al.*, 2019)*	China	Ex	G	-4% to -20%	demand for private car
	China (t-n)		G	-38.9%	
	China (FF.)		G	+10%	
	China (SB.)		G	+25%	
	China (t-n)		El	-48%	
	China (FF.)		El	-9%	
(Fromm *et al.*, 2019)	Amsterdam	Ex	NC	-10% to -22%	customer
	Berlin			-18% to -33%	
	Hamburg			-12% to -27%	
	Madrid			-4% to -9%	
	Rome			-7% to -16%	
	Vienna			-10% to -20%	
	Brussel			-16% to -28%	
	Copenhagen			-16% to -43%	
	Helsinki			-17% to -35%	
	Lisbon			-4% to -11%	
	London			-33% to -79%	
(Migliore, D'Orso and Caminiti, 2020)*	Europe	Ex	CNG	-38%	fleet
(Fernando *et al.*, 2020)*	USA	U+F +P	G	-19%	p.km p.km

Notes: (*PR, G-Gasoline, D-diesel, El-electricity, NC – not clear, U-Use phase, P-Production phase, F-energy processing, E-EoL, Ex – extended, Sub-modes: t-n – two-node, FF- free-floating, SB-station based))

Table A-3 Shortlisted sources – Carsharing: GHG results not compared with private vehicles

	Source		Source
1	(Cervero and Tsai, 2004)*	9	(Schulte and Voß, 2015)*
2	(Briceno *et al.*, 2005)*	10	(Rabbitt and Ghosh, 2016)*
3	(Martin and Shaheen, 2011)*	11	(Vasconcelos *et al.*, 2017)*
4	(Firnkorn and Müller, 2011)*	12	(Jung and Koo, 2018)*
5	(Rabbitt and Ghosh, 2013)*	13	(Amatuni *et al.*, 2020)*
6	(Mitropoulos and Prevedouros, 2014)*	14	(Luna *et al.*, 2020)*
7	(Steininger and Bachner, 2014)*	15	(Te and Lianghua, 2020)*
8	(Grischkat *et al.*, 2014)*		

Table A-4 Shortlisted sources – changes in GHG results Ridesourcing vs private vehicle

Source	Location (sub-mode)	Scope	Fuel type	GHG reduction compared to PC.	Functional unit
(Greenblatt and Shaheen, 2015)*	Glo	NC	El	-90%	mile or km
(Carranza *et al.*, 2016)	Los Angelis	U+P	HEV	-92.7%	miles driven
			NC	-88.9%	
(Jenn, 2020)*	California	U	El	-67%	km
	US 7 Metropolitan areas	U+F	G	+47%	trip mile
			El	-53%	
	(pooled-RH)		El	-68%	

Notes: (*PR, G-Gasoline, D-diesel, El-electricity, NC – not clear, U-Use phase, P-Production phase, F-energy processing, E-EoL, Ex – extended)

Table A-5 Shortlisted sources – Carpooling: GHG results not compared with private vehicles

Source	Location	Scope	Fuel type	GHG reduction compared to PC	Functional unit
(Mathez *et al.*, 2013)*	Montreal	NC	NC	-89%, -86%	person trip
(Javid, 2016)*	Multiple	NC	NC	-0.04% to -3.9%	NC
(Nurhadi *et al.*, 2017)*	Karlskrona	U+F+P+E	G	-20%	km/person
		U+F+P+E	BF	-30% to -40%	
		U+F+P+E, Battery: P+E	El	-50% to -70%	
(Mccarthy, 2017)*	Boston	U	G	-50%, -67%, -75%	passenger mile
		F	El	-50%, -67%, -75%	
(Coulombel *et al.*, 2018)*	Paris	NC	G,D	-68% to -77%	NC
(Yin *et al.*, 2018)*	Paris	NC	G,D	-11% to -18%	hour
				-29% to -36%	
(Ding *et al.*, 2019)*	China	U+F	G,D	-2%	demand for private cars
		U+F	El	-21%	
(Sinha and Tyagi, 2019)*	India	U	NC	-48%, -65%, -73%, -78%	Per passenger (NC)
(Fernando, Soo and Doolan, 2020)*	USA	U+F	G	0%	v.km
				-15%	p.km
	EU.			0%	v.km
				-28%	p.km
(Fernando *et al.*, 2020)*	USA	U+F+P	G	-26%	p.km
			El	-27%	p.km

Notes: *PR, G-Gasoline, D-diesel, El-electricity, NC – not clear, U-Use phase, P-Production phase, F-energy processing, E-EoL, Ex – extended

Table A-6 Shortlisted sources – Carpooling: GHG results not compared with private vehicle

	Source		Source
1	(Caulfield, 2009)	4	(Jalali *et al.*, 2017)
2	(Minett and Pearce, 2011)	5	(Guidotti *et al.*, 2017)
3	(Grischkat *et al.*, 2014)	6	(Yu *et al.*, 2017b)

Table A-7 Shortlisted sources – changes in GHG results Taxi compared with private vehicle

Source	Location	Scope	Fuel type	GHG reduction compared to PC	Functional unit
(Mathez *et al.*, 2013)*	Montreal	NC	NC	-89%, -86%	person trip
(Nurhadi *et al.*, 2017)*	Karlskrona	U+F+P+E	G	-20%	km/person
		U+F+P+E	BF	-30% to -40%	
		U+F+P+E, Battery: P+E	El	-50% to -70%	
(Mccarthy, 2017)*	Boston	U	G	-46%	passenger mile
		F	El	-20%	
(Vasconcelos *et al.*, 2017)*	Lisbon	U+F	NC	-6%	km
(Campíñez-Romero *et al.*, 2018)*	Madrid	NC	H2	-3.53%	year
(Lu *et al.*, 2018)*	Ann Arbor, Michigan	Ex	G	-6%	km
		Ex	El	-25%	
(Fernando, Soo and Doolan, 2020)*	USA	U+F	G	-8%	vkm
				+176%	p.km
	EU.			-10%	v.km
				+140%	p.km

Notes: *PR, G-Gasoline, D-diesel, El-electricity, NC – not clear, U-Use phase, P-Production phase, F-energy processing, E-EoL, Ex – extended

Table A-8 Shortlisted sources – Taxi: GHG results not compared with private vehicle

	Source		Source
1	(Baptista *et al.*, 2011)	10	(Lokhandwala and Cai, 2018)
2	(Ma and Wolfson, 2013)	11	(Nilrit, Sampanpanish and Bualert, 2018)
3	(Vedrenne *et al.*, 2014)	12	(Wu *et al.*, 2018)
4	(Qian and Li, 2014)	13	(Shinde, Dikshit and Singh, 2019)
5	(Bauer *et al.*, 2015)	14	(Li and Yu, 2019)
6	(Castel-Branco, Ribau and Silva, 2015)	15	(Gawron *et al.*, 2019)
7	(Shi *et al.*, 2016b)	16	(Girard *et al.*, 2019)
8	(Teixeira and Sodré, 2016)	17	(Kang and Lee, 2019)
9	(Cai *et al.*, 2017)		

B APPENDIX – CONSUMER PREFERENCE SECONDARY DATA

Table B-1 List of user preferences on carpooling attributes

Source	Trip purpose	Attribute														Location
		Comfort / Convenience	Time	Extra distance	Guaranteed ride-home	Software/tool	Routine-journeys	Incentives	Cost	Walking time to pick-up	Interaction comfort,	Safety	Usefulness of service	Sex of the driver	Transport anxiety	
(Ben-Akiva and Atherton, 1977)	W							1								
(Dumas and Dobson, 1979)		1														LA
(Tischer and Dobson, 1979)	W	1	1						1			1				LA - CBD
(Hunt and McMillan, 1997)	W		<u>1</u>	1	1											Calgary
(Palma and Rochat, 2000)	W	1	1						1							Geneva
(Washbrook, 2002)	W		<u>1</u>													Vancouver
(Nurul Habib, Tian and Zaman, 2011)	W					1	<u>1</u>									Edmonton
(Correia, Silva and Viegas, 2013)	W		1		1				<u>1</u>		-					Lisbon
(Malodia and Singla, 2016)	W		<u>1</u>						<u>1</u>	1						India
(Shaheen, Chan and Gaynor, 2016)	G	1	1						1							SF Bay
(Carroll, Caulfield and Ahern, 2017)	W,S		1						1							Dublin
(Carrese *et al.*, 2017)	G										1		1			Lazio
(Amirkiaee and Evangelopoulos, 2018)	G		1						1		1				1	USA
(Bansal *et al.*, 2020)			-											1		USA

Notes: W – to/from work journey, S – education purpose

Table B-2 List of user preferences on solo-ridesourcing attributes

Source	Trip purpose	Attribute																	Location
		Comfort	Time	Software/tool	Routine-journeys	Cost	Safety	Sales promotions	Service quality	Parking	Parking cost	Poor transit	Trip distance	Complaint mgt	Transparency - fees	Driver identification	Ease of payment	Personal space	
(Rayle *et al.*, 2014)	G		1							1						1			USA
(Lavieri and Bhat, 2019)*	G																		Dallas-Fort Worth Metropolitan Area
(Nguyen-Phuoc *et al.*, 2020)				1	-			1	1										Vietnam
(Clewlow and Mishra, 2017)	G									1	1								Boston, Chicago, Los Angeles, New York, San Francisco/ Bay Area, Seattle, and Washington, D.C.
(Alemi *et al.*, 2018)	S		-			-						1	1						California
(Henao, 2017)	S		1			<u>1</u>				1		1							Denver
(Rayle *et al.*, 2016)	S					1				1		1							
(Dhawan and Yadav, 2018)	P	1	-				1							1					Delhi

Source	Trip purpose	Attribute																	Location
		Comfort	Time	Software/tool	Routine-journeys	Cost	Safety	Sales promotions	Service quality	Parking	Parking cost	Poor transit	Trip distance	Complaint mgt	Transparency - fees	Driver identification	Ease of payment	Personal space	
(Schaller, 2018)	S	0				1				1									Boston, Chicago, Denver, Los Angeles, New York, San Francisco, Seattle and Washington DC
(Tirachini and del Río, 2019)		1				1	1												Santiago
(Tirachini and Gomez-Lobo, 2020)	S					1								1	1	1	1		Santiago
(Lippke and Noyce, 2020)		1	1		-	1	1			1	1							1	USA, incl Detroit
(Vij *et al.*, 2020)	G					1													Australia
(Zulhelmi *et al.*, 2018)	G	1			1	1	1												Malaysia
(Chen, 2017)	G		1			1													China

Notes: G-general, P – personal, S – education purpose, * Tech Savvy

Table B-3 List of user preferences on pooled-ridesourcing attributes

Source	Tripe purpose	Attributes					Location
		Comfort / Convenience	Time	Cost	Interaction comfort,	Privacy concerns	
(Sarriera *et al.*, 2017)	G		1	1	1		USA, incl Detroit
(Lavieri and Bhat, 2019)	S					1	Dallas-Fort Worth Metropolitan Area.
(Lippke and Noyce, 2020)	G	1	1	1		1	USA, incl Detroit
(Alonso-González *et al.*, 2020)	G		1	1			Netherlands
(Cui *et al.*, 2020)	G				1		USA, incl Detroit

Notes: G-general, S – education purpose

C APPENDIX – MODELLING SUPPORT DATA

Table C-1 Primary data - Time (door-to-door) and fare distribution summary

Parameter	Levels	Economy	Luxury	XL	Lux Black XL
Fare Distribution [USD]	15	24%	0%	0%	0%
	19	25%	0%	1%	0%
	21	22%	0%	5%	0%
	25	26%	2%	54%	0%
	40	3%	98%	40%	100%
Time distribution (door-to-door) [min]	15	4%	12%	3%	12%
	20	19%	19%	8%	18%
	25	25%	25%	18%	23%
	30	31%	24%	30%	22%
	40	22%	20%	41%	25%

Notes: round-trip to work in the US based on the Google map survey. Cities: Boston, Baltimore, Minneapolis, Los Angelis City, Total sample size = 211, Ridesourcing service provider – Lyft, Lux- luxury, XL – Extra Large body space

Table C-2 Primary data – Location-based summary – Time and Fare distribution

Sample		Sample size	Lyft: Economy			Lyft: Lux			Lyft: XL			Lyft: Lux Black XL		
Trip	Location		Fare [USD]	Waiting time [min]	Journey Time [min]	Fare [USD]	Waiting time [min]	Journey Time [min]	Fare [USD]	Waiting time [min]	Journey Time [min]	Fare [USD]	Waiting time [min]	Journey Time [min]
Morning (8-9 am)	Boston	30	20	13	35	45	11	34	34	14	36	61	12	34
	LA	34	29	10	29	56	7	26	47	12	31	85	7	26
	Baltimore	21	20	10	26	47	11	27	26	20	37	70	12	28
	Minneapolis	20	14	11	24	34	9	22	24	14	27	48	9	22
	Average		21	11	28	45	10	27	33	15	33	66	10	28
Afternoon (5-6pm)	Boston	30	20	14	33	43	11	30	32	13	31	58	13	31
	LA	39	27	8	31	56	6	28	42	16	38	84	7	29
	Baltimore	23	24	22	9	75	58	15	31	29	15	95	89	19
	Minneapolis	20	16	9	24	41	3	17	28	9	24	60	3	17
	Average		22	13	24	54	19	23	34	17	27	74	28	24

Notes: round-trip to work in the US based on the Google map survey. Ridesourcing service provider – Lyft, LA – Los Angelis City

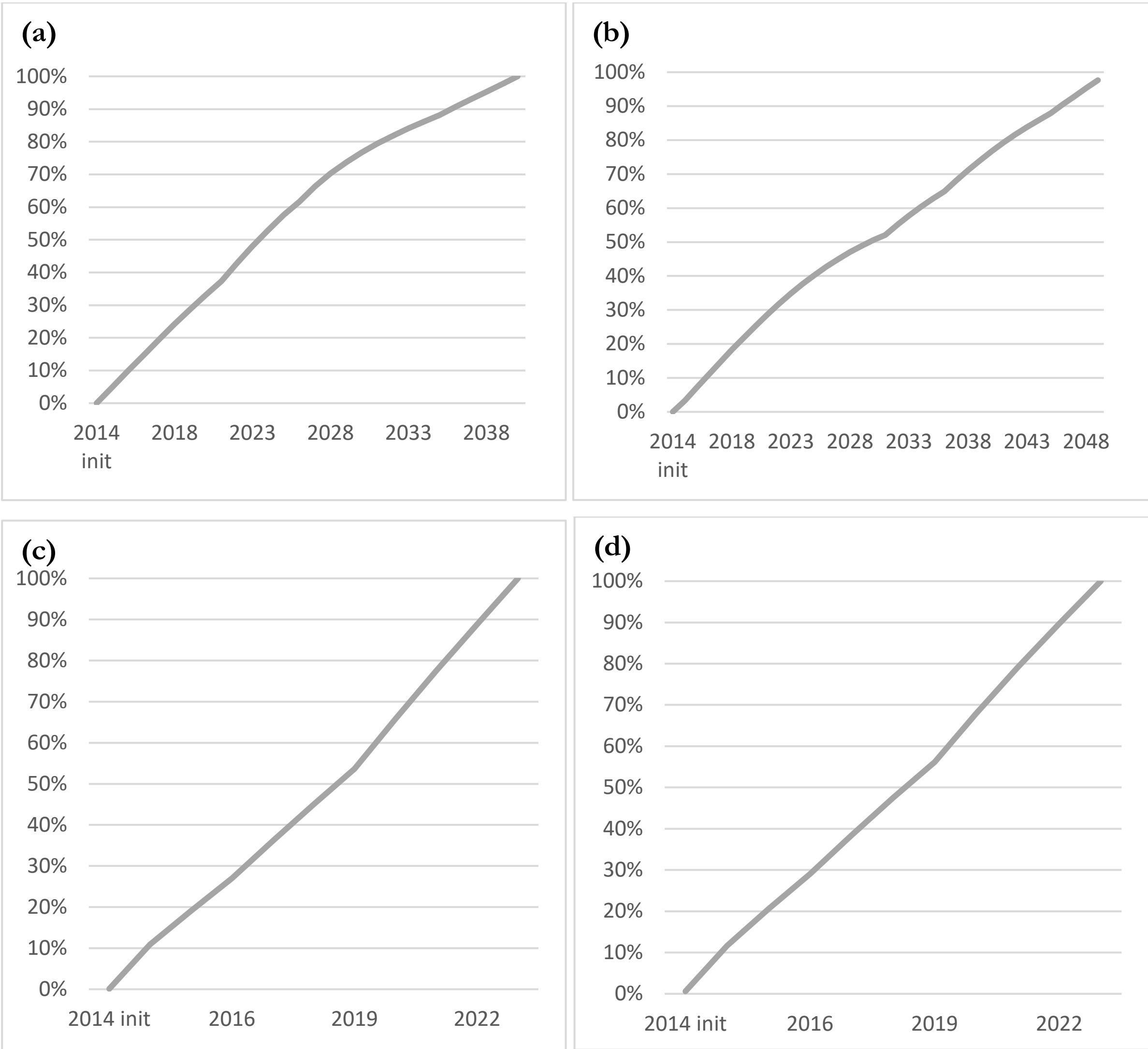

Figure C-1 Calculated cumulative vehicle scrappage rates

Note: (a) Sedan and Hatch - carpooling and private fleets, (b) SUVs - - carpooling and private fleets, (c) Sedan and Hatch – ridesourcing, (d) SUVs – ridesourcing; Assuming the vehicle was purchased in 2014, based on the vehicle survival data (Davis & Boundy (2021, pp. 3–20) and (S. Lu (2006, p. 8); for (c) and (d) - assuming the maximum age of a vehicle in a ridesourcing fleet is 15 years (Uber, 2021d) and no second life

Table C-3 Powertrain type composition data based on the policy scenario specifications

Mode, Body style	2014	2023	2030	2040	2050
CP, Sedan	78.8%	62.8%	50.4%	32.6%	27.7%
CP,SUV	17.0%	33.9%	47.0%	65.7%	71.3%
CP, Hatch	4.1%	3.3%	2.7%	1.7%	1.0%
sRS, Sedan	70.3%	45.9%	26.9%	27.3%	28.0%
sRS,SUV	25.5%	50.8%	70.5%	71.0%	71.0%
sRS, Hatch	4.1%	3.3%	2.7%	1.7%	1.0%
pRS, Sedan	20.0%	20.0%	20.0%	20.0%	20.0%
pRS,SUV	80.0%	80.0%	80.0%	80.0%	80.0%
pRS, Hatch	0.0%	0.0%	0.0%	0.0%	0.0%

Note: Data representing 5 years are presented aligned with the introduced time frames in Section 6.3

Table C-4 Vehicle body style composition data

Mode, Powertrain type	2014	2023	2030	2040	2050
Baseline scenario					
CP, Gasoline	97.7%	89.8%	46.5%	0.0%	0.0%
CP,HEV	2.3%	3.0%	3.5%	0.0%	0.0%
CP, BEV	0.1%	7.2%	50.0%	100.0%	100.0%
sRS, Gasoline	88.3%	77.5%	34.9%	0.0%	0.0%
sRS, BEV	11.6%	12.4%	0.0%	0.0%	0.0%
sRS, BEV	0.1%	10.1%	65.1%	100.0%	100.0%
pRS, Gasoline	97.0%	87.5%	40.0%	0.0%	0.0%
pRS, HEV	3.0%	4.8%	0.0%	0.0%	0.0%
pRS, BEV	0.0%	7.7%	60.0%	100.0%	100.0%
Baseline scenario					
CP, Gasoline	97.7%	72.0%	0.0%	0.0%	0.0%
CP,HEV	2.3%	2.2%	0.0%	0.0%	0.0%
CP, BEV	0.1%	25.8%	100.0%	100.0%	100.0%
sRS, Gasoline	88.3%	63.7%	0.0%	0.0%	0.0%
sRS, BEV	11.6%	10.6%	0.0%	0.0%	0.0%
sRS, BEV	0.1%	25.7%	100.0%	100.0%	100.0%
pRS, Gasoline	97.0%	70.6%	0.0%	0.0%	0.0%
pRS, HEV	3.0%	4.2%	0.0%	0.0%	0.0%
pRS, BEV	0.0%	25.2%	100.0%	100.0%	100.0%

Note: Data representing 5 years are presented aligned with the introduced time frames in Section 6.3

Table C-5 DPI profile - Production phase

Mode, Powertrain type, Body style	GHG emission per vehicle [gCO_2 eq/vehicle]			
	2014-2019	2020	2039	2040-2050
Baseline scenario				
CP,Sedan, Gasoline	5,185	5,253	6,553	6,553
CP,Sedan, Hybrid	5,400	5,471	6,821	6,821
CP,Sedan, BEV	10,480	10,482	10,524	10,524
CP,SUV, Gasoline	6,486	6,568	8,118	8,118
CP,SUV, Hybrid	6,791	6,873	8,442	8,442
CP,SUV, BEV	13,379	13,378	13,341	13,341
CP,Hatch, Gasoline	4,667	4,728	5,897	5,897
CP,Hatch, Hybrid	4,860	4,924	6,139	6,139
CP,Hatch, BEV	9,432	9,434	9,471	9,471
sRS,Sedan, Gasoline	5,185	5,253	6,553	6,553
sRS,Sedan, Hybrid	5,400	5,471	6,821	6,821
sRS,Sedan, BEV	10,480	10,482	10,524	10,524
sRS,SUV, Gasoline	6,486	6,568	8,118	8,118
sRS,SUV, Hybrid	6,791	6,873	8,442	8,442
sRS,SUV, BEV	13,379	13,378	13,341	13,341
sRS,Hatch, Gasoline	4,667	4,728	5,897	5,897
sRS,Hatch, Hybrid	4,860	4,924	6,139	6,139
sRS,Hatch, BEV	9,432	9,434	9,471	9,471
pRS,Sedan, Gasoline	5,704	5,779	7,208	7,208
pRS,Sedan, Hybrid	5,940	6,018	7,503	7,503
pRS,Sedan, BEV	11,527	11,530	11,576	11,576
pRS,SUV, Gasoline	7,135	7,225	8,930	8,930
pRS,SUV, Hybrid	7,470	7,560	9,286	9,286
pRS,SUV, BEV	14,717	14,715	14,675	14,675
pRS,Hatch, Gasoline	4,667	4,728	5,897	5,897
pRS,Hatch, Hybrid	4,860	4,924	6,139	6,139
pRS,Hatch, BEV	9,432	9,434	9,471	9,471
High BEV Adoption Scenario				
CP,Sedan, Gasoline	5,185	5,253	6,553	6,553
CP,Sedan, Hybrid	5,400	5,471	6,821	6,821
CP,Sedan, BEV	10,480	10,482	10,524	10,524
CP,SUV, Gasoline	6,486	6,568	8,118	8,118
CP,SUV, Hybrid	6,791	6,873	8,442	8,442
CP,SUV, BEV	13,379	13,378	13,341	13,341
CP,Hatch, Gasoline	4,667	4,728	5,897	5,897
CP,Hatch, Hybrid	4,860	4,924	6,139	6,139
CP,Hatch, BEV	9,432	9,434	9,471	9,471
sRS,Sedan, Gasoline	5,185	5,253	6,553	6,553
sRS,Sedan, Hybrid	5,400	5,471	6,821	6,821

Mode, Powertrain type, Body style	GHG emission per vehicle [gCO_2 eq/vehicle]			
	2014-2019	2020	2039	2040-2050
sRS,Sedan, BEV	10,480	10,482	10,524	10,524
sRS,SUV, Gasoline	6,486	6,568	8,118	8,118
sRS,SUV, Hybrid	6,791	6,873	8,442	8,442
sRS,SUV, BEV	13,379	13,378	13,341	13,341
sRS,Hatch, Gasoline	4,667	4,728	5,897	5,897
sRS,Hatch, Hybrid	4,860	4,924	6,139	6,139
sRS,Hatch, BEV	9,432	9,434	9,471	9,471
pRS,Sedan, Gasoline	5,704	5,779	7,208	7,208
pRS,Sedan, Hybrid	5,940	6,018	7,503	7,503
pRS,Sedan, BEV	11,527	11,530	11,576	11,576
pRS,SUV, Gasoline	7,135	7,225	8,930	8,930
pRS,SUV, Hybrid	7,470	7,560	9,286	9,286
pRS,SUV, BEV	14,717	14,715	14,675	14,675
pRS,Hatch, Gasoline	4,667	4,728	5,897	5,897
pRS,Hatch, Hybrid	4,860	4,924	6,139	6,139
pRS,Hatch, BEV	9,432	9,434	9,471	9,471

Note: Production phase DPI values represent the sum of raw material GHG emissions, manufacturing energy-related GHG emissions, and battery production-related GHG emissions, 2020 to 2039, a linear weight reduction is applied to achieve the GREET model lightweighting factors (Wang *et al.*, 2021).

Table C-6 DPI profile – Use phase

Mode, Powertrain type, Body style	GHG emission per vehicle [gCO_2 eq/km]			
	2014-2019	2020	2039	2040-2050
Baseline scenario				
CP,Sedan, Gasoline	0.256	0.255	0.228	0.228
CP,Sedan, Hybrid	0.187	0.186	0.165	0.165
CP,Sedan, BEV	0.116	0.083	0.054	0.054
CP,SUV, Gasoline	0.257	0.256	0.231	0.231
CP,SUV, Hybrid	0.188	0.187	0.167	0.167
CP,SUV, BEV	0.116	0.084	0.055	0.055
CP,Hatch, Gasoline	0.231	0.229	0.205	0.205
CP,Hatch, Hybrid	0.168	0.167	0.148	0.148
CP,Hatch, BEV	0.105	0.075	0.049	0.049
sRS,Sedan, Gasoline	0.256	0.255	0.228	0.228
sRS,Sedan, Hybrid	0.187	0.186	0.165	0.165
sRS,Sedan, BEV	0.116	0.083	0.054	0.054
sRS,SUV, Gasoline	0.257	0.256	0.231	0.231
sRS,SUV, Hybrid	0.188	0.187	0.167	0.167
sRS,SUV, BEV	0.116	0.084	0.055	0.055
sRS,Hatch, Gasoline	0.231	0.229	0.205	0.205
sRS,Hatch, Hybrid	0.168	0.167	0.148	0.148

Mode, Powertrain type, Body style	GHG emission per vehicle [gCO_2 eq/km]			
	2014-2019	2020	2039	2040-2050
pRS,Hatch, BEV	0.105	0.075	0.049	0.049
pRS,Sedan, Gasoline	0.319	0.319	0.279	0.279
pRS,Sedan, Hybrid	0.159	0.159	0.138	0.138
pRS,Sedan, BEV	0.091	0.091	0.082	0.082
pRS,SUV, Gasoline	0.413	0.413	0.361	0.361
pRS,SUV, Hybrid	0.195	0.195	0.168	0.168
pRS,SUV, BEV	0.091	0.091	0.082	0.082
pRS,Hatch, Gasoline	0.231	0.229	0.205	0.205
pRS,Hatch, Hybrid	0.168	0.167	0.148	0.148
pRS,Hatch, BEV	0.105	0.075	0.049	0.049
High BEV Adoption Scenario				
CP,Sedan, Gasoline	0.256	0.256	0.228	0.228
CP,Sedan, Hybrid	0.187	0.187	0.165	0.165
CP,Sedan, BEV	0.116	0.095	0.054	0.054
CP,SUV, Gasoline	0.257	0.257	0.231	0.231
CP,SUV, Hybrid	0.188	0.188	0.167	0.167
CP,SUV, BEV	0.116	0.095	0.055	0.055
CP,Hatch, Gasoline	0.231	0.231	0.205	0.205
CP,Hatch, Hybrid	0.168	0.168	0.148	0.148
CP,Hatch, BEV	0.105	0.086	0.049	0.049
sRS,Sedan, Gasoline	0.256	0.256	0.228	0.228
sRS,Sedan, Hybrid	0.187	0.187	0.165	0.165
sRS,Sedan, BEV	0.116	0.095	0.054	0.054
sRS,SUV, Gasoline	0.257	0.257	0.231	0.231
sRS,SUV, Hybrid	0.188	0.188	0.167	0.167
sRS,SUV, BEV	0.116	0.095	0.055	0.055
sRS,Hatch, Gasoline	0.231	0.231	0.205	0.205
sRS,Hatch, Hybrid	0.168	0.168	0.148	0.148
pRS,Hatch, BEV	0.105	0.086	0.049	0.049
pRS,Sedan, Gasoline	0.319	0.319	0.279	0.279
pRS,Sedan, Hybrid	0.159	0.159	0.138	0.138
pRS,Sedan, BEV	0.091	0.091	0.082	0.082
pRS,SUV, Gasoline	0.413	0.413	0.361	0.361
pRS,SUV, Hybrid	0.195	0.195	0.168	0.168
pRS,SUV, BEV	0.091	0.091	0.082	0.082
pRS,Hatch, Gasoline	0.231	0.231	0.205	0.205
pRS,Hatch, Hybrid	0.168	0.168	0.148	0.148
pRS,Hatch, BEV	0.105	0.086	0.049	0.049

Note: use phase DPI values represent the sum of combustion GHG emissions, refinery/electric grid related GHG emissions, and maintenance-related GHG emissions, 2020 to 2039, a linear weight reduction applied to achieve the GREET lightweighting factors (Wang *et al.*, 2021).

Table C-7 DPI – EoL profile

Mode, Powertrain type, Body style	GHG emission per vehicle [gCO_2 eq/vehicle]			
	2014-2019	2020	2039	2040-2050
Baseline scenario				
CP,Sedan, Gasoline	228	227	203	203
CP,Sedan, Hybrid	301	300	280	280
CP,Sedan, BEV	1,051	1,041	841	841
CP,SUV, Gasoline	287	286	269	269
CP,SUV, Hybrid	392	390	359	359
CP,SUV, BEV	1,351	1,338	1,088	1,088
CP,Hatch, Gasoline	205	204	183	183
CP,Hatch, Hybrid	271	270	252	252
CP,Hatch, BEV	946	942	781	781
sRS,Sedan, Gasoline	228	227	203	203
sRS,Sedan, Hybrid	301	300	280	280
sRS,Sedan, BEV	1,051	1,041	841	841
sRS,SUV, Gasoline	287	286	269	269
sRS,SUV, Hybrid	392	390	359	359
sRS,SUV, BEV	1,351	1,338	1,088	1,088
sRS,Hatch, Gasoline	205	204	183	183
sRS,Hatch, Hybrid	271	270	252	252
pRS,Hatch, BEV	946	942	781	781
pRS,Sedan, Gasoline	251	249	203	203
pRS,Sedan, Hybrid	331	329	280	280
pRS,Sedan, BEV	1,156	1,145	841	841
pRS,SUV, Gasoline	316	315	269	269
pRS,SUV, Hybrid	431	429	359	359
pRS,SUV, BEV	1,486	1,472	1,088	1,088
pRS,Hatch, Gasoline	225	224	183	183
pRS,Hatch, Hybrid	298	297	252	252
pRS,Hatch, BEV	1,041	1,037	781	781
High BEV Adoption Scenario				
CP,Sedan, Gasoline	228	227	203	203
CP,Sedan, Hybrid	301	300	280	280
CP,Sedan, BEV	1,051	1,041	841	841
CP,SUV, Gasoline	287	286	269	269
CP,SUV, Hybrid	392	390	359	359
CP,SUV, BEV	1,351	1,338	1,088	1,088
CP,Hatch, Gasoline	205	204	183	183
CP,Hatch, Hybrid	271	270	252	252
CP,Hatch, BEV	946	942	781	781
sRS,Sedan, Gasoline	228	227	203	203
sRS,Sedan, Hybrid	301	300	280	280

Mode, Powertrain type, Body style	GHG emission per vehicle [gCO_2 eq/vehicle]			
	2014-2019	2020	2039	2040-2050
sRS,Sedan, BEV	1,051	1,041	841	841
sRS,SUV, Gasoline	287	286	269	269
sRS,SUV, Hybrid	392	390	359	359
sRS,SUV, BEV	1,351	1,338	1,088	1,088
sRS,Hatch, Gasoline	205	204	183	183
sRS,Hatch, Hybrid	271	270	252	252
pRS,Hatch, BEV	946	942	781	781
pRS,Sedan, Gasoline	251	249	224	224
pRS,Sedan, Hybrid	331	329	308	308
pRS,Sedan, BEV	1,156	1,145	925	925
pRS,SUV, Gasoline	316	315	296	296
pRS,SUV, Hybrid	431	429	394	394
pRS,SUV, BEV	1,486	1,472	1,196	1,196
pRS,Hatch, Gasoline	225	224	201	201
pRS,Hatch, Hybrid	298	297	277	277
pRS,Hatch, BEV	1,041	1,037	859	859

Note: EoL phase DPI values represent the sum of treatment energy-related GHG emissions and battery recycling-related GHG emissions, 2020 to 2039, a linear weight reduction applied to achieve the GREET model lightweighting factors (Wang *et al.*, 2021).

Table C-8 Work trip GHG allocation factors

Mobility mode	Work trip allocation [%]
Private vehicles[1]	29%
Carpooling[2]	31%
Solo-ridesourcing[2]	41%
Pooled-ridesourcing[3]	44%

Note: [1]calculated based on the average annual vehicle miles for different trip purposes data from the National Household Transport Survey, 2017 (McGuckin and Fucci, 2018, p. 19), [2]factoriesed based on the deadheading factors (see Table 7-2) and private vehicle weights

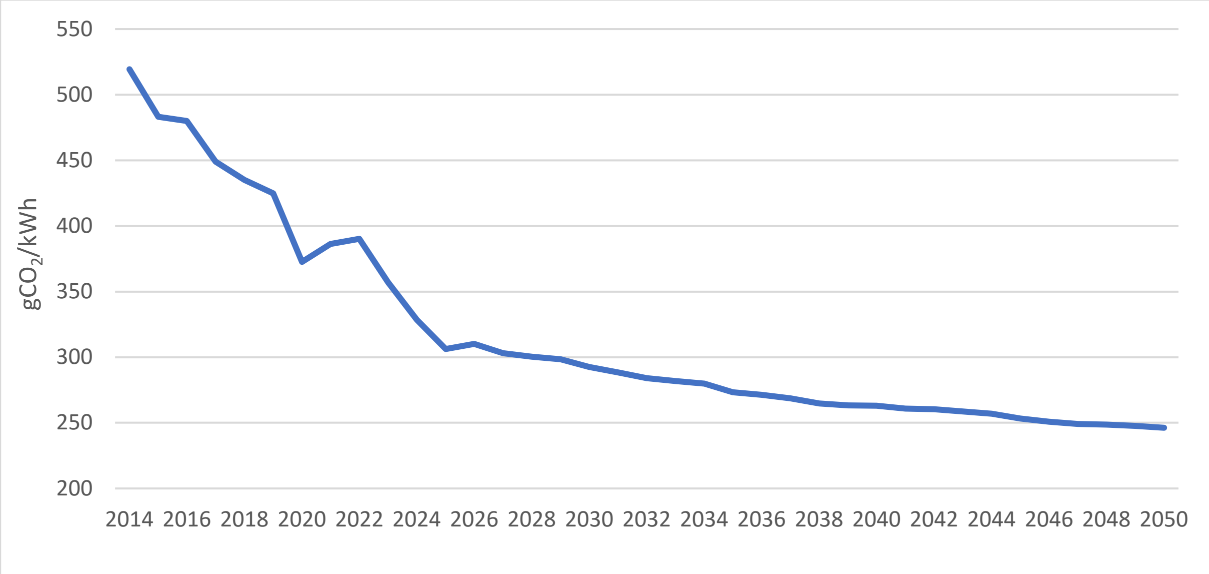

Figure C-2 US electric grid GHG factor

Note: Calculated based on U.S. Energy Information Administration - EIA (2016, 2019, 2021)

D APPENDIX – SURVEY QUESTIONNAIRE

Table D-1 Survey questionnaire

#	Question/Item	Response formats
Part 1		
1	A detailed introduction and Age consent (Ethics requirement)	o I am below 18years and agree to participate the survey o I am below 18years and agree to participate the survey o I am older than 18 years and agree to participate in this survey o I am older than 18 years and agree to participate in this survey o I DO NOT agree to participate this survey (Screen out) o I DO NOT agree to participate this survey
2	What was your city in pre-COVID-19 time?	o Arlington, VA o Atlanta, GA o Baltimore, MD o Bellevue, WA o Boston, MA o Bridgeport, CT o Buffalo, NY o Cambridge, MA o Chicago, IL o Cleveland, OH o Jersey City, NJ o Los Angeles, CA o Miami, FL o Minneapolis, MN o New Haven, CT o New Orleans, LA o New York, NY o Philadelphia, PA o Pittsburgh, PA o Portland, OR o San Francisco, CA o Urban Honolulu, HI o Washington, DC o Other: Other o Non-of the above
3	How frequently you travelled to work?	o Less than or once a month o Once a week o 2-3 times per week o Daily o I did not travel to/from work

#	Question/Item	Response formats
Part 2 – Choice-based conjoint analysis choice set (DCE model)		
Part 3 - to understand your mobility practices prior to the start of the COVID pandemic		
4	What was the most frequently used mobility mode for round-trip to work prior to the start of the COVID-19 pandemic? (if a multi-mode round-trip, select the most commonly used mode)	o Walk or Bicycle o Public transit o Own private car o Carpooling (Rideshare), Ride-hailing or pooled-Ride-hailing o Taxi o Motorbike o Other: Other
5	How did you hear about carpooling/rideshare prior to the start of the COVID-19 pandemic? carpooling - Formal or informal shared rides between drivers and passengers with similar origin-destination pairings (example: GoCarma, ridesharing.com) (if you heard through multiple sources, select the most influenced source)	o I had not heard of it before o WoM (known or credible user feedback) o Through marketing (social media, newspaper, internet-based advertisements, TV, radio, telemarketing o etc) o Other: Other
6	Did you use carpooling/rideshare for your round-trip to work prior to the start of the COVID-19 pandemic?	o Yes o No
7	How did you hear about ride-hailing prior to the start of the COVID-19 pandemic? ride-hailing - prearranged and on-demand transportation services for compensation in which drivers and passengers connect via digital applications (example: Uber, Lyft) (if you heard through multiple sources, select the most influenced source)	o Had not heard of it before o WoM (known or credible user feedback) o Through marketing (social media, newspaper, internet-based advertisements, TV, radio, telemarketing, etc) o Other: Other
8	Did you use ride-hailing for your round-trip to work prior to the start of the COVID-19 pandemic?	o Yes o No
9	How did you hear about pooled-ride-hailing prior to the start of the COVID-19 pandemic? pooled-ride-hailing - a trip is shared with one or more strangers (aside from the driver) and generally require multiple pick-up and drop-off points (example: UberPool, LyftShare) (if you heard through multiple sources, select the most influenced source)	o Had not heard of it before o WoM (known or credible user feedback) o Through marketing (social media, newspaper, internet-based advertisements, TV, radio, telemarketing o etc) o Other: Other

#	Question/Item	Response formats
10	Did you use pooled-ride-hailing for your round-trip to work prior to the start of the COVID-19 pandemic?	o Yes o No
11	Did you forgo or gave up owning a car by using Carpooling / Ride-hailing / pooled-Ride-hailing for round-trip to work prior to the start of the COVID-19 pandemic?	o Yes o No o I had given up/forgo, BUT I repurchased again
12	What mode had you used for round-trip to work before shifting to Carpooling / Ride-hailing / pooled-Ride-hailing?	o Walk o Public transit o Own private car o Carpooling was my first mobility mode for round-trip to work
13	How many miles per day you travelled round-trip to work (both directions) before the start of the COVID-19 pandemic? (type only the numbers	Numerical input
Part 4 – Demographic information		
14	Sex	o Male o Female o Other
15	Age [years]	o Below 18 o 18-24 o 25-34 o 35-54 o 55-64 o 65-75 o 76 above
16	Highest level of educational attainment	o Primary and Elementary (Grades 1 to 11) o High School graduate o Some college no degree o Associate degree (occupational or academic) o Bachelor's degree o Postgraduate (Masters, Professional, Doctoral, and above)
17	Household car/passenger vehicle ownership [number of cars per household] before the start of the COVID-19 pandemic	o Not owned a car o 1 car o 2 cars o 3 or more cars
18	Household car/passenger vehicle type (by fuel) you owned prior to the start of the COVID-19 pandemic?	o Gasoline o Hybrid o Electric Vehicle o Other

#	Question/Item	Response formats
19	Household gross income level [USD/annum] prior to the start of the COVID-19 pandemic	o Less than $10,000 o $10,000 to $14,999 o $15,000 to $24,999 o $25,000 to $34,999 o $35,000 to $49,999 o $50,000 to $64,999 o $65,000 to $74,999 o $75,000 or more
20	What is the size of your household?	o 1 o 2 o 3 o 4 or more
21	Would you like to share any additional comments?	Short answer

Notes: the choice-base conjoint analysis and screened-out messages appearing as questions were excluded

E Appendix – Modelling Outcomes (Extras)

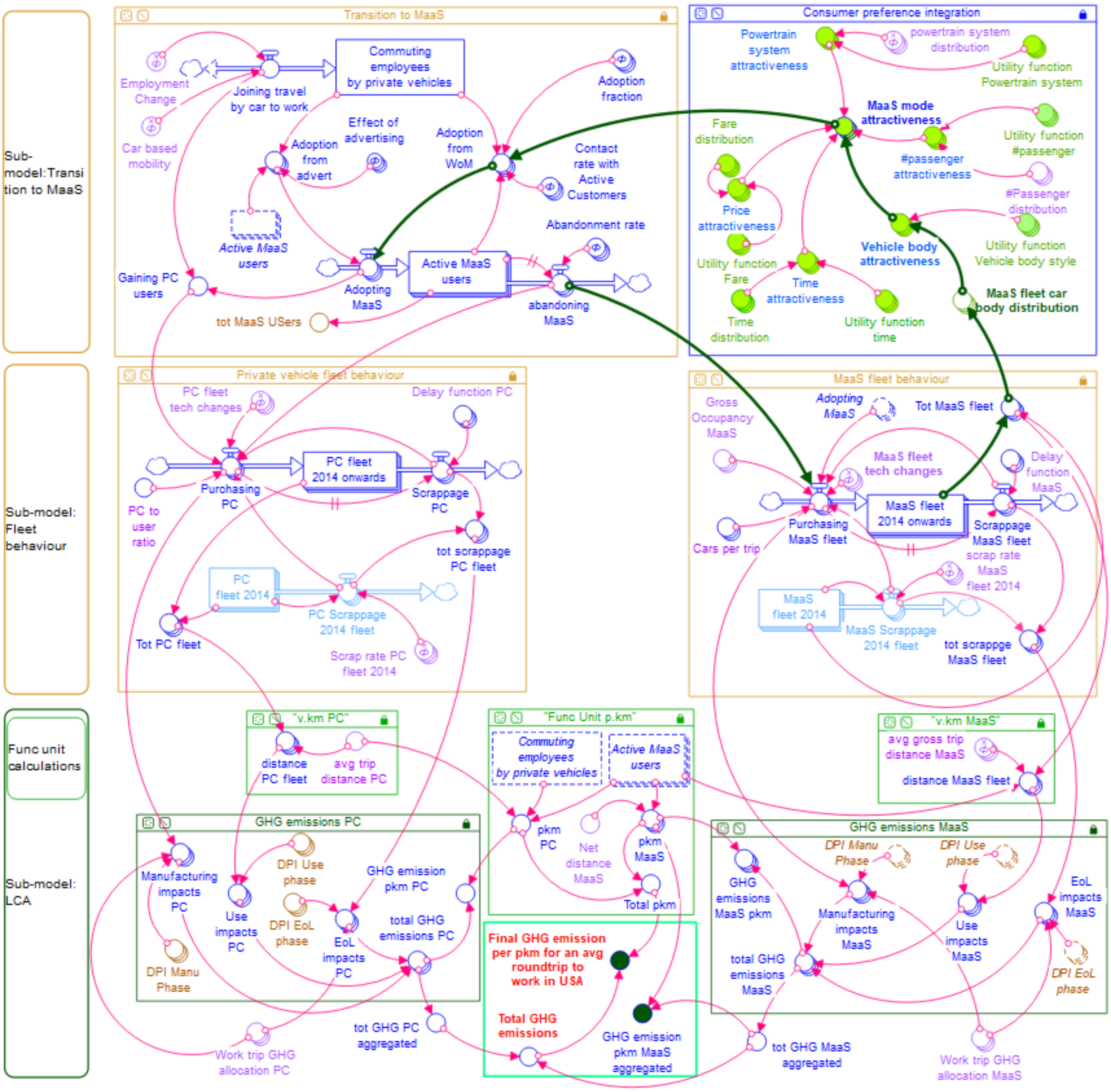

Figure E-1 Stock flow diagram of the Transition to MaaS dynamic GHG

Notes: Key to colour codes

SD model item	Font description
Sub-model, sub-model component	Dark green
Stock and flows	Blue
Converters – system defined	Blue
Converters – primary data-based	Bright green
Converters – secondary data-based	Purple
Converters – DPI	Brown

Table E-1 Historical data employed for the payoff calculations and system calibrations

Employee-related data on the drive alone and employment change				
Parameter (Source)	Time period and source application			
Employment change (Toossi, 2002; US Census Bureau, 2020a)	1980	1990	2000	2010 onwards 2050
	15,419,822	12,549,600	10,095,456	Using one-year estimates by the US Census Data
Private vehicle and car-based MaaS usage for work rides in the US				
Drove alone to work % (Office of Energy Efficiency and Renewable Energy, 2016; US Census Bureau, 2020a)	1980	1990	2000	2010 to 2019
	64.4%	73.2%	75.7%	76.6% to 75.9%
Carpool (Office of Energy Efficiency and Renewable Energy, 2016; US Census Bureau, 2020a)	19.7%	13.4%	12.2%	10.4% to 9.0%
Ridesourcing – estimated based on (US Census Bureau, 2020a; Schneider, 2021a, 2021b)	0%	0%	0%	Solo-ridesourcing: 2011 – 0.05% to 2019 - 0.65% | Pooled-ridesourcing: 2015 – 0.03% to 2019 – 0.18%

Table E-2 Modelling payoff calculation details - Baseline scenario

Method	**maxiter**	**init_step**	**tolerance**
Powell	25000	1e-7	1e-7
Element	Active MaaS users[CP]	Active MaaS users[sRS]	Active MaaS users[pRS]
Weight	auto	auto	auto
Comparison Type	Squared Error	Squared Error	Squared Error
Comparison Tolerance	0	0	0

Parameter:	Abandonment rate[CP]	Abandonment rate[sRS]	Abandonment rate[pRS]	Contact rate with Active Customers[CP]	Contact rate with Active Customers[sRS]	Contact rate with Active Customers[pRS]	Adoption fraction[CP]	Adoption fraction[sRS]	Adoption fraction[pRS]	Effect of advertising[CP]	Effect of advertising[sRS]	Effect of advertising[pRS]
min_value	0.15	0.19	0.15	1	1	1	0.000005	0.000005	0.000005	0.000001	0.000001	0.000001
max_value	0.2	0.2	0.2	333000	333000	333000	0.01	0.01	0.01	0.0009	0.0009	0.0009
scaling	1	1	1	1	1	1	1	1	1	1	1	1

	Abandonment rate[CP]	Abandonment rate[sRS]	Abandonment rate[pRS]	Contact rate with Active Customers[CP]	Contact rate with Active Customers[sRS]	Contact rate with Active Customers[pRS]	Adoption fraction[CP]	Adoption fraction[sRS]	Adoption fraction[pRS]	Effect of advertising[CP]	Effect of advertising[sRS]	Effect of advertising[pRS]	**Payoff1**
Starting at	0.19998548151	0.194708099339	0.151089342552	109.993935295	110.002307756	109.995630555	0.00583967253034	0.00867816545511	0.00442184012682	0.000001	0.00078911412698	0.000468304047225	
After 32 runs	0.199984814931	0.194708167972	0.151089363375	109.993935295	110.002307756	109.995630555	0.00583967251207	0.00867818356933	0.0044218871078	0.000001(min)	0.000789116590147	0.000468308320506	18.7986843747

Table E-3 Modelling payoff calculation – High BEV adoption scenario

Method	**maxiter**	**init_step**	**tolerance**
Powell	25000	1e-7	1e-7
Element	Active MaaS users[CP]	Active MaaS users[sRS]	Active MaaS users[pRS]
Weight	auto	auto	auto
Comparison Type	Squared Error	Squared Error	Squared Error
Comparison Tolerance	0	0	0

Parameter:	Abandonment rate[CP]	Abandonment rate[sRS]	Abandonment rate[pRS]	Contact rate with Active Customers[CP]	Contact rate with Active Customers[sRS]	Contact rate with Active Customers[pRS]	Adoption fraction[CP]	Adoption fraction[sRS]	Adoption fraction[pRS]	Effect of advertising[CP]	Effect of advertising[sRS]	Effect of advertising[pRS]
min_value	0.15	0.19	0.15	1	1	1	0.000005	0.000005	0.000005	0.000001	0.000001	0.000001
max_value	0.2	0.2	0.2	333000	333000	333000	0.01	0.01	0.01	0.0009	0.0009	0.0009
scaling	1	1	1	1	1	1	1	1	1	1	1	1

	Abandonment rate[CP]	Abandonment rate[sRS]	Abandonment rate[pRS]	Contact rate with Active Customers[CP]	Contact rate with Active Customers[sRS]	Contact rate with Active Customers[pRS]	Adoption fraction[CP]	Adoption fraction[sRS]	Adoption fraction[pRS]	Effect of advertising[CP]	Effect of advertising[sRS]	Effect of advertising[pRS]	**Payoff1**
Starting at	0.198683569315	0.194727639839	0.150907428822	109.994686776	110.002157406	109.996065934	0.005802954979 42	0.008677296627 31	0.004409364590 55	0.000001	0.000789261156 733	0.000468473123 667	
After 39 runs	0.198682492306	0.194727773811	0.15090754 28	109.994686777	110.002157406	109.996065934	0.005802916114 52	0.008677366463 11	0.004409309543 84	0.000001(min)	0.000789256783 277	0.000468471991 831	18.7998584436

	Abandonment rate[CP]	Abandonment rate[sRS]	Abandonment rate[pRS]	Contact rate with Active Customers[CP]	Contact rate with Active Customers[sRS]	Contact rate with Active Customers[pRS]	Adoption fraction [CP]	Adoption fraction [sRS]	Adoption fraction [pRS]	Effect of advertising[CP]	Effect of advertising[sRS]	Effect of advertising[pRS]
Lower	*	*	*	109.141858208	104.7627775149	49.1350552038	0.00574529679724	0.00822889324588	0.00195931240088	NaN	0.000749498829654	0.000385806509811
Value	0.198682492306	0.194727773811	0.1509075428	109.994686777	110.002157406	109.996065934	0.00580291611452	0.00867736646311	0.00440930954384	0.000001	0.000789256783277	0.000468471991831
Upper	NaN	*	*	110.850856874	115.004306165	161.14596124	0.00585368218276	0.00928726490443	0.0060723005827	*	0.000839980408491	0.000520085728315

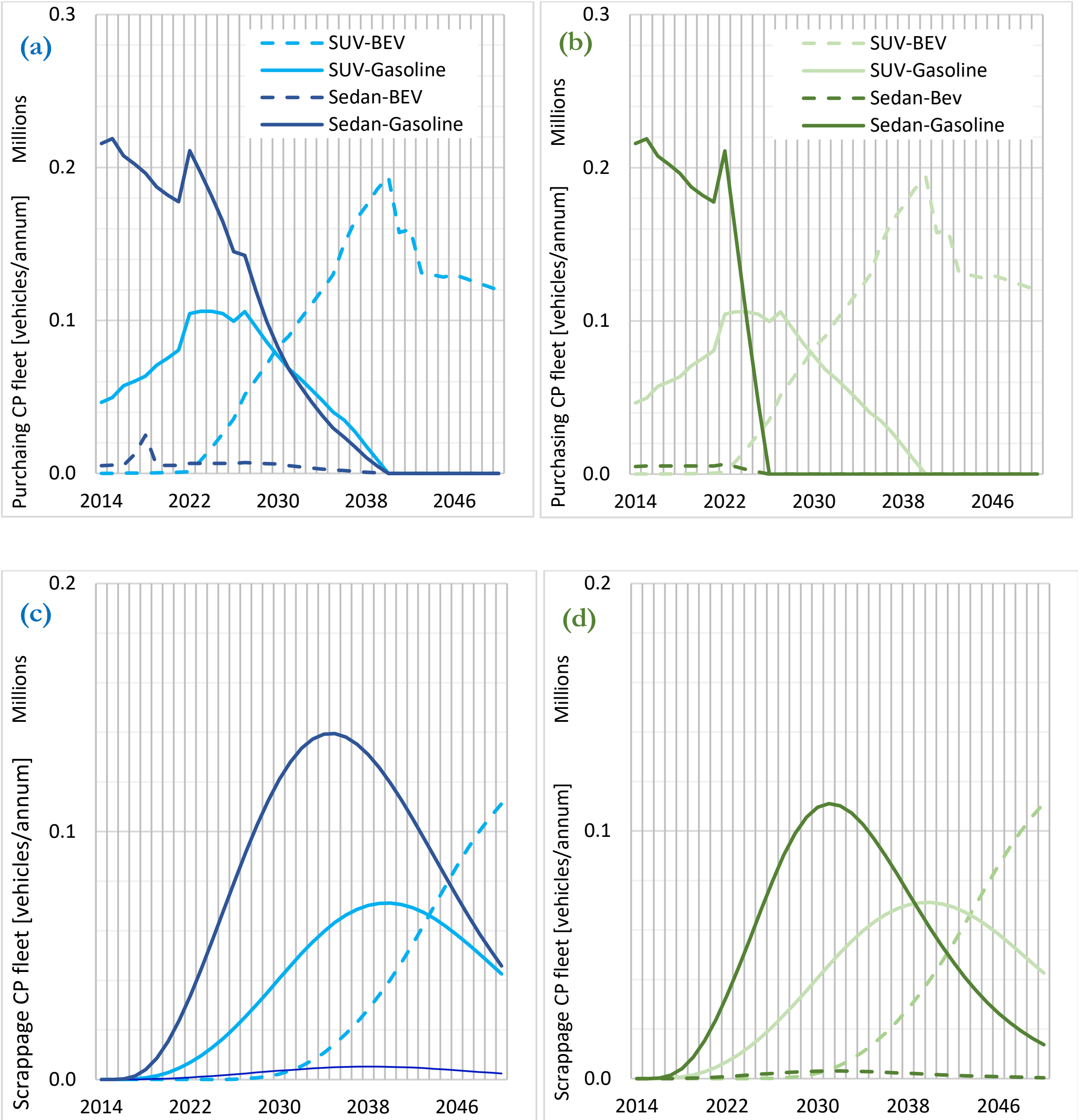

Figure E-2 Carpooling fleet behaviour: Purchasing (inflow) and Scrappage (outflow)

Notes: (a) Purchasing - Baseline scenario, (b) Purchasing - High BEV adoption scenario, (c) Scrappage - Baseline scenario, (d) Scrappage - High BEV adoption scenario *identical key with the purchasing*

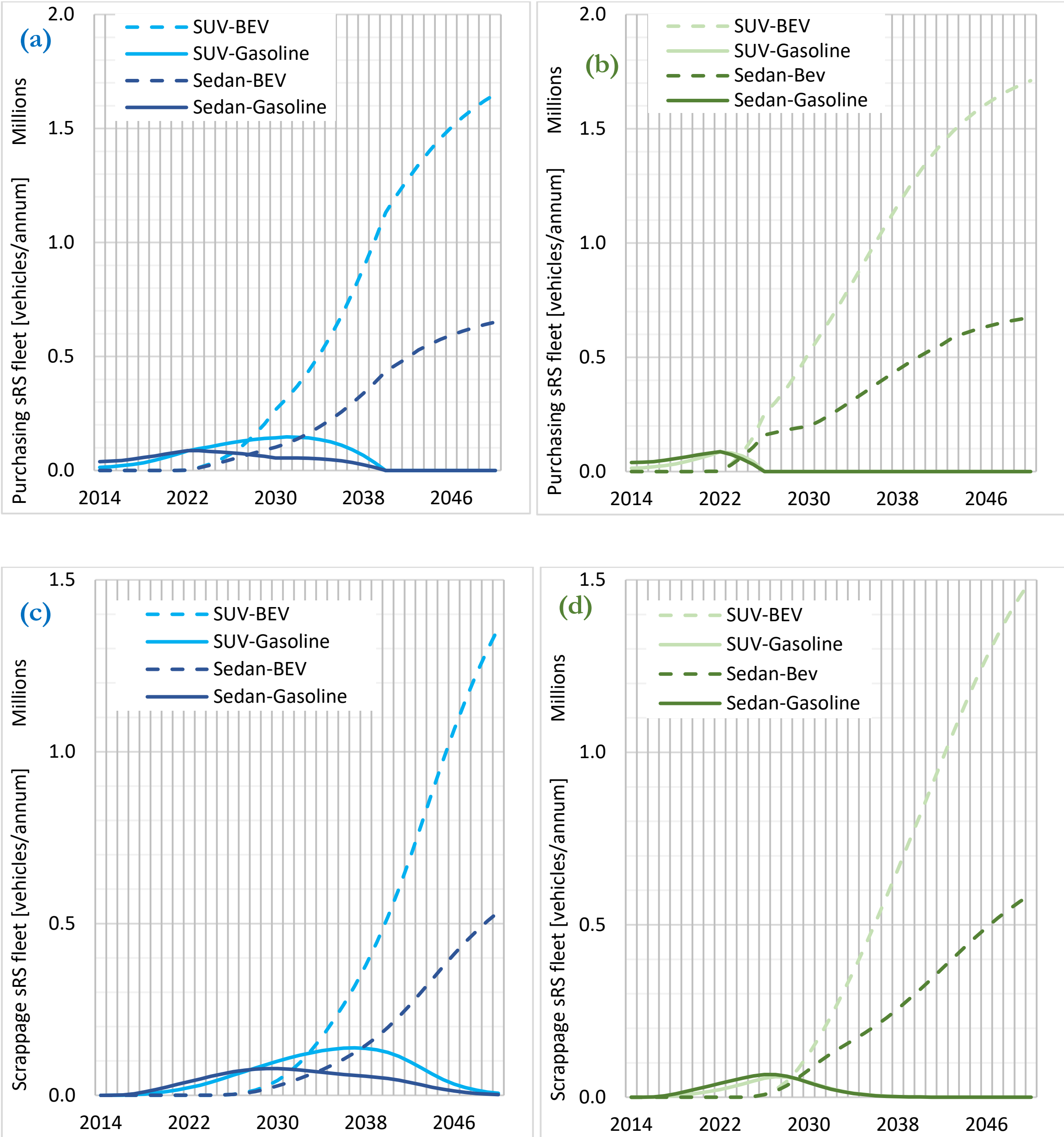

Figure E-3 Solo-ridesourcing fleet behaviour: Purchasing (inflow) and Scrappage (outflow)

Notes: (a) Purchasing - Baseline scenario, (b) Purchasing - High BEV adoption scenario, (c) Scrappage - Baseline scenario, (d) Scrappage - High BEV adoption scenario **identical key with the purchasing*

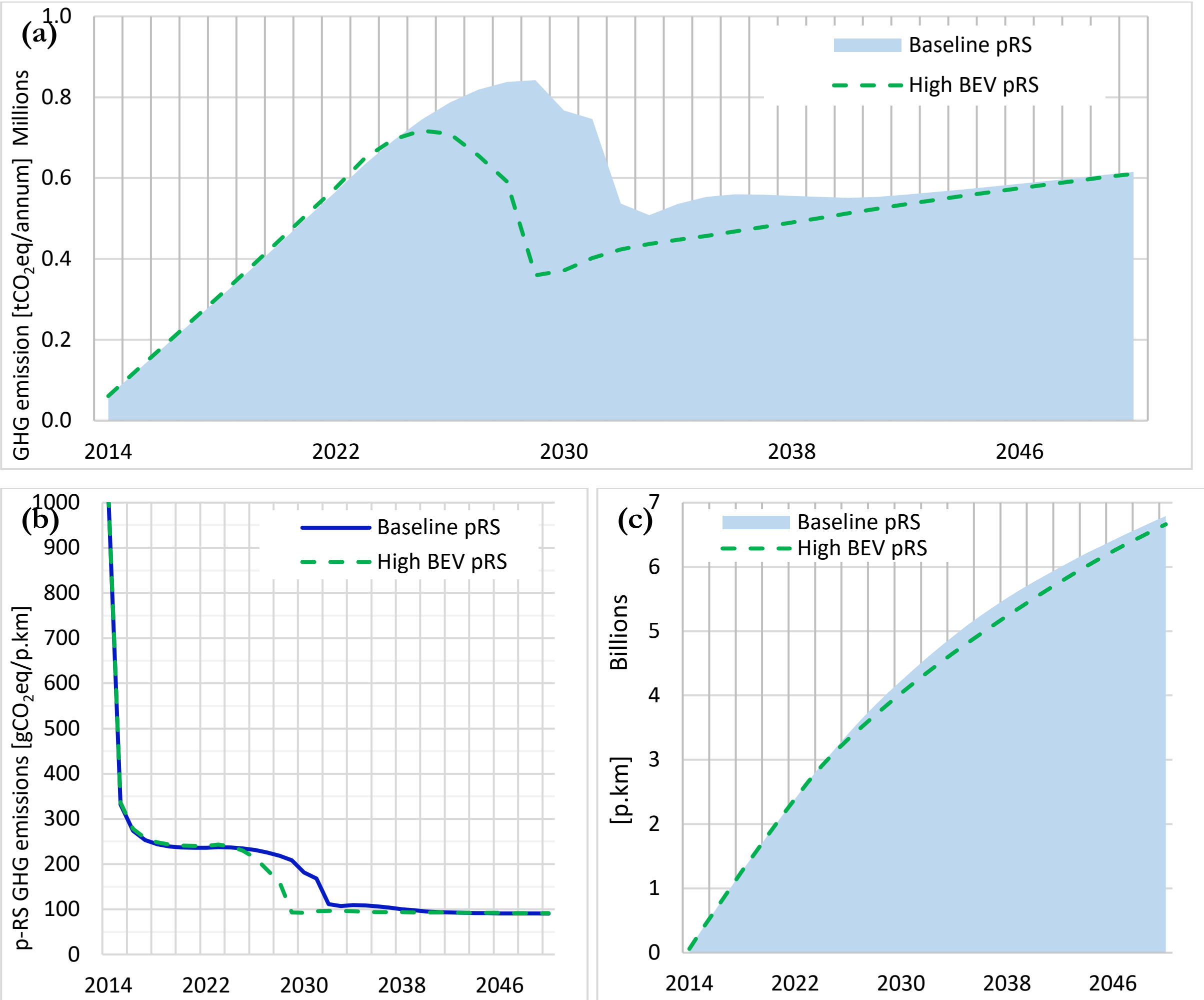

Figure E-4 Dynamic GHG results of the transition to MaaS – Pooled-ridesourcing

Notes: (a) Absolute GHG emissions, (b) Specific GHG emissions compared to p.km, (c) Passenger kilometres

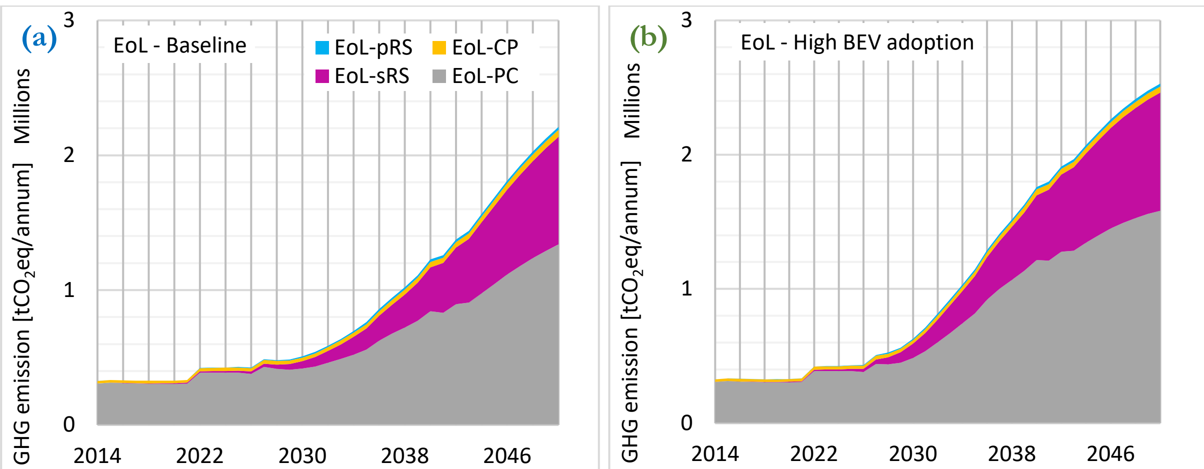

Figure E-5 Dynamic GHG emission results - car-based personal mobility modes – EoL phase

Notes: (a) Baseline scenario, (b) High BEV adoption scenario

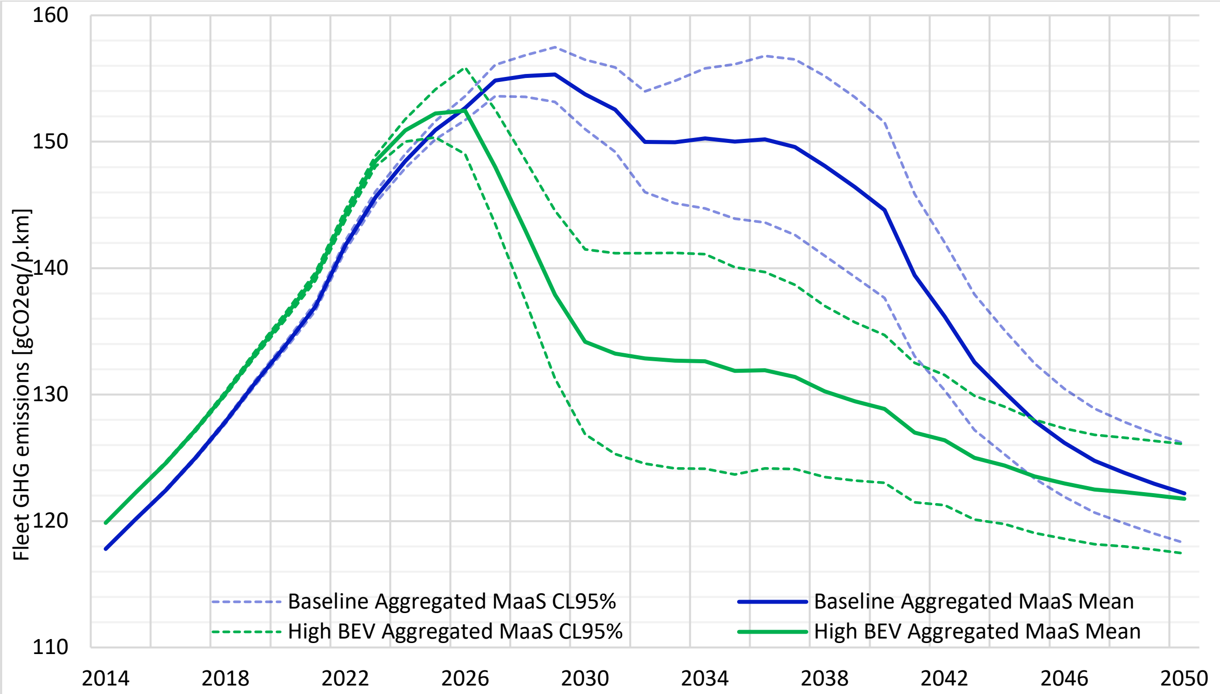

Figure E-6 Dynamic GHG emission results with confidence intervals – Aggregated car-based personal mobility modes

Notes: Specific GHG emissions compared to p.km. Solid line – mean, Dased lines - 95% confidence intervals

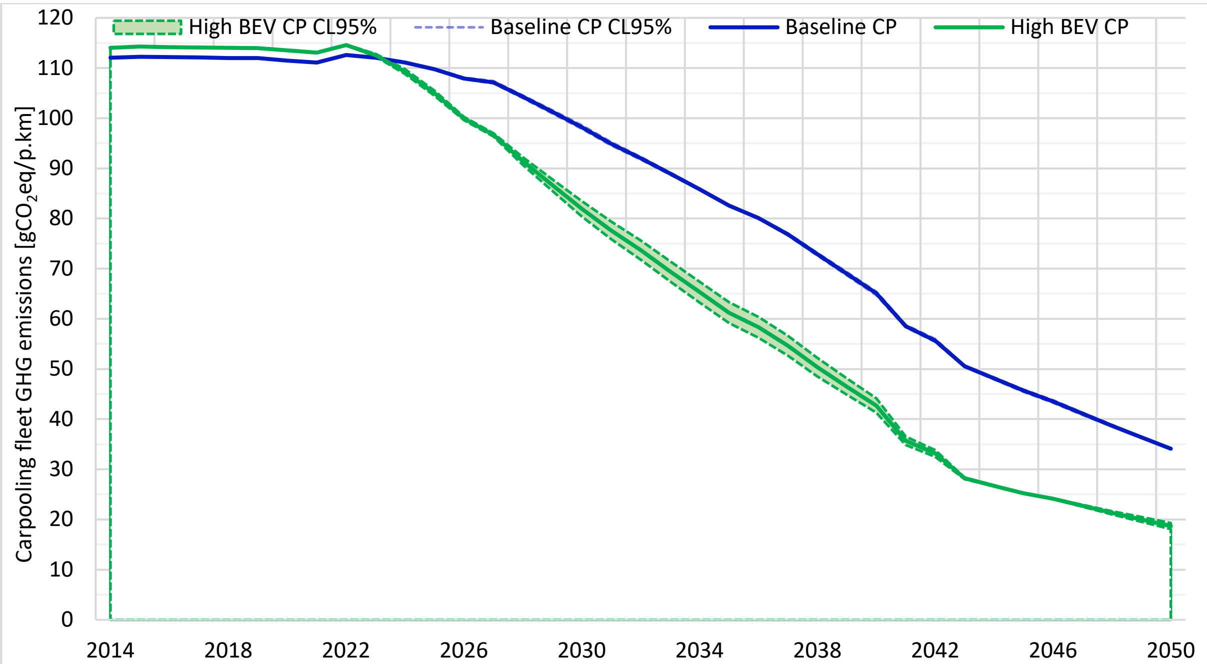

Figure E-7 Dynamic GHG emission results with confidence intervals – Carpooling

Notes: Specific GHG emissions compared to p.km. Solid line – mean, Shaded - 95% confidence intervals

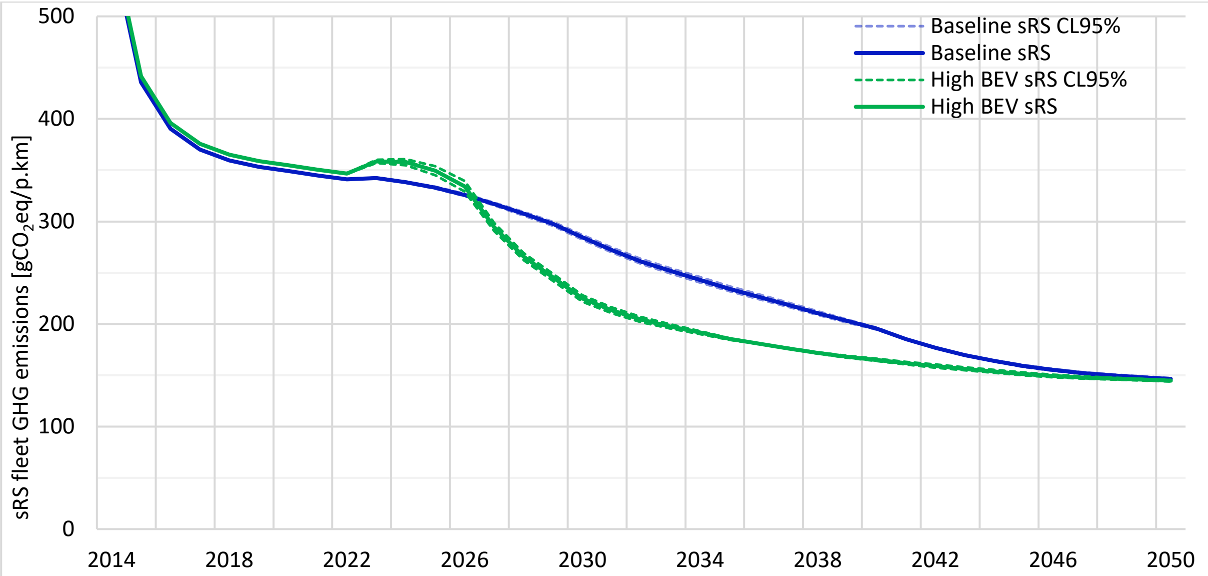

Figure E-8 Dynamic GHG emission results with confidence intervals – solo-ridesourcing

Notes: Specific GHG emissions compared to p.km. Solid line – mean, Shaded - 95% confidence intervals

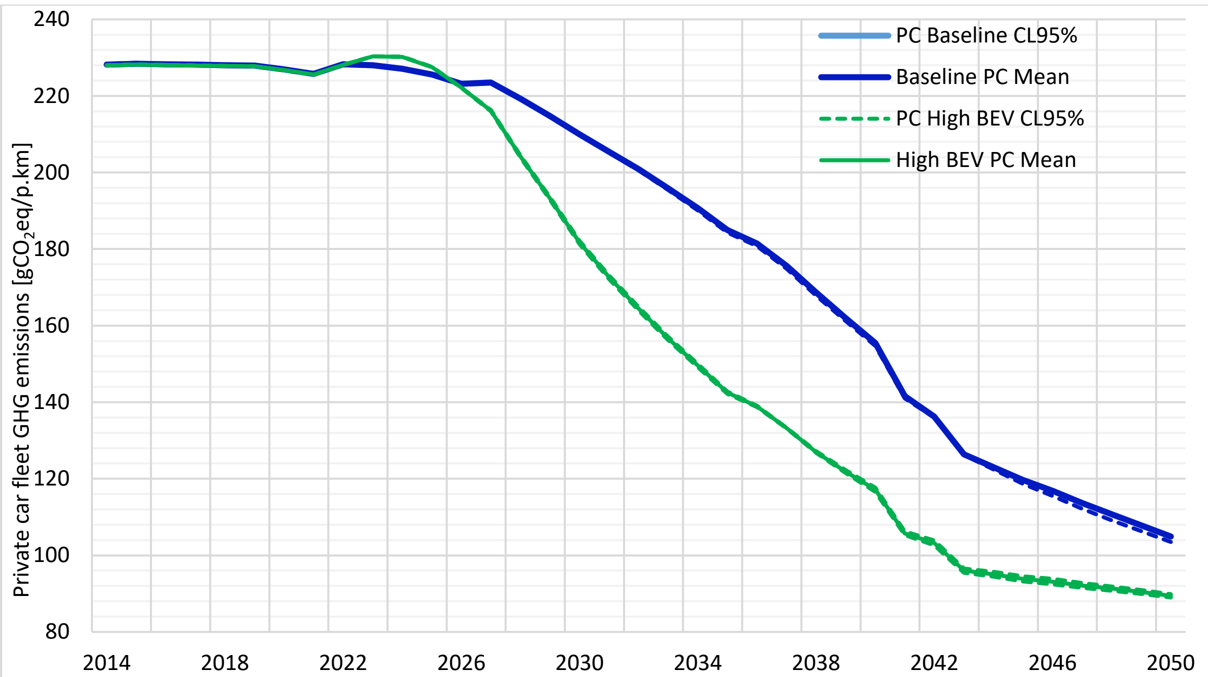

Figure E-9 Dynamic GHG emission results with confidence intervals – Private cars

Notes: Specific GHG emissions compared to p.km. Solid line – mean, Shaded - 95% confidence intervals

F Appendix – Sensitivity Analysis Findings

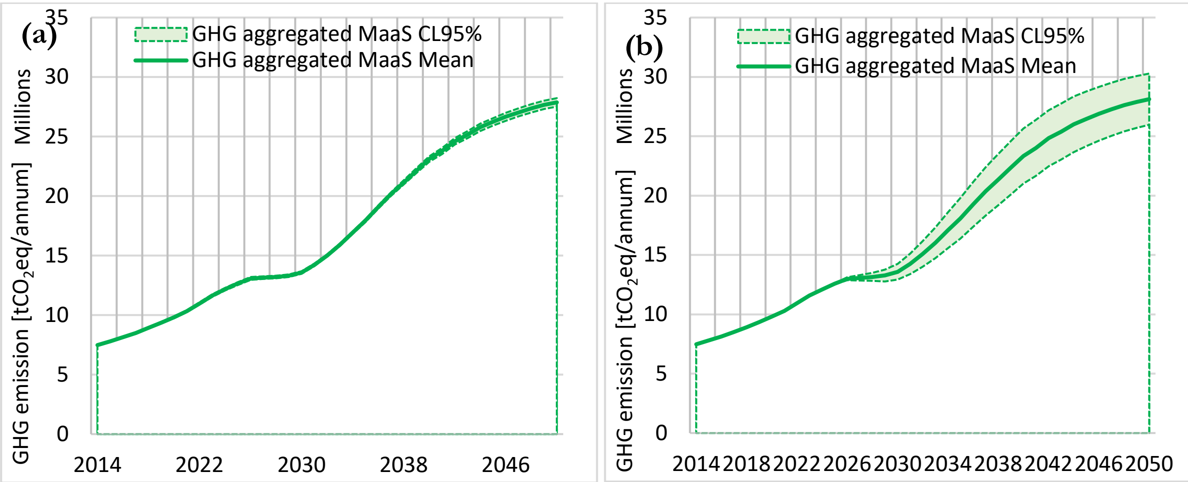

Figure F-1 Sensitivity analysis –Dynamic GHG emission - Aggregated MaaS, High BEV adoption

Note: (a) sensitivity test with control level 95% for body style only, (b) sensitivity test with control level 95% for powertrain type only

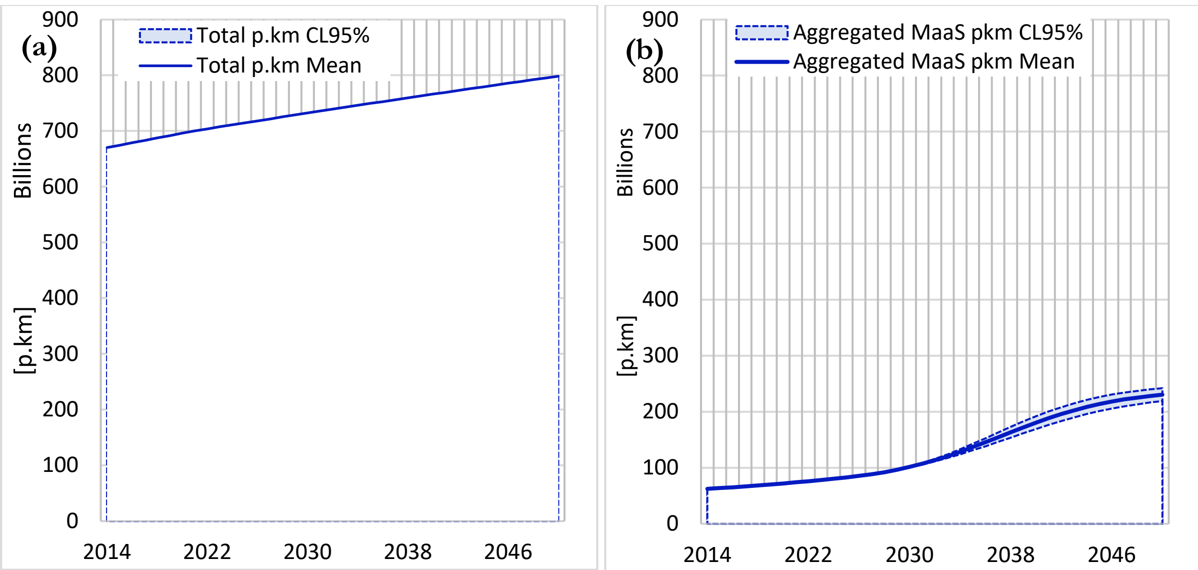

Figure F-2 Sensitivity analysis - passenger kilometres - Baseline scenario

Note: (a) sensitivity test with control level 95% for powertrain types, (b) Overall personal mobility, Right - Aggregated MaaS

G APPENDIX – SYSTEM DYNAMICS MODEL CODING

Notes: The model has 82 (830) variables (array expansion in parenthesis). In the root model, and 0 additional modules with nine sectors. Stocks: 6 (76), Flows: 9 (115), Converters: 67 (639), Constants: 32 (338), Equations: 44 (416), Graphicals: 0 (0), There are also 468 expanded macro variables.

Stella-generated SD simulation and formulation notes.

Top-Level Model:

Active_MaaS_users[CP](t) = Active_MaaS_users[CP](t - dt) + (Adopting_MaaS[CP] - abandoning_MaaS[CP]) * dt {NON-NEGATIVE}
  INIT Active_MaaS_users[CP] = 11514446
  UNITS: person
Active_MaaS_users[sRS](t) = Active_MaaS_users[sRS](t - dt) + (Adopting_MaaS[sRS] - abandoning_MaaS[sRS]) * dt {NON-NEGATIVE}
  INIT Active_MaaS_users[sRS] = 125157
  UNITS: person
Active_MaaS_users[pRS](t) = Active_MaaS_users[pRS](t - dt) + (Adopting_MaaS[pRS] - abandoning_MaaS[pRS]) * dt {NON-NEGATIVE}
  INIT Active_MaaS_users[pRS] = 11117
  UNITS: person
  UNITS: person
  INFLOWS:
  Adopting_MaaS[MaaS_Mode] = Adoption_from_advert+Adoption_from_WoM {UNIFLOW}
  UNITS: person/Year
  OUTFLOWS:
  abandoning_MaaS[MaaS_Mode] = Abandonment_rate*Active_MaaS_users {UNIFLOW}
  UNITS: person/Year
Commuting_employees_by_private_vehicles(t) = Commuting_employees_by_private_vehicles(t - dt) + (Joining_travel_by_car_to_work) * dt {NON-NEGATIVE}
  INIT Commuting_employees_by_private_vehicles = 125157020
  UNITS: person
  INFLOWS:
  Joining_travel_by_car_to_work = Employment_Change*Car_based_mobility
  UNITS: person/Year
MaaS_fleet_2014[CP, Sedan, Gasoline](t) = MaaS_fleet_2014[CP, Sedan, Gasoline](t - dt) + (- MaaS_Scrappage_2014_fleet[CP, Sedan, Gasoline]) * dt {NON-NEGATIVE}
  INIT MaaS_fleet_2014[CP, Sedan, Gasoline] = 4061458
  UNITS: cars
MaaS_fleet_2014[CP, Sedan, Hybrid](t) = MaaS_fleet_2014[CP, Sedan, Hybrid](t - dt) + (- MaaS_Scrappage_2014_fleet[CP, Sedan, Hybrid]) * dt {NON-NEGATIVE}
  INIT MaaS_fleet_2014[CP, Sedan, Hybrid] = 94685
  UNITS: cars
MaaS_fleet_2014[CP, Sedan, BEV](t) = MaaS_fleet_2014[CP, Sedan, BEV](t - dt) + (- MaaS_Scrappage_2014_fleet[CP, Sedan, BEV]) * dt {NON-NEGATIVE}
  INIT MaaS_fleet_2014[CP, Sedan, BEV] = 2361
  UNITS: cars
MaaS_fleet_2014[CP, SUV, Gasoline](t) = MaaS_fleet_2014[CP, SUV, Gasoline](t - dt) + (- MaaS_Scrappage_2014_fleet[CP, SUV, Gasoline]) * dt {NON-NEGATIVE}

INIT MaaS_fleet_2014[CP, SUV, Gasoline] = 876423
UNITS: cars
MaaS_fleet_2014[CP, SUV, Hybrid](t) = MaaS_fleet_2014[CP, SUV, Hybrid](t - dt) + (- MaaS_Scrappage_2014_fleet[CP, SUV, Hybrid]) * dt {NON-NEGATIVE}
INIT MaaS_fleet_2014[CP, SUV, Hybrid] = 20432
UNITS: cars
MaaS_fleet_2014[CP, SUV, BEV](t) = MaaS_fleet_2014[CP, SUV, BEV](t - dt) + (- MaaS_Scrappage_2014_fleet[CP, SUV, BEV]) * dt {NON-NEGATIVE}
INIT MaaS_fleet_2014[CP, SUV, BEV] = 509
UNITS: cars
MaaS_fleet_2014[CP, Hatch, Gasoline](t) = MaaS_fleet_2014[CP, Hatch, Gasoline](t - dt) + (- MaaS_Scrappage_2014_fleet[CP, Hatch, Gasoline]) * dt {NON-NEGATIVE}
INIT MaaS_fleet_2014[CP, Hatch, Gasoline] = 213761
UNITS: cars
MaaS_fleet_2014[CP, Hatch, Hybrid](t) = MaaS_fleet_2014[CP, Hatch, Hybrid](t - dt) + (- MaaS_Scrappage_2014_fleet[CP, Hatch, Hybrid]) * dt {NON-NEGATIVE}
INIT MaaS_fleet_2014[CP, Hatch, Hybrid] = 4983
UNITS: cars
MaaS_fleet_2014[CP, Hatch, BEV](t) = MaaS_fleet_2014[CP, Hatch, BEV](t - dt) + (- MaaS_Scrappage_2014_fleet[CP, Hatch, BEV]) * dt {NON-NEGATIVE}
INIT MaaS_fleet_2014[CP, Hatch, BEV] = 124
UNITS: cars
MaaS_fleet_2014[sRS, Sedan, Gasoline](t) = MaaS_fleet_2014[sRS, Sedan, Gasoline](t - dt) + (- MaaS_Scrappage_2014_fleet[sRS, Sedan, Gasoline]) * dt {NON-NEGATIVE}
INIT MaaS_fleet_2014[sRS, Sedan, Gasoline] = 49824
UNITS: cars
MaaS_fleet_2014[sRS, Sedan, Hybrid](t) = MaaS_fleet_2014[sRS, Sedan, Hybrid](t - dt) + (- MaaS_Scrappage_2014_fleet[sRS, Sedan, Hybrid]) * dt {NON-NEGATIVE}
INIT MaaS_fleet_2014[sRS, Sedan, Hybrid] = 6573
UNITS: cars
MaaS_fleet_2014[sRS, Sedan, BEV](t) = MaaS_fleet_2014[sRS, Sedan, BEV](t - dt) + (- MaaS_Scrappage_2014_fleet[sRS, Sedan, BEV]) * dt {NON-NEGATIVE}
INIT MaaS_fleet_2014[sRS, Sedan, BEV] = 29
UNITS: cars
MaaS_fleet_2014[sRS, SUV, Gasoline](t) = MaaS_fleet_2014[sRS, SUV, Gasoline](t - dt) + (- MaaS_Scrappage_2014_fleet[sRS, SUV, Gasoline]) * dt {NON-NEGATIVE}
INIT MaaS_fleet_2014[sRS, SUV, Gasoline] = 18078
UNITS: cars
MaaS_fleet_2014[sRS, SUV, Hybrid](t) = MaaS_fleet_2014[sRS, SUV, Hybrid](t - dt) + (- MaaS_Scrappage_2014_fleet[sRS, SUV, Hybrid]) * dt {NON-NEGATIVE}
INIT MaaS_fleet_2014[sRS, SUV, Hybrid] = 2385
UNITS: cars
MaaS_fleet_2014[sRS, SUV, BEV](t) = MaaS_fleet_2014[sRS, SUV, BEV](t - dt) + (- MaaS_Scrappage_2014_fleet[sRS, SUV, BEV]) * dt {NON-NEGATIVE}
INIT MaaS_fleet_2014[sRS, SUV, BEV] = 11
UNITS: cars
MaaS_fleet_2014[sRS, Hatch, Gasoline](t) = MaaS_fleet_2014[sRS, Hatch, Gasoline](t - dt) + (- MaaS_Scrappage_2014_fleet[sRS, Hatch, Gasoline]) * dt {NON-NEGATIVE}
INIT MaaS_fleet_2014[sRS, Hatch, Gasoline] = 2939

UNITS: cars
MaaS_fleet_2014[sRS, Hatch, Hybrid](t) = MaaS_fleet_2014[sRS, Hatch, Hybrid](t - dt) + (- MaaS_Scrappage_2014_fleet[sRS, Hatch, Hybrid]) * dt {NON-NEGATIVE}
INIT MaaS_fleet_2014[sRS, Hatch, Hybrid] = 388
UNITS: cars
MaaS_fleet_2014[sRS, Hatch, BEV](t) = MaaS_fleet_2014[sRS, Hatch, BEV](t - dt) + (- MaaS_Scrappage_2014_fleet[sRS, Hatch, BEV]) * dt {NON-NEGATIVE}
INIT MaaS_fleet_2014[sRS, Hatch, BEV] = 2
UNITS: cars
MaaS_fleet_2014[pRS, Sedan, Gasoline](t) = MaaS_fleet_2014[pRS, Sedan, Gasoline](t - dt) + (- MaaS_Scrappage_2014_fleet[pRS, Sedan, Gasoline]) * dt {NON-NEGATIVE}
INIT MaaS_fleet_2014[pRS, Sedan, Gasoline] = 770
UNITS: cars
MaaS_fleet_2014[pRS, Sedan, Hybrid](t) = MaaS_fleet_2014[pRS, Sedan, Hybrid](t - dt) + (- MaaS_Scrappage_2014_fleet[pRS, Sedan, Hybrid]) * dt {NON-NEGATIVE}
INIT MaaS_fleet_2014[pRS, Sedan, Hybrid] = 24
UNITS: cars
MaaS_fleet_2014[pRS, Sedan, BEV](t) = MaaS_fleet_2014[pRS, Sedan, BEV](t - dt) + (- MaaS_Scrappage_2014_fleet[pRS, Sedan, BEV]) * dt {NON-NEGATIVE}
INIT MaaS_fleet_2014[pRS, Sedan, BEV] = 0
UNITS: cars
MaaS_fleet_2014[pRS, SUV, Gasoline](t) = MaaS_fleet_2014[pRS, SUV, Gasoline](t - dt) + (- MaaS_Scrappage_2014_fleet[pRS, SUV, Gasoline]) * dt {NON-NEGATIVE}
INIT MaaS_fleet_2014[pRS, SUV, Gasoline] = 3080
UNITS: cars
MaaS_fleet_2014[pRS, SUV, Hybrid](t) = MaaS_fleet_2014[pRS, SUV, Hybrid](t - dt) + (- MaaS_Scrappage_2014_fleet[pRS, SUV, Hybrid]) * dt {NON-NEGATIVE}
INIT MaaS_fleet_2014[pRS, SUV, Hybrid] = 96
UNITS: cars
MaaS_fleet_2014[pRS, SUV, BEV](t) = MaaS_fleet_2014[pRS, SUV, BEV](t - dt) + (- MaaS_Scrappage_2014_fleet[pRS, SUV, BEV]) * dt {NON-NEGATIVE}
INIT MaaS_fleet_2014[pRS, SUV, BEV] = 0
UNITS: cars
MaaS_fleet_2014[pRS, Hatch, Gasoline](t) = MaaS_fleet_2014[pRS, Hatch, Gasoline](t - dt) + (- MaaS_Scrappage_2014_fleet[pRS, Hatch, Gasoline]) * dt {NON-NEGATIVE}
INIT MaaS_fleet_2014[pRS, Hatch, Gasoline] = 0
UNITS: cars
MaaS_fleet_2014[pRS, Hatch, Hybrid](t) = MaaS_fleet_2014[pRS, Hatch, Hybrid](t - dt) + (- MaaS_Scrappage_2014_fleet[pRS, Hatch, Hybrid]) * dt {NON-NEGATIVE}
INIT MaaS_fleet_2014[pRS, Hatch, Hybrid] = 0
UNITS: cars
MaaS_fleet_2014[pRS, Hatch, BEV](t) = MaaS_fleet_2014[pRS, Hatch, BEV](t - dt) + (- MaaS_Scrappage_2014_fleet[pRS, Hatch, BEV]) * dt {NON-NEGATIVE}
INIT MaaS_fleet_2014[pRS, Hatch, BEV] = 0
UNITS: cars
UNITS: cars
OUTFLOWS:
MaaS_Scrappage_2014_fleet[MaaS_Mode, Carbody, Powertrain] = scrap_rate_MaaS_fleet_2014*MaaS_fleet_2014 {UNIFLOW}

UNITS: cars/Years
MaaS_fleet_2014_onwards[MaaS_Mode, Carbody, Powertrain](t) =
MaaS_fleet_2014_onwards[MaaS_Mode, Carbody, Powertrain](t - dt) +
(Purchasing_MaaS_fleet[MaaS_Mode, Carbody, Powertrain] - Scrappage_MaaS_fleet[MaaS_Mode,
Carbody, Powertrain]) * dt {NON-NEGATIVE}
INIT MaaS_fleet_2014_onwards[MaaS_Mode, Carbody, Powertrain] = 1
UNITS: cars
INFLOWS:
Purchasing_MaaS_fleet[CP, Sedan, Gasoline] =
(Scrappage_MaaS_fleet[CP,Sedan,Gasoline]+Scrappage_MaaS_fleet[CP,Sedan,Hybrid]+Scrappage_MaaS
_fleet[CP,Sedan,BEV]+Scrappage_MaaS_fleet[CP,SUV,Gasoline]+Scrappage_MaaS_fleet[CP,SUV,Hybri
d]+Scrappage_MaaS_fleet[CP,SUV,BEV]+Scrappage_MaaS_fleet[CP,Hatch,Gasoline]+Scrappage_MaaS
_fleet[CP,Hatch,Hybrid]+Scrappage_MaaS_fleet[CP,Hatch,BEV]+MaaS_Scrappage_2014_fleet+((Adopti
ng_MaaS[CP]-
abandoning_MaaS[CP])*Cars_per_trip[CP]/Gross_Occupancy_MaaS[CP]))*MaaS_fleet_tech_changes[C
P,Sedan,Gasoline] {UNIFLOW}
UNITS: cars/Years
Purchasing_MaaS_fleet[CP, Sedan, Hybrid] =
(Scrappage_MaaS_fleet[CP,Sedan,Gasoline]+Scrappage_MaaS_fleet[CP,Sedan,Hybrid]+Scrappage_MaaS
_fleet[CP,Sedan,BEV]+Scrappage_MaaS_fleet[CP,SUV,Gasoline]+Scrappage_MaaS_fleet[CP,SUV,Hybri
d]+Scrappage_MaaS_fleet[CP,SUV,BEV]+Scrappage_MaaS_fleet[CP,Hatch,Gasoline]+Scrappage_MaaS
_fleet[CP,Hatch,Hybrid]+Scrappage_MaaS_fleet[CP,Hatch,BEV]+MaaS_Scrappage_2014_fleet+((Adopti
ng_MaaS[CP]-
abandoning_MaaS[CP])*Cars_per_trip[CP]/Gross_Occupancy_MaaS[CP]))*MaaS_fleet_tech_changes[C
P,Sedan,Hybrid] {UNIFLOW}
UNITS: cars/Years
Purchasing_MaaS_fleet[CP, Sedan, BEV] =
(Scrappage_MaaS_fleet[CP,Sedan,Gasoline]+Scrappage_MaaS_fleet[CP,Sedan,Hybrid]+Scrappage_MaaS
_fleet[CP,Sedan,BEV]+Scrappage_MaaS_fleet[CP,SUV,Gasoline]+Scrappage_MaaS_fleet[CP,SUV,Hybri
d]+Scrappage_MaaS_fleet[CP,SUV,BEV]+Scrappage_MaaS_fleet[CP,Hatch,Gasoline]+Scrappage_MaaS
_fleet[CP,Hatch,Hybrid]+Scrappage_MaaS_fleet[CP,Hatch,BEV]+MaaS_Scrappage_2014_fleet+((Adopti
ng_MaaS[CP]-
abandoning_MaaS[CP])*Cars_per_trip[CP]/Gross_Occupancy_MaaS[CP]))*MaaS_fleet_tech_changes[C
P,Sedan,Hybrid] {UNIFLOW}
UNITS: cars/Years
Purchasing_MaaS_fleet[CP, SUV, Gasoline] =
(Scrappage_MaaS_fleet[CP,Sedan,Gasoline]+Scrappage_MaaS_fleet[CP,Sedan,Hybrid]+Scrappage_MaaS
_fleet[CP,Sedan,BEV]+Scrappage_MaaS_fleet[CP,SUV,Gasoline]+Scrappage_MaaS_fleet[CP,SUV,Hybri
d]+Scrappage_MaaS_fleet[CP,SUV,BEV]+Scrappage_MaaS_fleet[CP,Hatch,Gasoline]+Scrappage_MaaS
_fleet[CP,Hatch,Hybrid]+Scrappage_MaaS_fleet[CP,Hatch,BEV]+MaaS_Scrappage_2014_fleet+((Adopti
ng_MaaS[CP]-
abandoning_MaaS[CP])*Cars_per_trip[CP]/Gross_Occupancy_MaaS[CP]))*MaaS_fleet_tech_changes[C
P,SUV,Gasoline] {UNIFLOW}
UNITS: cars/Years
Purchasing_MaaS_fleet[CP, SUV, Hybrid] =
(Scrappage_MaaS_fleet[CP,Sedan,Gasoline]+Scrappage_MaaS_fleet[CP,Sedan,Hybrid]+Scrappage_MaaS
_fleet[CP,Sedan,BEV]+Scrappage_MaaS_fleet[CP,SUV,Gasoline]+Scrappage_MaaS_fleet[CP,SUV,Hybri
d]+Scrappage_MaaS_fleet[CP,SUV,BEV]+Scrappage_MaaS_fleet[CP,Hatch,Gasoline]+Scrappage_MaaS
_fleet[CP,Hatch,Hybrid]+Scrappage_MaaS_fleet[CP,Hatch,BEV]+MaaS_Scrappage_2014_fleet+((Adopti
ng_MaaS[CP]-
abandoning_MaaS[CP])*Cars_per_trip[CP]/Gross_Occupancy_MaaS[CP]))*MaaS_fleet_tech_changes[C
P,SUV,Hybrid] {UNIFLOW}

UNITS: cars/Years
Purchasing_MaaS_fleet[CP, SUV, BEV] =
(Scrappage_MaaS_fleet[CP,Sedan,Gasoline]+Scrappage_MaaS_fleet[CP,Sedan,Hybrid]+Scrappage_MaaS_fleet[CP,Sedan,BEV]+Scrappage_MaaS_fleet[CP,SUV,Gasoline]+Scrappage_MaaS_fleet[CP,SUV,Hybrid]+Scrappage_MaaS_fleet[CP,SUV,BEV]+Scrappage_MaaS_fleet[CP,Hatch,Gasoline]+Scrappage_MaaS_fleet[CP,Hatch,Hybrid]+Scrappage_MaaS_fleet[CP,Hatch,BEV]+MaaS_Scrappage_2014_fleet+((Adopting_MaaS[CP]-abandoning_MaaS[CP])*Cars_per_trip[CP]/Gross_Occupancy_MaaS[CP]))*MaaS_fleet_tech_changes[CP,SUV,BEV] {UNIFLOW}
UNITS: cars/Years
Purchasing_MaaS_fleet[CP, Hatch, Gasoline] =
(Scrappage_MaaS_fleet[CP,Sedan,Gasoline]+Scrappage_MaaS_fleet[CP,Sedan,Hybrid]+Scrappage_MaaS_fleet[CP,Sedan,BEV]+Scrappage_MaaS_fleet[CP,SUV,Gasoline]+Scrappage_MaaS_fleet[CP,SUV,Hybrid]+Scrappage_MaaS_fleet[CP,SUV,BEV]+Scrappage_MaaS_fleet[CP,Hatch,Gasoline]+Scrappage_MaaS_fleet[CP,Hatch,Hybrid]+Scrappage_MaaS_fleet[CP,Hatch,BEV]+MaaS_Scrappage_2014_fleet+((Adopting_MaaS[CP]-abandoning_MaaS[CP])*Cars_per_trip[CP]/Gross_Occupancy_MaaS[CP]))*MaaS_fleet_tech_changes[CP,Hatch,Gasoline] {UNIFLOW}
UNITS: cars/Years
Purchasing_MaaS_fleet[CP, Hatch, Hybrid] =
(Scrappage_MaaS_fleet[CP,Sedan,Gasoline]+Scrappage_MaaS_fleet[CP,Sedan,Hybrid]+Scrappage_MaaS_fleet[CP,Sedan,BEV]+Scrappage_MaaS_fleet[CP,SUV,Gasoline]+Scrappage_MaaS_fleet[CP,SUV,Hybrid]+Scrappage_MaaS_fleet[CP,SUV,BEV]+Scrappage_MaaS_fleet[CP,Hatch,Gasoline]+Scrappage_MaaS_fleet[CP,Hatch,Hybrid]+Scrappage_MaaS_fleet[CP,Hatch,BEV]+MaaS_Scrappage_2014_fleet+((Adopting_MaaS[CP]-abandoning_MaaS[CP])*Cars_per_trip[CP]/Gross_Occupancy_MaaS[CP]))*MaaS_fleet_tech_changes[CP,Hatch,Hybrid] {UNIFLOW}
UNITS: cars/Years
Purchasing_MaaS_fleet[CP, Hatch, BEV] =
(Scrappage_MaaS_fleet[CP,Sedan,Gasoline]+Scrappage_MaaS_fleet[CP,Sedan,Hybrid]+Scrappage_MaaS_fleet[CP,Sedan,BEV]+Scrappage_MaaS_fleet[CP,SUV,Gasoline]+Scrappage_MaaS_fleet[CP,SUV,Hybrid]+Scrappage_MaaS_fleet[CP,SUV,BEV]+Scrappage_MaaS_fleet[CP,Hatch,Gasoline]+Scrappage_MaaS_fleet[CP,Hatch,Hybrid]+Scrappage_MaaS_fleet[CP,Hatch,BEV]+MaaS_Scrappage_2014_fleet+((Adopting_MaaS[CP]-abandoning_MaaS[CP])*Cars_per_trip[CP]/Gross_Occupancy_MaaS[CP]))*MaaS_fleet_tech_changes[CP,Hatch,BEV] {UNIFLOW}
UNITS: cars/Years
Purchasing_MaaS_fleet[sRS, Sedan, Gasoline] =
(Scrappage_MaaS_fleet[sRS,Sedan,Gasoline]+Scrappage_MaaS_fleet[sRS,Sedan,Hybrid]+Scrappage_MaaS_fleet[sRS,Sedan,BEV]+Scrappage_MaaS_fleet[sRS,SUV,Gasoline]+Scrappage_MaaS_fleet[sRS,SUV,Hybrid]+Scrappage_MaaS_fleet[sRS,SUV,BEV]+Scrappage_MaaS_fleet[sRS,Hatch,Gasoline]+Scrappage_MaaS_fleet[sRS,Hatch,Hybrid]+Scrappage_MaaS_fleet[sRS,Hatch,BEV]+MaaS_Scrappage_2014_fleet+((Adopting_MaaS[sRS]-abandoning_MaaS[sRS])*Cars_per_trip[sRS]/Gross_Occupancy_MaaS[sRS]))*MaaS_fleet_tech_changes[sRS,Sedan,Gasoline] {UNIFLOW}
UNITS: cars/Years
Purchasing_MaaS_fleet[sRS, Sedan, Hybrid] =
(Scrappage_MaaS_fleet[sRS,Sedan,Gasoline]+Scrappage_MaaS_fleet[sRS,Sedan,Hybrid]+Scrappage_MaaS_fleet[sRS,Sedan,BEV]+Scrappage_MaaS_fleet[sRS,SUV,Gasoline]+Scrappage_MaaS_fleet[sRS,SUV,Hybrid]+Scrappage_MaaS_fleet[sRS,SUV,BEV]+Scrappage_MaaS_fleet[sRS,Hatch,Gasoline]+Scrappage_MaaS_fleet[sRS,Hatch,Hybrid]+Scrappage_MaaS_fleet[sRS,Hatch,BEV]+MaaS_Scrappage_2014_fleet+((Adopting_MaaS[sRS]-

abandoning_MaaS[sRS])*Cars_per_trip[sRS]/Gross_Occupancy_MaaS[sRS]))*MaaS_fleet_tech_changes[sRS,Sedan,Hybrid] {UNIFLOW}
UNITS: cars/Years
Purchasing_MaaS_fleet[sRS, Sedan, BEV] =
(Scrappage_MaaS_fleet[sRS,Sedan,Gasoline]+Scrappage_MaaS_fleet[sRS,Sedan,Hybrid]+Scrappage_MaaS_fleet[sRS,Sedan,BEV]+Scrappage_MaaS_fleet[sRS,SUV,Gasoline]+Scrappage_MaaS_fleet[sRS,SUV,Hybrid]+Scrappage_MaaS_fleet[sRS,SUV,BEV]+Scrappage_MaaS_fleet[sRS,Hatch,Gasoline]+Scrappage_MaaS_fleet[sRS,Hatch,Hybrid]+Scrappage_MaaS_fleet[sRS,Hatch,BEV]+MaaS_Scrappage_2014_fleet+((Adopting_MaaS[sRS]-
abandoning_MaaS[sRS])*Cars_per_trip[sRS]/Gross_Occupancy_MaaS[sRS]))*MaaS_fleet_tech_changes[sRS,Sedan,BEV] {UNIFLOW}
UNITS: cars/Years
Purchasing_MaaS_fleet[sRS, SUV, Gasoline] =
(Scrappage_MaaS_fleet[sRS,Sedan,Gasoline]+Scrappage_MaaS_fleet[sRS,Sedan,Hybrid]+Scrappage_MaaS_fleet[sRS,Sedan,BEV]+Scrappage_MaaS_fleet[sRS,SUV,Gasoline]+Scrappage_MaaS_fleet[sRS,SUV,Hybrid]+Scrappage_MaaS_fleet[sRS,SUV,BEV]+Scrappage_MaaS_fleet[sRS,Hatch,Gasoline]+Scrappage_MaaS_fleet[sRS,Hatch,Hybrid]+Scrappage_MaaS_fleet[sRS,Hatch,BEV]+MaaS_Scrappage_2014_fleet+((Adopting_MaaS[sRS]-
abandoning_MaaS[sRS])*Cars_per_trip[sRS]/Gross_Occupancy_MaaS[sRS]))*MaaS_fleet_tech_changes[sRS,SUV,Gasoline] {UNIFLOW}
UNITS: cars/Years
Purchasing_MaaS_fleet[sRS, SUV, Hybrid] =
(Scrappage_MaaS_fleet[sRS,Sedan,Gasoline]+Scrappage_MaaS_fleet[sRS,Sedan,Hybrid]+Scrappage_MaaS_fleet[sRS,Sedan,BEV]+Scrappage_MaaS_fleet[sRS,SUV,Gasoline]+Scrappage_MaaS_fleet[sRS,SUV,Hybrid]+Scrappage_MaaS_fleet[sRS,SUV,BEV]+Scrappage_MaaS_fleet[sRS,Hatch,Gasoline]+Scrappage_MaaS_fleet[sRS,Hatch,Hybrid]+Scrappage_MaaS_fleet[sRS,Hatch,BEV]+MaaS_Scrappage_2014_fleet+((Adopting_MaaS[sRS]-
abandoning_MaaS[sRS])*Cars_per_trip[sRS]/Gross_Occupancy_MaaS[sRS]))*MaaS_fleet_tech_changes[sRS,SUV,Hybrid] {UNIFLOW}
UNITS: cars/Years
Purchasing_MaaS_fleet[sRS, SUV, BEV] =
(Scrappage_MaaS_fleet[sRS,Sedan,Gasoline]+Scrappage_MaaS_fleet[sRS,Sedan,Hybrid]+Scrappage_MaaS_fleet[sRS,Sedan,BEV]+Scrappage_MaaS_fleet[sRS,SUV,Gasoline]+Scrappage_MaaS_fleet[sRS,SUV,Hybrid]+Scrappage_MaaS_fleet[sRS,SUV,BEV]+Scrappage_MaaS_fleet[sRS,Hatch,Gasoline]+Scrappage_MaaS_fleet[sRS,Hatch,Hybrid]+Scrappage_MaaS_fleet[sRS,Hatch,BEV]+MaaS_Scrappage_2014_fleet+((Adopting_MaaS[sRS]-
abandoning_MaaS[sRS])*Cars_per_trip[sRS]/Gross_Occupancy_MaaS[sRS]))*MaaS_fleet_tech_changes[sRS,SUV,BEV] {UNIFLOW}
UNITS: cars/Years
Purchasing_MaaS_fleet[sRS, Hatch, Gasoline] =
(Scrappage_MaaS_fleet[sRS,Sedan,Gasoline]+Scrappage_MaaS_fleet[sRS,Sedan,Hybrid]+Scrappage_MaaS_fleet[sRS,Sedan,BEV]+Scrappage_MaaS_fleet[sRS,SUV,Gasoline]+Scrappage_MaaS_fleet[sRS,SUV,Hybrid]+Scrappage_MaaS_fleet[sRS,SUV,BEV]+Scrappage_MaaS_fleet[sRS,Hatch,Gasoline]+Scrappage_MaaS_fleet[sRS,Hatch,Hybrid]+Scrappage_MaaS_fleet[sRS,Hatch,BEV]+MaaS_Scrappage_2014_fleet+((Adopting_MaaS[sRS]-
abandoning_MaaS[sRS])*Cars_per_trip[sRS]/Gross_Occupancy_MaaS[sRS]))*MaaS_fleet_tech_changes[sRS,Hatch,Gasoline] {UNIFLOW}
UNITS: cars/Years
Purchasing_MaaS_fleet[sRS, Hatch, Hybrid] =
(Scrappage_MaaS_fleet[sRS,Sedan,Gasoline]+Scrappage_MaaS_fleet[sRS,Sedan,Hybrid]+Scrappage_MaaS_fleet[sRS,Sedan,BEV]+Scrappage_MaaS_fleet[sRS,SUV,Gasoline]+Scrappage_MaaS_fleet[sRS,SUV,Hybrid]+Scrappage_MaaS_fleet[sRS,SUV,BEV]+Scrappage_MaaS_fleet[sRS,Hatch,Gasoline]+Scrappage_MaaS_fleet[sRS,Hatch,Hybrid]+Scrappage_MaaS_fleet[sRS,Hatch,BEV]+MaaS_Scrappage_2014_fleet+((A

dopting_MaaS[sRS]-
abandoning_MaaS[sRS])*Cars_per_trip[sRS]/Gross_Occupancy_MaaS[sRS]))*MaaS_fleet_tech_changes[sRS,Hatch,Hybrid] {UNIFLOW}

UNITS: cars/Years

Purchasing_MaaS_fleet[sRS, Hatch, BEV] =
(Scrappage_MaaS_fleet[sRS,Sedan,Gasoline]+Scrappage_MaaS_fleet[sRS,Sedan,Hybrid]+Scrappage_MaaS_fleet[sRS,Sedan,BEV]+Scrappage_MaaS_fleet[sRS,SUV,Gasoline]+Scrappage_MaaS_fleet[sRS,SUV,Hybrid]+Scrappage_MaaS_fleet[sRS,SUV,BEV]+Scrappage_MaaS_fleet[sRS,Hatch,Gasoline]+Scrappage_MaaS_fleet[sRS,Hatch,Hybrid]+Scrappage_MaaS_fleet[sRS,Hatch,BEV]+MaaS_Scrappage_2014_fleet+((Adopting_MaaS[sRS]-
abandoning_MaaS[sRS])*Cars_per_trip[sRS]/Gross_Occupancy_MaaS[sRS]))*MaaS_fleet_tech_changes[sRS,Hatch,BEV] {UNIFLOW}

UNITS: cars/Years

Purchasing_MaaS_fleet[pRS, Sedan, Gasoline] =
(Scrappage_MaaS_fleet[pRS,Sedan,Gasoline]+Scrappage_MaaS_fleet[pRS,Sedan,Hybrid]+Scrappage_MaaS_fleet[pRS,Sedan,BEV]+Scrappage_MaaS_fleet[pRS,SUV,Gasoline]+Scrappage_MaaS_fleet[pRS,SUV,Hybrid]+Scrappage_MaaS_fleet[pRS,SUV,BEV]+Scrappage_MaaS_fleet[pRS,Hatch,Gasoline]+Scrappage_MaaS_fleet[pRS,Hatch,Hybrid]+Scrappage_MaaS_fleet[pRS,Hatch,BEV]+MaaS_Scrappage_2014_fleet+((Adopting_MaaS[pRS]-
abandoning_MaaS[pRS])*Cars_per_trip[pRS]/Gross_Occupancy_MaaS[pRS]))*MaaS_fleet_tech_changes[pRS,Sedan,Gasoline] {UNIFLOW}

UNITS: cars/Years

Purchasing_MaaS_fleet[pRS, Sedan, Hybrid] =
(Scrappage_MaaS_fleet[pRS,Sedan,Gasoline]+Scrappage_MaaS_fleet[pRS,Sedan,Hybrid]+Scrappage_MaaS_fleet[pRS,Sedan,BEV]+Scrappage_MaaS_fleet[pRS,SUV,Gasoline]+Scrappage_MaaS_fleet[pRS,SUV,Hybrid]+Scrappage_MaaS_fleet[pRS,SUV,BEV]+Scrappage_MaaS_fleet[pRS,Hatch,Gasoline]+Scrappage_MaaS_fleet[pRS,Hatch,Hybrid]+Scrappage_MaaS_fleet[pRS,Hatch,BEV]+MaaS_Scrappage_2014_fleet+((Adopting_MaaS[pRS]-
abandoning_MaaS[pRS])*Cars_per_trip[pRS]/Gross_Occupancy_MaaS[pRS]))*MaaS_fleet_tech_changes[pRS,Sedan,Hybrid] {UNIFLOW}

UNITS: cars/Years

Purchasing_MaaS_fleet[pRS, Sedan, BEV] =
(Scrappage_MaaS_fleet[pRS,Sedan,Gasoline]+Scrappage_MaaS_fleet[pRS,Sedan,Hybrid]+Scrappage_MaaS_fleet[pRS,Sedan,BEV]+Scrappage_MaaS_fleet[pRS,SUV,Gasoline]+Scrappage_MaaS_fleet[pRS,SUV,Hybrid]+Scrappage_MaaS_fleet[pRS,SUV,BEV]+Scrappage_MaaS_fleet[pRS,Hatch,Gasoline]+Scrappage_MaaS_fleet[pRS,Hatch,Hybrid]+Scrappage_MaaS_fleet[pRS,Hatch,BEV]+MaaS_Scrappage_2014_fleet+((Adopting_MaaS[pRS]-
abandoning_MaaS[pRS])*Cars_per_trip[pRS]/Gross_Occupancy_MaaS[pRS]))*MaaS_fleet_tech_changes[pRS,Sedan,BEV] {UNIFLOW}

UNITS: cars/Years

Purchasing_MaaS_fleet[pRS, SUV, Gasoline] =
(Scrappage_MaaS_fleet[pRS,Sedan,Gasoline]+Scrappage_MaaS_fleet[pRS,Sedan,Hybrid]+Scrappage_MaaS_fleet[pRS,Sedan,BEV]+Scrappage_MaaS_fleet[pRS,SUV,Gasoline]+Scrappage_MaaS_fleet[pRS,SUV,Hybrid]+Scrappage_MaaS_fleet[pRS,SUV,BEV]+Scrappage_MaaS_fleet[pRS,Hatch,Gasoline]+Scrappage_MaaS_fleet[pRS,Hatch,Hybrid]+Scrappage_MaaS_fleet[pRS,Hatch,BEV]+MaaS_Scrappage_2014_fleet+((Adopting_MaaS[pRS]-
abandoning_MaaS[pRS])*Cars_per_trip[pRS]/Gross_Occupancy_MaaS[pRS]))*MaaS_fleet_tech_changes[pRS,SUV,Gasoline] {UNIFLOW}

UNITS: cars/Years

Purchasing_MaaS_fleet[pRS, SUV, Hybrid] =
(Scrappage_MaaS_fleet[pRS,Sedan,Gasoline]+Scrappage_MaaS_fleet[pRS,Sedan,Hybrid]+Scrappage_MaaS_fleet[pRS,Sedan,BEV]+Scrappage_MaaS_fleet[pRS,SUV,Gasoline]+Scrappage_MaaS_fleet[pRS,SUV,Hybrid]+Scrappage_MaaS_fleet[pRS,SUV,BEV]+Scrappage_MaaS_fleet[pRS,Hatch,Gasoline]+Scrappage_

MaaS_fleet[pRS,Hatch,Hybrid]+Scrappage_MaaS_fleet[pRS,Hatch,BEV]+MaaS_Scrappage_2014_fleet+((Adopting_MaaS[pRS]-abandoning_MaaS[pRS])*Cars_per_trip[pRS]/Gross_Occupancy_MaaS[pRS]))*MaaS_fleet_tech_changes[pRS,SUV,Hybrid] {UNIFLOW}

UNITS: cars/Years

Purchasing_MaaS_fleet[pRS, SUV, BEV] = (Scrappage_MaaS_fleet[pRS,Sedan,Gasoline]+Scrappage_MaaS_fleet[pRS,Sedan,Hybrid]+Scrappage_MaaS_fleet[pRS,Sedan,BEV]+Scrappage_MaaS_fleet[pRS,SUV,Gasoline]+Scrappage_MaaS_fleet[pRS,SUV,Hybrid]+Scrappage_MaaS_fleet[pRS,SUV,BEV]+Scrappage_MaaS_fleet[pRS,Hatch,Gasoline]+Scrappage_MaaS_fleet[pRS,Hatch,Hybrid]+Scrappage_MaaS_fleet[pRS,Hatch,BEV]+MaaS_Scrappage_2014_fleet+((Adopting_MaaS[pRS]-abandoning_MaaS[pRS])*Cars_per_trip[pRS]/Gross_Occupancy_MaaS[pRS]))*MaaS_fleet_tech_changes[pRS,SUV,BEV] {UNIFLOW}

UNITS: cars/Years

Purchasing_MaaS_fleet[pRS, Hatch, Gasoline] = (Scrappage_MaaS_fleet[pRS,Sedan,Gasoline]+Scrappage_MaaS_fleet[pRS,Sedan,Hybrid]+Scrappage_MaaS_fleet[pRS,Sedan,BEV]+Scrappage_MaaS_fleet[pRS,SUV,Gasoline]+Scrappage_MaaS_fleet[pRS,SUV,Hybrid]+Scrappage_MaaS_fleet[pRS,SUV,BEV]+Scrappage_MaaS_fleet[pRS,Hatch,Gasoline]+Scrappage_MaaS_fleet[pRS,Hatch,Hybrid]+Scrappage_MaaS_fleet[pRS,Hatch,BEV]+MaaS_Scrappage_2014_fleet+((Adopting_MaaS[pRS]-abandoning_MaaS[pRS])*Cars_per_trip[pRS]/Gross_Occupancy_MaaS[pRS]))*MaaS_fleet_tech_changes[pRS,Hatch,Gasoline] {UNIFLOW}

UNITS: cars/Years

Purchasing_MaaS_fleet[pRS, Hatch, Hybrid] = (Scrappage_MaaS_fleet[pRS,Sedan,Gasoline]+Scrappage_MaaS_fleet[pRS,Sedan,Hybrid]+Scrappage_MaaS_fleet[pRS,Sedan,BEV]+Scrappage_MaaS_fleet[pRS,SUV,Gasoline]+Scrappage_MaaS_fleet[pRS,SUV,Hybrid]+Scrappage_MaaS_fleet[pRS,SUV,BEV]+Scrappage_MaaS_fleet[pRS,Hatch,Gasoline]+Scrappage_MaaS_fleet[pRS,Hatch,Hybrid]+Scrappage_MaaS_fleet[pRS,Hatch,BEV]+MaaS_Scrappage_2014_fleet+((Adopting_MaaS[pRS]-abandoning_MaaS[pRS])*Cars_per_trip[pRS]/Gross_Occupancy_MaaS[pRS]))*MaaS_fleet_tech_changes[pRS,Hatch,Hybrid] {UNIFLOW}

UNITS: cars/Years

Purchasing_MaaS_fleet[pRS, Hatch, BEV] = (Scrappage_MaaS_fleet[pRS,Sedan,Gasoline]+Scrappage_MaaS_fleet[pRS,Sedan,Hybrid]+Scrappage_MaaS_fleet[pRS,Sedan,BEV]+Scrappage_MaaS_fleet[pRS,SUV,Gasoline]+Scrappage_MaaS_fleet[pRS,SUV,Hybrid]+Scrappage_MaaS_fleet[pRS,SUV,BEV]+Scrappage_MaaS_fleet[pRS,Hatch,Gasoline]+Scrappage_MaaS_fleet[pRS,Hatch,Hybrid]+Scrappage_MaaS_fleet[pRS,Hatch,BEV]+MaaS_Scrappage_2014_fleet+((Adopting_MaaS[pRS]-abandoning_MaaS[pRS])*Cars_per_trip[pRS]/Gross_Occupancy_MaaS[pRS]))*MaaS_fleet_tech_changes[pRS,Hatch,BEV] {UNIFLOW}

UNITS: cars/Years

UNITS: cars/Years

OUTFLOWS:

Scrappage_MaaS_fleet[CP, Sedan, Gasoline] = DELAYN(Purchasing_MaaS_fleet[CP,Sedan,Gasoline], Delay_function_MaaS[CP,Sedan],4, 0) {UNIFLOW}

UNITS: cars/Years

Scrappage_MaaS_fleet[CP, Sedan, Hybrid] = DELAYN(Purchasing_MaaS_fleet[CP,Sedan,Hybrid], Delay_function_MaaS[CP,Sedan], 4, 0) {UNIFLOW}

UNITS: cars/Years

Scrappage_MaaS_fleet[CP, Sedan, BEV] = DELAYN((Purchasing_MaaS_fleet[CP,Sedan,BEV]), Delay_function_MaaS[CP,Sedan], 4, 0) {UNIFLOW}

UNITS: cars/Years

Scrappage_MaaS_fleet[CP, SUV, Gasoline] = DELAYN(Purchasing_MaaS_fleet[CP,SUV,Gasoline], Delay_function_MaaS[CP,SUV],4, 0) {UNIFLOW}
UNITS: cars/Years
Scrappage_MaaS_fleet[CP, SUV, Hybrid] = DELAYN((Purchasing_MaaS_fleet[CP,SUV,Hybrid]),Delay_function_MaaS[CP,SUV], 4, 0) {UNIFLOW}
UNITS: cars/Years
Scrappage_MaaS_fleet[CP, SUV, BEV] = DELAYN((Purchasing_MaaS_fleet[CP,SUV,BEV]),Delay_function_MaaS[CP,SUV], 4, 0) {UNIFLOW}
UNITS: cars/Years
Scrappage_MaaS_fleet[CP, Hatch, Gasoline] = DELAYN((Purchasing_MaaS_fleet[CP,Hatch,Gasoline]), Delay_function_MaaS[CP,Hatch], 4, 0) {UNIFLOW}
UNITS: cars/Years
Scrappage_MaaS_fleet[CP, Hatch, Hybrid] = DELAYN((Purchasing_MaaS_fleet[CP,Hatch,Hybrid]), Delay_function_MaaS[CP,Hatch], 4, 0) {UNIFLOW}
UNITS: cars/Years
Scrappage_MaaS_fleet[CP, Hatch, BEV] = DELAYN((Purchasing_MaaS_fleet[CP,Hatch,BEV]), Delay_function_MaaS[CP,Hatch], 4, 0) {UNIFLOW}
UNITS: cars/Years
Scrappage_MaaS_fleet[sRS, Sedan, Gasoline] = DELAYN(Purchasing_MaaS_fleet[sRS,Sedan,Gasoline], Delay_function_MaaS[sRS,Sedan],4, 0) {UNIFLOW}
UNITS: cars/Years
Scrappage_MaaS_fleet[sRS, Sedan, Hybrid] = DELAYN((Purchasing_MaaS_fleet[sRS,Sedan,Hybrid]), Delay_function_MaaS[sRS,Sedan], 4, 0) {UNIFLOW}
UNITS: cars/Years
Scrappage_MaaS_fleet[sRS, Sedan, BEV] = DELAYN((Purchasing_MaaS_fleet[sRS,Sedan,BEV]), Delay_function_MaaS[sRS,Sedan], 4, 0) {UNIFLOW}
UNITS: cars/Years
Scrappage_MaaS_fleet[sRS, SUV, Gasoline] = DELAYN((Purchasing_MaaS_fleet[sRS,SUV,Gasoline]), Delay_function_MaaS[sRS,SUV],4, 0) {UNIFLOW}
UNITS: cars/Years
Scrappage_MaaS_fleet[sRS, SUV, Hybrid] = DELAYN((Purchasing_MaaS_fleet[sRS,SUV,Hybrid]),Delay_function_MaaS[sRS,SUV], 4, 0) {UNIFLOW}
UNITS: cars/Years
Scrappage_MaaS_fleet[sRS, SUV, BEV] = DELAYN((Purchasing_MaaS_fleet[sRS,SUV,BEV]), Delay_function_MaaS[sRS,SUV], 4, 0) {UNIFLOW}
UNITS: cars/Years
Scrappage_MaaS_fleet[sRS, Hatch, Gasoline] = DELAYN((Purchasing_MaaS_fleet[sRS,Hatch,Gasoline]), Delay_function_MaaS[sRS,Hatch], 4, 0) {UNIFLOW}
UNITS: cars/Years
Scrappage_MaaS_fleet[sRS, Hatch, Hybrid] = DELAYN((Purchasing_MaaS_fleet[sRS,Hatch,Hybrid]), Delay_function_MaaS[sRS,Hatch], 4, 0) {UNIFLOW}
UNITS: cars/Years
Scrappage_MaaS_fleet[sRS, Hatch, BEV] = DELAYN((Purchasing_MaaS_fleet[sRS,Hatch,BEV]), Delay_function_MaaS[sRS,Hatch], 4, 0) {UNIFLOW}
UNITS: cars/Years

Scrappage_MaaS_fleet[pRS, Sedan, Gasoline] = DELAYN(Purchasing_MaaS_fleet[pRS,Sedan,Gasoline], Delay_function_MaaS[pRS,Sedan],4, 0) {UNIFLOW}
UNITS: cars/Years
Scrappage_MaaS_fleet[pRS, Sedan, Hybrid] = DELAYN((Purchasing_MaaS_fleet[pRS,Sedan,Hybrid]), Delay_function_MaaS[pRS,Sedan], 4, 0) {UNIFLOW}
UNITS: cars/Years
Scrappage_MaaS_fleet[pRS, Sedan, BEV] = DELAYN((Purchasing_MaaS_fleet[pRS,Sedan,BEV]), Delay_function_MaaS[pRS,Sedan], 4, 0) {UNIFLOW}
UNITS: cars/Years
Scrappage_MaaS_fleet[pRS, SUV, Gasoline] = DELAYN(Purchasing_MaaS_fleet[CP,SUV,Gasoline], Delay_function_MaaS[CP,SUV],4, 0) {UNIFLOW}
UNITS: cars/Years
Scrappage_MaaS_fleet[pRS, SUV, Hybrid] = DELAYN((Purchasing_MaaS_fleet[pRS,SUV,Hybrid]), Delay_function_MaaS[pRS,SUV], 4, 0) {UNIFLOW}
UNITS: cars/Years
Scrappage_MaaS_fleet[pRS, SUV, BEV] = DELAYN((Purchasing_MaaS_fleet[pRS,SUV,BEV]), Delay_function_MaaS[pRS,SUV], 4, 0) {UNIFLOW}
UNITS: cars/Years
Scrappage_MaaS_fleet[pRS, Hatch, Gasoline] = DELAYN((Purchasing_MaaS_fleet[pRS,Hatch,Gasoline]), Delay_function_MaaS[pRS,Hatch], 4, 0) {UNIFLOW}
UNITS: cars/Years
Scrappage_MaaS_fleet[pRS, Hatch, Hybrid] = DELAYN((Purchasing_MaaS_fleet[pRS,Hatch,Hybrid]), Delay_function_MaaS[pRS,Hatch], 4, 0) {UNIFLOW}
UNITS: cars/Years
Scrappage_MaaS_fleet[pRS, Hatch, BEV] = DELAYN((Purchasing_MaaS_fleet[pRS,Hatch,BEV]), Delay_function_MaaS[pRS,Hatch], 4, 0) {UNIFLOW}
UNITS: cars/Years
UNITS: cars/Years
PC_fleet_2014[Sedan, Gasoline](t) = PC_fleet_2014[Sedan, Gasoline](t - dt) + (- PC_Scrappage_2014_fleet[Sedan, Gasoline]) * dt {NON-NEGATIVE}
INIT PC_fleet_2014[Sedan, Gasoline] = 80199770
UNITS: cars
PC_fleet_2014[Sedan, Hybrid](t) = PC_fleet_2014[Sedan, Hybrid](t - dt) + (- PC_Scrappage_2014_fleet[Sedan, Hybrid]) * dt {NON-NEGATIVE}
INIT PC_fleet_2014[Sedan, Hybrid] = 2135718
UNITS: cars
PC_fleet_2014[Sedan, BEV](t) = PC_fleet_2014[Sedan, BEV](t - dt) + (- PC_Scrappage_2014_fleet[Sedan, BEV]) * dt {NON-NEGATIVE}
INIT PC_fleet_2014[Sedan, BEV] = 55187
UNITS: cars
PC_fleet_2014[SUV, Gasoline](t) = PC_fleet_2014[SUV, Gasoline](t - dt) + (- PC_Scrappage_2014_fleet[SUV, Gasoline]) * dt {NON-NEGATIVE}
INIT PC_fleet_2014[SUV, Gasoline] = 9478939
UNITS: cars
PC_fleet_2014[SUV, Hybrid](t) = PC_fleet_2014[SUV, Hybrid](t - dt) + (- PC_Scrappage_2014_fleet[SUV, Hybrid]) * dt {NON-NEGATIVE}
INIT PC_fleet_2014[SUV, Hybrid] = 69389

UNITS: cars
PC_fleet_2014[SUV, BEV](t) = PC_fleet_2014[SUV, BEV](t - dt) + (- PC_Scrappage_2014_fleet[SUV, BEV]) * dt {NON-NEGATIVE}
INIT PC_fleet_2014[SUV, BEV] = 637
UNITS: cars
PC_fleet_2014[Hatch, Gasoline](t) = PC_fleet_2014[Hatch, Gasoline](t - dt) + (- PC_Scrappage_2014_fleet[Hatch, Gasoline]) * dt {NON-NEGATIVE}
INIT PC_fleet_2014[Hatch, Gasoline] = 4216830
UNITS: cars
PC_fleet_2014[Hatch, Hybrid](t) = PC_fleet_2014[Hatch, Hybrid](t - dt) + (- PC_Scrappage_2014_fleet[Hatch, Hybrid]) * dt {NON-NEGATIVE}
INIT PC_fleet_2014[Hatch, Hybrid] = 112406
UNITS: cars
PC_fleet_2014[Hatch, BEV](t) = PC_fleet_2014[Hatch, BEV](t - dt) + (- PC_Scrappage_2014_fleet[Hatch, BEV]) * dt {NON-NEGATIVE}
INIT PC_fleet_2014[Hatch, BEV] = 2905
UNITS: cars
UNITS: cars
OUTFLOWS:
PC_Scrappage_2014_fleet[Carbody, Powertrain] = Scrap_rate_PC_fleet_2014*PC_fleet_2014 {UNIFLOW}
UNITS: cars/Years
PC_fleet_2014_onwards[Carbody, Powertrain](t) = PC_fleet_2014_onwards[Carbody, Powertrain](t - dt) + (Purchasing_PC[Carbody, Powertrain] - Scrappage_PC[Carbody, Powertrain]) * dt {NON-NEGATIVE}
INIT PC_fleet_2014_onwards[Carbody, Powertrain] = 1
UNITS: cars
INFLOWS:
Purchasing_PC[Sedan, Gasoline] = (Scrappage_PC[Sedan,Gasoline]+Scrappage_PC[Sedan,Hybrid]+Scrappage_PC[Sedan,BEV]+Scrappage_PC[SUV,Gasoline]+Scrappage_PC[SUV,Hybrid]+Scrappage_PC[SUV,BEV]+Scrappage_PC[Hatch,Gasoline]+Scrappage_PC[Hatch,Hybrid]+Scrappage_PC[Hatch,BEV]+PC_Scrappage_2014_fleet+PC_to_user_ratio*(Gaining_PC_users+abandoning_MaaS[CP]+abandoning_MaaS[sRS]+abandoning_MaaS[pRS]))*PC_fleet_tech_changes[Sedan,Gasoline] {UNIFLOW}
UNITS: cars/Years
Purchasing_PC[Sedan, Hybrid] = (Scrappage_PC[Sedan,Gasoline]+Scrappage_PC[Sedan,Hybrid]+Scrappage_PC[Sedan,BEV]+Scrappage_PC[SUV,Gasoline]+Scrappage_PC[SUV,Hybrid]+Scrappage_PC[SUV,BEV]+Scrappage_PC[Hatch,Gasoline]+Scrappage_PC[Hatch,Hybrid]+Scrappage_PC[Hatch,BEV]+PC_Scrappage_2014_fleet+PC_to_user_ratio*(Gaining_PC_users+abandoning_MaaS[CP]+abandoning_MaaS[sRS]+abandoning_MaaS[pRS]))*PC_fleet_tech_changes[Sedan,Hybrid] {UNIFLOW}
UNITS: cars/Years
Purchasing_PC[Sedan, BEV] = (Scrappage_PC[Sedan,Gasoline]+Scrappage_PC[Sedan,Hybrid]+Scrappage_PC[Sedan,BEV]+Scrappage_PC[SUV,Gasoline]+Scrappage_PC[SUV,Hybrid]+Scrappage_PC[SUV,BEV]+Scrappage_PC[Hatch,Gasoline]+Scrappage_PC[Hatch,Hybrid]+Scrappage_PC[Hatch,BEV]+PC_Scrappage_2014_fleet+PC_to_user_ratio*(Gaining_PC_users+abandoning_MaaS[CP]+abandoning_MaaS[sRS]+abandoning_MaaS[pRS]))*PC_fleet_tech_changes[Sedan,BEV] {UNIFLOW}
UNITS: cars/Years

Purchasing_PC[SUV, Gasoline] =
(Scrappage_PC[Sedan,Gasoline]+Scrappage_PC[Sedan,Hybrid]+Scrappage_PC[Sedan,BEV]+Scrappage_PC[SUV,Gasoline]+Scrappage_PC[SUV,Hybrid]+Scrappage_PC[SUV,BEV]+Scrappage_PC[Hatch,Gasoline]+Scrappage_PC[Hatch,Hybrid]+Scrappage_PC[Hatch,BEV]+PC_Scrappage_2014_fleet+PC_to_user_ratio*(Gaining_PC_users+abandoning_MaaS[CP]+abandoning_MaaS[sRS]+abandoning_MaaS[pRS]))*PC_fleet_tech_changes[SUV,Gasoline] {UNIFLOW}

UNITS: cars/Years

Purchasing_PC[SUV, Hybrid] =
(Scrappage_PC[Sedan,Gasoline]+Scrappage_PC[Sedan,Hybrid]+Scrappage_PC[Sedan,BEV]+Scrappage_PC[SUV,Gasoline]+Scrappage_PC[SUV,Hybrid]+Scrappage_PC[SUV,BEV]+Scrappage_PC[Hatch,Gasoline]+Scrappage_PC[Hatch,Hybrid]+Scrappage_PC[Hatch,BEV]+PC_Scrappage_2014_fleet+PC_to_user_ratio*(Gaining_PC_users+abandoning_MaaS[CP]+abandoning_MaaS[sRS]+abandoning_MaaS[pRS]))*PC_fleet_tech_changes[SUV,Hybrid] {UNIFLOW}

UNITS: cars/Years

Purchasing_PC[SUV, BEV] =
(Scrappage_PC[Sedan,Gasoline]+Scrappage_PC[Sedan,Hybrid]+Scrappage_PC[Sedan,BEV]+Scrappage_PC[SUV,Gasoline]+Scrappage_PC[SUV,Hybrid]+Scrappage_PC[SUV,BEV]+Scrappage_PC[Hatch,Gasoline]+Scrappage_PC[Hatch,Hybrid]+Scrappage_PC[Hatch,BEV]+PC_Scrappage_2014_fleet+PC_to_user_ratio*(Gaining_PC_users+abandoning_MaaS[CP]+abandoning_MaaS[sRS]+abandoning_MaaS[pRS]))*PC_fleet_tech_changes[SUV,BEV] {UNIFLOW}

UNITS: cars/Years

Purchasing_PC[Hatch, Gasoline] =
(Scrappage_PC[Sedan,Gasoline]+Scrappage_PC[Sedan,Hybrid]+Scrappage_PC[Sedan,BEV]+Scrappage_PC[SUV,Gasoline]+Scrappage_PC[SUV,Hybrid]+Scrappage_PC[SUV,BEV]+Scrappage_PC[Hatch,Gasoline]+Scrappage_PC[Hatch,Hybrid]+Scrappage_PC[Hatch,BEV]+PC_Scrappage_2014_fleet+PC_to_user_ratio*(Gaining_PC_users+abandoning_MaaS[CP]+abandoning_MaaS[sRS]+abandoning_MaaS[pRS]))*PC_fleet_tech_changes[Hatch,Gasoline] {UNIFLOW}

UNITS: cars/Years

Purchasing_PC[Hatch, Hybrid] =
(Scrappage_PC[Sedan,Gasoline]+Scrappage_PC[Sedan,Hybrid]+Scrappage_PC[Sedan,BEV]+Scrappage_PC[SUV,Gasoline]+Scrappage_PC[SUV,Hybrid]+Scrappage_PC[SUV,BEV]+Scrappage_PC[Hatch,Gasoline]+Scrappage_PC[Hatch,Hybrid]+Scrappage_PC[Hatch,BEV]+PC_Scrappage_2014_fleet+PC_to_user_ratio*(Gaining_PC_users+abandoning_MaaS[CP]+abandoning_MaaS[sRS]+abandoning_MaaS[pRS]))*PC_fleet_tech_changes[SUV,Hybrid] {UNIFLOW}

UNITS: cars/Years

Purchasing_PC[Hatch, BEV] =
(Scrappage_PC[Sedan,Gasoline]+Scrappage_PC[Sedan,Hybrid]+Scrappage_PC[Sedan,BEV]+Scrappage_PC[SUV,Gasoline]+Scrappage_PC[SUV,Hybrid]+Scrappage_PC[SUV,BEV]+Scrappage_PC[Hatch,Gasoline]+Scrappage_PC[Hatch,Hybrid]+Scrappage_PC[Hatch,BEV]+PC_Scrappage_2014_fleet+PC_to_user_ratio*(Gaining_PC_users+abandoning_MaaS[CP]+abandoning_MaaS[sRS]+abandoning_MaaS[pRS]))*PC_fleet_tech_changes[Hatch,BEV] {UNIFLOW}

UNITS: cars/Years

UNITS: cars/Years

OUTFLOWS:

Scrappage_PC[Sedan, Gasoline] = DELAYN((Purchasing_PC[Sedan,Gasoline]), Delay_function_PC[Sedan], 4, 0) {UNIFLOW}

UNITS: cars/Years

Scrappage_PC[Sedan, Hybrid] = DELAYN((Purchasing_PC[Sedan,Hybrid]), Delay_function_PC[Sedan], 4, 0) {UNIFLOW}

UNITS: cars/Years

Scrappage_PC[Sedan, BEV] = DELAYN((Purchasing_PC[Sedan,BEV]), Delay_function_PC[Sedan], 4, 0) {UNIFLOW}

UNITS: cars/Years
Scrappage_PC[SUV, Gasoline] = DELAYN((Purchasing_PC[SUV,Gasoline]), Delay_function_PC[SUV], 4, 0) {UNIFLOW}
UNITS: cars/Years
Scrappage_PC[SUV, Hybrid] = DELAYN((Purchasing_PC[SUV,Hybrid]), Delay_function_PC[SUV], 4, 0) {UNIFLOW}
UNITS: cars/Years
Scrappage_PC[SUV, BEV] = DELAYN((Purchasing_PC[SUV,BEV]), Delay_function_PC[SUV], 4, 0) {UNIFLOW}
UNITS: cars/Years
Scrappage_PC[Hatch, Gasoline] = DELAYN((Purchasing_PC[Hatch,Gasoline]), Delay_function_PC[Hatch], 4, 0) {UNIFLOW}
UNITS: cars/Years
Scrappage_PC[Hatch, Hybrid] = DELAYN((Purchasing_PC[Hatch,Hybrid]), Delay_function_PC[Hatch], 4, 0) {UNIFLOW}
UNITS: cars/Years
Scrappage_PC[Hatch, BEV] = DELAYN((Purchasing_PC[Hatch,BEV]), Delay_function_PC[Hatch], 4, 0) {UNIFLOW}
UNITS: cars/Years
UNITS: cars/Years

"#passenger_attractiveness"[CP] = EXP(Utility_function_#passenger[CP,passengers2]*"#Passenger_distribution"[CP,passengers2]+Utility_function_#passenger[CP,passengers3]*"#Passenger_distribution"[CP,passengers3]+Utility_function_#passenger[CP,passengers4]*"#Passenger_distribution"[CP,passengers4]+Utility_function_#passenger[CP,passengers5]*"#Passenger_distribution"[CP,passengers5])/(EXP(Utility_function_#passenger[CP,passengers2]*"#Passenger_distribution"[CP,passengers2]+Utility_function_#passenger[CP,passengers3]*"#Passenger_distribution"[CP,passengers3]+Utility_function_#passenger[CP,passengers4]*"#Passenger_distribution"[CP,passengers4]+Utility_function_#passenger[CP,passengers5]*"#Passenger_distribution"[CP,passengers5])+EXP(Utility_function_#passenger[pRS,passengers2]*"#Passenger_distribution"[pRS,passengers2]+Utility_function_#passenger[pRS,passengers3]*"#Passenger_distribution"[pRS,passengers3]+Utility_function_#passenger[pRS,passengers4]*"#Passenger_distribution"[pRS,passengers4]+Utility_function_#passenger[pRS,passengers5]*"#Passenger_distribution"[pRS,passengers5]))
UNITS: Dimensionless

"#passenger_attractiveness"[sRS] = 0
UNITS: Dimensionless

"#passenger_attractiveness"[pRS] = EXP(Utility_function_#passenger[pRS,passengers2]*"#Passenger_distribution"[pRS,passengers2]+Utility_function_#passenger[pRS,passengers3]*"#Passenger_distribution"[pRS,passengers3]+Utility_function_#passenger[pRS,passengers4]*"#Passenger_distribution"[pRS,passengers4]+Utility_function_#passenger[pRS,passengers5]*"#Passenger_distribution"[pRS,passengers5])/(EXP(Utility_function_#passenger[CP,passengers2]*"#Passenger_distribution"[CP,passengers2]+Utility_function_#passenger[CP,passengers3]*"#Passenger_distribution"[CP,passengers3]+Utility_function_#passenger[CP,passengers4]*"#Passenger_distribution"[CP,passengers4]+Utility_function_#passenger[CP,passengers5]*"#Passenger_distribution"[CP,passengers5])+EXP(Utility_function_#passenger[pRS,passengers2]*"#Passenger_distribution"[pRS,passengers2]+Utility_function_#passenger[pRS,passengers3]*"#Passenger_distribution"[pRS,passengers3]+Utility_function_#passenger[pRS,passengers4]*"#Passenger_distribution"[pRS,passengers4]+Utility_function_#passenger[pRS,passengers5]*"#Passenger_distribution"[pRS,passengers5]))
UNITS: Dimensionless
UNITS: Dimensionless

"#Passenger_distribution"[CP, passengers2] =.92
UNITS: Dimensionless

"#Passenger_distribution"[CP, passengers3] =.06
UNITS: Dimensionless
"#Passenger_distribution"[CP, passengers4] =.02
UNITS: Dimensionless
"#Passenger_distribution"[CP, passengers5] = 0
UNITS: Dimensionless
"#Passenger_distribution"[sRS, passengers2] = 0
UNITS: Dimensionless
"#Passenger_distribution"[sRS, passengers3] = 0
UNITS: Dimensionless
"#Passenger_distribution"[sRS, passengers4] = 0
UNITS: Dimensionless
"#Passenger_distribution"[sRS, passengers5] = 0
UNITS: Dimensionless
"#Passenger_distribution"[pRS, passengers2] =.93
UNITS: Dimensionless
"#Passenger_distribution"[pRS, passengers3] =.06
UNITS: Dimensionless
"#Passenger_distribution"[pRS, passengers4] =.01
UNITS: Dimensionless
"#Passenger_distribution"[pRS, passengers5] = 0
UNITS: Dimensionless
UNITS: Dimensionless
Abandonment_rate[CP] =.1
UNITS: Per Year
Abandonment_rate[sRS] =.1
UNITS: Per Year
Abandonment_rate[pRS] =.1
UNITS: Per Year
UNITS: Per Year
Adoption_fraction[MaaS_Mode] =.01
UNITS: Per Year
Adoption_from_advert[MaaS_Mode] =
Effect_of_advertising*(Commuting_employees_by_private_vehicles-Active_MaaS_users)
UNITS: person/year
Adoption_from_WoM[MaaS_Mode] =
Contact_rate_with_Active_Customers*Adoption_fraction*((MaaS_mode_attractiveness*Commuting_employees_by_private_vehicles)-
Active_MaaS_users)*Active_MaaS_users/Commuting_employees_by_private_vehicles
UNITS: person/year
avg_gross_trip_distance_MaaS[CP] = 23.10*260
UNITS: km/year
avg_gross_trip_distance_MaaS[sRS] = 28.93*260*2
UNITS: km/year
avg_gross_trip_distance_MaaS[pRS] = 30.6*260*2
UNITS: km/year
UNITS: km/year
avg_trip_distance_PC = 20.6*260

UNITS: km/year
Car_based_mobility =.65
UNITS: Dimensionless
Cars_per_trip[CP] = 1
UNITS: cars/trip
Cars_per_trip[sRS] = 0.5
UNITS: cars/trip
Cars_per_trip[pRS] = 0.5
UNITS: cars/trip
UNITS: cars/trip
Contact_rate_with_Active_Customers[MaaS_Mode] = 110
UNITS: Dimensionless
Delay_function_MaaS[CP, Sedan] = 15
UNITS: Per Year
Delay_function_MaaS[CP, SUV] = 16.5
UNITS: Per Year
Delay_function_MaaS[CP, Hatch] = 15
UNITS: Per Year
Delay_function_MaaS[sRS, Sedan] = 6.25
UNITS: Per Year
Delay_function_MaaS[sRS, SUV] = 6.25
UNITS: Per Year
Delay_function_MaaS[sRS, Hatch] = 6.25
UNITS: Per Year
Delay_function_MaaS[pRS, Sedan] = 6.25
UNITS: Per Year
Delay_function_MaaS[pRS, SUV] = 6.25
UNITS: Per Year
Delay_function_MaaS[pRS, Hatch] = 6.25
UNITS: Per Year
UNITS: Per Year
Delay_function_PC[Sedan] = 15
UNITS: Per Year
Delay_function_PC[SUV] = 16.5
UNITS: Per Year
Delay_function_PC[Hatch] = 15
UNITS: Per Year
UNITS: Per Year
distance_MaaS_fleet[CP, Sedan, Gasoline] = avg_gross_trip_distance_MaaS[CP]*Active_MaaS_users[CP]*Tot_MaaS_fleet[CP,Sedan,Gasoline]/(Tot_MaaS_fleet[CP,Sedan,Gasoline]+Tot_MaaS_fleet[CP,Sedan,Hybrid]+Tot_MaaS_fleet[CP,Sedan,BEV]+Tot_MaaS_fleet[CP,SUV,Gasoline]+Tot_MaaS_fleet[CP,SUV,Hybrid]+Tot_MaaS_fleet[CP,SUV,BEV]+Tot_MaaS_fleet[CP,Hatch,Gasoline]+Tot_MaaS_fleet[CP,Hatch,Hybrid]+Tot_MaaS_fleet[CP,Hatch,BEV]+Tot_MaaS_fleet[sRS,Sedan,Gasoline]+Tot_MaaS_fleet[sRS,Sedan,Hybrid]+Tot_MaaS_fleet[sRS,Sedan,BEV]+Tot_MaaS_fleet[sRS,SUV,Gasoline]+Tot_MaaS_fleet[sRS,SUV,Hybrid]+Tot_MaaS_fleet[sRS,SUV,BEV]+Tot_MaaS_fleet[sRS,Hatch,Gasoline]+Tot_MaaS_fleet[sRS,Hatch,Hybrid]+Tot_MaaS_fleet[sRS,Hatch,BEV]+Tot_MaaS_fleet[pRS,Sedan,Gasoline]+Tot_MaaS_fleet[pRS,Sedan,Hybrid]+Tot_MaaS_fleet[pRS,Sedan,BEV]+Tot_MaaS_fleet[pRS,SUV,Gasoline]+Tot_MaaS_fleet[pRS,SUV,Hybrid]+Tot_Maa

S_fleet[pRS,SUV,BEV]+Tot_MaaS_fleet[pRS,Hatch,Gasoline]+Tot_MaaS_fleet[pRS,Hatch,Hybrid]+Tot_MaaS_fleet[pRS,Hatch,BEV])

UNITS: cars*km/year

distance_MaaS_fleet[CP, Sedan, Hybrid] = avg_gross_trip_distance_MaaS[CP]*Active_MaaS_users[CP]*Tot_MaaS_fleet[CP,Sedan,Hybrid]/(Tot_MaaS_fleet[CP,Sedan,Gasoline]+Tot_MaaS_fleet[CP,Sedan,Hybrid]+Tot_MaaS_fleet[CP,Sedan,BEV]+Tot_MaaS_fleet[CP,SUV,Gasoline]+Tot_MaaS_fleet[CP,SUV,Hybrid]+Tot_MaaS_fleet[CP,SUV,BEV]+Tot_MaaS_fleet[CP,Hatch,Gasoline]+Tot_MaaS_fleet[CP,Hatch,Hybrid]+Tot_MaaS_fleet[CP,Hatch,BEV]+Tot_MaaS_fleet[sRS,Sedan,Gasoline]+Tot_MaaS_fleet[sRS,Sedan,Hybrid]+Tot_MaaS_fleet[sRS,Sedan,BEV]+Tot_MaaS_fleet[sRS,SUV,Gasoline]+Tot_MaaS_fleet[sRS,SUV,Hybrid]+Tot_MaaS_fleet[sRS,SUV,BEV]+Tot_MaaS_fleet[sRS,Hatch,Gasoline]+Tot_MaaS_fleet[sRS,Hatch,Hybrid]+Tot_MaaS_fleet[sRS,Hatch,BEV]+Tot_MaaS_fleet[pRS,Sedan,Gasoline]+Tot_MaaS_fleet[pRS,Sedan,Hybrid]+Tot_MaaS_fleet[pRS,Sedan,BEV]+Tot_MaaS_fleet[pRS,SUV,Gasoline]+Tot_MaaS_fleet[pRS,SUV,Hybrid]+Tot_MaaS_fleet[pRS,SUV,BEV]+Tot_MaaS_fleet[pRS,Hatch,Gasoline]+Tot_MaaS_fleet[pRS,Hatch,Hybrid]+Tot_MaaS_fleet[pRS,Hatch,BEV])

UNITS: cars*km/year

distance_MaaS_fleet[CP, Sedan, BEV] = avg_gross_trip_distance_MaaS[CP]*Active_MaaS_users[CP]*Tot_MaaS_fleet[CP,Sedan,BEV]/(Tot_MaaS_fleet[CP,Sedan,Gasoline]+Tot_MaaS_fleet[CP,Sedan,Hybrid]+Tot_MaaS_fleet[CP,Sedan,BEV]+Tot_MaaS_fleet[CP,SUV,Gasoline]+Tot_MaaS_fleet[CP,SUV,Hybrid]+Tot_MaaS_fleet[CP,SUV,BEV]+Tot_MaaS_fleet[CP,Hatch,Gasoline]+Tot_MaaS_fleet[CP,Hatch,Hybrid]+Tot_MaaS_fleet[CP,Hatch,BEV]+Tot_MaaS_fleet[sRS,Sedan,Gasoline]+Tot_MaaS_fleet[sRS,Sedan,Hybrid]+Tot_MaaS_fleet[sRS,Sedan,BEV]+Tot_MaaS_fleet[sRS,SUV,Gasoline]+Tot_MaaS_fleet[sRS,SUV,Hybrid]+Tot_MaaS_fleet[sRS,SUV,BEV]+Tot_MaaS_fleet[sRS,Hatch,Gasoline]+Tot_MaaS_fleet[sRS,Hatch,Hybrid]+Tot_MaaS_fleet[sRS,Hatch,BEV]+Tot_MaaS_fleet[pRS,Sedan,Gasoline]+Tot_MaaS_fleet[pRS,Sedan,Hybrid]+Tot_MaaS_fleet[pRS,Sedan,BEV]+Tot_MaaS_fleet[pRS,SUV,Gasoline]+Tot_MaaS_fleet[pRS,SUV,Hybrid]+Tot_MaaS_fleet[pRS,SUV,BEV]+Tot_MaaS_fleet[pRS,Hatch,Gasoline]+Tot_MaaS_fleet[pRS,Hatch,Hybrid]+Tot_MaaS_fleet[pRS,Hatch,BEV])

UNITS: cars*km/year

distance_MaaS_fleet[CP, SUV, Gasoline] = avg_gross_trip_distance_MaaS[CP]*Active_MaaS_users[CP]*Tot_MaaS_fleet[CP,SUV,Gasoline]/(Tot_MaaS_fleet[CP,Sedan,Gasoline]+Tot_MaaS_fleet[CP,Sedan,Hybrid]+Tot_MaaS_fleet[CP,Sedan,BEV]+Tot_MaaS_fleet[CP,SUV,Gasoline]+Tot_MaaS_fleet[CP,SUV,Hybrid]+Tot_MaaS_fleet[CP,SUV,BEV]+Tot_MaaS_fleet[CP,Hatch,Gasoline]+Tot_MaaS_fleet[CP,Hatch,Hybrid]+Tot_MaaS_fleet[CP,Hatch,BEV]+Tot_MaaS_fleet[sRS,Sedan,Gasoline]+Tot_MaaS_fleet[sRS,Sedan,Hybrid]+Tot_MaaS_fleet[sRS,Sedan,BEV]+Tot_MaaS_fleet[sRS,SUV,Gasoline]+Tot_MaaS_fleet[sRS,SUV,Hybrid]+Tot_MaaS_fleet[sRS,SUV,BEV]+Tot_MaaS_fleet[sRS,Hatch,Gasoline]+Tot_MaaS_fleet[sRS,Hatch,Hybrid]+Tot_MaaS_fleet[sRS,Hatch,BEV]+Tot_MaaS_fleet[pRS,Sedan,Gasoline]+Tot_MaaS_fleet[pRS,Sedan,Hybrid]+Tot_MaaS_fleet[pRS,Sedan,BEV]+Tot_MaaS_fleet[pRS,SUV,Gasoline]+Tot_MaaS_fleet[pRS,SUV,Hybrid]+Tot_MaaS_fleet[pRS,SUV,BEV]+Tot_MaaS_fleet[pRS,Hatch,Gasoline]+Tot_MaaS_fleet[pRS,Hatch,Hybrid]+Tot_MaaS_fleet[pRS,Hatch,BEV])

UNITS: cars*km/year

distance_MaaS_fleet[CP, SUV, Hybrid] = avg_gross_trip_distance_MaaS[CP]*Active_MaaS_users[CP]*Tot_MaaS_fleet[CP,SUV,Hybrid]/(Tot_MaaS_fleet[CP,Sedan,Gasoline]+Tot_MaaS_fleet[CP,Sedan,Hybrid]+Tot_MaaS_fleet[CP,Sedan,BEV]+Tot_MaaS_fleet[CP,SUV,Gasoline]+Tot_MaaS_fleet[CP,SUV,Hybrid]+Tot_MaaS_fleet[CP,SUV,BEV]+Tot_MaaS_fleet[CP,Hatch,Gasoline]+Tot_MaaS_fleet[CP,Hatch,Hybrid]+Tot_MaaS_fleet[CP,Hatch,BEV]+Tot_MaaS_fleet[sRS,Sedan,Gasoline]+Tot_MaaS_fleet[sRS,Sedan,Hybrid]+Tot_MaaS_fleet[sRS,Sedan,BEV]+Tot_MaaS_fleet[sRS,SUV,Gasoline]+Tot_MaaS_fleet[sRS,SUV,Hybrid]+Tot_MaaS_fleet[sRS,SUV,BEV]+Tot_MaaS_fleet[sRS,Hatch,Gasoline]+Tot_MaaS_fleet[sRS,Hatch,Hybrid]+Tot_MaaS_fleet[sRS,Hatch,BEV]+Tot_MaaS_fleet[pRS,Sedan,Gasoline]+Tot_MaaS_fleet[pRS,Sedan,Hybrid]+Tot_MaaS_fleet[pRS,Sedan,BEV]+Tot_MaaS_fleet[pRS,SUV,Gasoline]+Tot_MaaS_fleet[pRS,SUV,Hybrid]+Tot_MaaS_f leet[pRS,SUV,BEV]+Tot_MaaS_fleet[pRS,Hatch,Gasoline]+Tot_MaaS_fleet[pRS,Hatch,Hybrid]+Tot_MaaS_fleet[pRS,Hatch,BEV])

UNITS: cars*km/year

distance_MaaS_fleet[CP, SUV, BEV] = avg_gross_trip_distance_MaaS[CP]*Active_MaaS_users[CP]*Tot_MaaS_fleet[CP,SUV,BEV]/(Tot_MaaS_fleet[CP,Sedan,Gasoline]+Tot_MaaS_fleet[CP,Sedan,Hybrid]+Tot_MaaS_fleet[CP,Sedan,BEV]+Tot_MaaS_fleet[CP,SUV,Gasoline]+Tot_MaaS_fleet[CP,SUV,Hybrid]+Tot_MaaS_fleet[CP,SUV,BEV]+Tot_MaaS_fleet[CP,Hatch,Gasoline]+Tot_MaaS_fleet[CP,Hatch,Hybrid]+Tot_MaaS_fleet[CP,Hatch,BEV]+Tot_MaaS_fleet[sRS,Sedan,Gasoline]+Tot_MaaS_fleet[sRS,Sedan,Hybrid]+Tot_MaaS_fleet[sRS,Sedan,BEV]+Tot_MaaS_fleet[sRS,SUV,Gasoline]+Tot_MaaS_fleet[sRS,SUV,Hybrid]+Tot_MaaS_fleet[sRS,SUV,BEV]+Tot_MaaS_fleet[sRS,Hatch,Gasoline]+Tot_MaaS_fleet[sRS,Hatch,Hybrid]+Tot_MaaS_fleet[sRS,Hatch,BEV]+Tot_MaaS_fleet[pRS,Sedan,Gasoline]+Tot_MaaS_fleet[pRS,Sedan,Hybrid]+Tot_MaaS_fleet[pRS,Sedan,BEV]+Tot_MaaS_fleet[pRS,SUV,Gasoline]+Tot_MaaS_fleet[pRS,SUV,Hybrid]+Tot_MaaS_fleet[pRS,SUV,BEV]+Tot_MaaS_fleet[pRS,Hatch,Gasoline]+Tot_MaaS_fleet[pRS,Hatch,Hybrid]+Tot_MaaS_fleet[pRS,Hatch,BEV])

UNITS: cars*km/year

distance_MaaS_fleet[CP, Hatch, Gasoline] = avg_gross_trip_distance_MaaS[CP]*Active_MaaS_users[CP]*Tot_MaaS_fleet[CP,Hatch,Gasoline]/(Tot_MaaS_fleet[CP,Sedan,Gasoline]+Tot_MaaS_fleet[CP,Sedan,Hybrid]+Tot_MaaS_fleet[CP,Sedan,BEV]+Tot_MaaS_fleet[CP,SUV,Gasoline]+Tot_MaaS_fleet[CP,SUV,Hybrid]+Tot_MaaS_fleet[CP,SUV,BEV]+Tot_MaaS_fleet[CP,Hatch,Gasoline]+Tot_MaaS_fleet[CP,Hatch,Hybrid]+Tot_MaaS_fleet[CP,Hatch,BEV]+Tot_MaaS_fleet[sRS,Sedan,Gasoline]+Tot_MaaS_fleet[sRS,Sedan,Hybrid]+Tot_MaaS_fleet[sRS,Sedan,BEV]+Tot_MaaS_fleet[sRS,SUV,Gasoline]+Tot_MaaS_fleet[sRS,SUV,Hybrid]+Tot_MaaS_fleet[sRS,SUV,BEV]+Tot_MaaS_fleet[sRS,Hatch,Gasoline]+Tot_MaaS_fleet[sRS,Hatch,Hybrid]+Tot_MaaS_fleet[sRS,Hatch,BEV]+Tot_MaaS_fleet[pRS,Sedan,Gasoline]+Tot_MaaS_fleet[pRS,Sedan,Hybrid]+Tot_MaaS_fleet[pRS,Sedan,BEV]+Tot_MaaS_fleet[pRS,SUV,Gasoline]+Tot_MaaS_fleet[pRS,SUV,Hybrid]+Tot_MaaS_fleet[pRS,SUV,BEV]+Tot_MaaS_fleet[pRS,Hatch,Gasoline]+Tot_MaaS_fleet[pRS,Hatch,Hybrid]+Tot_MaaS_fleet[pRS,Hatch,BEV])

UNITS: cars*km/year

distance_MaaS_fleet[CP, Hatch, Hybrid] = avg_gross_trip_distance_MaaS[CP]*Active_MaaS_users[CP]*Tot_MaaS_fleet[CP,Hatch,Hybrid]/(Tot_MaaS_fleet[CP,Sedan,Gasoline]+Tot_MaaS_fleet[CP,Sedan,Hybrid]+Tot_MaaS_fleet[CP,Sedan,BEV]+Tot_MaaS_fleet[CP,SUV,Gasoline]+Tot_MaaS_fleet[CP,SUV,Hybrid]+Tot_MaaS_fleet[CP,SUV,BEV]+Tot_MaaS_fleet[CP,Hatch,Gasoline]+Tot_MaaS_fleet[CP,Hatch,Hybrid]+Tot_MaaS_fleet[CP,Hatch,BEV]+Tot_MaaS_fleet[sRS,Sedan,Gasoline]+Tot_MaaS_fleet[sRS,Sedan,Hybrid]+Tot_MaaS_fleet[sRS,Sedan,BEV]+Tot_MaaS_fleet[sRS,SUV,Gasoline]+Tot_MaaS_fleet[sRS,SUV,Hybrid]+Tot_MaaS_fleet[sRS,SUV,BEV]+Tot_MaaS_fleet[sRS,Hatch,Gasoline]+Tot_MaaS_fleet[sRS,Hatch,Hybrid]+Tot_MaaS_fleet[sRS,Hatch,BEV]+Tot_MaaS_fleet[pRS,Sedan,Gasoline]+Tot_MaaS_fleet[pRS,Sedan,Hybrid]+Tot_MaaS_fleet[pRS,Sedan,BEV]+Tot_MaaS_fleet[pRS,SUV,Gasoline]+Tot_MaaS_fleet[pRS,SUV,Hybrid]+Tot_MaaS_fleet[pRS,SUV,BEV]+Tot_MaaS_fleet[pRS,Hatch,Gasoline]+Tot_MaaS_fleet[pRS,Hatch,Hybrid]+Tot_MaaS_fleet[pRS,Hatch,BEV])

UNITS: cars*km/year

distance_MaaS_fleet[CP, Hatch, BEV] = avg_gross_trip_distance_MaaS[CP]*Active_MaaS_users[CP]*Tot_MaaS_fleet[CP,Hatch,BEV]/(Tot_MaaS_fleet[CP,Sedan,Gasoline]+Tot_MaaS_fleet[CP,Sedan,Hybrid]+Tot_MaaS_fleet[CP,Sedan,BEV]+Tot_MaaS_fleet[CP,SUV,Gasoline]+Tot_MaaS_fleet[CP,SUV,Hybrid]+Tot_MaaS_fleet[CP,SUV,BEV]+Tot_MaaS_fleet[CP,Hatch,Gasoline]+Tot_MaaS_fleet[CP,Hatch,Hybrid]+Tot_MaaS_fleet[CP,Hatch,BEV]+Tot_MaaS_fleet[sRS,Sedan,Gasoline]+Tot_MaaS_fleet[sRS,Sedan,Hybrid]+Tot_MaaS_fleet[sRS,Sedan,BEV]+Tot_MaaS_fleet[sRS,SUV,Gasoline]+Tot_MaaS_fleet[sRS,SUV,Hybrid]+Tot_MaaS_fleet[sRS,SUV,BEV]+Tot_MaaS_fleet[sRS,Hatch,Gasoline]+Tot_MaaS_fleet[sRS,Hatch,Hybrid]+Tot_MaaS_fleet[sRS,Hatch,BEV]+Tot_MaaS_fleet[pRS,Sedan,Gasoline]+Tot_MaaS_fleet[pRS,Sedan,Hybrid]+Tot_MaaS_fleet[pRS,Sedan,BEV]+Tot_MaaS_fleet[pRS,SUV,Gasoline]+Tot_MaaS_fleet[pRS,SUV,Hybrid]+Tot_MaaS_f leet[pRS,SUV,BEV]+Tot_MaaS_fleet[pRS,Hatch,Gasoline]+Tot_MaaS_fleet[pRS,Hatch,Hybrid]+Tot_MaaS_fleet[pRS,Hatch,BEV])

UNITS: cars*km/year

distance_MaaS_fleet[sRS, Sedan, Gasoline] = Tot_MaaS_fleet[sRS,Sedan,Gasoline]*avg_gross_trip_distance_MaaS[sRS]*Active_MaaS_users[sRS]/(Tot_MaaS_fleet[CP,Sedan,Gasoline]+Tot_MaaS_fleet[CP,Sedan,Hybrid]+Tot_MaaS_fleet[CP,Sedan,BEV]+Tot_MaaS_fleet[CP,SUV,Gasoline]+Tot_MaaS_fleet[CP,SUV,Hybrid]+Tot_MaaS_fleet[CP,SUV,BEV]+Tot_MaaS_fleet[CP,Hatch,Gasoline]+Tot_MaaS_fleet[CP,Hatch,Hybrid]+Tot_MaaS_fleet[CP,Hatch,BEV]+Tot_MaaS_fleet[sRS,Sedan,Gasoline]+Tot_MaaS_fleet[sRS,Sedan,Hybrid]+Tot_MaaS_fleet[sRS,Sedan,BEV]+Tot_MaaS_fleet[sRS,SUV,Gasoline]+Tot_MaaS_fleet[sRS,SUV,Hybrid]+Tot_MaaS_fleet[sRS,SUV,BEV]+Tot_MaaS_fleet[sRS,Hatch,Gasoline]+Tot_MaaS_fleet[sRS,Hatch,Hybrid]+Tot_MaaS_fleet[sRS,Hatch,BEV]+Tot_MaaS_fleet[pRS,Sedan,Gasoline]+Tot_MaaS_fleet[pRS,Sedan,Hybrid]+Tot_MaaS_fleet[pRS,Sedan,BEV]+Tot_MaaS_fleet[pRS,SUV,Gasoline]+Tot_MaaS_fleet[pRS,SUV,Hybrid]+Tot_MaaS_fleet[pRS,SUV,BEV]+Tot_MaaS_fleet[pRS,Hatch,Gasoline]+Tot_MaaS_fleet[pRS,Hatch,Hybrid]+Tot_MaaS_fleet[pRS,Hatch,BEV])

UNITS: cars*km/year

distance_MaaS_fleet[sRS, Sedan, Hybrid] = Tot_MaaS_fleet[sRS,Sedan,Hybrid]*avg_gross_trip_distance_MaaS[sRS]*Active_MaaS_users[sRS]/(Tot_MaaS_fleet[CP,Sedan,Gasoline]+Tot_MaaS_fleet[CP,Sedan,Hybrid]+Tot_MaaS_fleet[CP,Sedan,BEV]+Tot_MaaS_fleet[CP,SUV,Gasoline]+Tot_MaaS_fleet[CP,SUV,Hybrid]+Tot_MaaS_fleet[CP,SUV,BEV]+Tot_MaaS_fleet[CP,Hatch,Gasoline]+Tot_MaaS_fleet[CP,Hatch,Hybrid]+Tot_MaaS_fleet[CP,Hatch,BEV]+Tot_MaaS_fleet[sRS,Sedan,Gasoline]+Tot_MaaS_fleet[sRS,Sedan,Hybrid]+Tot_MaaS_fleet[sRS,Sedan,BEV]+Tot_MaaS_fleet[sRS,SUV,Gasoline]+Tot_MaaS_fleet[sRS,SUV,Hybrid]+Tot_MaaS_fleet[sRS,SUV,BEV]+Tot_MaaS_fleet[sRS,Hatch,Gasoline]+Tot_MaaS_fleet[sRS,Hatch,Hybrid]+Tot_MaaS_fleet[sRS,Hatch,BEV]+Tot_MaaS_fleet[pRS,Sedan,Gasoline]+Tot_MaaS_fleet[pRS,Sedan,Hybrid]+Tot_MaaS_fleet[pRS,Sedan,BEV]+Tot_MaaS_fleet[pRS,SUV,Gasoline]+Tot_MaaS_fleet[pRS,SUV,Hybrid]+Tot_MaaS_fleet[pRS,SUV,BEV]+Tot_MaaS_fleet[pRS,Hatch,Gasoline]+Tot_MaaS_fleet[pRS,Hatch,Hybrid]+Tot_MaaS_fleet[pRS,Hatch,BEV])

UNITS: cars*km/year

distance_MaaS_fleet[sRS, Sedan, BEV] = Tot_MaaS_fleet[sRS,Sedan,BEV]*avg_gross_trip_distance_MaaS[sRS]*Active_MaaS_users[sRS]/(Tot_MaaS_fleet[CP,Sedan,Gasoline]+Tot_MaaS_fleet[CP,Sedan,Hybrid]+Tot_MaaS_fleet[CP,Sedan,BEV]+Tot_MaaS_fleet[CP,SUV,Gasoline]+Tot_MaaS_fleet[CP,SUV,Hybrid]+Tot_MaaS_fleet[CP,SUV,BEV]+Tot_MaaS_fleet[CP,Hatch,Gasoline]+Tot_MaaS_fleet[CP,Hatch,Hybrid]+Tot_MaaS_fleet[CP,Hatch,BEV]+Tot_MaaS_fleet[sRS,Sedan,Gasoline]+Tot_MaaS_fleet[sRS,Sedan,Hybrid]+Tot_MaaS_fleet[sRS,Sedan,BEV]+Tot_MaaS_fleet[sRS,SUV,Gasoline]+Tot_MaaS_fleet[sRS,SUV,Hybrid]+Tot_MaaS_fleet[sRS,SUV,BEV]+Tot_MaaS_fleet[sRS,Hatch,Gasoline]+Tot_MaaS_fleet[sRS,Hatch,Hybrid]+Tot_MaaS_fleet[sRS,Hatch,BEV]+Tot_MaaS_fleet[pRS,Sedan,Gasoline]+Tot_MaaS_fleet[pRS,Sedan,Hybrid]+Tot_MaaS_fleet[pRS,Sedan,BEV]+Tot_MaaS_fleet[pRS,SUV,Gasoline]+Tot_MaaS_fleet[pRS,SUV,Hybrid]+Tot_MaaS_fleet[pRS,SUV,BEV]+Tot_MaaS_fleet[pRS,Hatch,Gasoline]+Tot_MaaS_fleet[pRS,Hatch,Hybrid]+Tot_MaaS_fleet[pRS,Hatch,BEV])

UNITS: cars*km/year

distance_MaaS_fleet[sRS, SUV, Gasoline] = Tot_MaaS_fleet[sRS,SUV,Gasoline]*avg_gross_trip_distance_MaaS[sRS]*Active_MaaS_users[sRS]/(Tot_MaaS_fleet[CP,Sedan,Gasoline]+Tot_MaaS_fleet[CP,Sedan,Hybrid]+Tot_MaaS_fleet[CP,Sedan,BEV]+Tot_MaaS_fleet[CP,SUV,Gasoline]+Tot_MaaS_fleet[CP,SUV,Hybrid]+Tot_MaaS_fleet[CP,SUV,BEV]+Tot_MaaS_fleet[CP,Hatch,Gasoline]+Tot_MaaS_fleet[CP,Hatch,Hybrid]+Tot_MaaS_fleet[CP,Hatch,BEV]+Tot_MaaS_fleet[sRS,Sedan,Gasoline]+Tot_MaaS_fleet[sRS,Sedan,Hybrid]+Tot_MaaS_fleet[sRS,Sedan,BEV]+Tot_MaaS_fleet[sRS,SUV,Gasoline]+Tot_MaaS_fleet[sRS,SUV,Hybrid]+Tot_MaaS_fleet[sRS,SUV,BEV]+Tot_MaaS_fleet[sRS,Hatch,Gasoline]+Tot_MaaS_fleet[sRS,Hatch,Hybrid]+Tot_MaaS_fleet[sRS,Hatch,BEV]+Tot_MaaS_fleet[pRS,Sedan,Gasoline]+Tot_MaaS_fleet[pRS,Sedan,Hybrid]+Tot_MaaS_fleet[pRS,Sedan,BEV]+Tot_MaaS_fleet[pRS,SUV,Gasoline]+Tot_MaaS_fleet[pRS,SUV,Hybrid]+Tot_Maa

S_fleet[pRS,SUV,BEV]+Tot_MaaS_fleet[pRS,Hatch,Gasoline]+Tot_MaaS_fleet[pRS,Hatch,Hybrid]+Tot_MaaS_fleet[pRS,Hatch,BEV])

UNITS: cars*km/year

distance_MaaS_fleet[sRS, SUV, Hybrid] =
Tot_MaaS_fleet[sRS,SUV,Hybrid]*avg_gross_trip_distance_MaaS[sRS]*Active_MaaS_users[sRS]/(Tot_MaaS_fleet[CP,Sedan,Gasoline]+Tot_MaaS_fleet[CP,Sedan,Hybrid]+Tot_MaaS_fleet[CP,Sedan,BEV]+Tot_MaaS_fleet[CP,SUV,Gasoline]+Tot_MaaS_fleet[CP,SUV,Hybrid]+Tot_MaaS_fleet[CP,SUV,BEV]+Tot_MaaS_fleet[CP,Hatch,Gasoline]+Tot_MaaS_fleet[CP,Hatch,Hybrid]+Tot_MaaS_fleet[CP,Hatch,BEV]+Tot_MaaS_fleet[sRS,Sedan,Gasoline]+Tot_MaaS_fleet[sRS,Sedan,Hybrid]+Tot_MaaS_fleet[sRS,Sedan,BEV]+Tot_MaaS_fleet[sRS,SUV,Gasoline]+Tot_MaaS_fleet[sRS,SUV,Hybrid]+Tot_MaaS_fleet[sRS,SUV,BEV]+Tot_MaaS_fleet[sRS,Hatch,Gasoline]+Tot_MaaS_fleet[sRS,Hatch,Hybrid]+Tot_MaaS_fleet[sRS,Hatch,BEV]+Tot_MaaS_fleet[pRS,Sedan,Gasoline]+Tot_MaaS_fleet[pRS,Sedan,Hybrid]+Tot_MaaS_fleet[pRS,Sedan,BEV]+Tot_MaaS_fleet[pRS,SUV,Gasoline]+Tot_MaaS_fleet[pRS,SUV,Hybrid]+Tot_MaaS_fleet[pRS,SUV,BEV]+Tot_MaaS_fleet[pRS,Hatch,Gasoline]+Tot_MaaS_fleet[pRS,Hatch,Hybrid]+Tot_MaaS_fleet[pRS,Hatch,BEV])

UNITS: cars*km/year

distance_MaaS_fleet[sRS, SUV, BEV] =
Tot_MaaS_fleet[sRS,SUV,BEV]*avg_gross_trip_distance_MaaS[sRS]*Active_MaaS_users[sRS]/(Tot_MaaS_fleet[CP,Sedan,Gasoline]+Tot_MaaS_fleet[CP,Sedan,Hybrid]+Tot_MaaS_fleet[CP,Sedan,BEV]+Tot_MaaS_fleet[CP,SUV,Gasoline]+Tot_MaaS_fleet[CP,SUV,Hybrid]+Tot_MaaS_fleet[CP,SUV,BEV]+Tot_MaaS_fleet[CP,Hatch,Gasoline]+Tot_MaaS_fleet[CP,Hatch,Hybrid]+Tot_MaaS_fleet[CP,Hatch,BEV]+Tot_MaaS_fleet[sRS,Sedan,Gasoline]+Tot_MaaS_fleet[sRS,Sedan,Hybrid]+Tot_MaaS_fleet[sRS,Sedan,BEV]+Tot_MaaS_fleet[sRS,SUV,Gasoline]+Tot_MaaS_fleet[sRS,SUV,Hybrid]+Tot_MaaS_fleet[sRS,SUV,BEV]+Tot_MaaS_fleet[sRS,Hatch,Gasoline]+Tot_MaaS_fleet[sRS,Hatch,Hybrid]+Tot_MaaS_fleet[sRS,Hatch,BEV]+Tot_MaaS_fleet[pRS,Sedan,Gasoline]+Tot_MaaS_fleet[pRS,Sedan,Hybrid]+Tot_MaaS_fleet[pRS,Sedan,BEV]+Tot_MaaS_fleet[pRS,SUV,Gasoline]+Tot_MaaS_fleet[pRS,SUV,Hybrid]+Tot_MaaS_fleet[pRS,SUV,BEV]+Tot_MaaS_fleet[pRS,Hatch,Gasoline]+Tot_MaaS_fleet[pRS,Hatch,Hybrid]+Tot_MaaS_fleet[pRS,Hatch,BEV])

UNITS: cars*km/year

distance_MaaS_fleet[sRS, Hatch, Gasoline] =
Tot_MaaS_fleet[sRS,Hatch,Gasoline]*avg_gross_trip_distance_MaaS[sRS]*Active_MaaS_users[sRS]/(Tot_MaaS_fleet[CP,Sedan,Gasoline]+Tot_MaaS_fleet[CP,Sedan,Hybrid]+Tot_MaaS_fleet[CP,Sedan,BEV]+Tot_MaaS_fleet[CP,SUV,Gasoline]+Tot_MaaS_fleet[CP,SUV,Hybrid]+Tot_MaaS_fleet[CP,SUV,BEV]+Tot_MaaS_fleet[CP,Hatch,Gasoline]+Tot_MaaS_fleet[CP,Hatch,Hybrid]+Tot_MaaS_fleet[CP,Hatch,BEV]+Tot_MaaS_fleet[sRS,Sedan,Gasoline]+Tot_MaaS_fleet[sRS,Sedan,Hybrid]+Tot_MaaS_fleet[sRS,Sedan,BEV]+Tot_MaaS_fleet[sRS,SUV,Gasoline]+Tot_MaaS_fleet[sRS,SUV,Hybrid]+Tot_MaaS_fleet[sRS,SUV,BEV]+Tot_MaaS_fleet[sRS,Hatch,Gasoline]+Tot_MaaS_fleet[sRS,Hatch,Hybrid]+Tot_MaaS_fleet[sRS,Hatch,BEV]+Tot_MaaS_fleet[pRS,Sedan,Gasoline]+Tot_MaaS_fleet[pRS,Sedan,Hybrid]+Tot_MaaS_fleet[pRS,Sedan,BEV]+Tot_MaaS_fleet[pRS,SUV,Gasoline]+Tot_MaaS_fleet[pRS,SUV,Hybrid]+Tot_MaaS_fleet[pRS,SUV,BEV]+Tot_MaaS_fleet[pRS,Hatch,Gasoline]+Tot_MaaS_fleet[pRS,Hatch,Hybrid]+Tot_MaaS_fleet[pRS,Hatch,BEV])

UNITS: cars*km/year

distance_MaaS_fleet[sRS, Hatch, Hybrid] =
Tot_MaaS_fleet[sRS,Hatch,Hybrid]*avg_gross_trip_distance_MaaS[sRS]*Active_MaaS_users[sRS]/(Tot_MaaS_fleet[CP,Sedan,Gasoline]+Tot_MaaS_fleet[CP,Sedan,Hybrid]+Tot_MaaS_fleet[CP,Sedan,BEV]+Tot_MaaS_fleet[CP,SUV,Gasoline]+Tot_MaaS_fleet[CP,SUV,Hybrid]+Tot_MaaS_fleet[CP,SUV,BEV]+Tot_MaaS_fleet[CP,Hatch,Gasoline]+Tot_MaaS_fleet[CP,Hatch,Hybrid]+Tot_MaaS_fleet[CP,Hatch,BEV]+Tot_MaaS_fleet[sRS,Sedan,Gasoline]+Tot_MaaS_fleet[sRS,Sedan,Hybrid]+Tot_MaaS_fleet[sRS,Sedan,BEV]+Tot_MaaS_fleet[sRS,SUV,Gasoline]+Tot_MaaS_fleet[sRS,SUV,Hybrid]+Tot_MaaS_fleet[sRS,SUV,BEV]+Tot_MaaS_fleet[sRS,Hatch,Gasoline]+Tot_MaaS_fleet[sRS,Hatch,Hybrid]+Tot_MaaS_fleet[sRS,Hatch,BEV]+Tot_MaaS_fleet[pRS,Sedan,Gasoline]+Tot_MaaS_fleet[pRS,Sedan,Hybrid]+Tot_MaaS_fleet[pRS,Sedan,BEV]+Tot_MaaS_fleet[pRS,SUV,Gasoline]+Tot_MaaS_fleet[pRS,SUV,Hybrid]+Tot_Maa

S_fleet[pRS,SUV,BEV]+Tot_MaaS_fleet[pRS,Hatch,Gasoline]+Tot_MaaS_fleet[pRS,Hatch,Hybrid]+Tot_MaaS_fleet[pRS,Hatch,BEV])

UNITS: cars*km/year

distance_MaaS_fleet[sRS, Hatch, BEV] =
Tot_MaaS_fleet[sRS,Hatch,BEV]*avg_gross_trip_distance_MaaS[sRS]*Active_MaaS_users[sRS]/(Tot_MaaS_fleet[CP,Sedan,Gasoline]+Tot_MaaS_fleet[CP,Sedan,Hybrid]+Tot_MaaS_fleet[CP,Sedan,BEV]+Tot_MaaS_fleet[CP,SUV,Gasoline]+Tot_MaaS_fleet[CP,SUV,Hybrid]+Tot_MaaS_fleet[CP,SUV,BEV]+Tot_MaaS_fleet[CP,Hatch,Gasoline]+Tot_MaaS_fleet[CP,Hatch,Hybrid]+Tot_MaaS_fleet[CP,Hatch,BEV]+Tot_MaaS_fleet[sRS,Sedan,Gasoline]+Tot_MaaS_fleet[sRS,Sedan,Hybrid]+Tot_MaaS_fleet[sRS,Sedan,BEV]+Tot_MaaS_fleet[sRS,SUV,Gasoline]+Tot_MaaS_fleet[sRS,SUV,Hybrid]+Tot_MaaS_fleet[sRS,SUV,BEV]+Tot_MaaS_fleet[sRS,Hatch,Gasoline]+Tot_MaaS_fleet[sRS,Hatch,Hybrid]+Tot_MaaS_fleet[sRS,Hatch,BEV]+Tot_MaaS_fleet[pRS,Sedan,Gasoline]+Tot_MaaS_fleet[pRS,Sedan,Hybrid]+Tot_MaaS_fleet[pRS,Sedan,BEV]+Tot_MaaS_fleet[pRS,SUV,Gasoline]+Tot_MaaS_fleet[pRS,SUV,Hybrid]+Tot_MaaS_fleet[pRS,SUV,BEV]+Tot_MaaS_fleet[pRS,Hatch,Gasoline]+Tot_MaaS_fleet[pRS,Hatch,Hybrid]+Tot_MaaS_fleet[pRS,Hatch,BEV])

UNITS: cars*km/year

distance_MaaS_fleet[pRS, Sedan, Gasoline] =
Tot_MaaS_fleet[pRS,Sedan,Gasoline]*Active_MaaS_users[pRS]*avg_gross_trip_distance_MaaS[pRS]*Active_MaaS_users[sRS]/(Tot_MaaS_fleet[CP,Sedan,Gasoline]+Tot_MaaS_fleet[CP,Sedan,Hybrid]+Tot_MaaS_fleet[CP,Sedan,BEV]+Tot_MaaS_fleet[CP,SUV,Gasoline]+Tot_MaaS_fleet[CP,SUV,Hybrid]+Tot_MaaS_fleet[CP,SUV,BEV]+Tot_MaaS_fleet[CP,Hatch,Gasoline]+Tot_MaaS_fleet[CP,Hatch,Hybrid]+Tot_MaaS_fleet[CP,Hatch,BEV]+Tot_MaaS_fleet[sRS,Sedan,Gasoline]+Tot_MaaS_fleet[sRS,Sedan,Hybrid]+Tot_MaaS_fleet[sRS,Sedan,BEV]+Tot_MaaS_fleet[sRS,SUV,Gasoline]+Tot_MaaS_fleet[sRS,SUV,Hybrid]+Tot_MaaS_fleet[sRS,SUV,BEV]+Tot_MaaS_fleet[sRS,Hatch,Gasoline]+Tot_MaaS_fleet[sRS,Hatch,Hybrid]+Tot_MaaS_fleet[sRS,Hatch,BEV]+Tot_MaaS_fleet[pRS,Sedan,Gasoline]+Tot_MaaS_fleet[pRS,Sedan,Hybrid]+Tot_MaaS_fleet[pRS,Sedan,BEV]+Tot_MaaS_fleet[pRS,SUV,Gasoline]+Tot_MaaS_fleet[pRS,SUV,Hybrid]+Tot_MaaS_fleet[pRS,SUV,BEV]+Tot_MaaS_fleet[pRS,Hatch,Gasoline]+Tot_MaaS_fleet[pRS,Hatch,Hybrid]+Tot_MaaS_fleet[pRS,Hatch,BEV])

UNITS: cars*km/year

distance_MaaS_fleet[pRS, Sedan, Hybrid] =
Tot_MaaS_fleet[pRS,Sedan,Hybrid]*Active_MaaS_users[pRS]*avg_gross_trip_distance_MaaS[pRS]*Active_MaaS_users[sRS]/(Tot_MaaS_fleet[CP,Sedan,Gasoline]+Tot_MaaS_fleet[CP,Sedan,Hybrid]+Tot_MaaS_fleet[CP,Sedan,BEV]+Tot_MaaS_fleet[CP,SUV,Gasoline]+Tot_MaaS_fleet[CP,SUV,Hybrid]+Tot_MaaS_fleet[CP,SUV,BEV]+Tot_MaaS_fleet[CP,Hatch,Gasoline]+Tot_MaaS_fleet[CP,Hatch,Hybrid]+Tot_MaaS_fleet[CP,Hatch,BEV]+Tot_MaaS_fleet[sRS,Sedan,Gasoline]+Tot_MaaS_fleet[sRS,Sedan,Hybrid]+Tot_MaaS_fleet[sRS,Sedan,BEV]+Tot_MaaS_fleet[sRS,SUV,Gasoline]+Tot_MaaS_fleet[sRS,SUV,Hybrid]+Tot_MaaS_fleet[sRS,SUV,BEV]+Tot_MaaS_fleet[sRS,Hatch,Gasoline]+Tot_MaaS_fleet[sRS,Hatch,Hybrid]+Tot_MaaS_fleet[sRS,Hatch,BEV]+Tot_MaaS_fleet[pRS,Sedan,Gasoline]+Tot_MaaS_fleet[pRS,Sedan,Hybrid]+Tot_MaaS_fleet[pRS,Sedan,BEV]+Tot_MaaS_fleet[pRS,SUV,Gasoline]+Tot_MaaS_fleet[pRS,SUV,Hybrid]+Tot_MaaS_fleet[pRS,SUV,BEV]+Tot_MaaS_fleet[pRS,Hatch,Gasoline]+Tot_MaaS_fleet[pRS,Hatch,Hybrid]+Tot_MaaS_fleet[pRS,Hatch,BEV])

UNITS: cars*km/year

distance_MaaS_fleet[pRS, Sedan, BEV] =
Tot_MaaS_fleet[pRS,Sedan,BEV]*Active_MaaS_users[pRS]*avg_gross_trip_distance_MaaS[pRS]*Active_MaaS_users[sRS]/(Tot_MaaS_fleet[CP,Sedan,Gasoline]+Tot_MaaS_fleet[CP,Sedan,Hybrid]+Tot_MaaS_fleet[CP,Sedan,BEV]+Tot_MaaS_fleet[CP,SUV,Gasoline]+Tot_MaaS_fleet[CP,SUV,Hybrid]+Tot_MaaS_fleet[CP,SUV,BEV]+Tot_MaaS_fleet[CP,Hatch,Gasoline]+Tot_MaaS_fleet[CP,Hatch,Hybrid]+Tot_MaaS_fleet[CP,Hatch,BEV]+Tot_MaaS_fleet[sRS,Sedan,Gasoline]+Tot_MaaS_fleet[sRS,Sedan,Hybrid]+Tot_MaaS_fleet[sRS,Sedan,BEV]+Tot_MaaS_fleet[sRS,SUV,Gasoline]+Tot_MaaS_fleet[sRS,SUV,Hybrid]+Tot_MaaS_fleet[sRS,SUV,BEV]+Tot_MaaS_fleet[sRS,Hatch,Gasoline]+Tot_MaaS_fleet[sRS,Hatch,Hybrid]+Tot_MaaS_fleet[sRS,Hatch,BEV]+Tot_MaaS_fleet[pRS,Sedan,Gasoline]+Tot_MaaS_fleet[pRS,Sedan,Hybrid]+Tot_MaaS_fleet[pRS,Sedan,BEV]+Tot_MaaS_fleet[pRS,SUV,Gasoline]+Tot_MaaS_fleet[pR

S,SUV,Hybrid]+Tot_MaaS_fleet[pRS,SUV,BEV]+Tot_MaaS_fleet[pRS,Hatch,Gasoline]+Tot_MaaS_flee t[pRS,Hatch,Hybrid]+Tot_MaaS_fleet[pRS,Hatch,BEV])

UNITS: cars*km/year

distance_MaaS_fleet[pRS, SUV, Gasoline] = Tot_MaaS_fleet[pRS,SUV, Gasoline]*Active_MaaS_users[pRS]*avg_gross_trip_distance_MaaS[pRS]*Active_MaaS_users[sRS]/(Tot_MaaS_fleet[CP,Sedan,Gasoline]+Tot_MaaS_fleet[CP,Sedan,Hybrid]+Tot_MaaS_fleet[CP,Sedan,BEV]+Tot_MaaS_fleet[CP,SUV,Gasoline]+Tot_MaaS_fleet[CP,SUV,Hybrid]+Tot_MaaS_fleet[CP,SUV,BEV]+Tot_MaaS_fleet[CP,Hatch,Gasoline]+Tot_MaaS_fleet[CP,Hatch,Hybrid]+Tot_MaaS_fleet[CP,Hatch,BEV]+Tot_MaaS_fleet[sRS,Sedan,Gasoline]+Tot_MaaS_fleet[sRS,Sedan,Hybrid]+Tot_MaaS_fleet[sRS,Sedan, BEV]+Tot_MaaS_fleet[sRS,SUV,Gasoline]+Tot_MaaS_fleet[sRS,SUV,Hybrid]+Tot_MaaS_fleet[sRS,SUV,BEV]+Tot_MaaS_fleet[sRS,Hatch,Gasoline]+Tot_MaaS_fleet[sRS,Hatch,Hybrid]+Tot_MaaS_fleet[sRS,Hatch,BEV]+Tot_MaaS_fleet[pRS,Sedan,Gasoline]+Tot_MaaS_fleet[pRS,Sedan,Hybrid]+Tot_MaaS_fleet[pRS,Sedan,BEV]+Tot_MaaS_fleet[pRS,SUV,Gasoline]+Tot_MaaS_fleet[pRS,SUV,Hybrid]+Tot_MaaS_fleet[pRS,SUV,BEV]+Tot_MaaS_fleet[pRS,Hatch,Gasoline]+Tot_MaaS_fleet[pRS,Hatch,Hybrid]+Tot_MaaS_fleet[pRS,Hatch,BEV])

UNITS: cars*km/year

distance_MaaS_fleet[pRS, SUV, Hybrid] = Tot_MaaS_fleet[pRS,SUV, Hybrid]*Active_MaaS_users[pRS]*avg_gross_trip_distance_MaaS[pRS]*Active_MaaS_users[sRS]/(Tot_MaaS_fleet[CP,Sedan,Gasoline]+Tot_MaaS_fleet[CP,Sedan,Hybrid]+Tot_MaaS_fleet[CP,Sedan,BEV]+Tot_MaaS_fleet[CP,SUV,Gasoline]+Tot_MaaS_fleet[CP,SUV,Hybrid]+Tot_MaaS_fleet[CP,SUV,BEV]+Tot_MaaS_fleet[CP,Hatch,Gasoline]+Tot_MaaS_fleet[CP,Hatch,Hybrid]+Tot_MaaS_fleet[CP,Hatch,BEV]+Tot_MaaS_fleet[sRS,Sedan,Gasoline]+Tot_MaaS_fleet[sRS,Sedan,Hybrid]+Tot_MaaS_fleet[sRS,Sedan, BEV]+Tot_MaaS_fleet[sRS,SUV,Gasoline]+Tot_MaaS_fleet[sRS,SUV,Hybrid]+Tot_MaaS_fleet[sRS,SUV,BEV]+Tot_MaaS_fleet[sRS,Hatch,Gasoline]+Tot_MaaS_fleet[sRS,Hatch,Hybrid]+Tot_MaaS_fleet[sRS,Hatch,BEV]+Tot_MaaS_fleet[pRS,Sedan,Gasoline]+Tot_MaaS_fleet[pRS,Sedan,Hybrid]+Tot_MaaS_fleet[pRS,Sedan,BEV]+Tot_MaaS_fleet[pRS,SUV,Gasoline]+Tot_MaaS_fleet[pRS,SUV,Hybrid]+Tot_MaaS_fleet[pRS,SUV,BEV]+Tot_MaaS_fleet[pRS,Hatch,Gasoline]+Tot_MaaS_fleet[pRS,Hatch,Hybrid]+Tot_MaaS_fleet[pRS,Hatch,BEV])

UNITS: cars*km/year

distance_MaaS_fleet[pRS, SUV, BEV] = Tot_MaaS_fleet[pRS,SUV, BEV]*Active_MaaS_users[pRS]*avg_gross_trip_distance_MaaS[pRS]*Active_MaaS_users[sRS]/(Tot_MaaS_fleet[CP,Sedan,Gasoline]+Tot_MaaS_fleet[CP,Sedan,Hybrid]+Tot_MaaS_fleet[CP,Sedan,BEV]+Tot_MaaS_fleet[CP,SUV,Gasoline]+Tot_MaaS_fleet[CP,SUV,Hybrid]+Tot_MaaS_fleet[CP,SUV,BEV]+Tot_MaaS_fleet[CP,Hatch,Gasoline]+Tot_MaaS_fleet[CP,Hatch,Hybrid]+Tot_MaaS_fleet[CP,Hatch,BEV]+Tot_MaaS_fleet[sRS,Sedan,Gasoline]+Tot_MaaS_fleet[sRS,Sedan,Hybrid]+Tot_MaaS_fleet[sRS,Sedan,BEV]+Tot_MaaS_fleet[sRS,SUV,Gasoline]+Tot_MaaS_fleet[sRS,SUV,Hybrid]+Tot_MaaS_fleet[sRS,SUV,BEV]+Tot_MaaS_fleet[sRS,Hatch,Gasoline]+Tot_MaaS_fleet[sRS,Hatch,Hybrid]+Tot_MaaS_fleet[sRS,Hatch,BEV]+Tot_MaaS_fleet[pRS,Sedan,Gasoline]+Tot_MaaS_fleet[pRS,Sedan,Hybrid]+Tot_MaaS_fleet[pRS,Sedan,BEV]+Tot_MaaS_fleet[pRS,SUV,Gasoline]+Tot_MaaS_fleet[pRS,SUV,Hybrid]+Tot_MaaS_fleet[pRS,SUV,BEV]+Tot_MaaS_fleet[pRS,Hatch,Gasoline]+Tot_MaaS_fleet[pRS,Hatch,Hybrid]+Tot_MaaS_fleet[pRS,Hatch,BEV])

UNITS: cars*km/year

distance_MaaS_fleet[pRS, Hatch, Gasoline] = Tot_MaaS_fleet[pRS,Hatch, Gasoline]*Active_MaaS_users[pRS]*avg_gross_trip_distance_MaaS[pRS]*Active_MaaS_users[sRS]/(Tot_MaaS_fleet[CP,Sedan,Gasoline]+Tot_MaaS_fleet[CP,Sedan,Hybrid]+Tot_MaaS_fleet[CP,Sedan,BEV]+Tot_MaaS_fleet[CP,SUV,Gasoline]+Tot_MaaS_fleet[CP,SUV,Hybrid]+Tot_MaaS_fleet[CP,SUV,BEV]+Tot_MaaS_fleet[CP,Hatch,Gasoline]+Tot_MaaS_fleet[CP,Hatch,Hybrid]+Tot_MaaS_fleet[CP,Hatch,BEV]+Tot_MaaS_fleet[sRS,Sedan,Gasoline]+Tot_MaaS_fleet[sRS,Sedan,Hybrid]+Tot_MaaS_fleet[sRS,Sedan, BEV]+Tot_MaaS_fleet[sRS,SUV,Gasoline]+Tot_MaaS_fleet[sRS,SUV,Hybrid]+Tot_MaaS_fleet[sRS,SUV,BEV]+Tot_MaaS_fleet[sRS,Hatch,Gasoline]+Tot_MaaS_fleet[sRS,Hatch,Hybrid]+Tot_MaaS_fleet[sRS,Hatch,BEV]+Tot_MaaS_fleet[pRS,Sedan,Gasoline]+Tot_MaaS_fleet[pRS,Sedan,Hybrid]+Tot_MaaS_fleet[pRS,Sedan,BEV]+Tot_MaaS_fleet[pRS,SUV,Gasoline]+Tot_MaaS_fleet[pRS,SUV,Hybrid]+Tot_Maa

S_fleet[pRS,SUV,BEV]+Tot_MaaS_fleet[pRS,Hatch,Gasoline]+Tot_MaaS_fleet[pRS,Hatch,Hybrid]+Tot_MaaS_fleet[pRS,Hatch,BEV])

UNITS: cars*km/year

distance_MaaS_fleet[pRS, Hatch, Hybrid] = Tot_MaaS_fleet[pRS,Hatch, Hybrid]*Active_MaaS_users[pRS]*avg_gross_trip_distance_MaaS[pRS]*Active_MaaS_users[sRS]/(Tot_MaaS_fleet[CP,Sedan,Gasoline]+Tot_MaaS_fleet[CP,Sedan,Hybrid]+Tot_MaaS_fleet[CP,Sedan,BEV]+Tot_MaaS_fleet[CP,SUV,Gasoline]+Tot_MaaS_fleet[CP,SUV,Hybrid]+Tot_MaaS_fleet[CP,SUV,BEV]+Tot_MaaS_fleet[CP,Hatch,Gasoline]+Tot_MaaS_fleet[CP,Hatch,Hybrid]+Tot_MaaS_fleet[CP,Hatch,BEV]+Tot_MaaS_fleet[sRS,Sedan,Gasoline]+Tot_MaaS_fleet[sRS,Sedan,Hybrid]+Tot_MaaS_fleet[sRS,Sedan,BEV]+Tot_MaaS_fleet[sRS,SUV,Gasoline]+Tot_MaaS_fleet[sRS,SUV,Hybrid]+Tot_MaaS_fleet[sRS,SUV,BEV]+Tot_MaaS_fleet[sRS,Hatch,Gasoline]+Tot_MaaS_fleet[sRS,Hatch,Hybrid]+Tot_MaaS_fleet[sRS,Hatch,BEV]+Tot_MaaS_fleet[pRS,Sedan,Gasoline]+Tot_MaaS_fleet[pRS,Sedan,Hybrid]+Tot_MaaS_fleet[pRS,Sedan,BEV]+Tot_MaaS_fleet[pRS,SUV,Gasoline]+Tot_MaaS_fleet[pRS,SUV,Hybrid]+Tot_MaaS_fleet[pRS,SUV,BEV]+Tot_MaaS_fleet[pRS,Hatch,Gasoline]+Tot_MaaS_fleet[pRS,Hatch,Hybrid]+Tot_MaaS_fleet[pRS,Hatch,BEV])

UNITS: cars*km/year

distance_MaaS_fleet[pRS, Hatch, BEV] = Tot_MaaS_fleet[pRS,Hatch, BEV]*Active_MaaS_users[pRS]*avg_gross_trip_distance_MaaS[pRS]*Active_MaaS_users[sRS]/(Tot_MaaS_fleet[CP,Sedan,Gasoline]+Tot_MaaS_fleet[CP,Sedan,Hybrid]+Tot_MaaS_fleet[CP,Sedan,BEV]+Tot_MaaS_fleet[CP,SUV,Gasoline]+Tot_MaaS_fleet[CP,SUV,Hybrid]+Tot_MaaS_fleet[CP,SUV,BEV]+Tot_MaaS_fleet[CP,Hatch,Gasoline]+Tot_MaaS_fleet[CP,Hatch,Hybrid]+Tot_MaaS_fleet[CP,Hatch,BEV]+Tot_MaaS_fleet[sRS,Sedan,Gasoline]+Tot_MaaS_fleet[sRS,Sedan,Hybrid]+Tot_MaaS_fleet[sRS,Sedan,BEV]+Tot_MaaS_fleet[sRS,SUV,Gasoline]+Tot_MaaS_fleet[sRS,SUV,Hybrid]+Tot_MaaS_fleet[sRS,SUV,BEV]+Tot_MaaS_fleet[sRS,Hatch,Gasoline]+Tot_MaaS_fleet[sRS,Hatch,Hybrid]+Tot_MaaS_fleet[sRS,Hatch,BEV]+Tot_MaaS_fleet[pRS,Sedan,Gasoline]+Tot_MaaS_fleet[pRS,Sedan,Hybrid]+Tot_MaaS_fleet[pRS,Sedan,BEV]+Tot_MaaS_fleet[pRS,SUV,Gasoline]+Tot_MaaS_fleet[pRS,SUV,Hybrid]+Tot_MaaS_fleet[pRS,SUV,BEV]+Tot_MaaS_fleet[pRS,Hatch,Gasoline]+Tot_MaaS_fleet[pRS,Hatch,Hybrid]+Tot_MaaS_fleet[pRS,Hatch,BEV])

UNITS: cars*km/year

UNITS: cars*km/year

distance_PC_fleet[Carbody, Powertrain] = avg_trip_distance_PC*Tot_PC_fleet

UNITS: cars*Kilometers/Years

DPI_EoL_phase[MaaS_Mode, Carbody, Powertrain] = 1

UNITS: kgCO_2/car

DPI_Manu_Phase[MaaS_Mode, Carbody, Powertrain] = 1

UNITS: kgCO_2/car

DPI_Use_phase[MaaS_Mode, Carbody, Powertrain] = 1

UNITS: kgCO_2/(car*km)

Effect_of_advertising[MaaS_Mode] = 0.000338

UNITS: Per Year

Employment_Change = 450000

UNITS: person/year

EoL_impacts_MaaS[MaaS_Mode, Carbody, Powertrain] = tot_scrappge_MaaS_fleet*DPI_EoL_phase*Work_trip_GHG_allocation_MaaS

UNITS: kgCO_2/year

EoL_impacts_PC[Carbody, Powertrain] = tot_scrappage_PC_fleet*DPI_EoL_phase[CP,Carbody,Powertrain]*Work_trip_GHG_allocation_PC

UNITS: kgCO_2/year

Fare_distribution[CP, $15] =.4

UNITS: Dimensionless

Fare_distribution[CP, $19] =.4

UNITS: Dimensionless
Fare_distribution[CP, $21] =.1
UNITS: Dimensionless
Fare_distribution[CP, $25] =.1
UNITS: Dimensionless
Fare_distribution[CP, $40] = 0
UNITS: Dimensionless
Fare_distribution[sRS, $15] = 0
UNITS: Dimensionless
Fare_distribution[sRS, $19] =.49
UNITS: Dimensionless
Fare_distribution[sRS, $21] =.22
UNITS: Dimensionless
Fare_distribution[sRS, $25] =.26
UNITS: Dimensionless
Fare_distribution[sRS, $40] =.03
UNITS: Dimensionless
Fare_distribution[pRS, $15] = 0
UNITS: Dimensionless
Fare_distribution[pRS, $19] =.01
UNITS: Dimensionless
Fare_distribution[pRS, $21] =.05
UNITS: Dimensionless
Fare_distribution[pRS, $25] =.54
UNITS: Dimensionless
Fare_distribution[pRS, $40] =.4
UNITS: Dimensionless
UNITS: Dimensionless
Final_GHG_emission_per_pkm_for_an_avg_roundtrip_to_work_in_USA =
Total_GHG_emissions/Total_pkm
UNITS: kgCO_2/(km*People)
Gaining_PC_users = Joining_travel_by_car_to_work-
(Adopting_MaaS[CP]+Adopting_MaaS[sRS]+Adopting_MaaS[pRS])
UNITS: person/Year
GHG_emission_pkm_MaaS_aggregated =
tot_GHG_MaaS_aggregated/(pkm_MaaS[CP]+pkm_MaaS[sRS]+pkm_MaaS[pRS])
UNITS: kgCO_2/(person*km)
GHG_emission_pkm_PC =
(total_GHG_emissions_PC[Sedan,Gasoline]+total_GHG_emissions_PC[Sedan,Hybrid]+total_GHG_emissions_PC[Sedan,BEV]+total_GHG_emissions_PC[SUV,Gasoline]+total_GHG_emissions_PC[SUV,Hybrid]+total_GHG_emissions_PC[SUV,BEV]+total_GHG_emissions_PC[Hatch,Gasoline]+total_GHG_emissions_PC[Hatch,BEV]+total_GHG_emissions_PC[Hatch,BEV])/pkm_PC
UNITS: kgCO_2/(person*km)
GHG_emissions_MaaS_pkm[CP] =
(total_GHG_emissions_MaaS[CP,Sedan,Gasoline]+total_GHG_emissions_MaaS[CP,Sedan,Hybrid]+total_GHG_emissions_MaaS[CP,Sedan,BEV]+total_GHG_emissions_MaaS[CP,SUV,Gasoline]+total_GHG_emissions_MaaS[CP,SUV,Hybrid]+total_GHG_emissions_MaaS[CP,SUV,BEV]+total_GHG_emissions_MaaS[CP,Hatch,Gasoline]+total_GHG_emissions_MaaS[CP,Hatch,Hybrid]+total_GHG_emissions_MaaS[CP,Hatch,BEV])/pkm_MaaS[CP]

UNITS: $kgCO_2$/(person*km)

GHG_emissions_MaaS_pkm[sRS] = (total_GHG_emissions_MaaS[sRS,Sedan,Gasoline]+total_GHG_emissions_MaaS[sRS,Sedan,Hybrid]+total_GHG_emissions_MaaS[sRS,Sedan,BEV]+total_GHG_emissions_MaaS[sRS,SUV,Gasoline]+total_GHG_emissions_MaaS[sRS,SUV,Hybrid]+total_GHG_emissions_MaaS[sRS,SUV,BEV]+total_GHG_emissions_MaaS[sRS,Hatch,Gasoline]+total_GHG_emissions_MaaS[sRS,Hatch,Hybrid]+total_GHG_emissions_MaaS[sRS,Hatch,BEV])/pkm_MaaS[sRS]

UNITS: $kgCO_2$/(person*km)

GHG_emissions_MaaS_pkm[pRS] = (total_GHG_emissions_MaaS[pRS,Sedan,Gasoline]+total_GHG_emissions_MaaS[pRS,Sedan,Hybrid]+total_GHG_emissions_MaaS[pRS,Sedan,BEV]+total_GHG_emissions_MaaS[pRS,SUV,Gasoline]+total_GHG_emissions_MaaS[pRS,SUV,Hybrid]+total_GHG_emissions_MaaS[pRS,SUV,BEV]+total_GHG_emissions_MaaS[pRS,Hatch,Gasoline]+total_GHG_emissions_MaaS[pRS,Hatch,Hybrid]+total_GHG_emissions_MaaS[pRS,Hatch,BEV])/pkm_MaaS[pRS]

UNITS: $kgCO_2$/(person*km)

UNITS: $kgCO_2$/(person*km)

Gross_Occupancy_MaaS[CP] = 2.18

UNITS: person/trip

Gross_Occupancy_MaaS[sRS] = 1

UNITS: person/trip

Gross_Occupancy_MaaS[pRS] = 2.23

UNITS: person/trip

UNITS: person/trip

MaaS_fleet_car_body_distribution[CP, Sedan] = (Tot_MaaS_fleet[CP,Sedan,Gasoline]+Tot_MaaS_fleet[CP,Sedan,Hybrid]+Tot_MaaS_fleet[CP,Sedan,BEV])/(Tot_MaaS_fleet[CP,Sedan,Gasoline]+Tot_MaaS_fleet[CP,Sedan,Hybrid]+Tot_MaaS_fleet[CP,Sedan,BEV]+(Tot_MaaS_fleet[CP,SUV,Gasoline]+Tot_MaaS_fleet[CP,SUV,Hybrid]+Tot_MaaS_fleet[CP,SUV,BEV])+(Tot_MaaS_fleet[CP,Hatch,Gasoline]+Tot_MaaS_fleet[CP,Hatch,Hybrid]+Tot_MaaS_fleet[CP,Hatch,BEV]))

UNITS: Dimensionless

MaaS_fleet_car_body_distribution[CP, SUV] = (Tot_MaaS_fleet[CP,SUV,Gasoline]+Tot_MaaS_fleet[CP,SUV,Hybrid]+Tot_MaaS_fleet[CP,SUV,BEV])/(Tot_MaaS_fleet[CP,Sedan,Gasoline]+Tot_MaaS_fleet[CP,Sedan,Hybrid]+Tot_MaaS_fleet[CP,Sedan,BEV]+(Tot_MaaS_fleet[CP,SUV,Gasoline]+Tot_MaaS_fleet[CP,SUV,Hybrid]+Tot_MaaS_fleet[CP,SUV,BEV])+(Tot_MaaS_fleet[CP,Hatch,Gasoline]+Tot_MaaS_fleet[CP,Hatch,Hybrid]+Tot_MaaS_fleet[CP,Hatch,BEV]))

UNITS: Dimensionless

MaaS_fleet_car_body_distribution[CP, Hatch] = (Tot_MaaS_fleet[CP,Hatch,Gasoline]+Tot_MaaS_fleet[CP,Hatch,Hybrid]+Tot_MaaS_fleet[CP,Hatch,BEV])/(Tot_MaaS_fleet[CP,Sedan,Gasoline]+Tot_MaaS_fleet[CP,Sedan,Hybrid]+Tot_MaaS_fleet[CP,Sedan,BEV]+(Tot_MaaS_fleet[CP,SUV,Gasoline]+Tot_MaaS_fleet[CP,SUV,Hybrid]+Tot_MaaS_fleet[CP,SUV,BEV])+(Tot_MaaS_fleet[CP,Hatch,Gasoline]+Tot_MaaS_fleet[CP,Hatch,Hybrid]+Tot_MaaS_fleet[CP,Hatch,BEV]))

UNITS: Dimensionless

MaaS_fleet_car_body_distribution[sRS, Sedan] = (Tot_MaaS_fleet[sRS,Sedan,Gasoline]+Tot_MaaS_fleet[sRS,Sedan,Hybrid]+Tot_MaaS_fleet[sRS,Sedan,BEV])/(Tot_MaaS_fleet[sRS,Sedan,Gasoline]+Tot_MaaS_fleet[sRS,Sedan,Hybrid]+Tot_MaaS_fleet[sRS,Sedan,BEV]+(Tot_MaaS_fleet[sRS,SUV,Gasoline]+Tot_MaaS_fleet[sRS,SUV,Hybrid]+Tot_MaaS_fleet[sRS,SUV,BEV])+(Tot_MaaS_fleet[sRS,Hatch,Gasoline]+Tot_MaaS_fleet[sRS,Hatch,Hybrid]+Tot_MaaS_fleet[sRS,Hatch,BEV]))

UNITS: Dimensionless

MaaS_fleet_car_body_distribution[sRS, SUV] = (Tot_MaaS_fleet[sRS,SUV,Gasoline]+Tot_MaaS_fleet[sRS,SUV,Hybrid]+Tot_MaaS_fleet[sRS,SUV,BEV])/(Tot_MaaS_fleet[sRS,Sedan,Gasoline]+Tot_MaaS_fleet[sRS,Sedan,Hybrid]+Tot_MaaS_fleet[sRS,Sedan,BEV]+(Tot_MaaS_fleet[sRS,SUV,Gasoline]+Tot_MaaS_fleet[sRS,SUV,Hybrid]+Tot_MaaS_fleet[sRS,SUV,BEV])+(Tot_MaaS_fleet[sRS,Hatch,Gasoline]+Tot_MaaS_fleet[sRS,Hatch,Hybrid]+Tot_MaaS_fleet[sRS,Hatch,BEV]))

UNITS: Dimensionless

MaaS_fleet_car_body_distribution[sRS, Hatch] = (Tot_MaaS_fleet[sRS,Hatch,Gasoline]+Tot_MaaS_fleet[sRS,Hatch,Hybrid]+Tot_MaaS_fleet[sRS,Hatch,BEV])/(Tot_MaaS_fleet[sRS,Sedan,Gasoline]+Tot_MaaS_fleet[sRS,Sedan,Hybrid]+Tot_MaaS_fleet[sRS,Sedan,BEV]+(Tot_MaaS_fleet[sRS,SUV,Gasoline]+Tot_MaaS_fleet[sRS,SUV,Hybrid]+Tot_MaaS_fleet[sRS,SUV,BEV])+(Tot_MaaS_fleet[sRS,Hatch,Gasoline]+Tot_MaaS_fleet[sRS,Hatch,Hybrid]+Tot_MaaS_fleet[sRS,Hatch,BEV]))

UNITS: Dimensionless

MaaS_fleet_car_body_distribution[pRS, Sedan] = (Tot_MaaS_fleet[pRS,Sedan,Gasoline]+Tot_MaaS_fleet[pRS,Sedan,Hybrid]+Tot_MaaS_fleet[pRS,Sedan,BEV])/(Tot_MaaS_fleet[pRS,Sedan,Gasoline]+Tot_MaaS_fleet[pRS,Sedan,Hybrid]+Tot_MaaS_fleet[pRS,Sedan,BEV]+(Tot_MaaS_fleet[pRS,SUV,Gasoline]+Tot_MaaS_fleet[pRS,SUV,Hybrid]+Tot_MaaS_fleet[pRS,SUV,BEV])+(Tot_MaaS_fleet[pRS,Hatch,Gasoline]+Tot_MaaS_fleet[pRS,Hatch,Hybrid]+Tot_MaaS_fleet[pRS,Hatch,BEV]))

UNITS: Dimensionless

MaaS_fleet_car_body_distribution[pRS, SUV] = (Tot_MaaS_fleet[pRS,SUV,Gasoline]+Tot_MaaS_fleet[pRS,SUV,Hybrid]+Tot_MaaS_fleet[pRS,SUV,BEV])/(Tot_MaaS_fleet[pRS,Sedan,Gasoline]+Tot_MaaS_fleet[pRS,Sedan,Hybrid]+Tot_MaaS_fleet[pRS,Sedan,BEV]+(Tot_MaaS_fleet[pRS,SUV,Gasoline]+Tot_MaaS_fleet[pRS,SUV,Hybrid]+Tot_MaaS_fleet[pRS,SUV,BEV])+(Tot_MaaS_fleet[pRS,Hatch,Gasoline]+Tot_MaaS_fleet[pRS,Hatch,Hybrid]+Tot_MaaS_fleet[pRS,Hatch,BEV]))

UNITS: Dimensionless

MaaS_fleet_car_body_distribution[pRS, Hatch] = (Tot_MaaS_fleet[pRS,Hatch,Gasoline]+Tot_MaaS_fleet[pRS,Hatch,Hybrid]+Tot_MaaS_fleet[pRS,Hatch,BEV])/(Tot_MaaS_fleet[pRS,Sedan,Gasoline]+Tot_MaaS_fleet[pRS,Sedan,Hybrid]+Tot_MaaS_fleet[pRS,Sedan,BEV]+(Tot_MaaS_fleet[pRS,SUV,Gasoline]+Tot_MaaS_fleet[pRS,SUV,Hybrid]+Tot_MaaS_fleet[pRS,SUV,BEV])+(Tot_MaaS_fleet[pRS,Hatch,Gasoline]+Tot_MaaS_fleet[pRS,Hatch,Hybrid]+Tot_MaaS_fleet[pRS,Hatch,BEV]))

UNITS: Dimensionless

UNITS: Dimensionless

MaaS_fleet_tech_changes[CP, Sedan, Gasoline] = 1

UNITS: Dimensionless

MaaS_fleet_tech_changes[CP, Sedan, Hybrid] = 1

UNITS: Dimensionless

MaaS_fleet_tech_changes[CP, Sedan, BEV] = 1

UNITS: Dimensionless

MaaS_fleet_tech_changes[CP, SUV, Gasoline] = 1

UNITS: Dimensionless

MaaS_fleet_tech_changes[CP, SUV, Hybrid] = 1

UNITS: Dimensionless

MaaS_fleet_tech_changes[CP, SUV, BEV] = 1

UNITS: Dimensionless

MaaS_fleet_tech_changes[CP, Hatch, Gasoline] = 1

UNITS: Dimensionless

MaaS_fleet_tech_changes[CP, Hatch, Hybrid] = 1

UNITS: Dimensionless
MaaS_fleet_tech_changes[CP, Hatch, BEV] = 1
UNITS: Dimensionless
MaaS_fleet_tech_changes[sRS, Sedan, Gasoline] = 1
UNITS: Dimensionless
MaaS_fleet_tech_changes[sRS, Sedan, Hybrid] = 1
UNITS: Dimensionless
MaaS_fleet_tech_changes[sRS, Sedan, BEV] = 1
UNITS: Dimensionless
MaaS_fleet_tech_changes[sRS, SUV, Gasoline] = 1
UNITS: Dimensionless
MaaS_fleet_tech_changes[sRS, SUV, Hybrid] = 1
UNITS: Dimensionless
MaaS_fleet_tech_changes[sRS, SUV, BEV] = 1
UNITS: Dimensionless
MaaS_fleet_tech_changes[sRS, Hatch, Gasoline] = 1
UNITS: Dimensionless
MaaS_fleet_tech_changes[sRS, Hatch, Hybrid] = 1
UNITS: Dimensionless
MaaS_fleet_tech_changes[sRS, Hatch, BEV] = 1
UNITS: Dimensionless
MaaS_fleet_tech_changes[pRS, Sedan, Gasoline] = 1
UNITS: Dimensionless
MaaS_fleet_tech_changes[pRS, Sedan, Hybrid] = 1
UNITS: Dimensionless
MaaS_fleet_tech_changes[pRS, Sedan, BEV] = 1
UNITS: Dimensionless
MaaS_fleet_tech_changes[pRS, SUV, Gasoline] = 1
UNITS: Dimensionless
MaaS_fleet_tech_changes[pRS, SUV, Hybrid] = 1
UNITS: Dimensionless
MaaS_fleet_tech_changes[pRS, SUV, BEV] = 1
UNITS: Dimensionless
MaaS_fleet_tech_changes[pRS, Hatch, Gasoline] = 1
UNITS: Dimensionless
MaaS_fleet_tech_changes[pRS, Hatch, Hybrid] = 1
UNITS: Dimensionless
MaaS_fleet_tech_changes[pRS, Hatch, BEV] = 1
UNITS: Dimensionless
UNITS: Dimensionless
MaaS_mode_attractiveness[CP] =
(("#passenger_attractiveness"[CP]+Vehicle_body_attractiveness[CP]+Price_attractiveness[CP]+Time_attractiveness[CP]+Powertrain_system_attractiveness[CP])/5)/((("#passenger_attractiveness"[CP]+Vehicle_body_attractiveness[CP]+Price_attractiveness[CP]+Time_attractiveness[CP]+Powertrain_system_attractiveness[CP])/5)+(("#passenger_attractiveness"[sRS]+Vehicle_body_attractiveness[sRS]+Price_attractiveness[sRS]+Time_attractiveness[sRS]+Powertrain_system_attractiveness[sRS])/4)+(("#passenger_attractiveness"[pRS]+Vehicle_body_attractiveness[pRS]+Price_attractiveness[pRS]+Time_attractiveness[pRS]+Powertrain_system_attractiveness[pRS])/5))

UNITS: Dimensionless

MaaS_mode_attractiveness[sRS] = (("#passenger_attractiveness"[sRS]+Vehicle_body_attractiveness[sRS]+Price_attractiveness[sRS]+Time_attractiveness[sRS]+Powertrain_system_attractiveness[sRS])/4)/((("#passenger_attractiveness"[CP]+Vehicle_body_attractiveness[CP]+Price_attractiveness[CP]+Time_attractiveness[CP]+Powertrain_system_attractiveness[CP])/5)+(("#passenger_attractiveness"[sRS]+Vehicle_body_attractiveness[sRS]+Price_attractiveness[sRS]+Time_attractiveness[sRS]+Powertrain_system_attractiveness[sRS])/4)+(("#passenger_attractiveness"[pRS]+Vehicle_body_attractiveness[pRS]+Price_attractiveness[pRS]+Time_attractiveness[pRS]+Powertrain_system_attractiveness[pRS])/5))

UNITS: Dimensionless

MaaS_mode_attractiveness[pRS] = (("#passenger_attractiveness"[pRS]+Vehicle_body_attractiveness[pRS]+Price_attractiveness[pRS]+Time_attractiveness[pRS]+Powertrain_system_attractiveness[pRS])/5)/((("#passenger_attractiveness"[CP]+Vehicle_body_attractiveness[CP]+Price_attractiveness[CP]+Time_attractiveness[CP]+Powertrain_system_attractiveness[CP])/5)+(("#passenger_attractiveness"[sRS]+Vehicle_body_attractiveness[sRS]+Price_attractiveness[sRS]+Time_attractiveness[sRS]+Powertrain_system_attractiveness[sRS])/4)+(("#passenger_attractiveness"[pRS]+Vehicle_body_attractiveness[pRS]+Price_attractiveness[pRS]+Time_attractiveness[pRS]+Powertrain_system_attractiveness[pRS])/5))

UNITS: Dimensionless

UNITS: Dimensionless

Manufacturing_impacts_MaaS[MaaS_Mode, Carbody, Powertrain] = Purchasing_MaaS_fleet*DPI_Manu_Phase*Work_trip_GHG_allocation_MaaS

UNITS: kgCO_2/year

Manufacturing_impacts_PC[Carbody, Powertrain] = Purchasing_PC*DPI_Manu_Phase[CP,Carbody,Powertrain]*Work_trip_GHG_allocation_PC

UNITS: kgCO_2/Years

Net_distance_MaaS = 20.6*260

UNITS: km/year

PC_fleet_tech_changes[Sedan, Gasoline] = 1

UNITS: Dimensionless

PC_fleet_tech_changes[Sedan, Hybrid] = 1

UNITS: Dimensionless

PC_fleet_tech_changes[Sedan, BEV] = 1

UNITS: Dimensionless

PC_fleet_tech_changes[SUV, Gasoline] = 1

UNITS: Dimensionless

PC_fleet_tech_changes[SUV, Hybrid] = 1

UNITS: Dimensionless

PC_fleet_tech_changes[SUV, BEV] = 1

UNITS: Dimensionless

PC_fleet_tech_changes[Hatch, Gasoline] = 1

UNITS: Dimensionless

PC_fleet_tech_changes[Hatch, Hybrid] = 1

UNITS: Dimensionless

PC_fleet_tech_changes[Hatch, BEV] = 1

UNITS: Dimensionless

UNITS: Dimensionless

PC_to_user_ratio = 1/1.18

UNITS: cars per person

pkm_MaaS[MaaS_Mode] = Net_distance_MaaS*Active_MaaS_users[MaaS_Mode]
UNITS: person*km/year

pkm_PC = (Commuting_employees_by_private_vehicles-Active_MaaS_users[CP]-Active_MaaS_users[sRS]-Active_MaaS_users[pRS])*avg_trip_distance_PC
UNITS: person*km/year

Powertrain_system_attractiveness[CP] = EXP(powertrain_system_distribution[CP,Gasoline]*Utility_function_Powertrain_system[CP,Gasoline]+powertrain_system_distribution[CP,Hybrid]*Utility_function_Powertrain_system[CP,Hybrid]+powertrain_system_distribution[CP,BEV]*Utility_function_Powertrain_system[CP,BEV])/(EXP(powertrain_system_distribution[CP,Gasoline]*Utility_function_Powertrain_system[CP,Gasoline]+powertrain_system_distribution[CP,Hybrid]*Utility_function_Powertrain_system[CP,Hybrid]+powertrain_system_distribution[CP,BEV]*Utility_function_Powertrain_system[CP,BEV])+EXP(powertrain_system_distribution[sRS,Gasoline]*Utility_function_Powertrain_system[sRS,Gasoline]+powertrain_system_distribution[sRS,Hybrid]*Utility_function_Powertrain_system[sRS,Hybrid]+powertrain_system_distribution[sRS,BEV]*Utility_function_Powertrain_system[sRS,BEV])+EXP(powertrain_system_distribution[pRS,Gasoline]*Utility_function_Powertrain_system[pRS,Gasoline]+powertrain_system_distribution[pRS,Hybrid]*Utility_function_Powertrain_system[pRS,Hybrid]+powertrain_system_distribution[pRS,BEV]*Utility_function_Powertrain_system[pRS,BEV]))
UNITS: Dimensionless

Powertrain_system_attractiveness[sRS] = EXP(powertrain_system_distribution[sRS,Gasoline]*Utility_function_Powertrain_system[sRS,Gasoline]+powertrain_system_distribution[sRS,Hybrid]*Utility_function_Powertrain_system[sRS,Hybrid]+powertrain_system_distribution[sRS,BEV]*Utility_function_Powertrain_system[sRS,BEV])/(EXP(powertrain_system_distribution[CP,Gasoline]*Utility_function_Powertrain_system[CP,Gasoline]+powertrain_system_distribution[CP,Hybrid]*Utility_function_Powertrain_system[CP,Hybrid]+powertrain_system_distribution[CP,BEV]*Utility_function_Powertrain_system[CP,BEV])+EXP(powertrain_system_distribution[sRS,Gasoline]*Utility_function_Powertrain_system[sRS,Gasoline]+powertrain_system_distribution[sRS,Hybrid]*Utility_function_Powertrain_system[sRS,Hybrid]+powertrain_system_distribution[sRS,BEV]*Utility_function_Powertrain_system[sRS,BEV])+EXP(powertrain_system_distribution[pRS,Gasoline]*Utility_function_Powertrain_system[pRS,Gasoline]+powertrain_system_distribution[pRS,Hybrid]*Utility_function_Powertrain_system[pRS,Hybrid]+powertrain_system_distribution[pRS,BEV]*Utility_function_Powertrain_system[pRS,BEV]))
UNITS: Dimensionless

Powertrain_system_attractiveness[pRS] = EXP(powertrain_system_distribution[pRS,Gasoline]*Utility_function_Powertrain_system[pRS,Gasoline]+powertrain_system_distribution[pRS,Hybrid]*Utility_function_Powertrain_system[pRS,Hybrid]+powertrain_system_distribution[pRS,BEV]*Utility_function_Powertrain_system[pRS,BEV])/(EXP(powertrain_system_distribution[CP,Gasoline]*Utility_function_Powertrain_system[CP,Gasoline]+powertrain_system_distribution[CP,Hybrid]*Utility_function_Powertrain_system[CP,Hybrid]+powertrain_system_distribution[CP,BEV]*Utility_function_Powertrain_system[CP,BEV])+EXP(powertrain_system_distribution[sRS,Gasoline]*Utility_function_Powertrain_system[sRS,Gasoline]+powertrain_system_distribution[sRS,Hybrid]*Utility_function_Powertrain_system[sRS,Hybrid]+powertrain_system_distribution[sRS,BEV]*Utility_function_Powertrain_system[sRS,BEV])+EXP(powertrain_system_distribution[pRS,Gasoline]*Utility_function_Powertrain_system[pRS,Gasoline]+powertrain_system_distribution[pRS,Hybrid]*Utility_function_Powertrain_system[pRS,Hybrid]+powertrain_system_distribution[pRS,BEV]*Utility_function_Powertrain_system[pRS,BEV]))
UNITS: Dimensionless
UNITS: Dimensionless

powertrain_system_distribution[CP, Gasoline] =.93
UNITS: Dimensionless

powertrain_system_distribution[CP, Hybrid] =.04
UNITS: Dimensionless

powertrain_system_distribution[CP, BEV] =.03
UNITS: Dimensionless
powertrain_system_distribution[sRS, Gasoline] =.78
UNITS: Dimensionless
powertrain_system_distribution[sRS, Hybrid] =.2
UNITS: Dimensionless
powertrain_system_distribution[sRS, BEV] =.01
UNITS: Dimensionless
powertrain_system_distribution[pRS, Gasoline] =.81
UNITS: Dimensionless
powertrain_system_distribution[pRS, Hybrid] =.19
UNITS: Dimensionless
powertrain_system_distribution[pRS, BEV] =.01
UNITS: Dimensionless
UNITS: Dimensionless
Price_attractiveness[CP] =
EXP(Utility_function_Fare[CP,$15]*Fare_distribution[CP,$15]+Utility_function_Fare[CP,$19]*Fare_distribution[CP,$19]+Utility_function_Fare[CP,$21]*Fare_distribution[CP,$21]+Utility_function_Fare[CP,$25]*Fare_distribution[CP,$25]+Utility_function_Fare[CP,$40]*Fare_distribution[CP,$40])/(EXP(Utility_function_Fare[CP,$15]*Fare_distribution[CP,$15]+Utility_function_Fare[CP,$19]*Fare_distribution[CP,$19]+Utility_function_Fare[CP,$21]*Fare_distribution[CP,$21]+Utility_function_Fare[CP,$25]*Fare_distribution[CP,$25]+Utility_function_Fare[CP,$40]*Fare_distribution[CP,$40])+EXP(Utility_function_Fare[sRS,$15]*Fare_distribution[sRS,$15]+Utility_function_Fare[sRS,$19]*Fare_distribution[sRS,$19]+Utility_function_Fare[sRS,$21]*Fare_distribution[sRS,$21]+Utility_function_Fare[sRS,$25]*Fare_distribution[sRS,$25]+Utility_function_Fare[sRS,$40]*Fare_distribution[sRS,$40])+EXP(Utility_function_Fare[pRS,$15]*Fare_distribution[pRS,$15]+Utility_function_Fare[pRS,$19]*Fare_distribution[pRS,$19]+Utility_function_Fare[pRS,$21]*Fare_distribution[pRS,$21]+Utility_function_Fare[pRS,$25]*Fare_distribution[pRS,$25]+Utility_function_Fare[pRS,$40]*Fare_distribution[pRS,$40]))
UNITS: Dimensionless
Price_attractiveness[sRS] =
EXP(Utility_function_Fare[sRS,$15]*Fare_distribution[sRS,$15]+Utility_function_Fare[sRS,$19]*Fare_distribution[sRS,$19]+Utility_function_Fare[sRS,$21]*Fare_distribution[sRS,$21]+Utility_function_Fare[sRS,$25]*Fare_distribution[sRS,$25]+Utility_function_Fare[sRS,$40]*Fare_distribution[sRS,$40])/(EXP(Utility_function_Fare[CP,$15]*Fare_distribution[CP,$15]+Utility_function_Fare[CP,$19]*Fare_distribution[CP,$19]+Utility_function_Fare[CP,$21]*Fare_distribution[CP,$21]+Utility_function_Fare[CP,$25]*Fare_distribution[CP,$25]+Utility_function_Fare[CP,$40]*Fare_distribution[CP,$40])+EXP(Utility_function_Fare[sRS,$15]*Fare_distribution[sRS,$15]+Utility_function_Fare[sRS,$19]*Fare_distribution[sRS,$19]+Utility_function_Fare[sRS,$21]*Fare_distribution[sRS,$21]+Utility_function_Fare[sRS,$25]*Fare_distribution[sRS,$25]+Utility_function_Fare[sRS,$40]*Fare_distribution[sRS,$40])+EXP(Utility_function_Fare[pRS,$15]*Fare_distribution[pRS,$15]+Utility_function_Fare[pRS,$19]*Fare_distribution[pRS,$19]+Utility_function_Fare[pRS,$21]*Fare_distribution[pRS,$21]+Utility_function_Fare[pRS,$25]*Fare_distribution[pRS,$25]+Utility_function_Fare[pRS,$40]*Fare_distribution[pRS,$40]))
UNITS: Dimensionless
Price_attractiveness[pRS] =
EXP(Utility_function_Fare[pRS,$15]*Fare_distribution[pRS,$15]+Utility_function_Fare[pRS,$19]*Fare_distribution[pRS,$19]+Utility_function_Fare[pRS,$21]*Fare_distribution[pRS,$21]+Utility_function_Fare[pRS,$25]*Fare_distribution[pRS,$25]+Utility_function_Fare[pRS,$40]*Fare_distribution[pRS,$40])/(EXP(Utility_function_Fare[CP,$15]*Fare_distribution[CP,$15]+Utility_function_Fare[CP,$19]*Fare_distribution[CP,$19]+Utility_function_Fare[CP,$21]*Fare_distribution[CP,$21]+Utility_function_Fare[CP,$25]*Fare_distribution[CP,$25]+Utility_function_Fare[CP,$40]*Fare_distribution[CP,$40])+EXP(Utility_function_Fare[sRS,$15]*Fare_distribution[sRS,$15]+Utility_function_Fare[sRS,$19]*Fare_distribution[sRS,$19]+Utility_function_Fare[sRS,$21]*Fare_distribution[sRS,$21]+Utility_function_Fare[sRS,$25]*Fare_distri

bution[sRS,$25]+Utility_function_Fare[sRS,$40]*Fare_distribution[sRS,$40])+EXP(Utility_function_Fare[pRS,$15]*Fare_distribution[pRS,$15]+Utility_function_Fare[pRS,$19]*Fare_distribution[pRS,$19]+Utility_function_Fare[pRS,$21]*Fare_distribution[pRS,$21]+Utility_function_Fare[pRS,$25]*Fare_distribution[pRS,$25]+Utility_function_Fare[pRS,$40]*Fare_distribution[pRS,$40]))

UNITS: Dimensionless

UNITS: Dimensionless

scrap_rate_MaaS_fleet_2014[MaaS_Mode, Carbody, Powertrain] = 1

UNITS: dmnl

Scrap_rate_PC_fleet_2014[Carbody, Powertrain] = 1

Time_attractiveness[CP] =
EXP(Utility_function_time[CP,min15]*Time_distribution[CP,min15]+Utility_function_time[CP,min20]*Time_distribution[CP,min20]+Utility_function_time[CP,min25]*Time_distribution[CP,min25]+Utility_function_time[CP,min30]*Time_distribution[CP,min30]+Utility_function_time[CP,min40]*Time_distribution[CP,min40])/(EXP(Utility_function_time[CP,min15]*Time_distribution[CP,min15]+Utility_function_time[CP,min20]*Time_distribution[CP,min20]+Utility_function_time[CP,min25]*Time_distribution[CP,min25]+Utility_function_time[CP,min30]*Time_distribution[CP,min30]+Utility_function_time[CP,min40]*Time_distribution[CP,min40])+EXP(Utility_function_time[sRS,min15]*Time_distribution[sRS,min15]+Utility_function_time[sRS,min20]*Time_distribution[sRS,min20]+Utility_function_time[sRS,min25]*Time_distribution[sRS,min25]+Utility_function_time[sRS,min30]*Time_distribution[sRS,min30]+Utility_function_time[sRS,min40]*Time_distribution[sRS,min40])+EXP(Utility_function_time[pRS,min15]*Time_distribution[pRS,min15]+Utility_function_time[pRS,min20]*Time_distribution[pRS,min20]+Utility_function_time[pRS,min25]*Time_distribution[pRS,min25]+Utility_function_time[pRS,min30]*Time_distribution[pRS,min30]+Utility_function_time[pRS,min40]*Time_distribution[pRS,min40]))

UNITS: Dimensionless

Time_attractiveness[sRS] =
EXP(Utility_function_time[sRS,min15]*Time_distribution[sRS,min15]+Utility_function_time[sRS,min20]*Time_distribution[sRS,min20]+Utility_function_time[sRS,min25]*Time_distribution[sRS,min25]+Utility_function_time[sRS,min30]*Time_distribution[sRS,min30]+Utility_function_time[sRS,min40]*Time_distribution[sRS,min40])/(EXP(Utility_function_time[CP,min15]*Time_distribution[CP,min15]+Utility_function_time[CP,min20]*Time_distribution[CP,min20]+Utility_function_time[CP,min25]*Time_distribution[CP,min25]+Utility_function_time[CP,min30]*Time_distribution[CP,min30]+Utility_function_time[CP,min40]*Time_distribution[CP,min40])+EXP(Utility_function_time[sRS,min15]*Time_distribution[sRS,min15]+Utility_function_time[sRS,min20]*Time_distribution[sRS,min20]+Utility_function_time[sRS,min25]*Time_distribution[sRS,min25]+Utility_function_time[sRS,min30]*Time_distribution[sRS,min30]+Utility_function_time[sRS,min40]*Time_distribution[sRS,min40])+EXP(Utility_function_time[pRS,min15]*Time_distribution[pRS,min15]+Utility_function_time[pRS,min20]*Time_distribution[pRS,min20]+Utility_function_time[pRS,min25]*Time_distribution[pRS,min25]+Utility_function_time[pRS,min30]*Time_distribution[pRS,min30]+Utility_function_time[pRS,min40]*Time_distribution[pRS,min40]))

UNITS: Dimensionless

Time_attractiveness[pRS] =
EXP(Utility_function_time[pRS,min15]*Time_distribution[pRS,min15]+Utility_function_time[pRS,min20]*Time_distribution[pRS,min20]+Utility_function_time[pRS,min25]*Time_distribution[pRS,min25]+Utility_function_time[pRS,min30]*Time_distribution[pRS,min30]+Utility_function_time[pRS,min40]*Time_distribution[pRS,min40])/(EXP(Utility_function_time[CP,min15]*Time_distribution[CP,min15]+Utility_function_time[CP,min20]*Time_distribution[CP,min20]+Utility_function_time[CP,min25]*Time_distribution[CP,min25]+Utility_function_time[CP,min30]*Time_distribution[CP,min30]+Utility_function_time[CP,min40]*Time_distribution[CP,min40])+EXP(Utility_function_time[sRS,min15]*Time_distribution[sRS,min15]+Utility_function_time[sRS,min20]*Time_distribution[sRS,min20]+Utility_function_time[sRS,min25]*Time_distribution[sRS,min25]+Utility_function_time[sRS,min30]*Time_distribution[sRS,min30]+Utility_function_time[sRS,min40]*Time_distribution[sRS,min40])+EXP(Utility_function_time[pRS,min15]*Time_distribution[pRS,min15]+Utility_function_time[pRS,min20]*Time_distribution[pRS,min20]+Utility_function_time[pRS,min25]*Time_distribution[pRS,min25]+Utility_function_time[pRS,min30]*Time_distribution[pRS,min30]+Utility_function_time[pRS,min40]*Time_distribution[pRS,min40]))

UNITS: Dimensionless
UNITS: Dimensionless
Time_distribution[CP, min15] =.05
UNITS: Dimensionless
Time_distribution[CP, min20] =.3
UNITS: Dimensionless
Time_distribution[CP, min25] =.25
UNITS: Dimensionless
Time_distribution[CP, min30] =.2
UNITS: Dimensionless
Time_distribution[CP, min40] =.2
UNITS: Dimensionless
Time_distribution[sRS, min15] =.04
UNITS: Dimensionless
Time_distribution[sRS, min20] =.19
UNITS: Dimensionless
Time_distribution[sRS, min25] =.25
UNITS: Dimensionless
Time_distribution[sRS, min30] =.31
UNITS: Dimensionless
Time_distribution[sRS, min40] =.22
UNITS: Dimensionless
Time_distribution[pRS, min15] =.03
UNITS: Dimensionless
Time_distribution[pRS, min20] =.08
UNITS: Dimensionless
Time_distribution[pRS, min25] =.18
UNITS: Dimensionless
Time_distribution[pRS, min30] =.3
UNITS: Dimensionless
Time_distribution[pRS, min40] =.41
UNITS: Dimensionless
UNITS: Dimensionless
tot_GHG_MaaS_aggregated =
(total_GHG_emissions_MaaS[CP,Sedan,Gasoline]+total_GHG_emissions_MaaS[CP,Sedan,Hybrid]+total_GHG_emissions_MaaS[CP,Sedan,BEV]+total_GHG_emissions_MaaS[CP,SUV,Gasoline]+total_GHG_emissions_MaaS[CP,SUV,Hybrid]+total_GHG_emissions_MaaS[CP,SUV,BEV]+total_GHG_emissions_MaaS[CP,Hatch,Gasoline]+total_GHG_emissions_MaaS[CP,Hatch,Hybrid]+total_GHG_emissions_MaaS[CP,Hatch,BEV])+(total_GHG_emissions_MaaS[sRS,Sedan,Gasoline]+total_GHG_emissions_MaaS[sRS,Sedan,Hybrid]+total_GHG_emissions_MaaS[sRS,Sedan,BEV]+total_GHG_emissions_MaaS[sRS,SUV,Gasoline]+total_GHG_emissions_MaaS[sRS,SUV,Hybrid]+total_GHG_emissions_MaaS[sRS,SUV,BEV]+total_GHG_emissions_MaaS[sRS,Hatch,Gasoline]+total_GHG_emissions_MaaS[sRS,Hatch,Hybrid]+total_GHG_emissions_MaaS[sRS,Hatch,BEV])+(total_GHG_emissions_MaaS[pRS,Sedan,Gasoline]+total_GHG_emissions_MaaS[pRS,Sedan,Hybrid]+total_GHG_emissions_MaaS[pRS,Sedan,BEV]+total_GHG_emissions_MaaS[pRS,SUV,Gasoline]+total_GHG_emissions_MaaS[pRS,SUV,Hybrid]+total_GHG_emissions_MaaS[pRS,SUV,BEV]+total_GHG_emissions_MaaS[pRS,Hatch,Gasoline]+total_GHG_emissions_MaaS[pRS,Hatch,Hybrid]+total_GHG_emissions_MaaS[pRS,Hatch,BEV])
UNITS: kgCO_2/year

tot_GHG_PC_aggregated =
total_GHG_emissions_PC[Sedan,Gasoline]+total_GHG_emissions_PC[Sedan,Hybrid]+total_GHG_emissions_PC[Sedan,BEV]+total_GHG_emissions_PC[SUV,Gasoline]+total_GHG_emissions_PC[SUV,Hybrid]+total_GHG_emissions_PC[SUV,BEV]+total_GHG_emissions_PC[Hatch,Gasoline]+total_GHG_emissions_PC[Hatch,Hybrid]+total_GHG_emissions_PC[Hatch,BEV]

UNITS: kgCO_2/year

Tot_MaaS_fleet[MaaS_Mode, Carbody, Powertrain] = MaaS_fleet_2014+MaaS_fleet_2014_onwards

UNITS: cars

tot_MaaS_USers = Active_MaaS_users[CP]+Active_MaaS_users[sRS]+Active_MaaS_users[pRS]

Tot_PC_fleet[Carbody, Powertrain] = PC_fleet_2014_onwards+PC_fleet_2014

UNITS: cars

tot_scrappage_PC_fleet[Carbody, Powertrain] = PC_Scrappage_2014_fleet+Scrappage_PC

UNITS: cars

tot_scrappge_MaaS_fleet[MaaS_Mode, Carbody, Powertrain] =
MaaS_Scrappage_2014_fleet+Scrappage_MaaS_fleet

Total_GHG_emissions = tot_GHG_PC_aggregated+tot_GHG_MaaS_aggregated

UNITS: kgCO_2/year

total_GHG_emissions_MaaS[MaaS_Mode, Carbody, Powertrain] =
Manufacturing_impacts_MaaS[MaaS_Mode,Carbody,Powertrain]+EoL_impacts_MaaS[MaaS_Mode,Carbody,Powertrain]+Use_impacts_MaaS[MaaS_Mode,Carbody,Powertrain]

UNITS: kgCO_2/year

total_GHG_emissions_PC[Carbody, Powertrain] =
Manufacturing_impacts_PC[Carbody,Powertrain]+Use_impacts_PC[Carbody,Powertrain]+EoL_impacts_PC[Carbody,Powertrain]

UNITS: kgCO_2/year

Total_pkm = pkm_PC+pkm_MaaS[CP]+pkm_MaaS[sRS]+pkm_MaaS[pRS]

UNITS: person*km/year

Use_impacts_MaaS[MaaS_Mode, Carbody, Powertrain] = distance_MaaS_fleet*DPI_Use_phase

UNITS: kgCO_2/year

Use_impacts_PC[Carbody, Powertrain] = distance_PC_fleet*DPI_Use_phase[CP,Carbody,Powertrain]

UNITS: kgCO_2/year

Utility_function_#passenger[CP, passengers2] = 2.8500

UNITS: Dimensionless

Utility_function_#passenger[CP, passengers3] =.9603

UNITS: Dimensionless

Utility_function_#passenger[CP, passengers4] = -2.0047

UNITS: Dimensionless

Utility_function_#passenger[CP, passengers5] = -1.8056

UNITS: Dimensionless

Utility_function_#passenger[sRS, passengers2] = 0

UNITS: Dimensionless

Utility_function_#passenger[sRS, passengers3] = 0

UNITS: Dimensionless

Utility_function_#passenger[sRS, passengers4] = 0

UNITS: Dimensionless

Utility_function_#passenger[sRS, passengers5] = 0

UNITS: Dimensionless

Utility_function_#passenger[pRS, passengers2] = 3.0735

UNITS: Dimensionless
Utility_function_#passenger[pRS, passengers3] = -.6244
UNITS: Dimensionless
Utility_function_#passenger[pRS, passengers4] = -2.4492
UNITS: Dimensionless
Utility_function_#passenger[pRS, passengers5] = 0
UNITS: Dimensionless
UNITS: Dimensionless
Utility_function_Fare[CP, $15] = 2.7007
UNITS: Dimensionless
Utility_function_Fare[CP, $19] = 0.5252
UNITS: Dimensionless
Utility_function_Fare[CP, $21] = -1.0719
UNITS: Dimensionless
Utility_function_Fare[CP, $25] = -2.1540
UNITS: Dimensionless
Utility_function_Fare[CP, $40] = 0
UNITS: Dimensionless
Utility_function_Fare[sRS, $15] = 0
UNITS: Dimensionless
Utility_function_Fare[sRS, $19] = 1.5190
UNITS: Dimensionless
Utility_function_Fare[sRS, $21] = 1.1304
UNITS: Dimensionless
Utility_function_Fare[sRS, $25] = 0.0078
UNITS: Dimensionless
Utility_function_Fare[sRS, $40] = -2.6572
UNITS: Dimensionless
Utility_function_Fare[pRS, $15] = 0
UNITS: Dimensionless
Utility_function_Fare[pRS, $19] = 2.0097
UNITS: Dimensionless
Utility_function_Fare[pRS, $21] = 1.1611
UNITS: Dimensionless
Utility_function_Fare[pRS, $25] = 0.3422
UNITS: Dimensionless
Utility_function_Fare[pRS, $40] = -3.5130
UNITS: Dimensionless
UNITS: Dimensionless
Utility_function_Powertrain_system[CP, Gasoline] = 2.2673
UNITS: Dimensionless
Utility_function_Powertrain_system[CP, Hybrid] =.3202
UNITS: Dimensionless
Utility_function_Powertrain_system[CP, BEV] = -2.5875
UNITS: Dimensionless
Utility_function_Powertrain_system[sRS, Gasoline] = 2.5620
UNITS: Dimensionless

Utility_function_Powertrain_system[sRS, Hybrid] = -.9478
UNITS: Dimensionless
Utility_function_Powertrain_system[sRS, BEV] = -1.6141
UNITS: Dimensionless
Utility_function_Powertrain_system[pRS, Gasoline] = 2.6316
UNITS: Dimensionless
Utility_function_Powertrain_system[pRS, Hybrid] =.2595
UNITS: Dimensionless
Utility_function_Powertrain_system[pRS, BEV] = -2.8911
UNITS: Dimensionless
UNITS: Dimensionless
Utility_function_time[CP, min15] = 2.2933
UNITS: Dimensionless
Utility_function_time[CP, min20] = 0.8181
UNITS: Dimensionless
Utility_function_time[CP, min25] = 0.0562
UNITS: Dimensionless
Utility_function_time[CP, min30] = -.6062
UNITS: Dimensionless
Utility_function_time[CP, min40] = -2.5614
UNITS: Dimensionless
Utility_function_time[sRS, min15] = 1.8790
UNITS: Dimensionless
Utility_function_time[sRS, min20] = 1.0025
UNITS: Dimensionless
Utility_function_time[sRS, min25] =.7870
UNITS: Dimensionless
Utility_function_time[sRS, min30] = -1.3714
UNITS: Dimensionless
Utility_function_time[sRS, min40] = -2.2972
UNITS: Dimensionless
Utility_function_time[pRS, min15] = 2.1991
UNITS: Dimensionless
Utility_function_time[pRS, min20] = 1.0762
UNITS: Dimensionless
Utility_function_time[pRS, min25] = 1.1009
UNITS: Dimensionless
Utility_function_time[pRS, min30] = -1.0525
UNITS: Dimensionless
Utility_function_time[pRS, min40] = -3.3236
UNITS: Dimensionless
UNITS: Dimensionless
Utility_function_Vehicle_body_style[CP, Sedan] = 2.3475
UNITS: Dimensionless
Utility_function_Vehicle_body_style[CP, SUV] = 0.1597
UNITS: Dimensionless
Utility_function_Vehicle_body_style[CP, Hatch] = -2.5072

UNITS: Dimensionless
Utility_function_Vehicle_body_style[sRS, Sedan] = 1.3442
UNITS: Dimensionless
Utility_function_Vehicle_body_style[sRS, SUV] = 1.4160
UNITS: Dimensionless
Utility_function_Vehicle_body_style[sRS, Hatch] = -2.7601
UNITS: Dimensionless
Utility_function_Vehicle_body_style[pRS, Sedan] = 2.5528
UNITS: Dimensionless
Utility_function_Vehicle_body_style[pRS, SUV] =.4172
UNITS: Dimensionless
Utility_function_Vehicle_body_style[pRS, Hatch] = -2.699
UNITS: Dimensionless
UNITS: Dimensionless
Vehicle_body_attractiveness[CP] =
EXP(MaaS_fleet_car_body_distribution[CP,Sedan]*Utility_function_Vehicle_body_style[CP,Sedan]+MaaS_fleet_car_body_distribution[CP,SUV]*Utility_function_Vehicle_body_style[CP,SUV]+MaaS_fleet_car_body_distribution[CP,Hatch]*Utility_function_Vehicle_body_style[CP,Hatch])/(EXP(MaaS_fleet_car_body_distribution[CP,Sedan]*Utility_function_Vehicle_body_style[CP,Sedan]+MaaS_fleet_car_body_distribution[CP,SUV]*Utility_function_Vehicle_body_style[CP,SUV]+MaaS_fleet_car_body_distribution[CP,Hatch]*Utility_function_Vehicle_body_style[CP,Hatch])+EXP(MaaS_fleet_car_body_distribution[sRS,Sedan]*Utility_function_Vehicle_body_style[sRS,Sedan]+MaaS_fleet_car_body_distribution[sRS,SUV]*Utility_function_Vehicle_body_style[sRS,SUV]+MaaS_fleet_car_body_distribution[sRS,Hatch]*Utility_function_Vehicle_body_style[sRS,Hatch])+EXP(MaaS_fleet_car_body_distribution[pRS,Sedan]*Utility_function_Vehicle_body_style[pRS,Sedan]+MaaS_fleet_car_body_distribution[pRS,SUV]*Utility_function_Vehicle_body_style[pRS,SUV]+MaaS_fleet_car_body_distribution[pRS,Hatch]*Utility_function_Vehicle_body_style[pRS,Hatch]))
UNITS: Dimensionless
Vehicle_body_attractiveness[sRS] =
EXP(MaaS_fleet_car_body_distribution[sRS,Sedan]*Utility_function_Vehicle_body_style[sRS,Sedan]+MaaS_fleet_car_body_distribution[sRS,SUV]*Utility_function_Vehicle_body_style[sRS,SUV]+MaaS_fleet_car_body_distribution[sRS,Hatch]*Utility_function_Vehicle_body_style[sRS,Hatch])/(EXP(MaaS_fleet_car_body_distribution[CP,Sedan]*Utility_function_Vehicle_body_style[CP,Sedan]+MaaS_fleet_car_body_distribution[CP,SUV]*Utility_function_Vehicle_body_style[CP,SUV]+MaaS_fleet_car_body_distribution[CP,Hatch]*Utility_function_Vehicle_body_style[CP,Hatch])+EXP(MaaS_fleet_car_body_distribution[sRS,Sedan]*Utility_function_Vehicle_body_style[sRS,Sedan]+MaaS_fleet_car_body_distribution[sRS,SUV]*Utility_function_Vehicle_body_style[sRS,SUV]+MaaS_fleet_car_body_distribution[sRS,Hatch]*Utility_function_Vehicle_body_style[sRS,Hatch])+EXP(MaaS_fleet_car_body_distribution[pRS,Sedan]*Utility_function_Vehicle_body_style[pRS,Sedan]+MaaS_fleet_car_body_distribution[pRS,SUV]*Utility_function_Vehicle_body_style[pRS,SUV]+MaaS_fleet_car_body_distribution[pRS,Hatch]*Utility_function_Vehicle_body_style[pRS,Hatch]))
UNITS: Dimensionless
Vehicle_body_attractiveness[pRS] =
EXP(MaaS_fleet_car_body_distribution[pRS,Sedan]*Utility_function_Vehicle_body_style[pRS,Sedan]+MaaS_fleet_car_body_distribution[pRS,SUV]*Utility_function_Vehicle_body_style[pRS,SUV]+MaaS_fleet_car_body_distribution[pRS,Hatch]*Utility_function_Vehicle_body_style[pRS,Hatch])/(EXP(MaaS_fleet_car_body_distribution[CP,Sedan]*Utility_function_Vehicle_body_style[CP,Sedan]+MaaS_fleet_car_body_distribution[CP,SUV]*Utility_function_Vehicle_body_style[CP,SUV]+MaaS_fleet_car_body_distribution[CP,Hatch]*Utility_function_Vehicle_body_style[CP,Hatch])+EXP(MaaS_fleet_car_body_distribution[sRS,Sedan]*Utility_function_Vehicle_body_style[sRS,Sedan]+MaaS_fleet_car_body_distribution[sRS,SUV]*Utility_function_Vehicle_body_style[sRS,SUV]+MaaS_fleet_car_body_distribution[sRS,Hatch]*Utility_function_Vehicle_body_style[sRS,Hatch])+EXP(MaaS_fleet_car_body_distribution[pRS,Sedan]*Utility_f

unction_Vehicle_body_style[pRS,Sedan]+MaaS_fleet_car_body_distribution[pRS,SUV]*Utility_function_Vehicle_body_style[pRS,SUV]+MaaS_fleet_car_body_distribution[pRS,Hatch]*Utility_function_Vehicle_body_style[pRS,Hatch]))
UNITS: Dimensionless
UNITS: Dimensionless
Work_trip_GHG_allocation_MaaS[CP, Sedan, Gasoline] =.34
UNITS: Dimensionless
Work_trip_GHG_allocation_MaaS[CP, Sedan, Hybrid] =.34
UNITS: Dimensionless
Work_trip_GHG_allocation_MaaS[CP, Sedan, BEV] =.49
UNITS: Dimensionless
Work_trip_GHG_allocation_MaaS[CP, SUV, Gasoline] =.35
UNITS: Dimensionless
Work_trip_GHG_allocation_MaaS[CP, SUV, Hybrid] =.35
UNITS: Dimensionless
Work_trip_GHG_allocation_MaaS[CP, SUV, BEV] =.49
UNITS: Dimensionless
Work_trip_GHG_allocation_MaaS[CP, Hatch, Gasoline] =.34
UNITS: Dimensionless
Work_trip_GHG_allocation_MaaS[CP, Hatch, Hybrid] =.34
UNITS: Dimensionless
Work_trip_GHG_allocation_MaaS[CP, Hatch, BEV] =.49
UNITS: Dimensionless
Work_trip_GHG_allocation_MaaS[sRS, Sedan, Gasoline] =.4
UNITS: Dimensionless
Work_trip_GHG_allocation_MaaS[sRS, Sedan, Hybrid] =.4
UNITS: Dimensionless
Work_trip_GHG_allocation_MaaS[sRS, Sedan, BEV] =.58
UNITS: Dimensionless
Work_trip_GHG_allocation_MaaS[sRS, SUV, Gasoline] =.38
UNITS: Dimensionless
Work_trip_GHG_allocation_MaaS[sRS, SUV, Hybrid] =.38
UNITS: Dimensionless
Work_trip_GHG_allocation_MaaS[sRS, SUV, BEV] =.55
UNITS: Dimensionless
Work_trip_GHG_allocation_MaaS[sRS, Hatch, Gasoline] =.4
UNITS: Dimensionless
Work_trip_GHG_allocation_MaaS[sRS, Hatch, Hybrid] =.4
UNITS: Dimensionless
Work_trip_GHG_allocation_MaaS[sRS, Hatch, BEV] =.58
UNITS: Dimensionless
Work_trip_GHG_allocation_MaaS[pRS, Sedan, Gasoline] =.43
UNITS: Dimensionless
Work_trip_GHG_allocation_MaaS[pRS, Sedan, Hybrid] =.43
UNITS: Dimensionless
Work_trip_GHG_allocation_MaaS[pRS, Sedan, BEV] =.61
UNITS: Dimensionless

Work_trip_GHG_allocation_MaaS[pRS, SUV, Gasoline] =.4
UNITS: Dimensionless
Work_trip_GHG_allocation_MaaS[pRS, SUV, Hybrid] =.4
UNITS: Dimensionless
Work_trip_GHG_allocation_MaaS[pRS, SUV, BEV] =.58
UNITS: Dimensionless
Work_trip_GHG_allocation_MaaS[pRS, Hatch, Gasoline] =.43
UNITS: Dimensionless
Work_trip_GHG_allocation_MaaS[pRS, Hatch, Hybrid] =.43
UNITS: Dimensionless
Work_trip_GHG_allocation_MaaS[pRS, Hatch, BEV] =.61
UNITS: Dimensionless
UNITS: Dimensionless
Work_trip_GHG_allocation_PC[Sedan, Gasoline] =.31
UNITS: Dimensionless
Work_trip_GHG_allocation_PC[Sedan, Hybrid] =.31
UNITS: Dimensionless
Work_trip_GHG_allocation_PC[Sedan, BEV] =.44
UNITS: Dimensionless
Work_trip_GHG_allocation_PC[SUV, Gasoline] =.31
UNITS: Dimensionless
Work_trip_GHG_allocation_PC[SUV, Hybrid] =.31
UNITS: Dimensionless
Work_trip_GHG_allocation_PC[SUV, BEV] =.44
UNITS: Dimensionless
Work_trip_GHG_allocation_PC[Hatch, Gasoline] =.31
UNITS: Dimensionless
Work_trip_GHG_allocation_PC[Hatch, Hybrid] =.31
UNITS: Dimensionless
Work_trip_GHG_allocation_PC[Hatch, BEV] =.44
UNITS: Dimensionless
UNITS: Dimensionless